SINGLE NUCLEOTIDE POLYMORPHISMS ASSOCIATED WITH THE HUMAN ELECTROENCEPHALOGRAM DURING DESFLURANE ANAESTHESIA

A thesis

submitted in partial fulfilment

of the requirements for the degree

of

Master of Science in Biological Sciences

at

The University of Waikato

by

Claire Vignette Mulholland

THE UNIVERSITY OF
WAIKATO
Te Whare Wānanga o Waikato

2012

Abstract

General anaesthesia is an induced state that enables a person to endure surgical procedures without pain or recollection. There is substantial individual variability in the response to anaesthesia and in order to avoid adverse effects caused by either under- or over-sedation, anaesthetic drug administration must be tailored to suit the individual patient. This requires a means to monitor the depth of general anaesthesia. The electroencephalogram (EEG) records the electrical activity of the brain and enables effects of anaesthetic drugs on brain functioning to be monitored. Quantitative EEG monitors, such as the Bispectral (BIS) index monitor, process the raw EEG and provide a numerical output that is often used to measure the depth of general anaesthesia during surgery. Due to a number of factors including clinical conditions and genetic variability in the EEG, the BIS value can at times be misleading.

To identify genetic variations associated with EEG phenotypes relevant to anaesthesia monitoring, an association analysis was performed for 34 single nucleotide polymorphisms (SNPs) in a sample of 125 surgical patients undergoing general, gynaecological or orthopaedic surgery. During surgery, patients were anaesthetised with the volatile anaesthetic agent desflurane, the depth of anaesthesia was measured using BIS monitoring and the raw was also EEG recorded. SNP genotyping was performed for 13 SNPs in five candidate genes; *SGIP1*, *GABRA2*, *CACNA1G*, *HCN1* and *HCN2*, using the polymerase chain reaction and restriction fragment length polymorphism analysis. An additional 21 SNPs in 15 genes involved in various inflammatory and other immune-related pathways were genotyped by Sequenom MassARRAY at the Australian Genome Research Facility.

Six SNPs in five different genes were found to be associated with spindle amplitude (*SGIP1*, *GABRA2*, *HCN1*, *IL1B* and *MYD88*), and a further five SNPs were associated with either delta frequency (*IL10*), or end tidal desflurane concentration (ETDC) (*CACNA1G*, *CRP*, *MYD88* and *TGFB1*). The strongest

associations were identified for a single SNP located in the 3' UTR of *MYD88* (rs6853). The rs6853 A/G genotype was associated with higher median spindle amplitude ($p = 0.0040$) and spindle amplitude relative to ETDC ($p = 0.0006$), and lower EDTC ($p = 0.0095$) than the A/A genotype. No rs6853 G/G homozygotes were identified in the study sample.

MYD88 acts as an adaptor protein in the interleukin-1 receptor and toll-like receptor signalling pathways. Within the brain, cytokines are thought to act as neuronal modulators and influence neurotransmitter signalling and ion channel activity. The association of *MYD88* with spindle amplitude, in conjunction with *IL1B*, suggests that cytokines may influence the EEG during general anaesthesia. Thus cytokine mediated regulation of neuronal activity is speculated to underlie the reported associations. All reported effect sizes were small (0.77- to 1.55-fold) and associated genes had four distinct types of function; ion channels, neurotransmitter signalling, endocytosis, and cytokine signalling. This suggests that numerous genes in different pathways, each with a small, possibly additive effect, are involved in regulating the EEG during general anaesthesia.

Acknowledgements

I would first like to thank my supervisors Dr Ray Cursons and Professor Jamie Sleigh for their expertise and guidance throughout this research. Also, thanks to Professor Dick Wilkins for his initial supervision and for getting me started on this project. Olivia and Greg – thanks for your all technical and other lab related support, and Greg and Richard for your much appreciated proof-reading.

I would also like to acknowledge and thank the researchers at the Australian Genome Research Facility for the additional genotyping data, as well as the anaesthetists and everyone else involved in the larger study that has made this project possible. Much appreciation and thanks goes to those groups that have helped fund this degree, and for their recognition; The University of Waikato Masters Research Scholarship, The Freemasons Charity, The Todd Foundation and The Brian Perry Charitable Trust.

To all of my lab mates – especially Becca, Tania, Nadine, and Jo, cheers for all of your encouragement and advice. You guys have made this time a lot of fun, Queenstown in particular! All of my other friends – thanks for putting up with me and for your understanding. Finally, a huge thank you to my family for your unwavering support and encouragement – you guys are awesome.

Table of Contents

List of Figures

Chapter 4: Discussion

Appendix

List of Tables

List of Abbreviations

AGRF	Australian Genome Research Facility
BBB	Blood-brain barrier
BIS	Bispectral
bp	Base pairs
BSA	Bovine serum albumin
cAMP	Cyclic adenosine monophosphate
Ca_v	Voltage gated calcium channel
CEU	Caucasian of European descent
Ch.	Chromosome
CME	Clathrin-mediated endocytosis
CNS	Central nervous system
CSF	Cerebrospinal fluid
CTAB	Cetyltrimethylammonium bromide
DEPC	Diethyl pyrocarbonate
DNA	Deoxyribonucleic acid
dNTP	Deoxyribonucleotide triphosphate
ECR	Evolutionary conserved region
EDTA	Ethylenediaminetetraacetic acid
EEG	Electroencephalogram
EM	Expectation-maximization
EPSP	Excitatory postsynaptic potential
ETAC	End tidal anaesthetic concentration
ETDC	End tidal desflurane concentration
GABA	Gamma-aminobutyric acid
GITC	Guanidinium isothiocyanate
GWAS	Genome-wide association study
HCN	Hyperpolarisation-activated cyclic nucleotide gated
hr	Hour(s)

HWE	Hardy Weinberg equilibrium
Hz	Hertz
I_h	Hyperpolarisation activated mixed cation current
IL	Interleukin
IL-1R	Interleukin-1 receptor
IPSP	Inhibitory postsynaptic potential
I_t	Low-threshold calcium current
kb	Kilobase(s)
KW-ANOVA	Kruskal-Wallis one-way analysis of variance
l	Litre(s)
LD	Linkage disequilibrium
LPS	Lipopolysaccharide
LTS	Low threshold spike
M	Molar
mA	Milliamp(s)
MAF	Minor allele frequency
mb	Megabase(s)
min	Minute(s)
miRNA	Micro RNA
ml	Millilitre(s)
mM	Millimolar
NCBI	National Centre for Biotechnology Information
ng	Nanogram(s)
NREM	Non-rapid eye movement
PCR	Polymerase chain reaction
PY	Pyramidal (neuron)
qEEG	Quantitative EEG
REM	Rapid eye movement
RFLP	Restriction fragment length polymorphism
rpm	Revolutions per minute
SB	Sodium borate
sec	Second(s)
SNP	Single nucleotide polymorphism
T_a	Annealing temperature

TC	Thalamocortical (neuron)
TE	Tris-EDTA
TLR	Toll-like receptor
T_m	Melting Temperature
TNF	Tumor necrosis factor
TR	Thalamic reticular (neuron)
Tris	Tris(hydroxymethyl)aminomethane
TRN	Thalamic reticular nucleus
T_{td}	Touchdown temperature
U	Units of enzyme
UCSC	University of California Santa Cruz
µg	Microgram(s)
µl	Microlitre(s)
µM	Micromolar
µV	Microvolts
UV	Ultraviolet
V	Volt(s)
V3/R27/CEU	Version 3, Release 27, CEU population

Chapter 1: Introduction and Literature Review

1.1 General introduction

Every year thousands of New Zealanders undergo operations that require the use of general anaesthesia to enable them to endure surgical procedures without pain or recollection. It is widely accepted that there is substantial variability in the quantity of anaesthetic agents required to induce adequate anaesthesia and that following surgery, the pain experienced by patients can be highly variable [1]. To ensure appropriate dosage of anaesthetic drugs and avoid adverse effects caused by either under- or over-sedation, a reliable and accurate method of monitoring the depth of anaesthesia is required.

One tool that is now commonly used to monitor general anaesthesia during surgery is the electroencephalogram (EEG). The EEG records the electrical activity of the brain and reflects its rhythmic activity. EEG patterns reflect a person's state of consciousness and can be used to assess the effects of anaesthetics on cortical activity – allowing the EEG to be used to gauge the depth of anaesthesia and assist anaesthetic administration. Various quantitative EEG (qEEG) monitors, such as the bispectral (BIS) index monitor, have been developed to process the raw EEG and provide a numerical output that is used to **guide** the titration of anaesthetics during surgery. Previous studies have reported the depth of anaesthesia, as measured by qEEG monitors, can influence post-operative pain [2], and that the use of these monitors during surgery can reduce the risk of post-operative recall [3, 4].

This research is part of larger study aimed at determining the influence of the depth of anaesthesia, as measured by the BIS monitor, on post-operative pain levels. The BIS is a dimensionless numerical variable that ranges from 0-100 and reflects of consciousness. BIS monitors are commonly used in anaesthesia monitoring, however, due to factors including clinical conditions and genetic variability in the EEG, the BIS value can at times be misleading.

Many features of brain oscillations are largely genetically determined, resulting in inter-individual differences in the EEG that can contribute to a misleading BIS value. While numerous studies have investigated genetic variations associated with the EEG in psychiatric disorders, variations influencing the EEG during general anaesthesia have not yet been investigated. The aim of this research was to investigate genetic variably in the form of single nucleotide polymorphisms (SNPs) associated with the EEG during general anaesthesia. As genetic differences can confound interpretation of the EEG, a better understanding of the genetic variability underlying individual EEG variability may lead to improved use of the EEG in anaesthesia monitoring and reduced post-operative pain.

1.2 General anaesthesia

General anaesthesia is a controlled and reversible state comprised of multiple components – sedation, amnesia, analgesia, and immobility – that enable a person to endure surgical procedures without pain or recollection. While the exact mechanisms of general anaesthesia are still poorly understood, a generalised decrease in cortical activity and the blockade of external sensory information transfer from the thalamus to the cortex is presumed to be involved [5].

Both genetic and clinical factors influence anaesthetic drug requirements and the response to anaesthesia [6], occasionally resulting in either under- or over-sedation [7]. Under-sedation can potentially result in a patient remembering events from the surgery (post-operative recall), which can lead to psychological disturbances such as anxiety, nightmares and post-traumatic stress disorder [8-10]. The incidence of post-operative recall is estimated at 1-2 patients per 1000 [11-13], however this risk is substantially increased during certain high risk

procedures, such as cardiac surgery [14] and caesarean section [15]. Over-sedation can also compromise patient outcome and can potentially result in complications such as cardiovascular and respiratory suppression [7].

1.2.1 Monitoring the depth of general anaesthesia

Because of the variability in the way individuals respond to anaesthesia, drug administration must be tailored to suit the individual patient. This requires monitoring the depth of anaesthesia and titrating anaesthetic agents to achieve a desirable level of sedation.

Traditionally, anaesthetists monitored various physiological parameters such as respiration rate, heart rate, blood pressure and pupil size, to gauge the depth of anaesthesia (reviewed in [16]). The absence of responsiveness, while an important sign of adequate anaesthesia, is an unreliable predictor of the depth of anaesthesia, largely due to the administration of muscle relaxants that suppress movement without removing consciousness [13, 17]. Other techniques evolved to assist anaesthesia monitoring include the isolated forearm technique [18] and measuring the exhaled concentration of volatile anaesthetics (end tidal anaesthetic concentration (ETAC)). ETAC provides a measure of the alveolar concentration of anaesthetic agent which is thought to reflect levels in the brain. More recently, the EEG has been gaining popularity as a tool to monitor the depth of anaesthesia as it enables the effects of anaesthetics on cortical functioning to be monitored [19]. Incorporation of EEG monitoring with current monitoring techniques is suggested to better enable the patient's level of sedation to be estimated [11, 19]. Better measurement of the depth of anaesthesia may lead to more appropriate administration of anaesthetic agents, subsequently reducing the potential for adverse effects caused by either over- or under-sedation.

1.3 The electroencephalogram

The EEG provides a graphical representation of the spontaneous electrical activity of the brain. It was discovered in the 1920's by Hans Berger who reported the first human EEG recording in 1929 [20]. Nowadays, the EEG is widely used in both research and clinical settings, including applications in psychiatry, diagnostics and anaesthesia monitoring.

The EEG recording is obtained by placing electrodes on the scalp that detect the combined electrical activity of large numbers of neurons located primarily in the cerebral cortex [21]. Differences in voltage between pairs of electrodes at different sites on the head are measured and amplified, and the resultant EEG recording provides a graphical representation of these voltage differences over time (Figure 1.1).

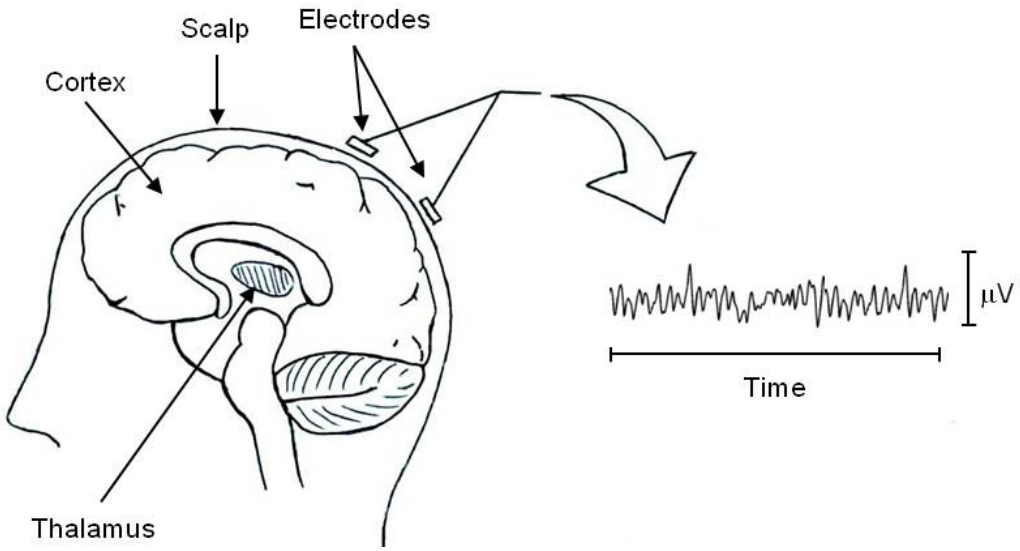

Figure 1.1: The human brain and EEG recording.
Electrodes placed on the scalp measure the voltage difference between two locations on the head and the EEG recording provides a graphical representation of these voltage differences over time.

1.3.1 Genesis of the EEG signal

The primary generators of the EEG signal are the large excitatory pyramidal (PY) neurons located in layers III, IV and V of the cerebral cortex [21]. The combined synchronous activity of large numbers of these neurons creates extracellular voltage fields that are able to be detected by scalp electrodes [21-23] .

It is not axonal action potentials but rather synaptic activity in the dendrites of cortical PY neurons that provide the predominant source of the EEG signal [21, 22]. Excitatory postsynaptic potentials (EPSPs) and inhibitory postsynaptic potentials (IPSPs), generate extracellular currents that are able to summate both temporally and spatially to produce local electric fields of both sufficient duration and strength to be detected by scalp electrodes [21, 24]. While synaptic activity provides the most significant source of the EEG signal, other non-synaptic sources can potentially contribute to extracellular current flow and therefore to the EEG signal. Non-synaptic contributors to the EEG signal include calcium mediated action potentials (Ca^{2+} spikes) and the after hyperpolarisation following Ca^{2+} spikes [21, 25]. Sodium action potentials (Na^{+} spikes) are usually of too short duration (<2 μs) to contribute to scalp recorded EEG, except during synchronous events such as epileptic activity [21, 24].

1.3.2 EEG rhythms

The EEG reflects the rhythmic activity of the brain. Wave-like fluctuations occur when periodic sequences of synchronised action potential bursts generate EPSPs in large numbers of cortical PY cells that summate to produce major depolarisations, resulting in fluctuations in local field potentials that appear as oscillations in the EEG [24]. These oscillations are classified on the basis of frequency into five major classes of brain oscillations (Table 1.1).

Table 1.1: Brain oscillations categorised by frequency.
Hz = hertz (number of oscillations per second).

Wave category	Frequency (Hz)
Delta (δ)	0.5 - 4.0
Theta (θ)	4.0 - 7.0
Alpha (α)	7.0 - 13.0
Beta (β)	13.0 - 30.0
Gamma (γ)	30.0 - 80.0

EEG oscillatory activity reflects the functional state of the brain and changes in both the signal frequency and amplitude are observed with different states. In the awake state and during rapid eye movement (REM) sleep, the EEG is predominated by low amplitude, high frequency, alpha and beta waves [22]. In these states rapid patterns are observed and the EEG is said to be desynchronised [26]. During non-REM (NREM) sleep and anaesthesia, there is a shift in the EEG signal from rapid low-amplitude, high-frequency activity, to high-amplitude, low-frequency rhythmic activity (synchronised EEG) [26, 27]. Delta and spindle waves are particularly prominent features of the synchronised EEG [27] and these rhythms reflect important changes in thalamocortical activity (Section 1.3.3). Spindle waves are groups of waxing and waning 7 to 14 Hz oscillations that last 1 to 3 seconds and recur every 3 to 10 seconds [28] (Section 1.4.3). These rhythmic oscillations are a hallmark of NREM sleep and are also an important feature of the EEG during general anaesthesia [29].

1.3.3 EEG patterns during general anaesthesia

The anaesthetised EGG is similar to that seen during NREM sleep and is characterised by low frequency delta and theta waves, the loss of alpha and beta waves, and the appearance of spindle waves that become slower and longer as the depth of anaesthesia increases [5, 22]. The most important signs of anaesthesia are likely the absence of fast waves, and the presence of spindle waves superimposed against background of slow waves [22].

During both sleep and anaesthesia, the shift to synchronised EEG activity reflects important changes in thalamic activity. The thalamus acts as a gateway regulating the flow of information to the cortex [28] and a decrease in its activity is an important feature of loss of consciousness [22]. During waking, the thalamus is depolarised and in this state acts a relay station forwarding sensory information to the cortex. During slow wave sleep and anaesthesia the thalamus becomes hyperpolarised and in this state the transfer of information from the thalamus to the cortex is blocked [5, 29]. The appearance of spindle and delta waves on the EEG indicate thalamic hyperpolarisation, and thus the blockade of sensory information transfer through to the cortex [29].

1.4 Generation of synchronised EEG activity

The synchronised EEG observed during sleep and anaesthesia results from rhythmic neuronal activity co-ordinated by sub-cortical pacemaker activity in the brain [26]. The main brain regions involved in the generation of synchronised EEG activity, such as spindle and delta waves, are the thalamus and the cerebral cortex [28], and the primary cell types involved are the thalamocortical (TC) neurons and the GABA-ergic thalamic reticular (TR) neurons of the thalamic reticular nucleus (TRN) [28]. Neurons in these structures have intrinsic oscillatory properties [26, 28, 30] and interactions with other neurons are thought to modulate this oscillatory activity [31]. Both the intrinsic properties of these neurons and their interactions are important for the generation of widespread rhythmic brain activity [32, 33].

Thalamic neurons can fire in two distinct firing modes: the ‘tonic mode’ (also known as the transmission mode) and the ‘burst mode’ (also known as the oscillatory mode) [34]. The desynchronised EEG occurs when thalamic neurons fire in the tonic mode. In this mode, TC neurons fire tonic Na^+ spikes at depolarised membrane potentials and the thalamus acts as a relay station for sensory information to be forwarded to the cortex [27]. Accordingly, the tonic mode is generally associated with the awake state and also REM sleep [34]. The burst mode is associated with the synchronised EEG and occurs during NREM

sleep and anaesthesia. In the burst firing mode, thalamic neurons are hyperpolarised and fire in a uniform repetitive pattern and in this state, information transfer from the thalamus to the cortex is blocked [5, 29].

The switch from the tonic mode to the burst mode of firing involves alterations in neurotransmitter release from the brainstem, resulting in hyperpolarisation of the resting membrane potential [27, 28, 35]. Hyperpolarisation activates a series of ionic currents that play an important role in the burst mode and the generation of synchronised EEG activity. Two highly important currents involved in the burst mode of firing are the low-threshold calcium current (I_t) and the hyperpolarisation-activated mixed cation current (I_h). These two currents are thought to operate in tandem to generate rhythmic burst firing in thalamocortical networks [27].

1.4.1 Low-threshold calcium current

The low-threshold calcium current (I_t) is an inward flowing Ca^{2+} current that is active near the resting membrane potential and exhibits voltage dependent activation and inactivation [36]. This current was first identified in nervous tissue in the 1980's following the discovery of low threshold spikes (LTS) in inferior olive and thalamic neurons by Llinás and colleagues (reviewed in [36]). I_t plays an important role in neuronal oscillations and cardiac and neuronal pacemaker activity [36, 37], and is implicated in various other processes including pain processing [38, 39] and fertilization [40]. I_t has also been associated with various disorders such as epilepsy [41], neuropathic pain [42], hypertension [43] and cardiac hypertrophy [44].

Underlying I_t are low voltage gated T-type Ca^{2+} channels (T-type Ca^{2+} channels, also known as low voltage activated Ca^{2+} channels). T-type Ca^{2+} channels are characterised by their low-voltage threshold for activation and inactivation, fast inactivation, selectivity for Ca^{2+}, and tiny single channel conductance [37]. These channels activate around the resting membrane potential (about -65mV), are inactivated by membrane depolarisation and de-inactivated by membrane repolarisation [27, 37, 45].

I_t is inactive at the more depolarised membrane potentials associated with the tonic firing mode [34]. During the burst firing mode, the resting membrane potential is more negative and I_t plays an important role in the generation of synchronised EEG activity by promoting LTS and rebound burst firing [46]. Rebound burst firing is the phenomenon whereby neurons can be triggered to fire after hyperpolarisation. This involves action potentials known as low threshold spikes that are generated from a membrane potential more negative than the Na^+ spike threshold. Hyperpolarisation, such as that induced by the arrival of IPSPs, removes the inactivation of I_t and when the membrane potential returns to its resting level voltage dependent activation of I_t occurs. The activation of I_t results in a Ca^{2+} influx into the cell (Ca^{2+} spike) that depolarises the membrane to the point where Na^+ channels are able to open, resulting in a burst of Na^+ action potentials called rebound bursts (reviewed in [36]).

1.4.2 Hyperpolarisation-activated mixed cation current

The hyperpolarisation-activated mixed cation current (I_h) is an inwardly directed mixed Na^+/K^+ current that is activated by hyperpolarisation and closes at positive membrane potentials. cAMP is a direct modulator I_h of and acts to shift the activation curve toward more positive potentials [47]. I_h plays a central role in the generation and regulation of spontaneous rhythmic activity in both the brain and cardiac pacemaker cells, and also contributes to numerous other neuronal functions including working memory, motor learning, determination of the resting membrane potential and synaptic transmission (reviewed in [48, 49]). Misregulation of I_h is thought contribute to a number of neurological disorders including epilepsy and chronic pain (reviewed in [50]).

Underling I_h are hyperpolarisation-activated cyclic nucleotide gated (HCN) channels. There are four HCN subunit isoforms (HCN1-4) and these assemble into either homo- or hetero-tetrameric I_h channels that form a pore across the cell membrane [51]. The four HCN subunit isoforms differ both in their activation kinetics [52] and degree of regulation by cAMP (reviewed in [49]). The co-assembly of different HCN subunits to form heterotetrameric I_h channels substantially increases the functional diversity of these channels [51, 53, 54].

1.4.3 Spindle oscillations

Spindles oscillations are bursts of 7 to 14 Hz oscillations that generally last 1 to 3 seconds and recur every 3 to 10 seconds [28] (Figure 1.2). The appearance of these rhythmic oscillations on the EEG is a useful correlate for anaesthesia monitoring they indicate hyperpolarisation of the thalamus and a switch to the burst firing mode [5, 29].

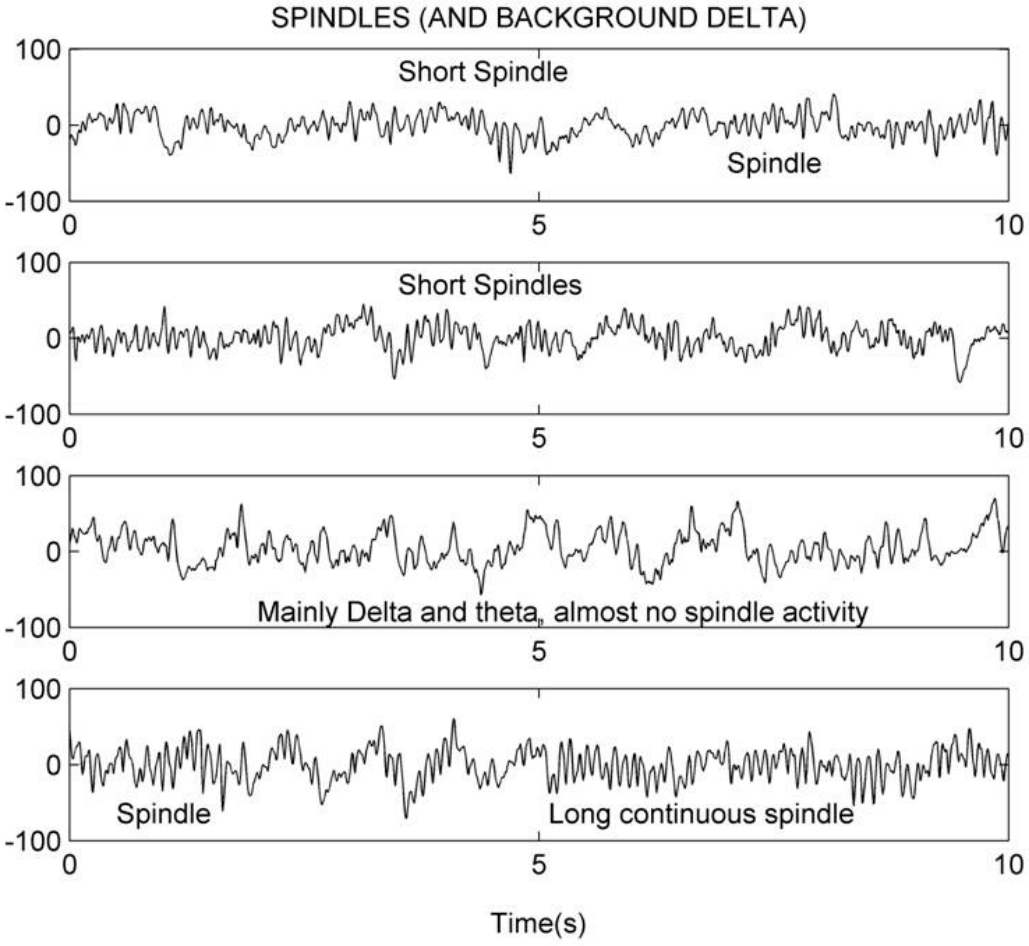

Figure 1.2: The EEG showing varying amounts of spindle activity.
Image kindly supplied by Professor Jamie Sleigh (Department of Anaesthesiology, Waikato Clinical School, University of Auckland, Auckland, New Zealand).

Spindle waves were first described by Loomis in the 1930's [55]. They are primarily generated in the thalamus by a reciprocal interaction between TC and TR neurons [28, 56, 57] through the interplay of synaptic interconnections and intrinsic membrane properties [33]. Rhythmic cycles of action potential bursts in TR cells impose IPSPs on TC neurons via GABA-ergic synapses [33] that

hyperpolarise TC neurons, resulting in the de-inactivation of I_t and the subsequent activation of I_t during the repolarising phase [56, 57]. Activation of I_t generates LTS and rebound bursts in TC neurons, which then fire EPSPs back to TR neurons to restart the cycle [56, 57]. TC neurons also forward this activity onto the cortex, imposing EPSPs on PY neurons, that are visible in the EEG as spindle waves [28]. A small number of cells are involved in spindle wave initiation and they then spread into synchronised network oscillations through the progressive recruitment of neighbouring neurons [58]. Within the thalamus, TR cells are thought to play a central role in the initiation of spindle oscillations and also to act as the oscillatory pacemaker by setting TC firing at the spindle frequency (reviewed in [59]).

The cortex is also thought to play an important role in the initiation, synchronization and termination of spindle oscillations [60, 61]. In addition to cortical inputs, spindle termination is thought to involve upregulation of I_h. LTS is accompanied by a rise in intracellular Ca^{2+}. This increases cAMP levels leading to persistent I_h activation, which in turn depolarises TC cells sufficiently to inactivate the I_t current and thus end the spindle. Immediately following the spindle, intracellular Ca^{2+} remains high resulting in residual upregulation of I_h which is thought to determine the refractory period between spindles [62-64]. Blockage of I_h either by the application of Cs^+ or the drug ZD7288 (a bradycardiac agent), has been demonstrated to abolish the spindle wave refractory period, resulting in the generation of continuous spindle oscillations [62].

1.4.4 Delta oscillations

Delta oscillations lie in the 0.5 to 3.5 Hz frequency range and are primarily associated with deep sleep [23]. These oscillations are also seen during general anaesthesia and are important correlates for anaesthesia monitoring as they indicate thalamic hyperpolarisation and blockade of sensory information transfer to the cortex [29].

The delta oscillation is an intrinsic rhythm generated in the thalamus in TC neurons at membrane potentials more negative than that required for spindle wave generation [32]. This rhythm involves the interaction of I_h and I_t at hyperpolarised

membrane potentials, resulting in the generation of spontaneous and self sustained oscillations in the delta frequency range [28]. At hyperpolarised membrane potentials, activation of I_t generates LTS and rebound burst firing causing a membrane depolarisation that deactivates I_h and inactivates I_t. Decline of the rebound burst creates a hyperpolarising overshoot, removing the inactivation of I_t and activating I_h. I_h then gradually depolarises the membrane leading to the activation of I_t – restarting of the cycle [65]. While the interaction between I_h and I_t is able to generate intrinsic delta rhythms in single TC neurons, the cortex is hypothesised to both potentiate the delta rhythm and synchronise thalamic neurons via thalamocortical networks, resulting in the appearance of delta waves in the EEG [66].

1.5 Using the EEG to monitor anaesthesia

1.5.1 q EEG monitors and the BIS index

A predictable series of changes occur in the EEG as a person transitions from fully awake to asleep, or as one becomes anaesthetised (Section 1.3.3). qEEG monitors algorithmically process the raw EEG to generate a numerical output known as a qEEG index that reflects state of consciousness [22]. The qEEG index is used to guide the titration of anaesthetic agents to achieve a number within a recommended range. These monitors are often used to estimate the depth of general anaesthesia and assess the risk of intra-operative recall during surgery [22]. Numerous indices are commercially available such as the BIS index (Aspect Medical Systems, Newton, MA), spectral entropy (GE Healthcare, Helsinki, Finland), and the cerebral state index (Danmeter, Odense, Denmark).

The BIS index was first introduced in 1992 and is now the most widely used and investigated qEEG index [7]. The BIS monitor processes the raw EEG recorded from a single EEG channel measured on the patient's forehead to derive the BIS value. The BIS index is a dimensionless numerical variable that provides a quantitative measure of cortical activity, allowing the effects of anaesthetics on consciousness, memory formation, and analgesia, to be assessed during surgery

[67] (reviewed in [68]). BIS values range from 0-100 and inversely reflect level of sedation; a BIS value of zero indicates the absence of brain activity (isoelectric EEG) whereas a value of 100 indicates full consciousness. BIS values of 40-60 are generally recommended as a suitable target for surgery, and have been associated with a low probability of responsiveness and recall during general anaesthesia [69, 70]. When anaesthetic drug delivery was titrated within this range, the use of BIS monitors during surgery has been reported to lead to an approximately 80% reduction in the incidence of recall [3, 4], and also to promote faster emergence and improved post-operative recovery [71-73]. Furthermore, the BIS value has also been shown to correlate with the probability of movement in response to surgical incision [74, 75], however, this correlation becomes weaker when analgesics are used in conjunction with other anaesthetic agents [76].

1.5.2 Reliability of the BIS value

While there are numerous studies demonstrating the use of BIS monitors in anaesthesia management to improve patient care, there are also reports in which the BIS value has been erroneous. For example, case reports document patients experiencing explicit intra-operative recall despite having BIS values <50 [77, 78]. While the above examples represent extreme cases, they highlight the fact that the BIS value can at times be misleading and cannot be relied on as a sole means to estimate anaesthetic depth. A number of factors can contribute to a misleading BIS value including various clinical conditions, electromyography artefacts and environmental artefacts such as interference from electronic devices (reviewed in [79]). Furthermore, the BIS value is not independent of the anaesthetic agent used whereby different drugs can elicit varying changes in the EEG [79].

In addition to various clinical and environmental factors that can affect the BIS value, BIS values also demonstrate significant variability between individuals potentially making it difficult to accurately use the BIS monitor to predict sedation level [80]. Between individuals there can be marked differences in the raw EEG, these differences are largely genetically determined [81] and can confound interpretation of the BIS value. For example, spindle wave patterns have been demonstrated to show considerable variability between individuals during normal

sleep [82] and clinical observations have shown that some patients lack spindle waves during general anaesthesia (unpublished observation).

1.6 Genetics of human brain oscillations

The EEG is relatively stable in individuals and high high-retest correlations are observed in healthy adults [83-85]. The majority of EEG characteristics are largely genetically determined [81], with genetic factors contributing strongly to important characteristics of the sleep, waking and anaesthetised EEG. Twin studies investigating heritability of the EEG have demonstrated higher concordance between monozygotic twins than dizygotic twins and unrelated individuals [86, 87], this is also observed in monozygotic twins raised apart [88]. EEG spectral power analysis has demonstrated high heritability for the various frequency bands; the average heritability of the alpha, beta, theta, and delta frequencies have been estimated to be 89%, 86%, 89% and 76%, respectively [89].

Because of the stability and high heritability of the EEG, phenotypes based on measures of EEG power and amplitude represent useful correlates for genetic analysis. Accordingly, the EEG is often used as an endophenotype (an intermediate phenotype that is involved in the pathway between genotype and clinical outcome [90]) to study to genetic factors involved in psychiatric disorders. The use of the EEG as an endophenotype is thought to aid the search of genes associated with complex disorders as the EEG more closely reflects the function of genes that predispose to such disorders than clinical diagnosis and symptoms alone [91]. Using this approach, numerous studies have investigated genetic variations contributing to EEG variability in the context of disorders such as alcoholism [92-95] and schizophrenia/psychosis [96, 97]. This has led to the identification of numerous genes predicted to influence the resting EEG that may also be involved in predisposition to alcoholism, including *SGIP1* [95], *GABRA2* [92, 98] and *CRH-BP* [93, 99] and *HRT3B* [94].

Despite the important clinical application of the EEG in anaesthesia monitoring, studies investigating genetic variation and the EEG during general anaesthesia have not been published to date.

1.7 Anaesthesia, surgery and inflammation

1.7.1 Inflammation

Inflammation is an immune response characterised by five cardinal signs; *rubor* (redness), *tumor* (swelling), *calor* (heat) and *dolor* (pain) and *functio laesa* (loss of function). The inflammatory response plays an essential role in host defence and can be activated in response to pathogenic infection, tissue injury, or by immune stimulation. It is a dynamic process that consists of four main components; inflammatory inducers, sensors, mediators and target tissues [100].

As well as playing a vital role in the immune response to infection, inflammation is also a contributing factor to many chronic diseases including diabetes, osteoporosis and cardiovascular disease (reviewed in [101]). Inflammation is also thought to have a potential role in many central nervous system (CNS) diseases including epilepsy, neurodegenerative disorders, multiple sclerosis, and even some psychiatric disorders such as schizophrenia and depression [102, 103].

1.7.2 Cytokines and immune system-to-brain communication

Cytokines are small protein molecules involved in cell-cell signalling. They exert their effects by binding to specific receptors on target cells, activating intra-cellular signalling cascades that regulate gene transcription. Cytokines play an important role as mediators of the inflammatory response, including regulating the production of other cytokines [104].

During systemic inflammation, cytokines are secreted primarily by peripheral immune cells, such as macrophages and monocytes [105]. These cytokines, or their signals, are able to reach the CNS, thus there is bi-directional communication

between the brain and immune system [106]. Tumor necrosis factor (TNF) α, and the interleukins (IL) IL-1 and IL-6, are thought to be the primary mediators of immune system-to-brain communication [106]. Cytokines cannot freely cross the blood-brain barrier (BBB) but can reach the brain by passive transport through leaky areas of the BBB, active transport across the BBB [106]. Cytokine signals may also be transmitted via nerve fibres and humoral mechanisms [106]. Furthermore, cytokines are known to be expressed by various brain cells, including glial cells, astrocytes and neurons (reviewed in [107]).

Within the brain, cytokines have been implicated in various aspects of normal brain functioning, including sleep regulation, neuroendocrine functioning and neuronal development [105], as well in pathological conditions such as seizure generation and epilepsy [108]. Numerous studies on rodents have reported elevated mRNA levels of TNFα, IL-1, IL-6, and the IL-1 receptor (IL-1R) following immune activation induced by peripheral endotoxin administration [109-114], suggesting that the systemic inflammatory response may affect brain functioning by inducing pro-inflammatory cytokine expression in the brain [109]. Accordingly, peripheral immune stimulation by endotoxin administration has been found to influence the sleep EEG and sleep patterns, resulting in increased delta activity during NREM sleep in rats [115] and humans [116], and increased alpha and beta activity in humans [117]. However, conflicting results have also been reported [118].

Increasing evidence suggests that cytokines may influence neurotransmitter signalling and ion channel activity in the brain to regulate neuronal excitability and synaptic plasticity (reviewed in [105, 119]). Although the exact mechanisms by which cytokines exert such effect remains unclear, post-translational modification has been suggested as one possible mechanism, as effects have been shown to occur rapidly within seconds or minutes of exposure. Effects have also been observed following prolonged exposure – suggesting cytokine mediated effects on gene expression [119].

1.7.3 Surgery, anaesthesia and the inflammatory response

Surgery is a highly invasive process that induces a systemic inflammatory response essential for tissue repair, pathogen elimination and the maintenance of homeostasis. The normal inflammatory response to surgery consists of immunological, hormonal and metabolic components and involves a balance between pro- and anti-inflammatory factors [120]. Initially, pro-inflammatory cytokines such as IL-1, IL-6 and TNFα, are released at the site of damage and induce immune activation and an inflammatory response. Inflammatory stimulation predominates for the first 36 hrs and over the next few days is balanced by a compensatory suppressive response that involves the release of anti-inflammatory cytokines including IL-10, IL-1R antagonist, and soluble TNF receptors [120]. The extent of the inflammatory response to surgery is usually well- controlled and appropriately balanced in healthy patients and is related to the invasiveness of the surgical procedure [120]. Dysregulation of this response can lead to post-operative complications such as sepsis, impaired wound healing and systemic inflammatory response syndrome [120].

The inflammatory response to surgery is influenced by various factors such as genetics, age, other medications, pre-existing conditions and also anaesthetic drugs [121, 122]. The ability of anaesthetic agents to modulate inflammatory processes was first demonstrated over 100 years ago and during more recent decades, effects of various anaesthetics on the immune response have been widely studied both *in vitro* and *in vivo* (reviewed in [120, 122]). In general, anaesthetic agents are considered to have immuno-suppressive effects. Different anaesthetics modulate the inflammatory response to surgery either via direct effects on immune cells, or, indirectly by influencing the stress response, disturbing the balance between pro- and anti-inflammatory responses, resulting in a slight immune-suppression of limited duration.[122-124]. Although the exact nature and extent of these effects remain unclear, it is apparent that both the type of anaesthetic and the concentration administered influence the effects of anaesthetics on immune cells [120, 122]. Effects are generally considered to be small and clinically insignificant in healthy patients relative to the impact of surgical trauma [120], but may be of much greater clinical importance in patients with significant pre-existing conditions and elderly patients [122, 123].

1.8 Personalised medicine and pharmacogenomics

Personalised medicine refers to the customisation of healthcare in which genetic and other information, such as biochemical measurements, are used to tailor medical practice and treatment to best suit the individual.

One major area in which personalised medicine may lead to improved health care outcomes is in drug administration and prescription. There is a wide degree of heterogeneity in individual response to pharmaceuticals which can be due to numerous factors including age, sex, other clinical conditions, and inheritance [1, 125, 126]. The disciplines of pharmacogenetics and pharmacogenomics (collectively referred to here as pharmacogenomics) study the genetic basis underling individual variation in drug response. Pharmacogenomic studies tend to focus on genetic variation in the form of SNPs (Section 1.8.1). Cancer chemotherapy provides an example of progress in pharmacogenomics that has led to improved treatment outcomes by allowing treatment to be customised based on the genetic profile of the tumor cells [127].

It is widely accepted that there is considerable variability in anaesthesia requirements and recovery from anaesthesia between patients. Along with various clinical factors, genetic variation also contributes to the pharmacology of anaesthetics and it is thought that multiple genes and gene variants underlie this variability [128]. The response to anaesthesia can be influenced by genetic differences in receptors and ion channels [6], as well as transport proteins and enzymes involved in drug metabolism [1]. These differences have important clinical implications for the anaesthetist [1], thus this area represents an important focus for pharmacogenomics research. While understanding the genetic variability contributing to anaesthetic response has clear implications for clinical practice, understanding the genetic variability associated with the EEG during general anaesthesia may augment advances in this area by improving anaesthesia monitoring.

The identification of genetic variants associated with EEG traits of importance to anaesthesia monitoring, such as spindle and delta wave features, may lead to improved use of qEEG monitors in anaesthesia monitoring by allowing the incorporation of genetic data into the BIS or other algorithms, or through the

development of new algorithms. Improved monitoring in conjunction with personalised anaesthetic drug administration using pharmacogenomic information, may lead to improved anaesthetic administration and consequently better patient outcomes, potentially reducing side effects and post-operative pain.

1.8.1 Single nucleotide polymorphisms

SNPs are single base pair differences in the human genome present in >1% of the population. There an estimated ~7 million common SNPs with minor allele frequencies (MAF) >5%, and a further ~4 million with MAFs between 1 and 5% [129]. While allele frequencies of SNPs can vary considerably between populations, the majority of common SNPs are found in most major human populations [130]. SNPs account for the majority of variants in the human genome and are predicted to occur approximately once every 800-100 bp [131, 132].

Genome-wide association studies (GWAS) and candidate gene studies generally use common DNA variants in the form of SNPs to identify genes and genomic regions associated with particular traits or disease risk. GWAS test thousands of SNPs spread across the entire genome for potential associations, whereas candidate gene studies select a subset of SNPs in a gene, or genes, of interest to genotype and test for associations with the phenotype of interest. These studies have identified hundreds of loci associated with disease susceptibility, the vast majority of which are located in non-coding regions [133].

SNPs in non-coding regions may have functional effects on phenotype if they occur in regulatory regions and affect levels of gene expression. Alternatively, associations of non-coding SNPs with disease may be due to linkage disequilibrium (LD) with functional SNPs either in non-coding or protein coding regions. LD refers to the non-random association of SNP loci on the same chromosome [134, 135]. Segments of the genome in high LD are unlikely to have been interrupted by recombination, and such segments are referred to as haplotype blocks. Within these blocks, SNP alleles correlate in a predictable way and limited combinations of alleles – known as haplotypes – are observed [134, 135].

1.9 Study design

This research applied a candidate gene type approach to identify SNPs associated with the EEG during general anaesthesia with desflurane (herein referred to simply as general anaesthesia). Participants were surgical patients who had the raw EEG recorded during surgery and the depth of anaesthesia measured using the BIS monitor. For each patient, a short EEG segment (epoch) was selected from the middle of the surgery for analysis. Five candidate genes were selected for inclusion in this study (Section 1.10) and two to three SNPs in each gene were chosen to be genotyped. Genotyping was performed using the polymerase chain reaction (PCR) and restriction fragment length polymorphism (RFLP) analysis (collectively referred to as PCR-RFLP) (Section 2.2). Statistical analysis was used to test SNPs for associations with spindle and delta wave features, and with anaesthetic agent concentration.

For the larger study this research was part of, a number of patient DNA samples were also sent to the Australian Genome Research Facility (AGRF, Brisbane, Australia) and genotyped for SNPs 15 different inflammatory and immune-related genes (Section 1.11). Genotyping results were provided for incorporation into this study and these SNPs were also tested for associations with the EEG.

1.10 Candidate genes

Five candidate genes were specifically selected for inclusion in this study (Table 1.2). The first two of these genes – *SGIP1* and *GABRA2* – were selected on the basis of results from previous association studies [92, 95] and on their physiological roles. The remaining three genes – *CACNA1G*, *HCN1* and *HCN2* – were chosen based on their roles in the generation of synchronised neuronal activity.

Table 1.2: Basic information on candidate genes selected for inclusion in this study.

Official Symbol	Location	Official name	Role of gene product
SGIP1	1p31.3	SH3-domain GRB2-like (endophilin) interacting protein 1	Involved in recycling receptors, ion channels and other membrane proteins in neuronal cells.
GABRA2	4p12	Gamma-aminobutyric acid (GABA) A receptor alpha 2	Neurotransmitter receptor in the brain for the inhibitory neurotransmitter GABA.
HCN1	5p12	Hyperpolarisation-activated cyclic nucleotide-gated potassium channel 1	Mixed cationic ion channel in neuronal cells, underlies I_h.
CACNA1G	17q22	Calcium channel, voltage-dependent, T type, alpha 1G subunit	T-type Ca^{2+} ion channel in neuronal cells, underlies I_t.
HCN2	19p13.3	Hyperpolarisation-activated cyclic nucleotide-gated potassium channel 2	Mixed cationic ion channel in neuronal cells, underlies I_h.

1.10.1 *SGIP1*

The human gene *SGIP1* encodes a highly conserved endocytic adaptor protein predominantly expressed in the brain known as SH3-domain GRB2-like (endophilin) interacting protein 1 (NCBI Gene ID: 84251) [136]. *SGIP1* is located on the forward strand of chromosome 1 at 1p31.3, spans approximately 211 kb, and consists of 27 exons [136] (Figure 1.3) (Figure 2.2a).

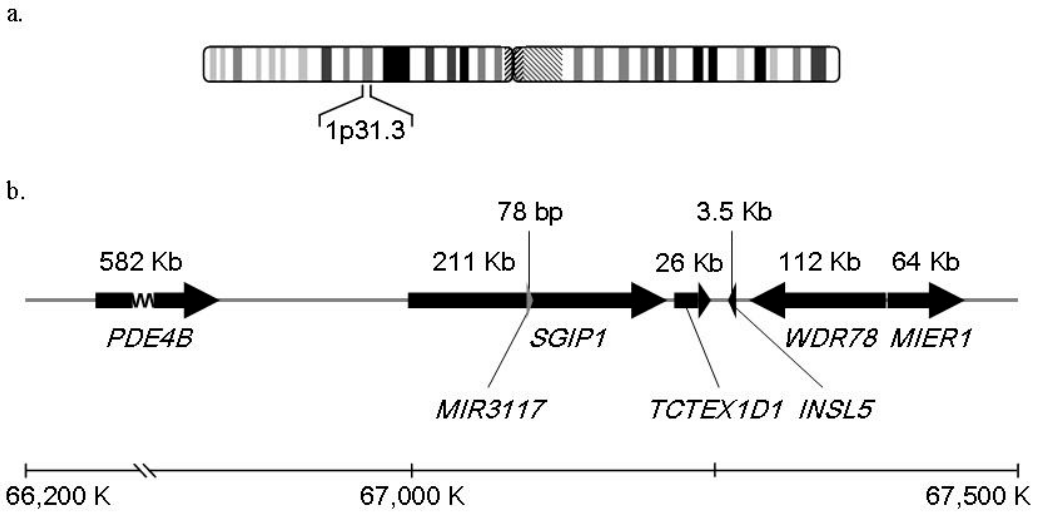

Figure 1.3: Location and genomic context of *SGIP1*.
a. Chromosome 1 showing locus 1p31.3; b. Genomic region of 1p31.3 containing S*GIP1* and neighbouring genes. (Figure based on NCBI human genome build 37.3).

SGIP1 was first identified as a central regulator of energy homeostasis in *Psammomys obesus*, a polygenic rodent model of obesity [136]. The protein it encodes has been shown to as function as an endocytic protein [136], and a direct role for the splice variant SGIP1α in clathrin-mediated endocytosis (CME) has been demonstrated using knockdown, over-expression and co-localisation studies [137]. In neuronal cells, CME regulates the uptake of channels, transporters and other membrane proteins, and also mediates the internalization of several signalling receptors, thereby modulating signal transduction [138]. CME is also a central pathway for the recycling of synaptic vesicles at the nerve terminal following synaptic transmission [139].

A recent GWAS by Hodgkinson et al. (2010) identified eight SNPs in *SGIP1* associated with resting theta power in Plains American Indians [95]. *SGIP1* was

found to account for 8.8% of the variance in theta power in this sample, and for 3.5% of the variance in a replicate US Caucasian sample. Several other genes involved in cell trafficking processes were also associated with the EEG at threshold or sub-threshold significance. Variability in such genes is suggested to influence neuronal membrane component uptake and recycling, consequently influencing neuronal excitability [95], which is then reflected in the EEG.

1.10.2 *GABRA2*

Gamma-aminobutyric acid (GABA) is the primary inhibitory neurotransmitter in the mammalian brain (Stephenson 1988). GABA exerts its inhibitory effects by binding to one of three types of receptors; $GABA_A$, $GABA_B$ and $GABA_C$. $GABA_A$ receptors are ligand-gated chloride ion channels that mediate the majority of fast synaptic inhibition in the brain [140]. These receptors are assembled from a combination of five subunits from six different subunit classes; α, β, γ, ε, ρ and μ [140]. Different combinations of these subunits confer different physiological and pharmacological properties increasing the diversity of $GABA_A$ receptors [140]. $GABA_A$ receptors are been proposed as targets for many general anaesthetics (reviewed in [141]). Nearly all general anaesthetics have been demonstrated to potentiate GABA-ergic currents, and generally at higher doses to activate $GABA_A$ receptors in the absence of GABA [141].

There are six members of the α subunit class (α1- α6) and the majority of $GABA_A$ receptors contain α subunits as well as β and γ. In humans, the $GABA_A$ α2 subunit is encoded for by the gene *GABRA2* (NCBI Gene ID: 2555). *GABRA2* is comprised of 10 exons, spans approximately 140 kb and is located amongst a cluster of $GABA_A$ receptor genes on the reverse strand of chromosome 4 at 4p12 [142] (Figure 1.4) (Figure 2.2b). *GABRA2* mRNA is subject to both alternative splicing and alternative promoter use, leading to the production of numerous isoforms with varying levels of expression throughout the brain [143].

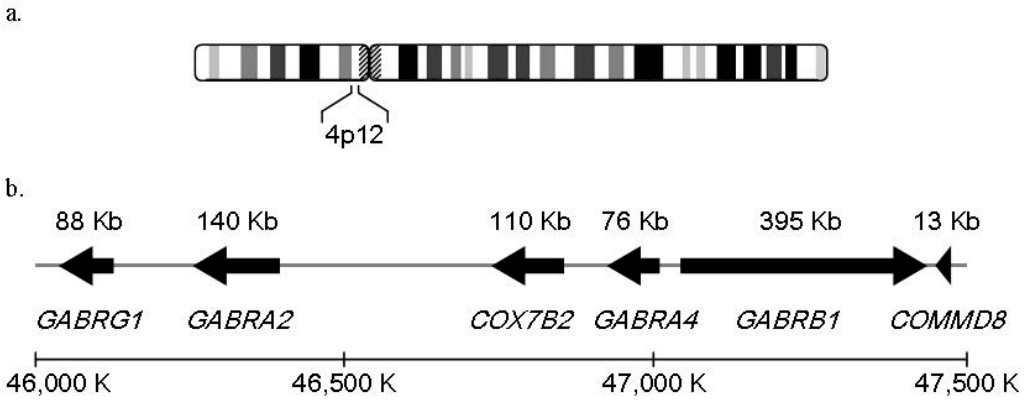

Figure 1.4: Location and genomic context of *GABRA2*.
a. Chromosome 4 showing locus 4p12; b. 1.5 mb region on 4p12 containing the $GABA_A$ receptor gene cluster harbouring *GABRA2*. (Figure based on NCBI human genome build 37.3).

GABRA2 variability has previously been associated with increased beta power in the resting EEG [92, 144]. The association of *GABRA2* with the EEG was first identified in a study by Edenberg et al. (2004) using the EEG as an endophenotype to investigate the genetics of alcohol dependency [92]. Numerous candidate gene studies have reported associations between *GABRA2* variation and alcohol dependence and related phenotypes, and this gene is now considered a confirmed locus for susceptibility to alcohol dependency (reviewed in [145]). The association of *GABRA2* with both the beta frequency band and alcohol dependence has lead to the hypothesis that *GABRA2* variability might influence susceptibility to alcohol dependence by modulating neuronal excitability [92].

Based on the role of GABA-ergic signalling spindle wave generation (Section 1.4.3); the role of $GABA_A$ receptors as targets for many general anaesthetics; the previously identified association of *GABRA2* with beta frequencies; and the postulated role of this gene in regulating neuronal activity, it is hypothesised that *GABRA2* variability might also influence anaesthetic response and the EEG during general anaesthesia.

1.10.3 *CACNA1G*

The human gene *CACNA1G* encodes the T-type Ca^{2+} channel subunit α1G, also known as $Ca_v3.1$ (NCBI Gene ID: 8913). *CACNA1G* maps to chromosome 17 at 17q22, spans approximately 66.5 kb on the forward strand and consists of 38 exons [146, 147] (Figure 1.5) (Figure 2.2d). *CACNAG1* is subject to extensive alternative splicing that is both developmentally regulated [148] and tissue specific [149]. Alternative splicing of *CACNA1G* transcripts serves to increase the diversity of T-type Ca^{2+} channels and has been shown to modify channel gating properties [148, 150]. 15 sites of transcript variation have been identified: 11 sites of alternative splicing in the open reading frame, two alternative 5' UTR promoter sites and two alternative 3' UTR polyadenylation sites [146, 148].

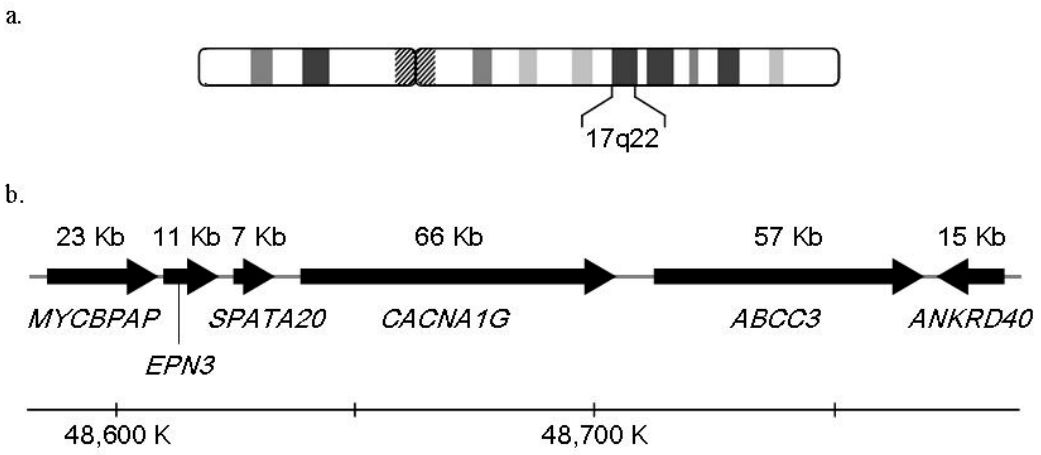

Figure 1.5: Location and genomic context of *CACNA1G*.
a. Chromosome 17 showing locus 17q22; b. ~200 kb region of 17q22 containing *CACNA1G* and neighbouring genes. (Figure based on NCBI human genome build 37.3).

T-type Ca^{2+} channels belong to the voltage gated Ca^{2+} channel (Ca_v) family, which includes both low (T-type) and high (L-, P/Q-, N- and R-types) voltage activated members. The different members of this family mediate the different voltage regulated Ca^{2+} currents. Ca_v channels are heteromultimers and the channel subtype is determined solely by the principle pore forming α1 subunit [151]. The various α1 subunits are encoded for by Ca_v channel α1 subunit gene family which contains three subfamilies (Ca_v1-3) that arose by an ancient gene duplication [152].

CACNA1G belongs to the Ca_v3 gene subfamily which encodes the T-type $\alpha1$ subunits. There are two other genes in this subfamily; *CACNA1H* and *CACNA1I*, which encode the $\alpha1H$ ($Ca_v3.2$) and $\alpha1I$ ($Ca_v3.3$) subunits, respectively. The three T-type $\alpha1$ subunits each have different biophysical properties (reviewed in [153]) and the expression pattern of the three Ca_v3 genes is unique and complementary to a great extent [154]. The $\alpha1G$ subunit is predominantly expressed in the brain, with particularly high levels of expression observed in the thalamus [147, 149, 154].

T-type Ca^{2+} channels mediate I_t and this current plays an important role in the generation of synchronised EEG activity, including delta and spindle waves (Sections 1.4.4 and 1.4.3). The importance of $Ca_v3.1$ channels in the generation synchronised EEG activity has been demonstrated in mice lacking functional $Ca_v3.1$. Within the thalamus, $Ca_v3.1$ channels are the primary generators of LTS [153]. LTS and burst firing has been shown to be absent in TC neurons of *CACNA1G*$^{-/-}$ mice [155], accordingly, these mice show altered slow wave EEG activity during natural sleep and under urethane anaesthesia, with both a loss of spindle oscillations and decreased delta activity compared to wild type mice [156].

Because of the important role of I_t in the generation of synchronised EEG activity; the role of $Ca_v3.1$ channels in promoting LTS in the thalamus; and the altered slow wave EEG activity observed in *CACNA1G*$^{-/-}$ mice, variability in *CACNA1G* is suggested to potentially underlie some of the variability in the EEG observed under general anaesthesia.

1.10.4 *HCN1* and *HCN2*

The human gene *HCN1* encodes the hyperpolarisation-activated cyclic nucleotide-gated channel subunit 1 (HCN1), also known as brain cyclic nucleotide gated 1 (BCNG-1). *HCN1* is located in a relatively gene poor region on the reverse strand of chromosome 5 at 5p12, spans approximately 437 kb and is comprised of 8 exons (NCBI Gene ID: 348980) (Figure 1.6) (Figure 2.2c). *HCN2* encodes the hyperpolarisation-activated cyclic nucleotide-gated channel subunit 2 (HCN2), also known as brain cyclic nucleotide gated 2 (BCNG-2). *HCN2* is located on the forward strand of chromosome 19 at 19p13.3, consists of 8 exons and spans

approximately 27 kb (NCBI Gene ID: 610) (Figure 1.7) (Figure 2.2e). The protein products of these genes are 890 (*HCN1*) and 189 (*HCN2*), amino acids long and alternative splicing variants have not been identified for either gene (Ensembl: ENSG00000164588 (*HCN1*) and ENSG00000099822 (*HCN2*)).

HCN1 and *HCN2* were first discovered and cloned in the late 1990's along with the other two members of the HCN gene family, *HCN3* and *HCN4* [157-159]. In the brain, HCN channels mediate the important pacemaker current I_h (Section 1.4.2). I_h plays a key role in delta wave generation (Section 1.4.4) and is thought to be involved in regulating the periodicity of spindle waves (Section 1.4.3).

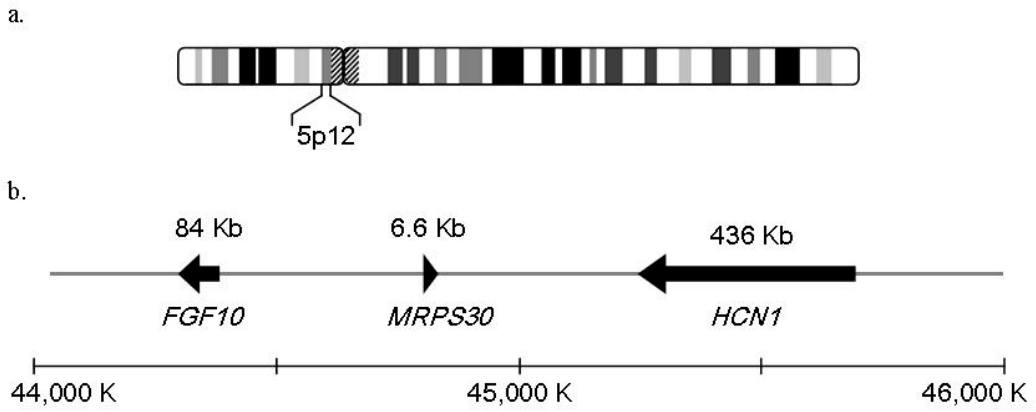

Figure 1.6: Location and genomic context of *HCN1*.
a. Chromosome 5 showing location of locus 5p12; b. 2 mb region of 5p12-5p11 containing *HCN1* and neighbouring genes. (Figure based on NCBI human genome build 37.3).

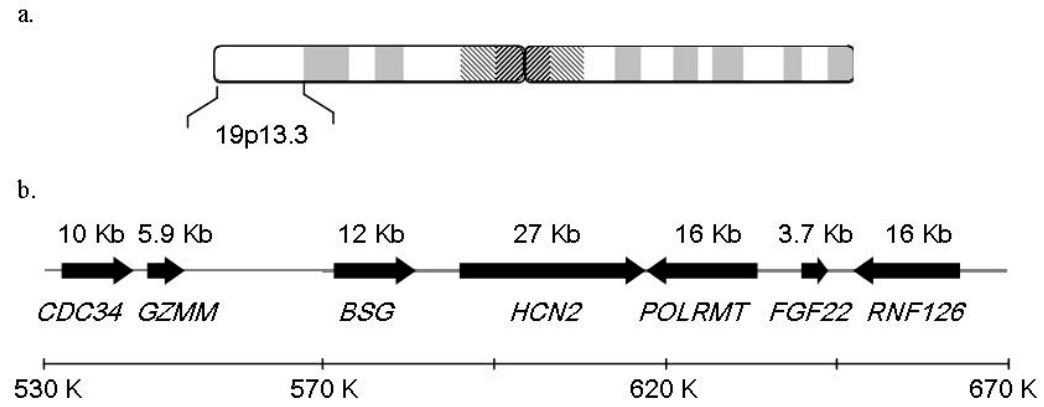

Figure 1.7: Location and genomic context of *HCN2*.
a. Chromosome 19 showing location of locus 19p13.3; b. ~140 kb region of 19p13.3 containing *HCN2* and neighbouring genes. (Figure based on NCBI human genome build 37.3).

Expression of the HCN gene family has been well studied at both the transcript and protein levels in the mouse and rat brain. All four genes have been found to be expressed in the brain and multiple isoforms can be expressed in the same cell [52, 160]. *HCN2* is widely distributed throughout the brain and is particularly highly expressed in the thalamus and brain stem. *HCN1* shows a more localised distribution and is predominantly expressed in the neocortex, hippocampus and cerebellum [158, 160-162]. There is considerable overlap in the expression of *HCN1* and *HCN2* [160], and sub-cellular localization of these subunits has also been shown with the highest channel density found in the distal dendrites of neuronal cells [161, 163].

Using *HCN2*$^{-/-}$ mice, Ludwig et al. (2003) have demonstrated that I_h in TC neurons is predominately generated by HCN2, and that HCN2 plays a vital role in determining the resting membrane potential of these cells [164]. *HCN2*$^{-/-}$ TC relay neurons were found to exhibit a near total loss of I_h and fired in the burst mode rather than the tonic mode as observed in wild type cells [164]. While HCN2 channels appear to play a critical role in regulating neuronal excitability in TC neurons, HCN1 channels appear to fulfil this role in PY neurons. The dendrites of *HCN1*$^{-/-}$ PY neurons have been demonstrated to display a loss of I_h resulting in enhanced excitability, suggesting a crucial role for HCN1 in the generation of I_h and the regulation of excitability in PY neurons [165]. These observations also correspond well with expression data showing that *HCN1* is the most predominantly expressed HCN gene in the cortex, and *HCN2* in the thalamus [160].

HCN channels have also been implicated as potential targets of anaesthetics. Volatile anaesthetics have been demonstrated to inhibit I_h in brainstem motor neurons [166, 167], and intravenous anaesthetics to inhibit I_h in thalamic and TC relay neurons [168, 169]. The inhibition of I_h by volatile anaesthetics involves a hyperpolarising shift in the voltage dependence of activation and a decrease in current amplitude; these effects represent actions on the HCN1 and HCN2 subunits, respectively [170].

Based on the essential role of I_h in the generation of synchronised EEG; the effects of *HCN1* and *HCN2* knockout on PY and TC neurons, respectively; and the role of HCN channels as anaesthetic targets, it is speculated that variability in

either *HCN1* and/or *HCN2* may influence the generation of synchronised EEG activity and be associated with differences in the EEG during general anaesthesia.

1.11 Inflammatory genes

Several candidate genes involved in various inflammatory and other immune-related pathways were investigated for associations with post-operative pain for the larger study this research was part of. The majority of these genes are involved in cytokine signalling and inflammatory pathways and therefore this set of genes will be collectively referred to as 'inflammatory genes'. SNPs in or near 15 inflammatory genes were selected and genotyped by researchers at AGRF (Table 1.3), and genotyping information was provided for incorporation into the present study.

Based on the role of cytokines in immune-to-brain communication and their ability to modulate ion channels in the brain and influence neuronal excitability (Section 1.7.2), variability in genes involved in these signalling pathways might also influence the EEG during general anaesthesia.

Table 1.3: Information on candidate inflammatory genes

Information on genes involved in various inflammatory and immune pathways selected for genotyping by AGRF. Ch. = chromosome; TLR = toll-like receptor signalling.

Official Symbol	Ch.	Official Name	Function
IL6R	1	Interleukin 6 Receptor	Cytokine receptor
CRP	1	C-reactive protein, pentraxin-related	Involved in various host defence functions
IL10	1	Interleukin 10	Anti-inflammatory cytokine
IL1B	2	Interleukin 1 beta	Pro-inflammatory cytokine
MYD88	3	Myeloid Differentiation Primary Response Gene (88)	Signal transducer in IL-1 & TLR signalling pathways
IL2	4	Interleukin 2	Pro-inflammatory cytokine
TLR2	4	Toll Like Receptor 2	TLR signalling
TNF	6	Tumor Necrosis Factor	Pro-inflammatory cytokine
OPRM1	6	Opioid Receptor, Mu 1	Opioid receptor
IL6	7	Interleukin 6	Pro-inflammatory cytokine
LY96	8	Lymphocyte Antigen 96	TLR signalling
TLR4	9	Toll Like Receptor 4	TLR signalling
CASP1	11	Caspase 1	Protease. Activates inactive IL-1 precursor. Can promote apoptosis.
BDNF	11	Brain-Derived Neurotrophic Factor	Nerve growth factor
TGFB1	19	Transforming growth factor, beta 1	Anti-inflammatory cytokine

1.12 Research objectives

The main objective of this study was to identify genetic polymorphisms associated with brain oscillations during general anaesthesia. The identification of such variants may improve our understanding of genetic factors influencing the EEG during general anaesthesia and may help provide a genetic explanation for clinical observations, such as the absence of spindles in some patients. This may lead to improved understanding of how genetic variability can influence the BIS value, and lead to improved use of the BIS index in anaesthesia monitoring.

1.12.1 Aim

The primary aim of this research was to identify genetic variants in the form of SNPs associated with human brain oscillations as recorded by the EEG during general anaesthesia in specifically selected candidate genes and various inflammatory and immune-related genes.

1.12.2 Hypotheses

Hypothesis One

Polymorphisms in, or near, the candidate genes; *SGIP1, CACNA1G, GABRA2 HCN* and *HCN2*, will influence brain oscillations as recorded by the EEG during general anaesthesia. A null hypothesis proposes that brain oscillations during general anaesthesia are not affected by variation in, or near, these genes.

Hypothesis Two

Polymorphisms in, or near, inflammatory pathway and related genes may affect human brain oscillations as recorded by the EEG during general anaesthesia. A null hypothesis proposes that variability in or near inflammatory and related genes will not influence brain oscillations during general anaesthesia.

Chapter 2: Materials and Methods

2.1 Samples

This research was part of larger study investigating post-operative pain levels and use of the BIS monitor to measure the depth of anaesthesia during surgery. Ethical approval was obtained from the Northern X Ethics Committee (reference number NTX/09/06/047) and from the University of Waikato School of Science and Engineering Human Research Ethics Committee (reference number 103).

Participants undergoing general, gynaecological or orthopaedic surgery were recruited from Waikato Hospital and North Shore Hospitals. Written consent was obtained from each participant and basic personal and medical details were recorded including age, sex, ethnicity, and operation type.

During surgery, patients were anaesthetised with the volatile anaesthetic agent desflurane. The depth of anaesthesia was estimated with BIS monitoring, and anaesthesia was titrated to achieve a BIS value within a given range. The raw EEG was also recorded intra-operatively and processed by the anaesthetist following surgery. For each patient, the anaesthetist selected a 60 sec EEG epoch recorded during the middle of the surgery that was representative of the EEG throughout. Median BIS value, median delta amplitude and frequency, median spindle amplitude and frequency, and median end tidal desflurane concentration (ETDC), were determined for the selected epoch. Quantitative processed EEG and ETDC data was then provided by the anaesthetist in spreadsheet format.

1 ml of peripheral whole blood was obtained at surgical closure by a medical doctor and was placed in a collection tube containing 4 ml of a 5 M guanidinium isothiocyanate (GITC) solution (Appendix 6.1) [171]. This was transported from

the hospital to the Molecular Genetics Laboratory at the University of Waikato (C.2.03) and stored at room temperature until DNA extraction.

2.1.1 Isolation of genomic DNA from blood

Total genomic DNA was extracted from each blood sample using the following protocol:

1 ml of the blood/GITC solution was placed in a labelled 1.7 ml eppendorf tube and 100 µl of 3 M sodium acetate and 0.7 ml of phenol:chloroform was added. The tube was shaken vigorously and placed on a rotator wheel for 15 min, followed by centrifugation at 13,000 rpm for 15 min at 4ºC. The aqueous layer containing the DNA was transferred to new labelled tube using a transfer pipette. An additional extraction was then performed using the same procedure as above, with an equal volume of chloroform in place of phenol:chloroform.

Following extraction, an equal volume of isopropanol was added and the tube was inverted a few times then left on ice for 15 min to allow the DNA to precipitate. After precipitation, the tube was centrifuged at 13,000 rpm for 15 min at 4ºC and the supernatant discarded. The precipitate was then washed with 1 ml 70% ethanol and centrifuged at 13,000 rpm for 5 min at 4ºC. The supernatant was removed and discarded using a transfer pipette, and any residual ethanol was briefly spun down in a centrifuge and removed using an autopipette. Any remaining ethanol was evaporated by leaving the tube to stand at room temperature for a short period. Finally, 50 µl of TE buffer (Appendix 6.1) was added to re-suspend the pellet and samples were stored at 4˚C until required.

2.1.2 Cetyltrimethylammonium bromide DNA cleanup

For DNA samples that failed to amplify, a cleanup of extracted DNA using cetyltrimethylammonium bromide (CTAB) was trialled to improve the quality of the DNA sample for PCR.

In this protocol, 50 µl of the extracted DNA solution was placed in a clean 1.7 ml eppendorf tube and diluted with TE buffer to a final volume of 570 µl. 30 µl of 30% SDS was then added and the tube was incubated for 1 hr at 37°C. After

incubation, 100 µl of 5 mM NaCl was added, followed by 80 µl CTAB/NaCl (Appendix 6.1). Tubes were incubated at 65°C for 10 min, and the DNA was then extracted using an equal volume of chloroform. The tube was shaken vigorously then placed on a rotator wheel for 15 min, followed by centrifugation at 13,000 rpm for 15 min at 4ºC. The aqueous layer containing the DNA was transferred to new labelled tube and an equal volume of isopropanol was added to precipitate the DNA. Following DNA precipitation, the tube was centrifuged at 13,000 rpm for 15 min at 4ºC and the supernatant discarded. The pellet was washed with 1 ml 70% ethanol and centrifuged at 13,000 rpm for 5 min at 4ºC. The supernatant was removed and discarded, and any residual ethanol was briefly spin down in a centrifuge and removed. The tube was left to stand at room temperature for a short period to evaporate any remaining ethanol, and the pellet was then re-suspended in 25 µl of TE buffer.

2.1.3 Column DNA extraction

DNA recovery kits (Zymoclean Gel DNA Recovery Kit™) were used to further purify DNA samples that failed to amplify. This kit is designed to extract DNA from agarose gel slices and it is also capable of extracting DNA from TE buffer. Three volumes of the supplied ADB Buffer™ were added to each volume of DNA solution in a 1.7 ml eppendorf tube and this was incubated at 37°C for 10 min. The solution was then transferred to a Zymo-Spin I™ column placed in a collection tube, and centrifuged for 1 min at 13,000 rpm. The flow through was discarded and 200 µl of the supplied wash buffer was added to the column. This was then centrifuged for 30 sec at 13,000 rpm, the flow through discarded, and the wash step repeated. The column was then placed in a new 1.7 ml tube and depending on the amount and starting concentration of DNA solution, 20 - 40 µl of TE buffer was added directly to the column. The column was then centrifuged at 13,000 rpm for 1 min to elute the DNA.

2.1.4 DNA quantification

DNA was quantified in ng/µl and purity assessed by the 260/280 ratio using a Nanodrop ND-1000 spectrophotometer. A 260/280 ratio of 1.8 – 2.0 was considered ideal, indicating a sample free from protein, RNA, phenol or other contaminants. Working DNA samples were prepared by diluting a small amount of stock DNA solution with TE buffer to a concentration of approximately 100 ng/µl

2.2 Genotyping of candidate genes by PCR-RFLP

PCR-RFLP assays were custom designed to genotype 13 SNPs in five candidate genes; *SGIP1*, *GABRA2*, *CACNA1G*, *HCN1* and *HCN2* (Table 2.1). Briefly, for each genotyping assay customised designed primer pairs were first used to amplify a small genomic region containing the SNP of interest by PCR. PCR products were then digested with a restriction enzyme specific to the assay that would either cut, or not cut, the product depending on the allele present at the SNP loci of interest. Digested PCR products were separated by agarose gel electrophoresis and visualised under UV light, allowing genotype to be determined from the banding pattern present (Figure 2.1).

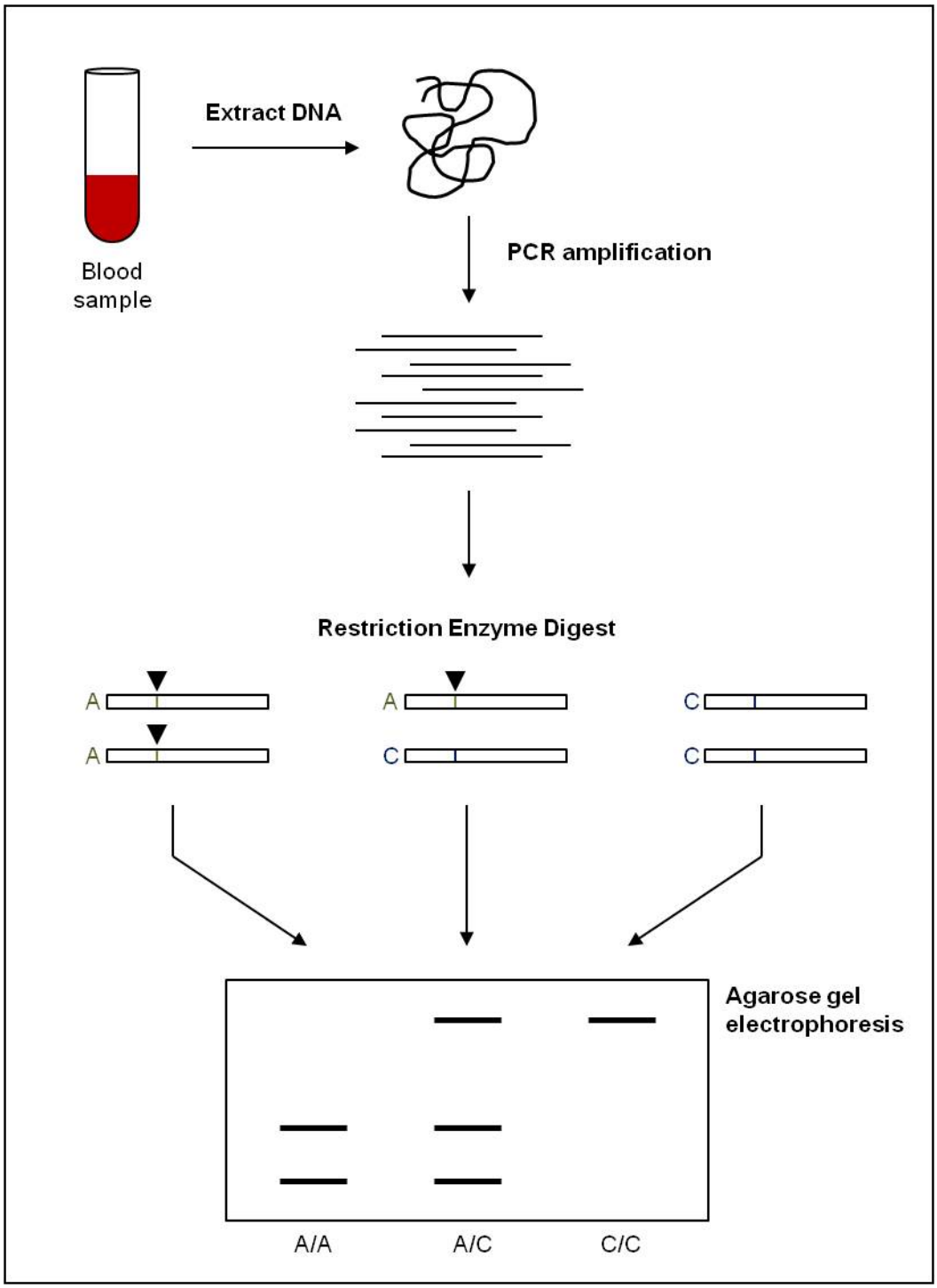

Figure 2.1: Diagram outlining PCR-RFLP genotyping method.
The restriction enzyme will either cut, or not cut, the PCR product depending on the SNP allele present. In the example shown, the A allele is cut (indicated by a solid black triangle) into a small and medium sized fragments, and the C allele is uncut. The rate at which DNA fragments migrate through the agarose gel depends on their size, allowing digestion product fragments to be separated and genotype to be determined from the fragmentation pattern.

2.2.1 SNP selection

Two to three SNPs in each candidate gene were selected for genotyping by PCR-RFLP (Table 2.1).

Three intronic SNPs in each of *SGIP1* and *GABRA2*, were chosen for genotyping based on results from previous association studies [92, 95]. SNPs in the remaining three genes – *CACNA1G*, *HCN1* and *HCN2* – were selected using database information to identify SNP loci with potential functional effects on gene regulation or splicing. Selected SNPs were also required to have a MAF of at least 15%. Databases utilised were the UCSC Genome Browser (http://genome.ucsc.edu. Assembly: Feb 2009, GRCh37/hg19) [172], the ECR Browser (http://ecrbrowser.dcode.org/) [173], NCBI dbSNP (http://www.ncbi.nlm.nih.gov/snp/), and the International HapMap project (http://hapmap.ncbi.nlm.nih.gov. Project data: Phase II+III, #27, Feb 09, Caucasian population) [174].

Table 2.1 provides summary information on all 13 SNPs genotyped by PCR-RFLP, including MAFs for the HapMap Caucasian population (sample of Caucasians of European descent (CEU)), and Figure 2.2 shows the position of SNPs genotyped in each candidate gene.

Table 2.1: Information on SNPs genotyped by PCR-RFLP.

[1] Position of SNP in Human Reference Sequence build 37.3.

[2] MAF for the HapMap Caucasian population, unless otherwise indicated. * MAF for pilot HapMap Caucasian population. [¥] MAF for pilot HapMap Yoruban population.

"from 3'/5'" indicates approximate distance of SNP from gene 3'/5' end.

Ch. = Chromosome. SNPs are listed in order of chromosomal position. Data retrieved April 2012 from NCBI dbSNP.

Gene	SNP	Location	Position[1]	Alleles	MAF[2]
SGIP1	rs10889635	Intronic	65184790 (Ch.1)	A/G	0.442 (G)
	rs6681460	Intronic	65232536 (Ch.1)	A/G	0.451 (A)
	rs2146904	Intronic	65269889 (Ch.1)	A/G	0.390 (A)
GABRA2	rs572227	~250 bp from 3'	45569517 (Ch.4)	G/A	0.456 (A)
	rs279845	Intronic	45647787 (Ch.4)	A/T	0.473 (A)
	rs279841	Intronic	45658827 (Ch.4)	A/G	0.446 (A)
HCN1	rs13361609	~1.5 kb from 5'	45650903 (Ch.5)	C/T	0.341 (C)
	rs13187565	~10 kb from 5'	45660979 (Ch.5)	G/T	0.456 (T)
CACNA1G	rs7501581	~1.5 kb from 5'	44004613 (Ch.17)	C/G	0.400 (G)*
	rs8066527	Intronic (near splice site)	44060878 (Ch.17)	C/T	0.300 (T)*
	rs8066269	Exonic (missense)	44069812 (Ch.17)	G/T	0.153 (T)[¥]
HCN2	rs7254543	~4 kb from 5'	585805 (Ch. 19)	A/C	0.221 (A)
	rs873634	~1.5 kb from 5'	588305 (Ch. 19)	G/T	0.195 (G)

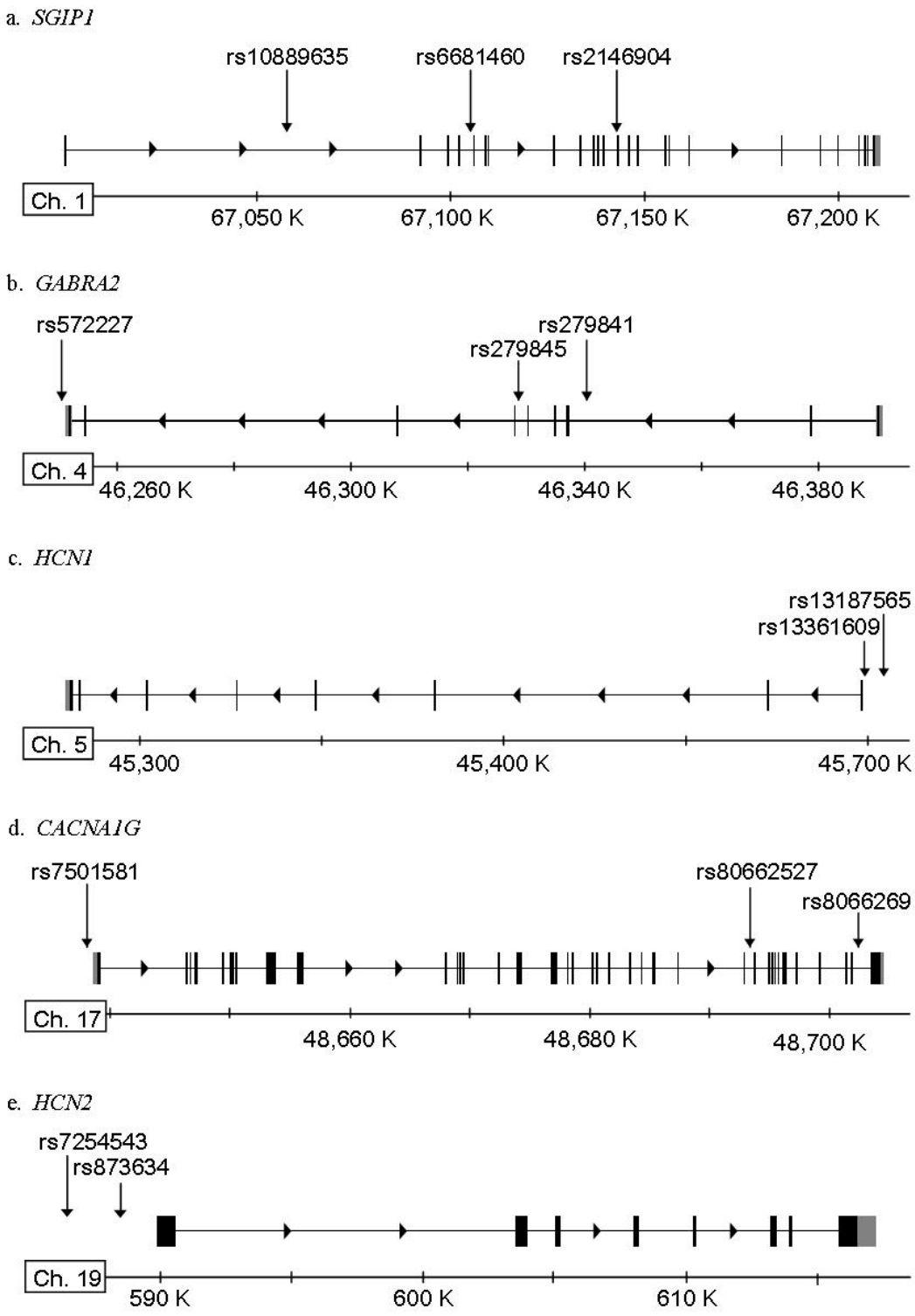

Figure 2.2: Structure of candidate genes showing position of SNPs genotyped by PCR-RFLP.

a. *SGIP*; b. *GABRA2*; c. *HCN1*; d. *CACNA1G*; and e. *HCN2*. Ch. = chromosome.

(Created using data from the UCSC Genome Browser and NCBI Gene (Reference sequence GRCh37.p5 Primary Assembly) (http://www.ncbi.nlm.nih.gov/gene)).

2.2.2 PCR-RFLP assay design

PCR-RFLP assays were designed for each SNP using the NCBI dbSNP database and the free online tools WatCut (watcut.uwaterloo.ca/watcut/watcut/template.php), Primer3 (version 0.4.0) (http://frodo.wi.mit.edu/primer3/) Primer-BLAST (http://www.ncbi.nlm.nih.gov/tools/primer-blast/) and NEBcutter V2.0 (http://tools.neb.com/NEBcutter2/).

WatCut was first used to identify restriction enzymes that would cleave only one variant sequence, thereby enabling the two SNP alleles to be distinguished. The 300 bp sequence flanking each side of the SNP was retrieved from NCBI dbSNP and this sequence was used to design specific primer pairs using Primer3 (Table 2.2).

Primer pairs were designed to flank the SNP of interest, with the 3' end of each primer ideally being at least 30 bp from the restriction enzyme cut site in order to make restriction digest fragments easy to distinguish. Where required, artificial restriction enzyme cut sites were created by incorporating a mismatch near, but not directly next to, the 3' end of either the forward or reverse primer. This results in the incorporation of a new base near the SNP and the mismatch site artificially generates a sequence in the PCR product that is recognised by a specific restriction enzyme for one allele but not the other. Expected PCR products for each allele were then input into NEBcutter V2.0 and a custom digest was performed using the restriction enzyme specific to the assay to determine expected fragment sizes and banding pattern.

To reduce the probability of non specific priming, Primer-BLAST was used to check the specificity of each primer pair against the human genome. Primer binding regions were also checked for known polymorphisms using the UCSC Genome Browser.

2.3 PCR protocols

2.3.1 Standard PCR

For each PCR-RFLP assay, PCR was first used to amply a short segment of DNA containing the SNP of interest using specifically designed primers (Table 2.2).

20 μl PCR reactions were prepared for each sample containing 0.5 units (U) HOT FIREPol® DNA polymerase (Solis BioDyne), the supplied buffer at x1 concentration, 2.0 mM $MgCl_2$, 250 μM dNTPs and 0.2 μM of each primer. Approximately 100 ng of extracted DNA was added to each reaction tube, excluding the negative control.

PCR thermal cycling parameters were as follows:

1. Initial denaturation and DNA polymerase activation: 95°C for 15 min
2. Denaturation: 95°C for 20 sec
3. Annealing: T_a°C for 30 sec
4. Elongation: 72°C for 30 sec
5. Repeat steps 2-4 for 34 more cycles
6. Final elongation: 72°C for 1 min

The annealing temperature (T_a) used was specific for each primer pair (Table 2.2). To determine the annealing temperature for each reaction, the annealing temperature was initially set approximately 5°C below the average melting temperature (T_m) for the primer pair. This was then either slightly modified if needed to either reduce non-specific priming or improve yield. Final annealing temperatures used in PCR-RFLP assays are shown in Table 2.2.

This protocol was used for all SNPS with the exception of SNP rs8066527 and rs7254543. For these two SNPs the optimum annealing temperature was first determined by gradient PCR (Section 2.3.2) and a touchdown PCR protocol was then trialled and used for genotyping (Section 2.3.3).

Table 2.2: PCR reaction information for SNPs genotyped by PCR-RFLP.
Mismatches incorporated to create artificial restriction enzyme sites are shown in lower case. A touchdown protocol was used for SNPs rs8066527 and rs7254543, $(T_{td})^1$ = final touchdown temperature (Section 2.3.3).

SNP	Primer sequence (5'-3')	Product size (bp)	T_a
rs10889635	F: AGGAGAAATACTTGGGCCAACC R: TGACCTACATTCTCAGTGACGC	364	60˚C
rs6681460	F: GAGGAAGATCTAGGATACAGCCACT R: GAAGGTTCTGTGCCTTGATTACAcC	193	60˚C
rs2146904	F: CTCTAGATGCACCCTGTATATTTACTGTTgA R: AAGCAGTGACCGGACATGTAATCTT	201	60˚C
rs572227	F: TTACGGGTGCTGGAGACTG R: TGCCAATTAACTGCCCTTCT	234	60˚C
rs279845	F: TGCCATGTTTGCTACAGGTT R: CTCTCCTTGCAAAAACACAGAG	213	60˚C
rs279841	F: CCCTCTTGTCTCTACTCATAcA R: AGCTAGAAAACTGGCTCAACCT	174	50˚C
rs13361609	F: ATCTCCCTTGCGCTCTTGAA R: CAGGGCAAGATTCTCTTTGA	192	48˚C
rs13187565	F: CTACCAACAAAGAGGCCATT R: GAACTGTGGAGTTTTGTAAACTGgTA	222	48˚C
rs7501581	F: GTGGTGCAGCCTTAGGAGAG R: AAGCACTCTCCCAACACTTG	196	55˚C
rs8066527	F: AGCAGCCCCAGGTAGG**c**G R: AAGATGATACCCACCCTCAAGG	169	60˚C $(T_{td})^1$
rs8066269	F: CCTCGCTTTGCTCGTCTACT R: AACACAGGCTACTACCAGCA	239	55˚C
rs7254543	F: GGCCCTCTCCTCCCTgTA R: TCTCATGCTAGCAGCCTCTCT	194	55˚C $(T_{td})^1$
rs873634	F: GCTGAAGGGGGTCTTTTTATG R: CACAGCCCTCCTTGTGACTT	199	55˚C

2.3.2 Gradient PCR

To avoid the non-specific priming observed in test reactions for SNPs rs8066527 and rs7254543, gradient PCR was used to determine the optimum annealing temperature.

110 µl PCR reactions were prepared containing 0.5 U HOT FIREPol® DNA polymerase (Solis BioDyne), the supplied buffer at x1 concentration, 2.0 mM $MgCl_2$, 250 µM dNTPs and 0.2 µM of each primer. 10 µl of this reaction mixture was transferred into a clean PCR tube as the negative control. Approximately 500 ng of extracted DNA was added to the remaining 100 µl and this was then aliquoted into 10 individual PCR tubes. PCR was performed using an annealing temperature gradient for step 3, with the negative control placed at an intermediate annealing temperature.

Thermal cycling parameters for gradient PCR were as follows:

1. Initial denaturation and DNA polymerase activation: 95°C for 15 min
2. Denaturation: 95°C for 20 sec
3. Annealing temperature gradient: 51°C to 62°C for rs8066527
   45°C to 55°C for rs7254543
4. Elongation: 72°C for 30 sec
5. Repeat steps 2-4 for 34 more cycles
6. Final elongation: 72°C for 1 min

PCR products were separated by gel electrophoresis on 1 – 1.5% agarose/sodium borate (SB) gels and visualised under UV light (Section 2.4). The optimum annealing temperature was determined by visual inspection of product yield and non-specific amplification at each annealing temperature.

2.3.3 Touchdown PCR

For SNPs rs806627 and rs7254543, a touchdown PCR protocol was trialled and applied for PCR-RFLP assays to reduce non-specific priming.

In this modified PCR protocol, the annealing temperature of the early cycles was set higher than the expected annealing temperature and was subsequently reduced by 1°C per cycle until a desired 'touchdown' temperature (T_{td}) was reached. The touchdown temperature was then used as the annealing temperature for the remaining cycles. Final touchdown temperatures used for PCR-RFLP are shown in Table 2.3.

PCR reactions were set up as for standard PCR (Section 2.3) and thermal cycling parameters were set as follows:

Phase one:

1. Initial denaturation and DNA polymerase activation: 95°C for 15 min
2. Denaturation: 95°C for 20 sec
3. Annealing: T_{td} + 10°C for 30 sec, reduced by 1°C per cycle
4. Elongation: 72°C for 30 sec
5. Repeat steps 2 - 4 for 9 more cycles until T_{td} reached

Phase two:

1. Denaturation: 95°C for 20 sec
2. Annealing: T_{td} for 30 sec
3. Elongation: 72°C for 30 sec
4. Repeat steps 1 - 3 for 34 more cycles
5. Final elongation: 72°C for 1 min

Table 2.3: Touchdown PCR reaction information.
Mismatches incorporated to create artificial restriction enzyme sites are shown in lower case. T_{td} = touchdown temperature.

SNP	Primer sequence (5'-3')	Product size (bp)	T_{td}
rs8066527	F: AGCAGCCCCAGGTAGGcG R: AAGATGATACCCACCCTCAAGG	169	60˚C
rs7254543	F: GGCCCTCTCCTCCCTgTA R: TCTCATGCTAGCAGCCTCTCT	194	55˚C

2.3.4 Spiked PCR

To determine if the failure of some samples to amplify by PCR was due to the presence of inhibitors, spiked PCR reactions were used.

20 μl PCR reactions were prepared containing 0.5 U HOT FIREPol® DNA polymerase (Solis BioDyne), the supplied buffer at x1 concentration, 2.0 mM $MgCl_2$, 250 μM dNTPs and 0.2 μM of the forward and reverse primers for SNP rs13187456. Approximately 100 ng of DNA from a sample known to amplify was added to each reaction tube, excluding the negative control. An additional 100 ng of DNA from a sample that failed to amplify was then added to each tube excluding the negative and positive controls.

PCR thermal cycling parameters were as follows:

1. Initial denaturation and DNA polymerase activation: 95°C for 15 min
2. Denaturation: 95°C for 20 sec
3. Annealing: 48 °C for 30 sec
4. Elongation: 72°C for 30 sec
5. Repeat steps 2-4 for 34 more cycles, for a total of 35 cycles.
6. Final elongation: 72°C for 1 min

Gel electrophoresis (Section 2.4) using 1% agarose/SB gels, was used to determine if amplification was successful. Successful amplification of the positive control and failed amplification of spiked reactions would indicate the presence of an inhibitor in the DNA solution used to the spike the PCR.

2.4 Agarose gel electrophoresis

PCR and restriction enzyme digest products were separated on 1 – 2.5% (w/v) agarose/SB gels containing ethidium bromide, in x1 SB running buffer (Appendix 6.1) run at 100 V, using an Owl gel electrophoresis separation system. 5 - 10 μl of each sample was first mixed with a gel loading buffer (Appendix 6.1) and then loaded into a well. Gels were run for as long as required to achieve a desired level of resolution. Products were then visualised under UV light on a trans-illuminator (Life Technologies, Gibco BRL UV Trans-illuminator, TFX-35M) and a 100 bp ladder (Solis BioDyne) was used to estimate product/fragment size.

2.5 Restriction enzyme digests

PCR products were digested with 1 - 2 U of restriction enzyme specific to the assay and the total reaction volume was bought up to 25 μl by addition of the supplied restriction enzyme buffer and Milli-Q water. Where specified by the enzyme manufacturer, digestion reactions were supplemented with bovine serum albumin (BSA) at 100 μg/ml. Digestion reactions were performed in a shaking incubator (Eppendorf, thermomixer comfort) at 900 rpm at the optimum temperature, with the exception of rs13361609, which was incubated in an MJ Research PCT-200 Peltier Thermal Cycler. Table 2.4 provides information on restriction enzyme digest conditions and expected fragment sizes of digestion products.

The genotype of each sample was able to be inferred from the sizes and pattern of digested PCR product fragments using agarose gel electrophoresis (Section 2.4). The percentage of agarose used in gels varied depending on the size of the diagnostic fragments. Digestions cleaving small fragments (<40 bp) were run on 2–2.5% agarose/SB gels to obtain finer resolution, whereas digestions removing larger fragments were able to be separated on 1–1.5% agarose/SB gels (Table 2.4).

Table 2.4: Restriction enzyme digest information.
Restriction enzyme and number of units used in each assay are given along with incubation temperature, expected fragment sizes and the percentage of agarose used in gels.
* Supplemented with BSA at a concentration of 100 μg/ml.

SNP	Restriction Enzyme	Incubation	Fragment sizes (bp)	Agarose (%)
rs10889635	XbaI (2 U)*	37˚C for 2 hrs	A 201/163 G 364	1.0
rs6681460	MnlI (2 U)	37˚C for 2 hrs	A 160/33 G 193	2.0
rs2146904	BclI (2 U)	50˚C for 2 hrs	A 172/29 G 201	2.0
rs572227	DraIII (2 U)*	37˚C for 2 hrs	G 120/114 A 234	1.0
rs279845	HinfI (2 U)	37˚C for 2 hrs	A 173/40 T 213	1.5
rs279841	NspI (2 U)*	37˚C for 2 hrs	G 150/24 A 174	2.0
rs13361609	TaiI (1 U)	65˚C for 6 hrs	C 143/49 T 192	1.5
rs13187565	RsaI (2 U)	37˚C for 1 hr	G 197/25 T 222	2.0
rs7501581	Tsp451 (1 U)*	65˚C for 4 hrs	G 142/54 C 196	1.5
rs8066527	CfoI (2 U)*	37˚C for 1 hr	C 151/18 T 169	2.5
rs8066269	AluI (2 U)	37˚C for 1 hr	T 149/39/38/13 G 187/39/13	1.5
rs7254543	Hpy166II (2 U)	37°C for 1hr	A 176/18 C 194	2.5
rs873634	HaeIII (2 U)	37˚C for 2 hrs	G 82/74/43 T 156/43	2.0

2.6 Sequencing

To confirm that the correct genomic fragment had been amplified, one sample for each PCR-RFLP assay was sequenced in both the forward and reverse directions. Samples were first amplified by PCR and the PCR product was then cleaned up and used as the sequencing template.

2.6.1 Template preparation

40 µl PCR reactions were prepared containing 1U HOT FIREPol® DNA polymerase (Solis BioDyne), the supplied buffer at x1 concentration, 2 mM $MgCl_2$, 250 µM dNTPs and 0.2 µM of each primer. 10 µl of the reaction was aliquoted into a separate tube as a negative control and approximately 150 ng of extracted DNA was added to the remaining 30 µl as a template. PCR cycling parameters and annealing temperatures were the same as those used for PCR-RFLP assays (Section 2.3; Table 2.2).

Following thermal cycling, 5 µl of each PCR reaction was separated by gel electrophoresis on 1% agarose/SB gels (Section 2.4) and the DNA ladder was used to estimate both product size and DNA concentration.

The remaining 25 µl of PCR product was then cleaned up for sequencing using Exonuclease I and Alkaline Phosphatase. These enzymes remove any remaining primers and free dNTPs, respectively. 10 U Exonuclease I (Fermentas) and 1 U rAPid Alkaline Phosphatase (Roche) was added to each PCR reaction, tubes were vortexed and then incubated for 15 min at 37°C, followed by a 15 min incubation at 85°C.

Solutions were then sent to the University of Waikato Sequencing Facility (Hamilton, New Zealand) for sequencing using an Applied Biosystems 3130xl Genetic Analyzer. Each PCR product was sequenced in both the forward and reverse direction using the appropriate forward and reverse PCR primers as sequencing primers.

2.6.2 Sequence analysis

Sequencing reaction results were provided in FASTA format along with a printout of the electropherogram. The electropherogram printout was used to examine the quality of the read and determine reliable start and end points for the sequence. The free online software FASTA Sequence Comparison (http://fasta.bioch.virginia.edu/fasta_www2/) was used to align forward and reverse sequences for each primer pair and a final sequence was determined for each PCR product. Any mismatches in the alignment were checked using the electropherogram printout. Final sequences were entered into NCBI nucleotide BLAST (BLASTN 2.2.26+) (http://blast.ncbi.nlm.nih.gov/) [175], to search the human genome for similar sequences, allowing confirmation that the correct region had been amplified. The position and genotype of the SNP of interest in each sequence was also determined from the electropherogram and checked against genotyping results.

2.7 Genotyping of inflammatory genes by MassARRAY

21 SNPs in or near 15 different genes involved in various inflammatory and related pathways were selected for genotyping by researchers at AGRF (Table 1.3, Table 2.5). 100 samples were sent to AGRF and were genotyped for these SNPS with custom-designed multiplex analysis using Sequenom MassARRAY technology (iPlex Gold).

Completed genotyping data was provided in an excel spreadsheet along with calculated genotype and allele frequencies. This data was then paired with EEG and other patient data.

Table 2.5: Information on SNPs genotyped by MassARRAY at AGRF.

[1] Position of SNP in Human Reference Sequence build 37.3.

[2] MAF for the HapMap Caucasian population.

"from 5'" indicates approximate distance of SNP from gene 5' end.

Synom. = Synonymous coding SNP. Ch. = Chromosome. Data retrieved April 2012 from NCBI dbSNP.

Gene	SNP	Location	Position[1]	Alleles	MAF[2]
IL6R	rs8192284	Exonic (missense)	154426970 (Ch.1)	A/C	0.354 (C)
CRP	rs2794521	~600 bp from 5'	159685096 (Ch.1)	C/T	0.317 (C)
IL10	rs1800871	~800 bp from 5'	206946634 (Ch.1)	C/T	0.173 (T)
	rs1800896	~1 kb from 5'	206946897 (Ch.1)	A/G	0.469 (A)
IL1B	rs1143634	Exonic (synom.)	113590390 (Ch.2)	C/T	0.208 (T)
	rs1143627	~30 bp from 5'	113594387 (Ch.2)	C/T	0.363 (C)
	rs16944	~500 bp from 5'	113594867 (Ch.2)	A/G	0.358 (A)
MYD88	rs6853	3' UTR	38184370 (Ch.3)	A/G	0.115 (G)
IL2	rs2069762	~200 bp from 5'	123377980 (Ch.4)	G/T	0.232 (G)
TLR2	rs3804100	Exonic (synom.)	154625409 (Ch.4)	C/T	0.051 (C)
TNF	rs1800629	~200 bp from 5'	31543031 (Ch.6)	A/G	0.173 (A)
OPRM1	rs1799971	Exonic (missense)	154360797 (Ch.6)	A/G	0.155 (G)
IL6	rs10499563	~6 kb from 5'	22760488 (Ch.7)	C/T	0.195 (C)
LY96	rs11466004	Exonic (missense)	74941275 (Ch.8)	C/T	0.028 (T)
TLR4	rs4986790	Exonic (missense)	120475302 (Ch.9)	A/G	0.035 (G)
	rs4986791	Exonic (missense)	120475602 (Ch.9)	C/T	0.045 (T)
BDNF	rs6265	Exonic (missense)	27679916 (Ch.11)	A/G	0.195 (A)
CASP1	rs554344	~1 kb from 5'	104895197 (Ch.11)	C/G	0.192 (C)
	rs580253	Exonic (synom.)	104900488 (Ch.11)	C/T	0.192 (T)
TGFB1	rs11466314	~450 bp from 5'	41860236 (Ch.19)	A/G	0.021 (A)
	rs1800469	~500 bp from 5'	41860296 (Ch.19)	C/T	0.288 (T)

2.8 Analysis of genotyping data

Raw genotyping results from PCR-RFLP assays and MassARRAY were input into Microsoft Office Excel spreadsheet along with corresponding EEG trait values for each sample. Within the excel document, separate sheets were used to format data to be exported to Haploview, SNPAnalyzer 1.2A and the statistical software NCSS.

2.8.1 Haploview

The free software Haploview [176] was used to check SNPs for adherence to the Hardy Weinberg equilibrium (HWE), to examine patterns of LD between SNPs, and to estimate haplotypes and their frequencies. SNP genotyping data was converted to a tab-delimited text file for importation into Haploview as specified in the user's manual. Fields requiring pedigree and case-control information were filled with a zero.

Haploview was also used to construct LD plots and to infer haplotypes and their frequencies for selected genes using HapMap Caucasian data. Data was imported directly into the Haploview software using the download feature in Haploview, and by specifying the chromosome and start and end points in kb.

2.8.2 SNPAnalyzer 1.2A

The expectation-maximization (EM) algorithm in the free online software SNPAnalyzer 1.2A (http://snp.istech.info/istech/board/detail.jsp) was used to reconstruct three SNP haplotypes for *SGIP1*, *GABRA2* and *IL1B.* For importation into SNPAnalyzer 1.2A, genotyping data was converted to a tab-delimited text file as specified in the user's manual.

2.8.3 Association analysis: NCSS

The statistical software NCSS was used to perform statistical tests to examine associations between SNPs and quantitative EEG traits. All statistical tests performed were non-parametric tests as these methods do not require data to be normally distributed.

Summary statistics and histograms were produced for all EEG traits and ETDC and the Shapiro-Wilk W test was used to determine if variability was normally distributed. Linear regression analysis was performed to examine correlations between different EEG traits and the BIS value, and between the EEG and ETDC.

Kruskal-Wallis one-way analysis of variance (KW-ANOVA) was used to identify SNPs with potential associations with the EEG or ETDC, and box and whisker plots enabled data to be visualised categorised by genotype. KW-ANOVA was performed for each SNP, with each EEG trait, to identify SNPs with a significant difference in the median between genotypes.

SNPs that were putatively associated with the EEG or ETDC ($p < 0.05$) were further examined. Mann-Whitney U tests were used to identify SNP genotypes with significant differences in the median and to test SNPs for associations with the EEG and ETDC in recessive, dominant, and over-dominant models. The dominant, recessive and over-dominant models are tests for the minor allele; if “D” is the major allele and “d” is the minor allele the dominant model compares [dd + dD] vs. DD, the recessive model compares dd vs. [dD + DD], and the over-dominant model compares dD vs. [dd + DD]. To determine effect sizes, fold differences were calculated for each comparison by dividing the median value for one genotype by the median for the other.

Chapter 3: Results

3.1 Participants

137 participants undergoing general, gynaecological, or orthopaedic surgery were recruited and the raw EEG was recorded for 125 patients who were therefore retained for inclusion in the present study.

The age range of participants in this study was 17 – 67 years (mean = 42.3 years) and 82% were female (Table 3.1). The high proportion of female participants was largely due the high proportion of gynaecological patients (51%) recruited. Of the remaining patients (general and orthopaedic), there was also a higher proportion of females (62%) than males (38%).

Table 3.1: Basic summary information on study participants (n = 125).
NZ Euro. = New Zealand European; Poly/M = Polynesian and Maori; N/S = Not Specified; Gynae. = Gynaecological; Ortho. = Orthopaedic.

Gender		**Ethnicity**				**Surgery type**		
M	**F**	**NZ Euro.**	**Asian**	**Poly/M**	**N/S**	**General**	**Gynae.**	**Ortho.**
23	102	96	10	18	1	46	64	15

3.2 EEG Data and anaesthetic administration

EEG signal processing was performed by the anaesthetist on a selected 60 sec epoch recorded during the middle of surgery. The median was determined for the following EEG traits; spindle amplitude, spindle frequency, delta amplitude and delta frequency (n = 125) (N.B. logarithmic transformation applied to spindle and delta amplitude). Median BIS value (n = 100) and ETDC (n = 122) were also determined for the selected epoch. Processed data was supplied in spreadsheet format, and spindle amplitude relative to ETDC (relative spindle amplitude) was calculated using the supplied data (Equation 3.1) (n = 122).

$$\frac{\text{Spindle amplitude}}{\text{ETDC}} = \text{Relative spindle amplitude} \qquad \text{(Equation 3.1)}$$

Summary statistics were calculated for all EEG traits and ETDC using the statistical software NCSS. The distribution of each variable was visualised using histograms (Figure 3.1), and distributions were tested for normality using the Shapiro-Wilk W test. Spindle and ETDC showed a normal distribution ($p > 0.05$) whereas normality was rejected for BIS value ($p = 0.0014$), spindle frequency ($p = <0.0001$), delta frequency ($p = <0.0001$), delta amplitude ($p = 0.0047$) and relative spindle amplitude ($p = 0.0099$).

Table 3.2: Summary statistics for quantitative EEG data and ETDC.
Min. = minimum; Max. = maximum; Med. = median; Std.Dev. = standard deviation.

Variable	Min.	Max.	Range	Med.	Mean	Std. Dev.	n
ETDC (%)	2.12	9.46	7.34	5.46	5.58	1.31	122
BIS value	22	81	59	39	40	11.27	100
Delta amplitude (Log(μV))	3.36	10.22	6.86	5.83	5.89	0.99	125
Delta frequency (Hz)	0.50	2.25	1.75	0.63	0.71	0.26	125
Spindle amplitude (Log(μV))	0.19	3.23	3.04	1.86	1.83	0.63	125
Spindle frequency (Hz)	7.13	16.50	9.38	9.38	9.73	2.02	125
Relative spindle amplitude	0.034	0.844	0.811	0.339	0.357	0.173	122

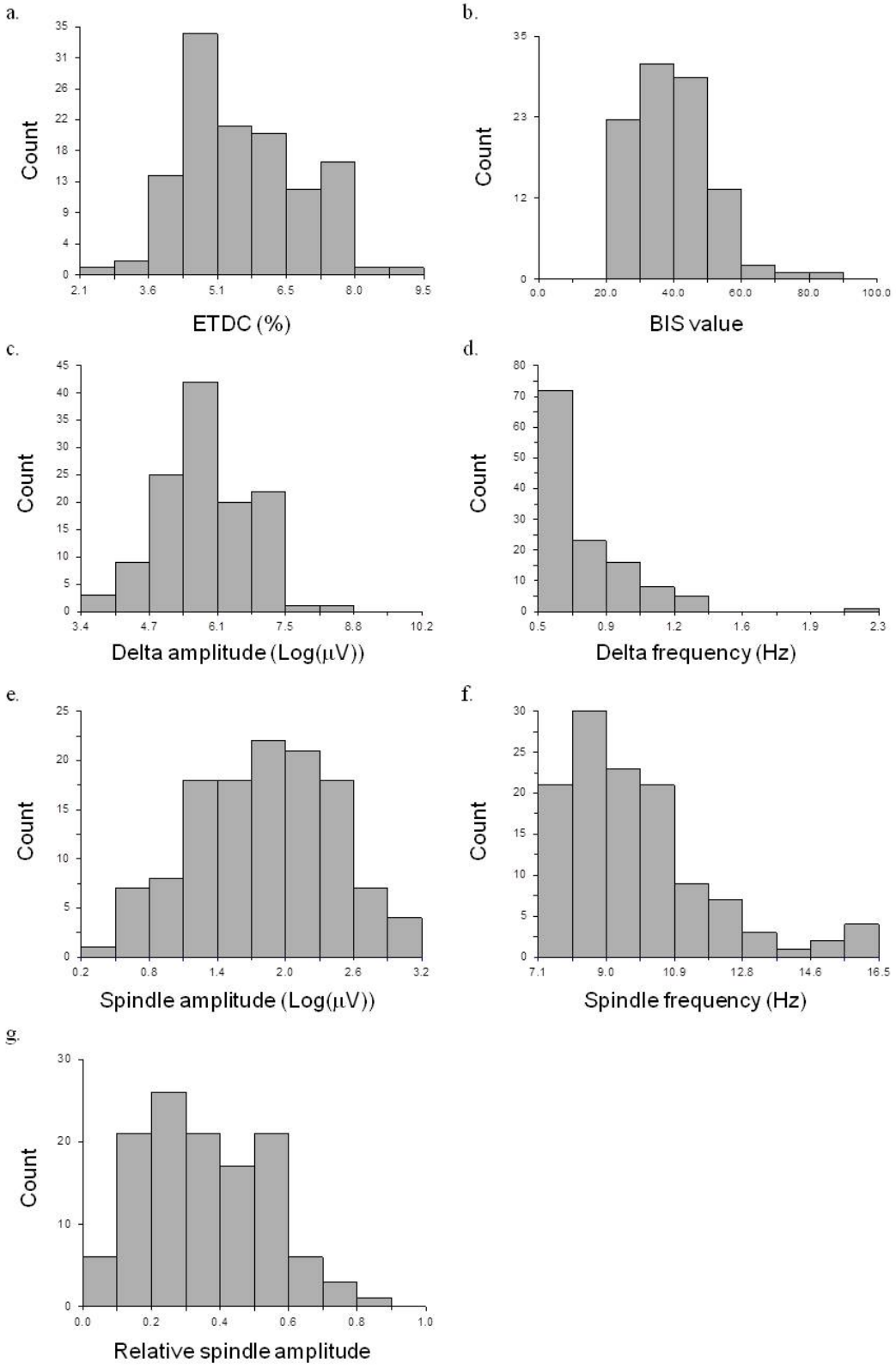

Figure 3.1: Histograms showing distributions of EEG data and ETDC.

a. ETDC; b. BIS value; c. Delta amplitude; d. Delta frequency; e. Spindle amplitude; f. Spindle frequency; g. Relative spindle amplitude.

3.2.1 EEG correlation analysis

Scatter plots and linear regression analyses were used to analyse relationships between ETDC, BIS value, and EEG traits (Figure 3.2). Were required, data was transformed using the square root or Log^{10} of the dependent variable in order to meet the necessary assumptions of the linear regression model. The full results from this analysis are presented in Appendix Table 6.2.

A weak correlation was observed between BIS value and ETDC (r = -0.227, p = 0.023) (Figure 3.2a). Modest correlations were observed between spindle amplitude and ETDC (r = -0.467, p = <0.0001), and delta amplitude and BIS value (r = -0.469, p = <0.0001) (Figure 3.2b,d). Weak correlations were also observed between delta amplitude and ETDC (r = 0.265, p = 0.0032) (Figure 3.2c).

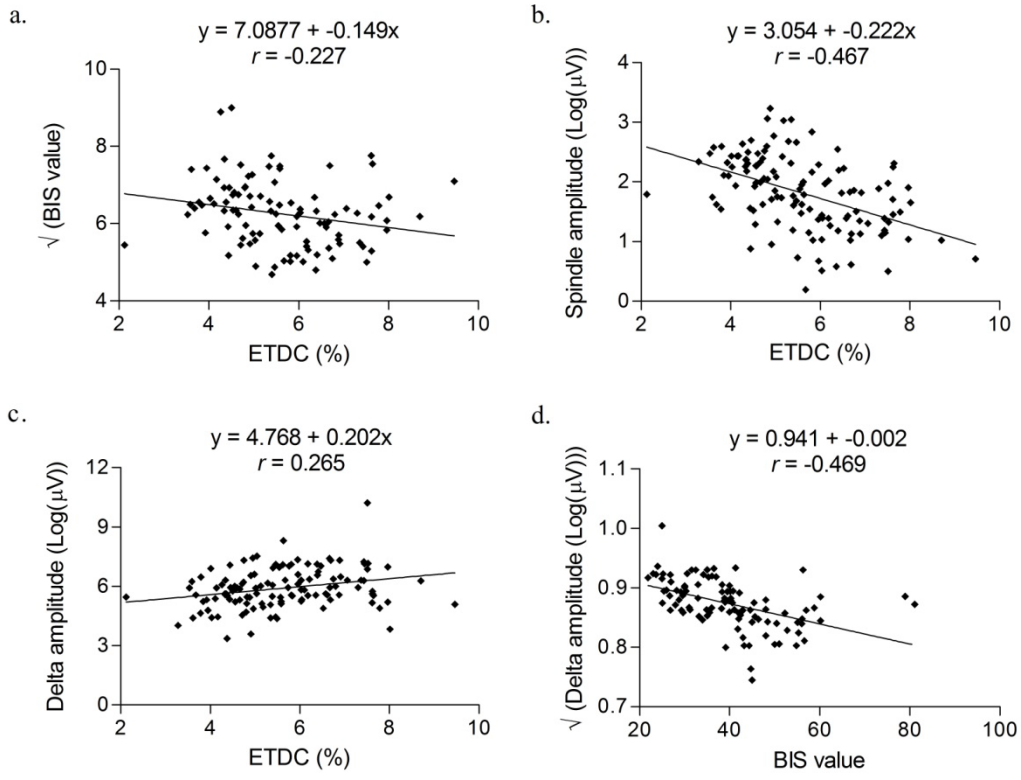

Figure 3.2: Scatter plots and regression lines showing relationships between EEG traits, BIS value and ETDC.

a. BIS value and ETDC; b. Spindle amplitude and ETDC; c. Delta amplitude and ETDC; d. Delta amplitude and BIS value.

3.3 Isolation of genomic DNA

Prior to the beginning of this study, DNA had already been extracted from approximately 110 samples using a phenol:chloroform extraction method (Section 2.1.1). As part of the current project, DNA was extracted from the remaining samples.

Using the phenol:chloroform extraction protocol, DNA that reliably amplified by PCR was able to be obtained for >90% of samples. For a small number of samples, PCR was either completely or frequently unsuccessful, requiring further purification steps to obtain higher quality DNA. A CTAB cleanup method was first trialled to improve the quality of samples that failed to amplify (Section 2.1.2). This method was unsuccessful (Section 3.3.1), and using spiked PCR (Section 2.3.4) it was determined that the failure of some samples to amplify was likely due to the presence of an inhibitor in the DNA solution (Section 3.3.2). A column DNA extraction using a commercial kit (Zymoclean Gel DNA Recovery Kit™) was then trialled to remove any inhibitors (Section 2.1.3). This kit successfully extracting DNA from samples that failed to amplify (Section 3.3.3), and was used to further purify samples if required. The final protocol used for the isolation and purification of DNA from blood samples is shown in the flow chart below (Figure 3.3).

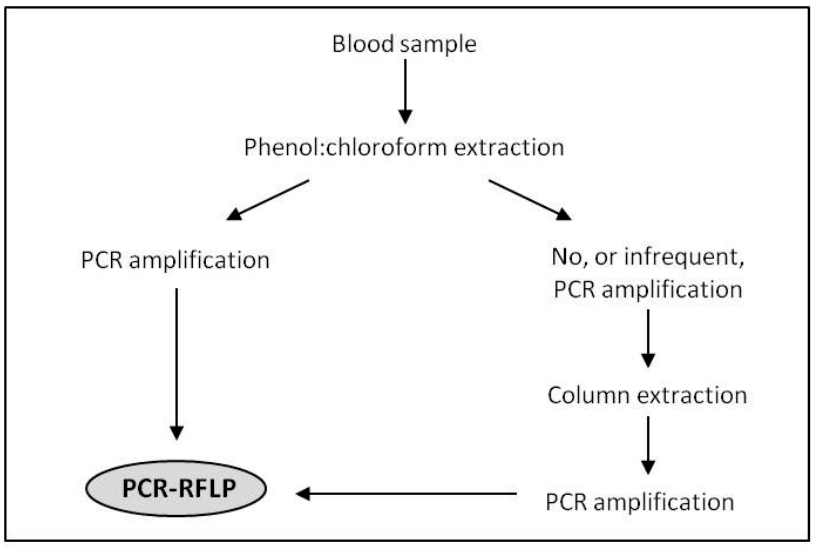

Figure 3.3: Flow chart outlining final protocol used for isolation and purification of genomic DNA for PCR-RFLP assays.

3.3.1 CTAB Cleanup

An additional DNA cleanup protocol using CTAB (Section 2.1.2) was trialled for three DNA samples that frequently failed to amplify (samples IDs; 23, 34, 75). Briefly, 50 µl of the originally isolated DNA was incubated with SDS, NaCl and CTAB. Following incubation, DNA was re-extracted with chloroform and then precipitated using isopropanol and re-suspended in 25 µl of TE.

This protocol was found to markedly increase the 260:230 ratio with minimal effect on the 260:280 ratio (Table 3.3). On average, approximately two-thirds of the DNA was recovered. While the CTAB method was found to improve the quality of DNA samples as determined by 260:230 ratio, these three samples still failed to amplify during PCR.

Table 3.3: Nanodrop results showing the effect of CTAB cleanup on DNA quality.
Nanodrop readings from DNA samples isolated from blood and from the same samples after clean up using CTAB.

Sample ID	Before CTAB cleanup			After CTAB cleanup		
	260:280	260:230	ng/µl	260:280	260:230	ng/µl
23	1.78	1.52	104	1.82	2.25	130
34	1.83	1.83	273	1.84	2.26	480
75	1.84	1.67	65	1.81	2.17	73

3.3.2 Spiked PCR

Spiked PCR reactions were used to determine if the failure to amplify during PCR was due to presence of inhibitors. Four PCR reactions were prepared using a sample known to amplify and three of these were spiked with DNA from sample numbers 23, 34 and 75 and the remaining reaction was left unspiked as a positive control. PCR reactions failed when spiked with DNA from samples 23, 34 and 75, whereas the positive unspiked control successfully amplified, demonstrating that the failure of these samples to amplify was likely due to the presence of a contaminant in the DNA solution (Figure 3.4).

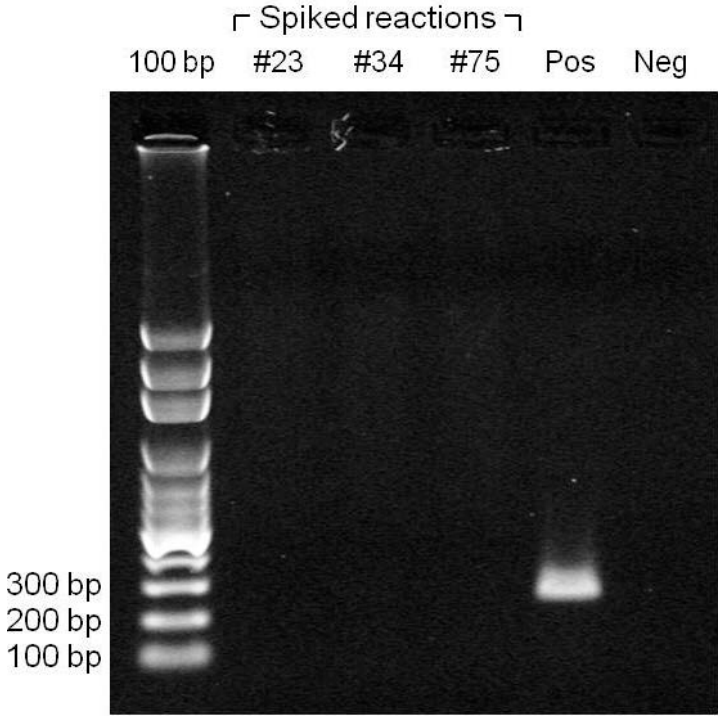

Figure 3.4: Gel image of spiked PCR results.
Spiked PCR reaction products separated on a 1% agarose/SB gel. Pos = positive control, Neg = negative control. PCR reactions spiked with DNA from samples 23, 34 and 75 failed to amplify, whereas the positive unspiked control successfully amplified.

3.3.3 Column DNA extraction

The three samples used for CTAB cleanup were used to trial an additional purification using a Zymoclean Gel DNA Recovery Kit™ (Section 2.1.3). This kit uses a column to absorb DNA from a buffer solution, and once DNA was absorbed the column was washed twice and the DNA eluted with TE buffer.

Following column purification with this kit, all three samples successfully amplified during PCR. 260:280 ratios were slightly improved, however, 260:230 ratios decreased (Table 3.4). A substantial reduction in the total amount of DNA in solution was also observed, with approximately only half the DNA being recovered.

Following this result, any DNA samples frequently failing to amplify by PCR were re-purified from the original solutions using the Zymoclean Gel DNA Recovery Kit™ with the omission of the CTAB protocol. Using this approach, DNA was able to be obtained from 123 samples that reliably amplified and gave results for at least 10 of the 13 genotyped SNPs.

Table 3.4: Nanodrop results showing the effect of column extraction (Zymoclean Gel DNA Recovery Kit™) on DNA quality.
260:280 and 260:230 ratios and DNA concentration are shown for three samples cleaned up using CTAB before and after column extraction. Approximately 50% of total DNA was lost during extraction (DNA concentration shown does not reflect the extent of this loss as differing amounts of starting DNA solution and TE buffer for elution were used depending on the amount and concentration of starting DNA solution).

Sample ID	Before column purification			After column purification		
	260:280	260:230	ng/µl	260:280	260:230	ng/µl
23	1.82	2.25	130	1.85	1.48	26.1
34	1.84	2.26	480	1.90	1.63	28.5
75	1.81	2.17	73	1.91	1.77	34

3.4 PCR optimisation

For all PCR reactions, the annealing temperature was initially set approximately 5°C below the average primer T_m and if required this was adjusted slightly to improve amplification or reduce non-specific priming. This approach was successful for establishing the annealing temperature to be used for the majority of PCR-RFLP assays. Due to poor priming specificity, the optimum annealing temperature for primer pairs designed to amplify rs8066527 (*CACNA1G*) and rs7254543 (*HCN2*) was first determined by gradient PCR and then a touchdown protocol was trialled and implemented to improve priming specificity.

3.4.1 Gradient PCR

The optimum annealing temperature for rs8066527 and rs7254543 was determined by gradient PCR (Section 2.3.2). The annealing temperature gradient ranged from 51.0°C to 62.1°C for rs8066527, and from 45°C to 55.2°C for rs7254543.

For rs8066527, an annealing temperature of approximately 55°C was determined to give maximal yield of the correct PCR product but substantial levels of non-specific priming were still observed (Figure 3.5). Even at annealing temperatures as high as 62°C, >5°C higher than the lowest T_m of the primer pair, non-specific priming still occurred.

For rs7254543 annealing temperature had a little effect on yield of the correct product (Figure 3.6). At annealing temperatures below 52°C substantial non-specific priming still occurred, and at higher annealing temperatures (53.1 – 55.2°C) non-specific priming was markedly reduced but still weakly visible.

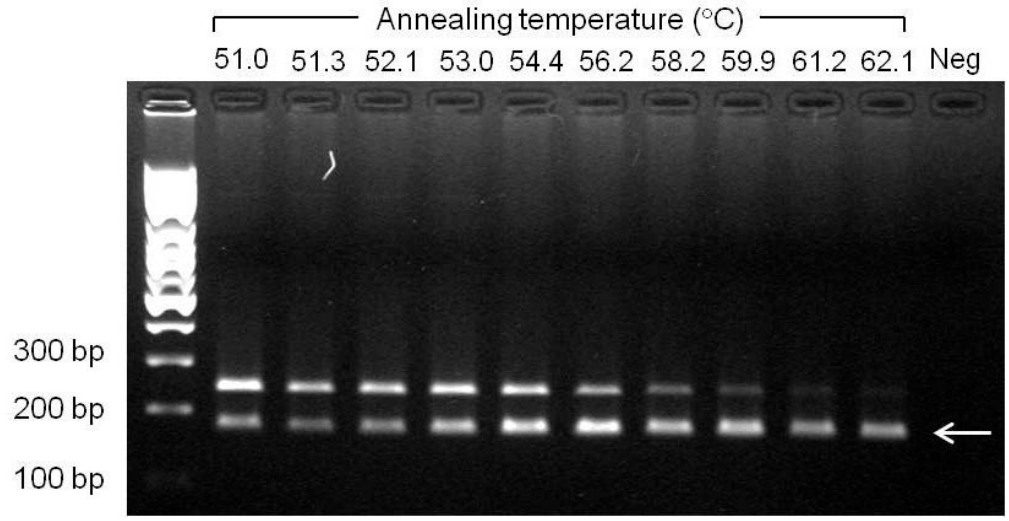

Figure 3.5: Gel electrophoresis image showing gradient PCR results for rs8066527 (*CACNA1G*).
PCR products were separated on a 1.5% agarose/SB gel. The correct product band is indicated with a white arrow. Neg = negative control.

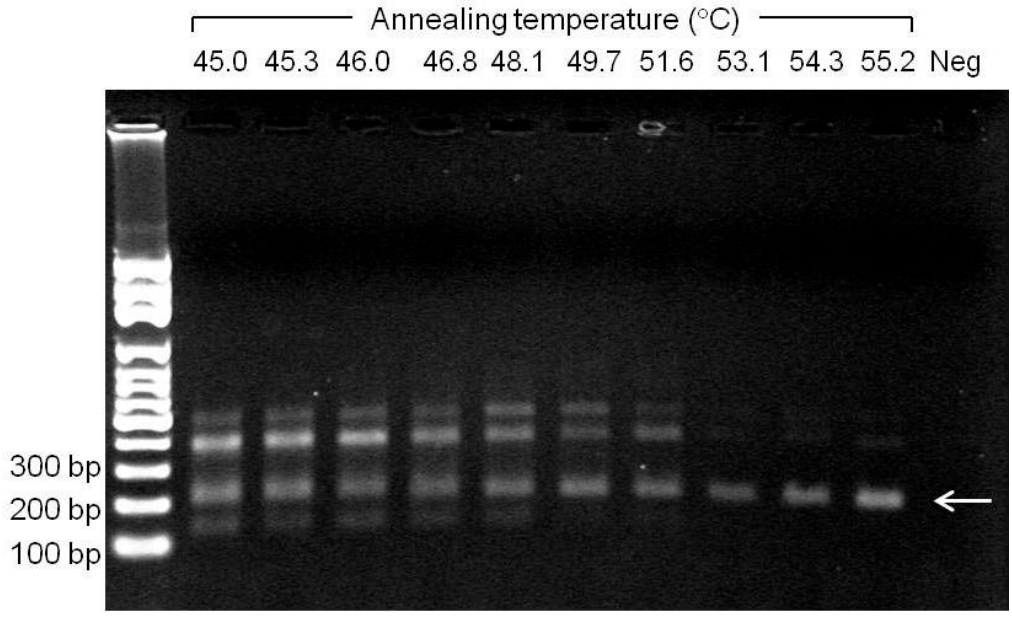

Figure 3.6: Gel electrophoresis image showing gradient PCR results for rs7254543 (*HCN1*).
PCR products were separated on a 1% agarose/SB gel. The correct product band is indicated with a white arrow. Neg = negative control.

3.4.2 Touchdown PCR

A touchdown PCR protocol was trialled and implemented for primer pairs rs8066527 and rs7254543 to reduce non-specific priming and to improve yield (Section 2.3.3). At the higher annealing temperatures in the early cycles, only very specific binding occurs, allowing for enrichment of the correct product over any non-specific products. Using the lower touchdown temperature for the remaining cycles serves to increase the yield of the desired product [177, 178].

For rs8066527 two touchdown temperatures were trialled; 55°C, as this annealing temperature was found to give maximum yield of the correct PCR product, and 60°C which resulted in reduced non-specific product but also slightly reduced product yield (Figure 3.5). A 55°C touchdown temperature was found to increase product yield relative to the standard protocol and as a result only 30 cycles for phase two were required to give a desirable yield, but, non-specific priming was not reduced (Figure 3.7). Increasing the touchdown temperature to 60°C was found to reduce non-specific priming, and when 35 cycles were performed for phase two a desirable product yield was obtained.

For rs7254534 a touchdown temperature of 50°C was trialled. This temperature resulted in the elimination of non-specific priming and a suitable product yield for PCR-RFLP when 35 cycles were performed for phase two (Figure 3.19 shows final PCR-RFLP assay using a 50°C touchdown temperature).

Based on the results from these trials, touchdown protocols were used for PCR in PCR-RFLP assays for rs8066527 and rs7254534. A 55°C touchdown temperature was used for rs8066527, 50°C for rs7254534, and 35 cycles for phase two of thermal cycling for both reactions.

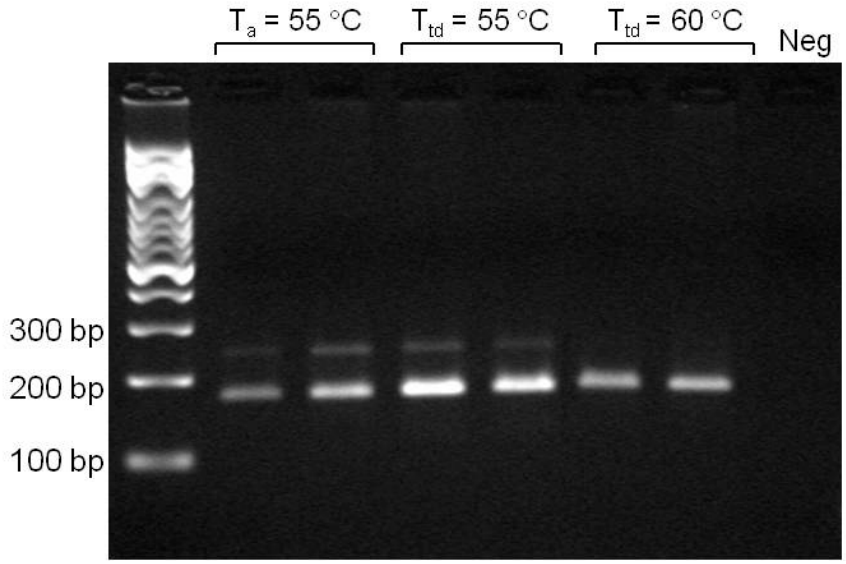

Figure 3.7: Gel electrophoresis image showing touchdown PCR results for rs8066527 (*CACNA1G*).
A standard PCR protocol for rs8066527 using an annealing temperature of 55°C (T_a = 55°C), compared with touchdown protocols using touchdown temperatures of 55°C (x30 cycles for phase two) (T_{td} = 55°C), and 60°C (x35 cycles for phase two) (T_{td} = 60°C). Neg = negative control.

3.5 PCR-RFLP assays

Briefly, PCR was first used to amplify a small genomic region (169-364 bp) containing the SNP of interest using custom designed primers. PCR products were digested with a restriction enzyme specific to the assay at the optimum temperature for that enzyme and digested PCR products were separated by gel electrophoresis and visualised by UV trans-illumination. A 100 bp DNA ladder was used to estimate the size of the fragments and the genotype of each sample was determined from the fragmentation pattern (Section 2.2-2.5).

PCR-RFLP assays were successfully designed and optimised that enabled genotyping for each of the 13 selected SNPs. Figures 3.8-3.20 show example gel image results from each PCR-RFLP assay. Primer-dimer was observed for some primer pairs, however, this did not seem to have significant impact on amplification efficiency, nor did it impair genotyping.

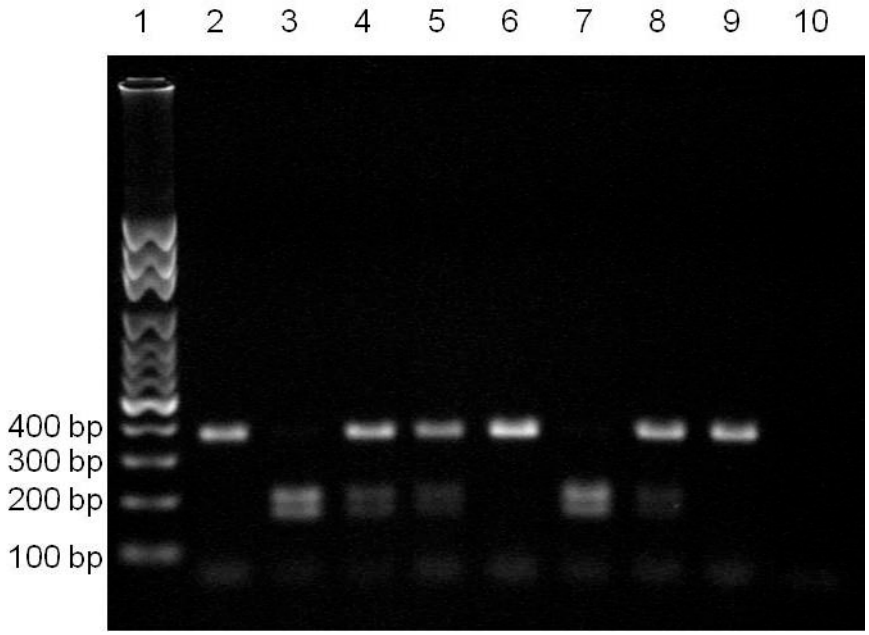

Figure 3.8: Example gel electrophoresis image of PCR-RFLP results for r10889635 (*SGIP1*).
Lane 1 – 100 bp ladder; lanes 3, 7 – A/A homozygous; lanes 2, 6, 9 – G/G homozygous; lanes 4, 5, 8 – A/G heterozygous; lane 10 – negative control. Products separated on a 1% agarose/SB gel.

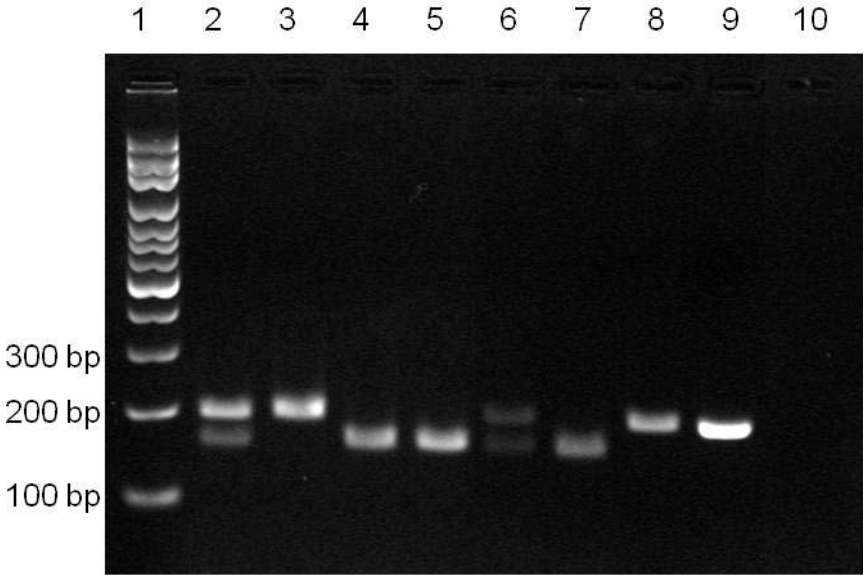

Figure 3.9: Example gel electrophoresis image of PCR-RFLP results for rs6681460 (*SGIP1*).
Lane 1 – 100 bp ladder; lanes 4, 5, 7 – A/A homozygous; lanes 3, 8, 9 – G/G homozygous; lanes 2, 6 – A/G heterozygous; lane 10 – negative control. Products separated on a 2% agarose/SB gel.

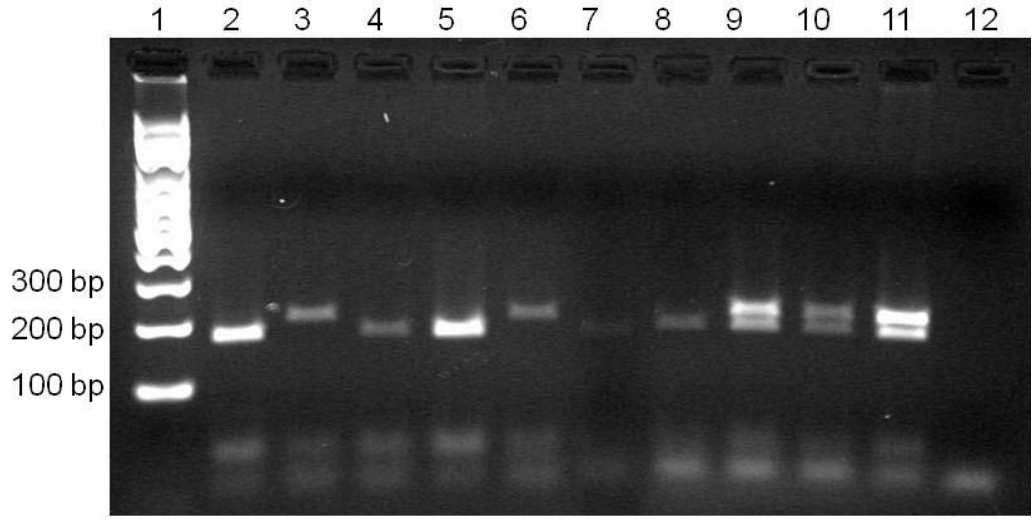

Figure 3.10: Example gel electrophoresis image of PCR-RFLP results for rs2146904 (*SGIP1*).
Lane 1 – 100 bp ladder; lanes 2, 4, 5, 7, 8 – A/A homozygous (weak amplification for lane 7, PCR-RFLP was repeated for this sample and confirmed genotype); lanes 3, 6 – G/G homozygous; lanes 9, 10, 11 – A/G heterozygous; lane 12 – negative control. Products separated on a 2% agarose/SB gel.

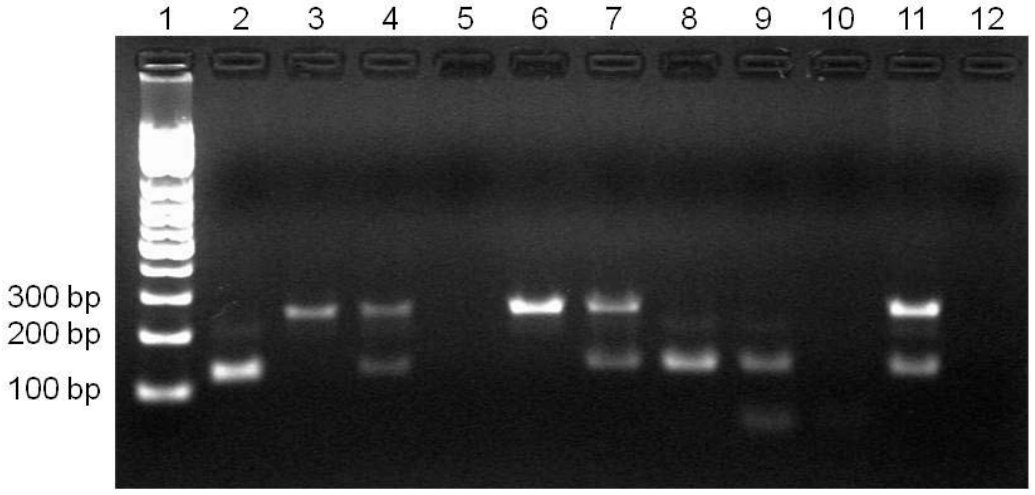

Figure 3.11: Example gel electrophoresis image of PCR-RFLP results for rs572227 (*GABRA2*).
Lane 1 – 100 bp ladder; lanes 2, 8, 9 – G/G homozygous; lanes 3, 6 – A/A homozygous; lanes – 4, 7, 11 – A/G heterozygous; lanes 5, 10 – no amplification; lane 12 – negative control. Products separated on a 1% agarose/SB gel.

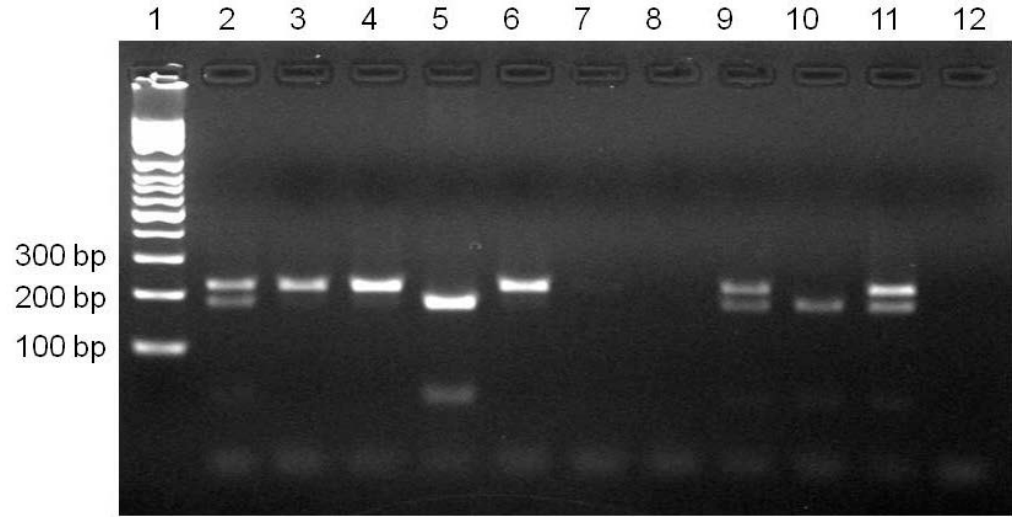

Figure 3.12: Example gel electrophoresis image of PCR-RFLP results for rs279845 (*GABRA2*).
Lane 1 – 100 bp ladder; lanes 5, 10 – A/A homozygous; lanes 3, 4, 6 – T/T homozygous; lanes 2, 9, 11 – A/T heterozygous; lanes 7, 8 – no amplification; lane 12 – negative control. Products separated on a 1.5% agarose/SB gel.

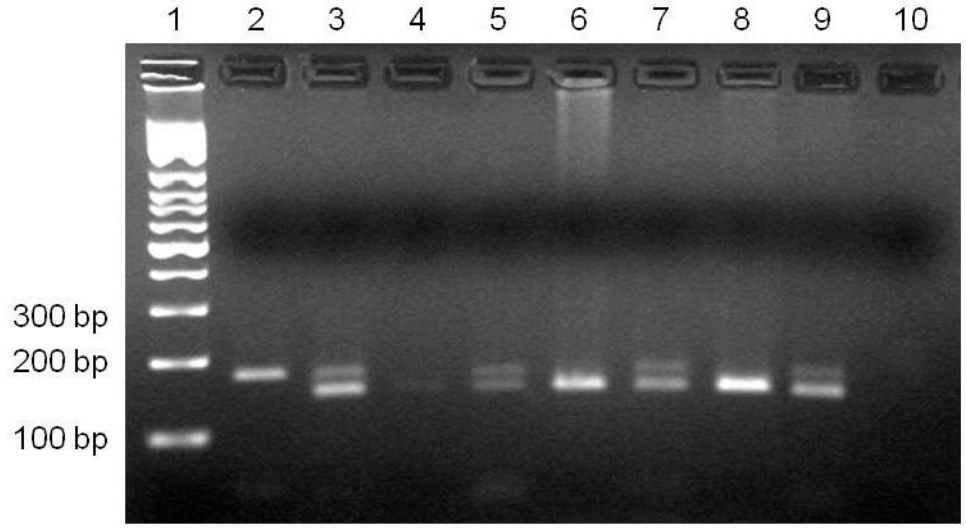

Figure 3.13: Example gel electrophoresis image of PCR-RFLP results for rs279841 (*GABRA2*).
Lane 1 – 100 bp ladder; lanes 6, 8 – G/G homozygous; lane 2 – A/A homozygous; lanes 3, 5, 7 – A/G heterozygous; lane 4 – no amplification; lane 12 – negative control. Products separated on a 2% agarose/SB gel.

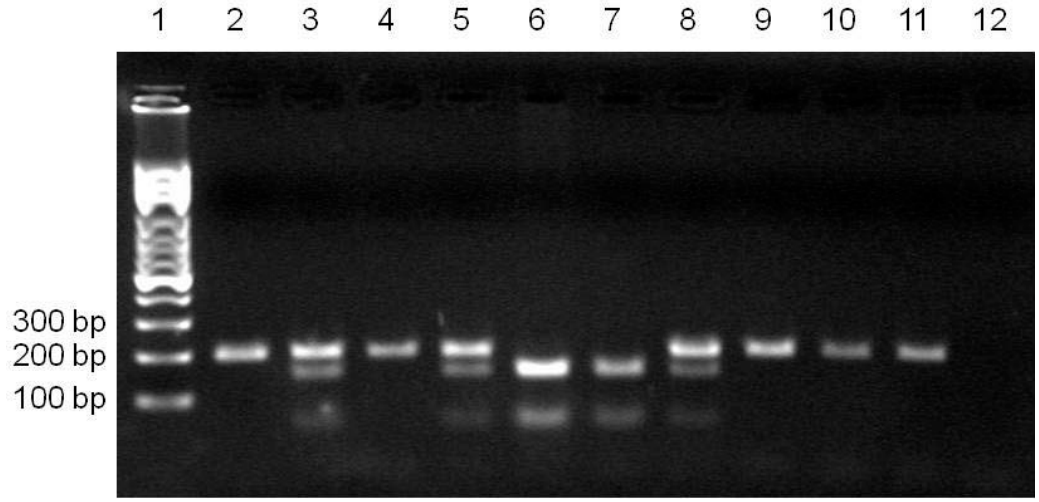

Figure 3.14: Example gel electrophoresis image of PCR-RFLP results for rs13361609 (*HCN1).*

Lane 1 – 100 bp ladder; lanes 6, 7 – C/C homozygous; lanes 2, 4, 9, 10, 11 – T/T homozygous; lanes 3, 5, 8 – C/T heterozygous; lane 12 – negative control. Products separated on a 1.5% agarose/SB gel.

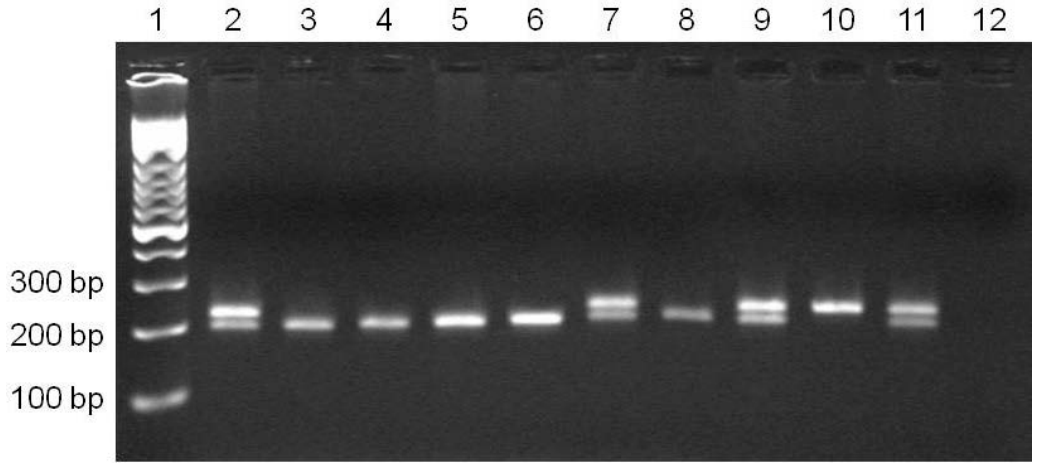

Figure 3.15: Example gel electrophoresis image of PCR-RFLP results for rs13187565 (*HCN1).*

Lane 1 – 100 bp ladder; lanes 3, 4, 5, 6, 8 – G/G homozygous; lane 10 – T/T homozygous; lanes 2, 7, 9, 11 – G/T heterozygous; lane 12 – negative control. Products separated on a 2% agarose/SB gel.

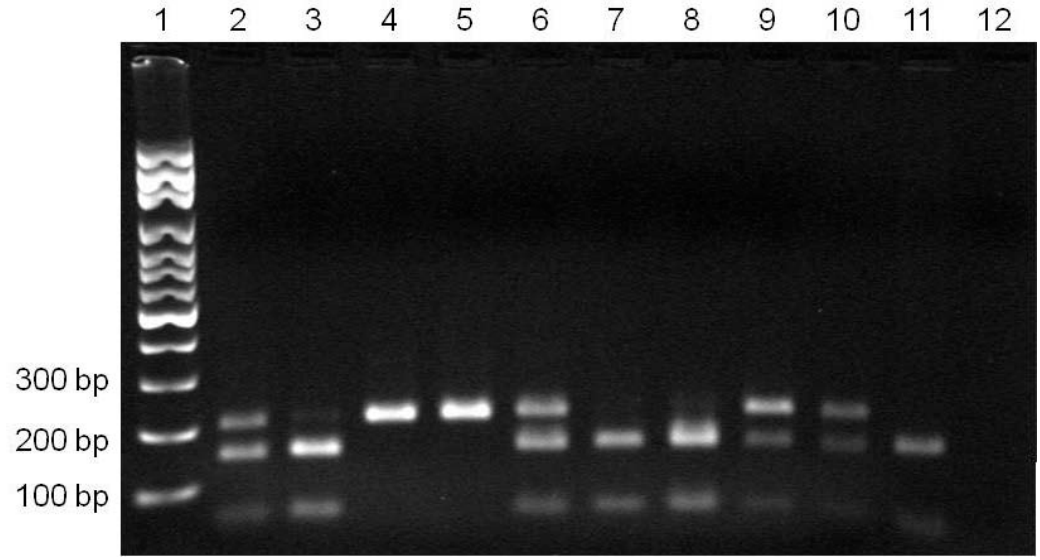

Figure 3.16: Example gel electrophoresis image of PCR-RFLP results for rs750581 (*CACNA1G).*
Lane 1 – 100 bp ladder; lanes 3, 7, 8, 11 – G/G homozygous; lanes 4, 5 – C/C homozygous; lanes – 2, 6, 9, 10 G/C heterozygous; lane 12 – negative control. Products separated on a 1.5% agarose/SB gel.

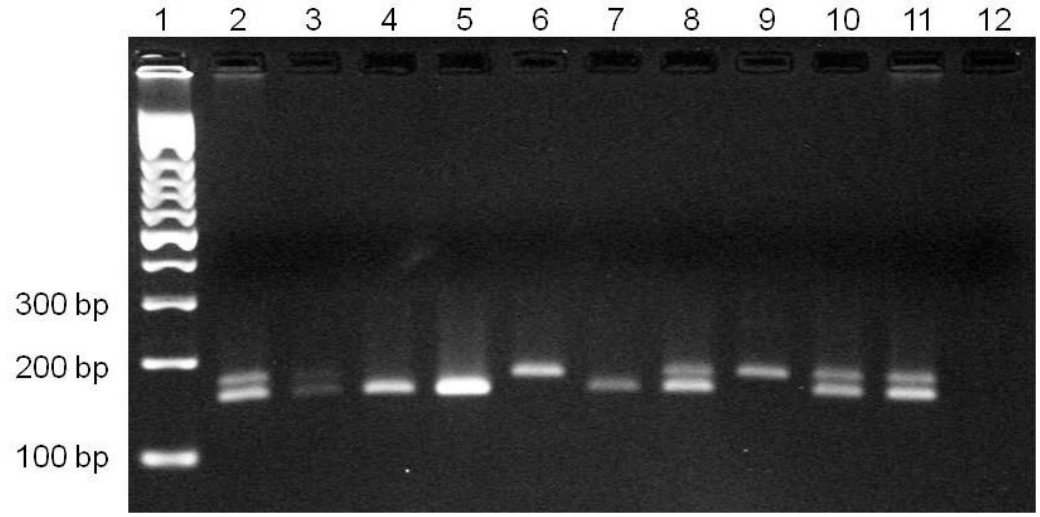

Figure 3.17: Example gel electrophoresis image of PCR-RFLP results for rs8066527 (*CACNA1G).*
Lane 1 – 100 bp ladder; lanes 4, 5, 7 – C/C homozygous; lanes 6, 9 – T/T homozygous; lanes 2, 3, 8,10, 11 – C/T heterozygous; lane 12 – negative control. Products separated on a 2.5% agarose/SB gel.

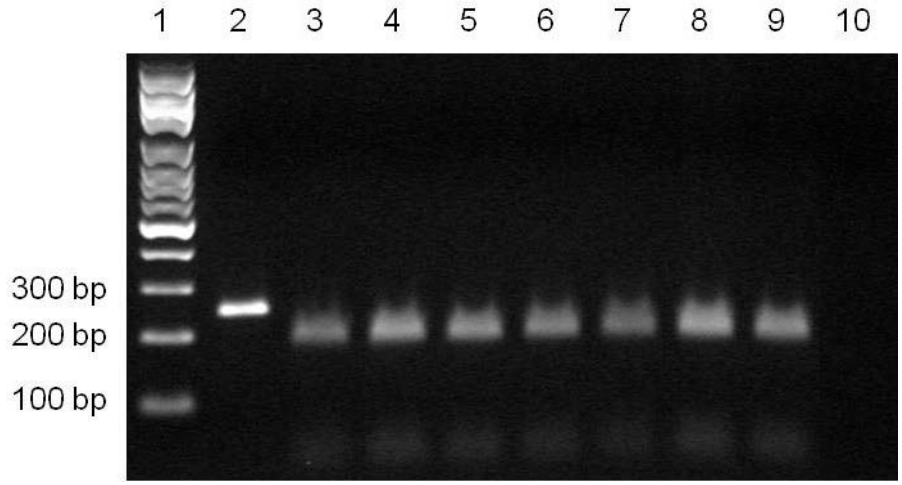

Figure 3.18: Example gel electrophoresis image of PCR-RFLP results for rs8066269 (*CACNA1G*).
Lane 1 – 100 bp ladder; lane 2 – undigested sample; lanes 3 to 10 – G/G homozygous; lane 11 – negative control. Products separated on a 1.5% agarose/SB gel.

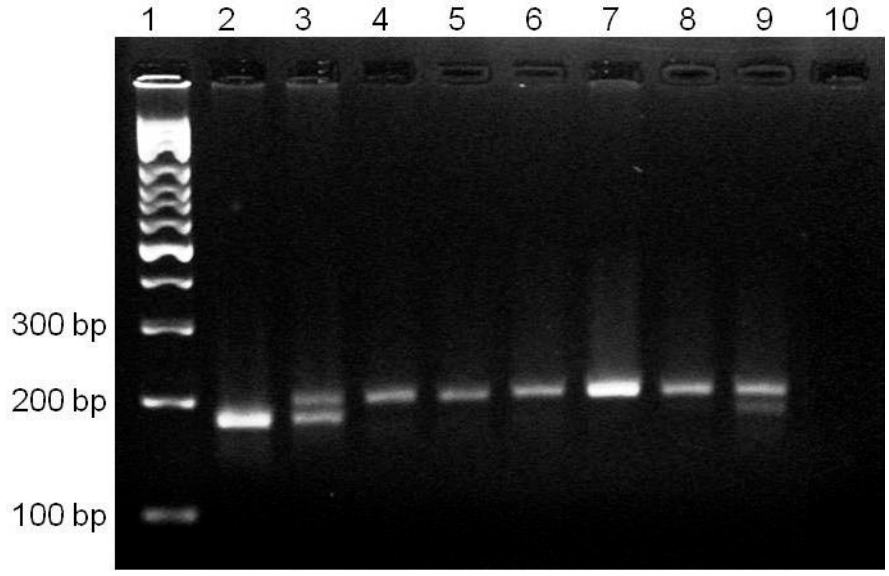

Figure 3.19: Example gel electrophoresis image of PCR-RFLP results for rs7254543 (*HCN2*).
Lane 1 – 100 bp ladder; lane 2 – A/A homozygous; lanes 4, 5, 6, 7, 8 – C/C homozygous; lanes 3, 9, – G/T heterozygous lane 10 – negative control. Products separated on a 2.5% agarose/SB gel.

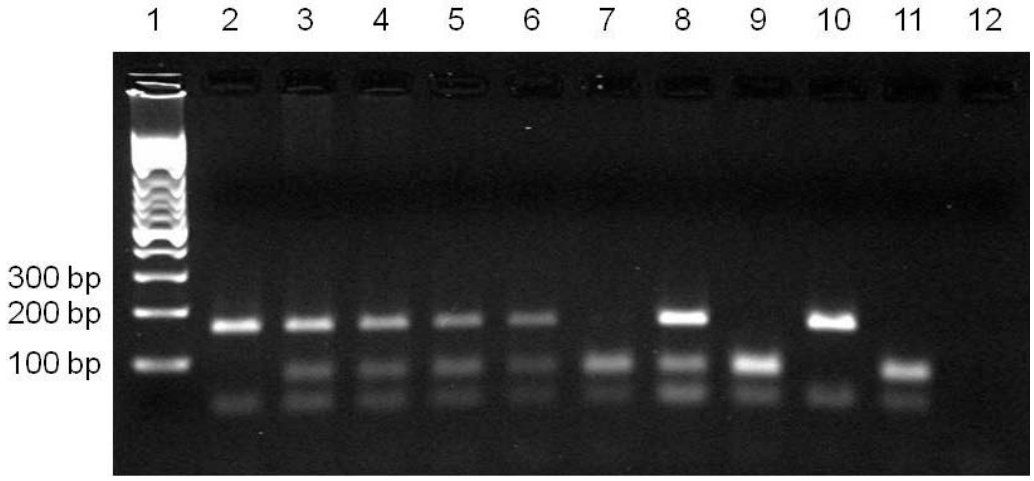

Figure 3.20: Example gel electrophoresis image of PCR-RFLP results for rs873634 (*HCN2*).
Lane 1 – 100 bp ladder; lanes 7, 9, 11 – G/G homozygous; lanes 2, 10 – T/T homozygous; lanes 3, 4, 5, 6, 8 – G/T heterozygous; lane 12 – negative control. Products separated on a 2% agarose/SB gel.

3.6 Conformation by sequencing

To ensure that the correct region had been amplified for each PCR-RFLP assay, one sample was sequenced in the forward and reverse directions for all primer pairs (Section 2.6). DNA sequences were then input into NCBI BLAST and queried against the human genome (all assemblies) (Figure 3.21). All primer pairs were found to amplify the correct genomic region and SNP genotypes determined by PCR-RFLP corresponded with sequencing results for all sequenced samples (Appendix 6.4).

```
Molecule type:  nucleic acid
Query Length:   363
Database Name:  Genome (all assemblies)
Description:    Homo sapiens build 37.3 genome database
(reference assembly GRCh37.p5 [GCF_000001405.17] and alternate
assemblies HuRef [GCF_000002125.1] and CRA_TCAGchr7v2
[GCF_000002135.2])
Program:        BLASTN 2.2.26+
```

Figure 3.21: BLAST search parameters used to check alignment of PCR products against the human genome.

3.7 Genotyping results

3.7.1 PCR-RFLP genotyping results

Following completion of PCR-RFLP assays, genotyping results were input into a Microsoft Excel spreadsheet. Raw genotyping results for PCR-RFLP are shown in Appendix Table 6.3.

Excel was used to determine the number of samples successfully genotyped for each PCR-RFLP assay and to assist calculations of MAF and genotype frequencies (Table 3.5). Of the 125 samples included in this study, genotyping results were obtained for 95-100% of samples for each individual SNP, with the exception of rs8066269. For rs8066269 only 25 samples were genotyped and all were found to be homozygous for the G allele. Excluding rs8066269, MAFs ranged from 0.238 – 0.419 (mean = 0.367) and minor genotype frequencies from 0.074 - 0.234 (mean = 0.156).

3.7.2 MassARRAY genotyping results

100 DNA samples included in this study were genotyped with custom-designed multiplex analysis using Sequenom MassARRAY technology (iPlex Gold) at AGRF. Completed genotyping data was provided in excel format and then paired with EEG and other patient data. Raw genotyping data is shown in Appendix Table 6.4.

Of the 100 samples genotyped by Sequenom MassARRAY, genotypes were determined for 88-99% of samples for each individual SNP (Table 3.6). Two SNPs (rs11466314 and rs11466004) were found not to be polymorphic in this sample and were therefore excluded from further analysis. All three genotypes were present for 16 of the remaining SNPs, and no patients were found to be homozygous for the minor allele for SNPs rs3804100, rs4986790 and rs4986791. Of the 19 polymorphic SNPs, MAFs ranged from 0.036 to 0.429 (mean = 0.215) and minor genotype frequencies from 0.000 to 0.192 (mean = 0.068).

Table 3.5: Summary of genotyping results for SNPs genotyped by PCR-RFLP.

Gene	SNP	n	Genotype frequencies			MAF
SGIP1	rs10889635	124	0.169 (G/G)	0.4768 (A/G)	0.355 (A/A)	0.407 (G)
	rs6681460	123	0.170 (A/A)	0.407 (A/G)	0.423 (G/G)	0.374 (A)
	rs2146904	124	0.170 (A/A)	0.427 (A/G)	0.403 (G/G)	0.383 (A)
GABRA2	rs572227	125	0.152 (A/A)	0.472 (A/G)	0.376 (A/G)	0.388 (A)
	rs279845	125	0.168 (A/A)	0.496 (A/T)	0.336 (A/T)	0.416 (A)
	rs279841	123	0.146 (A/A)	0.472 (A/G)	0.382 (G/G)	0.382 (A)
HCN1	rs13361609	122	0.074 (C/C)	0.328 (C/T)	0.598 (T/T)	0.238 (C)
	rs13187565	124	0.234 (T/T)	.371 (G/T)	0.395 (G/G)	0.419 (T)
CACNA1G	rs7501581	125	0.152 (G/G)	0.432 (C/G)	0.416 (C/C)	0.368 (G)
	rs8066527	123	0.155 (T/T)	0.398 (C/T)	0.447 (C/C)	0.354 (T)
	rs8066269	25	0.000 (T/T)	0.00 (G/T)	1.00 (G/G)	0.000 (T)
HCN2	rs7254543	119	0.151 (A/A)	0.336 (A/C)	0.513 (C/C)	0.319 (A)
	rs873634	122	0.131 (G/G)	0.443 (G/T)	0.426 (T/T)	0.352 (G)

Table 3.6: Summary of genotyping results for SNPs genotyped by MassARRAY at AGRF.

Gene	SNP	n	Genotype frequencies			MAF
IL6R	rs8192284	97	0.175 (C/C)	0.371 (A/C)	0.454 (A/A)	0.361 (C)
CRP	rs2794521	97	0.082 (C/C)	0.320 (C/T)	0.598 (T/T)	0.242 (C)
IL10	rs1800871	99	0.101 (T/T)	0.343 (C/T)	0.556 (C/C)	0.273 (T)
	rs1800896	99	0.192 (G/G)	0.475 (A/G)	0.333 (A/A)	0.429 (G)
IL1B	rs1143634	99	0.020 (T/T)	0.232 (C/T)	0.747 (C/C)	0.136 (T)
	rs1143627	97	0.134 (C/C)	0.495 (C/T)	0.371 (T/T)	0.381 (C)
	rs16944	99	0.121 (A/A)	0.515 (A/G)	0.364 (G/G)	0.379 (A)
MYD88	rs6853	98	0.000 (G/G)	0.153 (A/G)	0.847 (A/A)	0.077 (G)
IL2	rs2069762	93	0.151 (G/G)	0.419 (G/T)	0.430 (T/T)	0.360 (G)
TLR2	rs3804100	99	0.010 (C/C)	0.172 (C/T)	0.818 (T/T)	0.096 (C)
TNF	rs1800629	99	0.020 (A/A)	0.192 (A/G)	0.788 (G/G)	0.116 (A)
OPRM1	rs1799971	99	0.020 (GG)	0.253 (AG)	0.727 (AA)	0.146 (G)
IL6	rs10499563	88	0.011 (C/C)	0.239 (C/T)	0.750 (T/T)	0.131 (C)
LY96	rs11466004	90	0.000 (T/T)	0.000 (C/T)	1.000 (C/C)	0.000 (T)
TLR4	rs4986790	97	0.000 (G/G)	0.072 (A/G)	0.928 (A/A)	0.036 (G)
	rs4986791	98	0.000 (T/T)	0.112 (C/T)	0.888 (C/C)	0.056 (T)
BDNF	rs6265	99	0.051 (A/A)	0.232 (A/G)	0.717 (G/G)	0.167 (A)
CASP1	rs554344	98	0.031 (C/C)	0.286 (C/G)	0.684 (G/G)	0.173 (C)
	rs580253	98	0.041 (T/T)	0.235 (C/T)	0.724 (C/C)	0.158 (T)
TGFB1	rs11466314	98	0.000 (A/A)	0.000 (A/G)	1.000 (G/G)	0.000 (A)
	rs1800469	99	0.131 (T/T)	0.475 (C/T)	0.394 (C/C)	0.369 (T)

3.8 Haploview

The software Haploview was used to check for adherence to HWE, calculate LD between SNPS, and to estimate haplotypes and their frequencies.

For importation into Haploview, raw genotyping data was formatted as specified in the user manual and then converted into tab-delimited text files. Two separate Haploview input files were created; one providing information on SNPs genotyped by PCR-RFLP and the other on SNPs genotyped by MassARRAY. Each file contained information on sample number, gender, and genotype for each study participant. Fields were filled with a zero where pedigree information or case control status was required. An excerpt of the Haploview importation file for SNPs genotyped by PCR-RFLP is shown in Figure 3.22.

A	B	C	D	E	F	G		
0	1	0	0	2	0	1 3	1 3	1 3
0	2	0	0	2	0	1 1	3 3	3 3
0	3	0	0	1	0	1 1	3 3	3 3
0	4	0	0	2	0	3 3	1 3	1 3
0	5	0	0	2	0	1 3	1 3	1 3

Figure 3.22: Excerpt of Haploview input file.
Information is shown for on sample numbers 1-5 for *SGIP1* SNPs. Column A – pedigree name; B – sample ID number; C – father's ID number; D – mother's ID number; E – gender (1 = male, 2 = female); F – affection status; G – genotypes for rs10889635, rs6681460 and rs2146904 (0 = unknown, 1 = A, 2 = C, 3 = G, T = 4).

3.8.1 Adherence to HWE

Haploview was used to test each SNP for adherence to HWE as a quality control measure. For any given SNP, the sum of the major and minor allele frequencies (p and q, respectively) equals one (equation 3.2). If a SNP is in HWE then the observed genotypes are a simple function of the major and minor allele frequencies (Equation 3.3).

$$p + q = 1 \qquad \text{(Equation 3.2)}$$

$$p^2 + 2pq + q^2 = 1 \qquad \text{(Equation 3.3)}$$

If observed genotype frequencies deviate significantly from those predicted by Equation 3.3 then that SNP is not in HWE. Haploview compares observed heterozygosity with that predicted, and any significant deviations ($p < 0.05$) indicate that SNP is not in HWE.

All of the SNPs genotyped by MassARRAY, and 11 of the 13 SNPs genotyped by PCR-RFLP, were found to adhere to HWE ($p > 0.05$). For two SNPs, rs13187565 and rs7254543, observed heterozygosity deviated significantly from expected ($p = 0.0117$ and $p = 0.0219$, respectively) (Appendix; Table 6.5). Adherence to HWE was therefore rejected for these SNPs and they were excluded from further analysis.

3.8.2 LD and haplotype estimation

LD values for SNP loci in the same gene were calculated in Haploview. Both D' and r^2 values were calculated, and LD plots were generated for genes in which three or more SNPs were genotyped.

D' provides a measure of the recombinational history between SNPs. D' = 1.00 indicates two SNP loci have not been separated by recombination (complete LD), D' values <1.00 indicate linkage has been disrupted by recombination, and D' = 0 implies complete independence between loci. r^2 is the correlation co-efficient and provides information on both LD and allele frequencies. $r^2 = 1$ indicates SNPs have been separated by recombination and also have the same allele frequencies (perfect LD), thus the allele present at one SNP loci perfectly predicts the allele present at the other. Based on D', SNP loci were assigned as either being in high (D' ≥ 0.90), moderate (D' ≥ 0.70) or weak (D' < 0.70) LD. LD data was also obtained directly from the HapMap database for the HapMap Caucasian population (phase II+III, #27, Feb 09) for comparison with results obtained in the present study.

Haploview was used to infer three-SNP haplotypes and estimate haplotype frequency (HF) for each gene containing three genotyped SNPs (*SGIP1*, *GABRA2* and *IL1B*). Haplotypes with HF ≥ 0.05 were considered common and HF < 0.05 as rare. LD plots, haplotypes, and haplotype frequencies, were also inferred for the HapMap Caucasian population for several of the genes included in this study

(Appendix; 6.6). Data was downloaded directly into Haploview using the HapMap download feature (Version 3, Release 27, CEU population – herein referred to as V3/R27/CEU).

3.8.2.1 SNPs genotyped by PCR-RFLP

D' values ranged from 0.155 to 0.961 (mean = 0.791), and r^2 from 0.008 to 0.817 (mean = 0.624), for pairs of SNP loci in the same gene (Table 3.7**).** The highest D' values were observed between SNPs located in *GABRA2*. SNPs in both *SGIP1* and *GABRA2* were found to be in moderate to high LD whereas weak LD was observed between SNPs in *CACNA1G*. Haploview identified eight three-SNP haplotypes for *SGIP1* and six for *GABRA2* (Figure 3.23c-d). Two common haplotypes were observed in both genes, along with six rare haplotypes in *SGIP1*, and four in *GABRA2*.

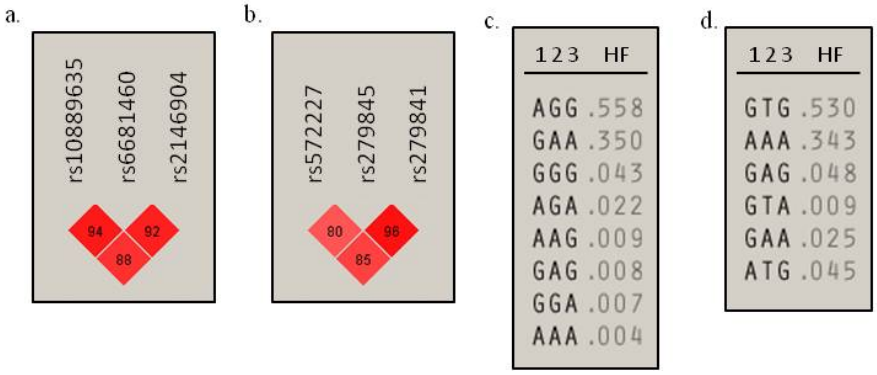

Figure 3.23: LD plots and haplotypes for genes genotyped by PCR-RFLP.
LD plots constructed in Haploview for a. *SGIP1*; and b. *GABRA2*. The value in each square corresponds level of LD between SNP loci in D', for example, a value of 94 corresponds to D' = 0.94. Dark red squares indicate high levels of LD.
Haplotypes and their estimated frequencies inferred in Haploview for d. *SGIP1* (1 = rs10889635, 2 = rs6681460, 3 = rs2146904); and e. *GABRA2* (1 = rs572227, 2 = 279845, 3 = rs279841).

Table 3.7: LD values for SNP loci in the same gene genotyped by PCR-RFLP.
Haploview results determined for this study are shown (Genotyped) along with LD data for the HapMap Caucasian population. Distance between loci for each SNP pair is also shown. N/D = no HapMap data.

Gene	SNP 1	SNP 2	Genotyped		HapMap		Distance (bp)
			D'	r^2	D'	r^2	
SGIP1	rs10889635	rs6681460	0.942	0.761	1.000	0.960	47746
	rs10889635	rs2146904	0.888	0.713	0.957	0.878	85099
	rs6681460	rs2146904	0.927	0.817	1.000	1.000	37353
GABRA2	rs572227	279845	0.809	0.583	0.876	0.710	78270
	rs572227	279841	0.854	0.705	0.882	0.777	89310
	279845	279841	0.961	0.780	0.959	0.850	11040
CACNA1G	rs7501581	rs8066527	0.155	0.008	N/D	N/D	56265

3.8.2.2 SNPs genotyped by MassARRAY

Between pairs of SNP loci in the same gene genotyped by MassARRAY, D' values ranged from 0.790 to 1.000 (mean = 0.931), and r^2 from 0.060 to 0.857 (mean = 0.488) (Table 3.8). Complete LD (D' = 1) was observed between SNPs in *IL10*, *TLR4*, *CASP1* and between one pair of SNP in *IL1B*. The three SNPs in *IL1B* were found to be in moderate to strong LD (Figure 3.24a). Four three-SNP haplotypes; two common and two rare, were identified for *IL1B* (Figure 3.24b).

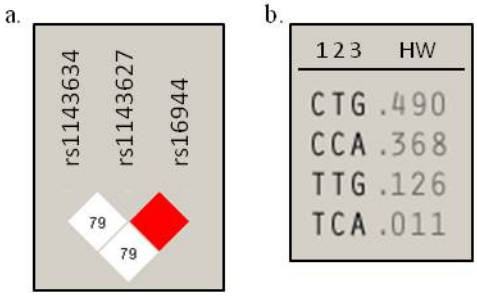

Figure 3.24: LD plots and haplotypes for *IL1B*.
a. LD plot for *IL1B*. The value in each square corresponds level of LD between two SNP loci in D', for example, a value of 79 corresponds to D' = 0.79 and empty squares correspond to D' = 1. Dark red squares indicate high levels of LD. b. *IL1B* haplotypes and their estimated frequencies (1 = rs1143634, 2 = rs1143627, 3 = rs16944).

Table 3.8: LD values for SNP loci in the same gene genotyped by MassARRAY.
Haploview results determined for this study are shown (Genotyped) along with LD data for the HapMap Caucasian population. Distance between SNP loci for each SNP pair is also shown.

Gene	SNP 1	SNP 2	Genotyped		HapMap		Distance (bp)
			D'	r^2	D'	r^2	
IL10	rs1800871	rs1800896	1.000	0.282	1.000	0.255	263
IL1B	rs1143634	rs1143627	0.795	0.063	0.551	0.064	3997
	rs1143634	rs16944	0.790	0.060	0.538	0.058	4477
	rs1143627	rs16944	1.000	0.978	1.000	0.982	480
TLR4	rs4986790	rs4986791	1.000	0.689	1.000	0.742	300
CASP1	rs554344	rs580253	1.000	0.857	1.000	1.000	5291

3.9 Halplotype phasing

The EM algorithm in SNPAnalyzer 1.2A was used to estimate haplotypes and infer haplotype phase for three-SNP haplotypes in *SGIP1*, *GABRA2* and *IL1B.* Raw unphased data was formatted as specified in the user's manual and converted into tab-delimited text files for input in SNPAnalyzer 1.2A. Input files contained information on SNP ID, sample ID and genotype (Figure 3.25). Any samples with incomplete genotyping data for the gene of interest were excluded from this analysis.

NAME	rs10889635	rs6681460	rs2146904
1	AG	AG	AG
2	AA	GG	GG
3	AA	GG	GG
4	GG	AG	AG
5	AG	AG	AG

Figure 3.25: Excerpt of SNPAnalyzer 1.2A input file for *SGIP1*.
Row one provides information on SNP ID, and subsequent rows list sample ID followed by genotypes for each SNP.

The EM algorithm identified the same three-SNP haplotypes constructed by Haploview and provided similar frequency estimates for *SGIP1* and *GABRA2* (Table 3.9a-b). For *IL1B*, the EM algorithm identified one additional rare

haplotype (CCG, HF = 0.005) and frequency estimates for the remaining four *IL1B* haplotypes were similar for both Haploview and EM (Table 3.9c).

Table 3.9: EM constructed haplotypes and their estimated frequencies.
a. *SGIP1*; b. *GABRA2*; and c. *IL1B.*

a.

SGIP1 **Haplotypes**	**HF**
AGG	0.550
GAA	0.351
GGG	0.040
AGA	0.020
AAG	0.012
AAA	0.008
GAG	0.008
GGA	0.008

b.

GABRA2 **Haplotypes**	**HF**
GTG	0.528
AAA	0.350
GAG	0.049
ATG	0.041
GAA	0.024
GTA	0.008

c.

IL1B **Haplotypes**	**HF**
CTG	0.485
CCA	0.371
TTG	0.134
TCA	0.005
CCG	0.005

Haplotype phase was also inferred for each sample using the EM algorithm in SNPAnalyzer 1.2A, and the probability of each haplotype call was also determined. A probability threshold of 90% was chosen for accepting the haplotype call and considering phase resolved. Overall, probabilities ranged from 37-100% (mean = 76%) and only 57%, 51% and 51% of haplotypes calls met the 90% threshold for *SGIP1*, *GABRA2* and *IL1B*, respectively (Appendix; Table 6.7).

3.10 Association analysis

The software NCSS was used to perform statistical tests to examine associations between SNPs and quantitative EEG traits and ETDC. Because spindle frequency, delta amplitude and BIS value failed tests for normality, only non-parametric statistical tests were performed.

3.10.1 Association of SNPs in candidate genes

Of the 13 SNPs genotyped by PCR-RFLP, 10 passed quality control checks on MAF and adherence to HWE (Section 3.8.1) and were tested for associations with the EEG. KW-ANOVA identified associations with either the EEG or ETDC for four SNPs located in or near four different genes ($p < 0.05$). Two SNPs were found to associate with spindle amplitude; rs6681406 (*SGIP1*) and rs279841 (*GABRA2*). rs6681406 (*SGIP1*) was also associated with relative spindle along with rs873634 (*HCN2*). A single SNP, rs7501581 (*CACNA1G*) was found to be associated with ETDC (Table 3.10).

Table 3.10: Association of SNPs genotyped by PCR-RFLP with ETDC and the EEG.

SNPs were tested for associations with ETDC and the EEG using KW-ANOVA. *p*-values for each test are shown and significant *p*-values are marked with a single ($p < 0.05$) or double ($p < 0.01$) asterisk. n_1 = number of samples tested for association with EEG traits excluding relative spindle amplitude (Relative spindle); n_2 = number of samples tested for association with ETDC and relative spindle amplitude.

Gene	SNP	ETDC	Delta amplitude	Delta frequency	Spindle amplitude	Spindle frequency	Relative spindle	n_1	n_2
SGIP1	rs10889635	0.0811	0.8439	0.9393	0.1332	0.5794	0.0715	124	121
	rs6681460	0.1144	0.6770	0.7231	0.0362*	0.7778	0.0357*	123	120
	rs2146904	0.3684	0.3826	0.7475	0.2210	0.8189	0.2237	124	121
GABRA2	rs572227	0.9726	0.7549	0.9319	0.8308	0.2104	0.9335	125	122
	rs279845	0.1925	0.4287	0.7060	0.1034	0.0637	0.0838	125	122
	rs279841	0.1643	0.8264	0.7933	0.0427*	0.0836	0.0674	123	120
HCN1	rs13361609	0.3434	0.4488	0.6217	0.6851	0.7335	0.4962	122	119
CACNA1G	rs7501581	0.0097**	0.2120	0.7041	0.3645	0.6478	0.0889	125	122
	rs8066527	0.6222	0.9922	0.5267	0.6929	0.2286	0.6225	123	120
HCN2	rs873634	0.1109	0.7936	0.2860	0.1406	0.9137	0.0474*	122	119

3.10.1.1 Associations with spindle amplitude

Three SNPs in or near three different genes – *SGIP1, GABRA2* and *HCN2* – were found to be associated with spindle amplitude and/or relative spindle amplitude (Figure 3.26). For each of these SNPs, the strongest associations were observed in recessive models, and the minor allele was associated higher median spindle amplitude (Table 3.11, Table 3.12).

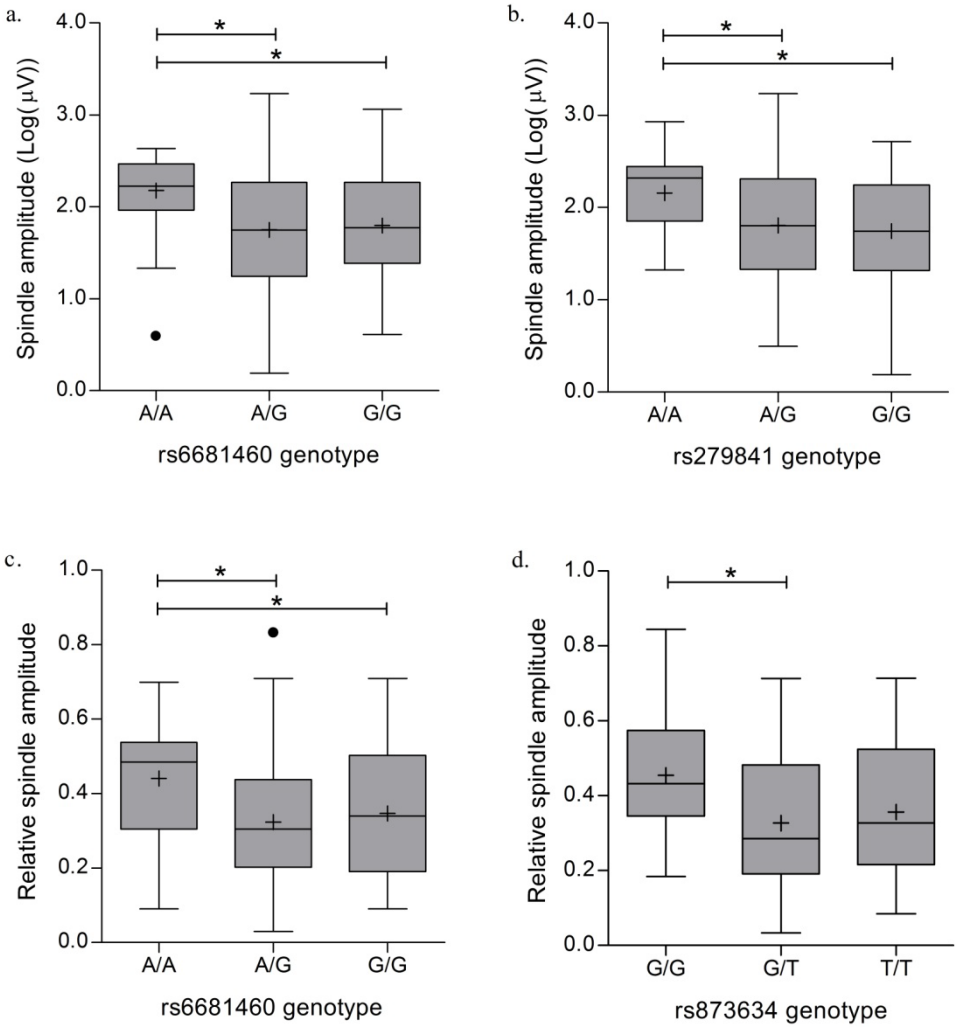

Figure 3.26: Association of SNPs genotyped by PCR-RFLP with spindle amplitude and relative spindle amplitude.

Association of a. rs6681460 (SGIP1) with spindle amplitude; b. rs279841 (GABRA2) with spindle amplitude; c. rs6681460 with relative spindle amplitude; and d. rs873634 (HCN2) with relative spindle amplitude. Box and whisker plots show median, minimum, maximum, and upper and lower quartiles for each genotype. The mean is marked with a cross and black circles denote outliers. Significant differences in median are indicated with a single asterisk ($p < 0.05$) (Appendix; Table 6.9, Table 6.10).

Table 3.11: Individual SNP effects on spindle amplitude for associated SNPs genotyped by PCR-RFLP.
R = recessive model; D = dominant model; OD = over-dominant model. Significant *p*-values are marked with a single ($p < 0.05$) or double ($p < 0.01$) asterisk.

SNP	Model	Genotype/s	n	Median (95% CI)	Fold Diff.	*p*-value
rs6681406	R	A/A	21	2.18 (1.93-2.43)	1.25	0.0103*
(*SGIP1*)		A/G + G/G	102	1.75 (1.56-1.93)		
	D	A/A + A/G	71	1.93 (1.75-2.16)	1.09	0.4440
		G/G	52	1.77 (1.50-1.99)		
	OD	A/A + G/G	73	1.93 (1.73-2.08)	1.10	0.2322
		A/G	50	1.75 (1.51-1.98)		
rs279841	R	A/A	18	2.32 (1.95-2.44)	1.28	0.0124*
(*GABRA2*)		A/G + G/G	105	1.81 (1.62-1.97)		
	D	A/A + A/G	76	1.94 (1.73-2.11)	1.07	0.3040
		G/G	47	1.81 (1.54-2.06)		
	OD	A/A + G/G	65	1.95 (1.71-2.16)	1.08	0.4412
		A/G	58	1.80 (1.61-1.99)		

Table 3.12: Individual SNP effects on relative spindle amplitude for associated SNPs genotyped by PCR-RFLP.
R = recessive model; D = dominant model; OD = over-dominant model. Significant *p*-values are marked with a single ($p < 0.05$) or double ($p < 0.01$) asterisk.

SNP	Model	Genotype/s	n	Median (95% CI)	Fold Diff.	*p*-value
rs6681406	R	A/A	20	0.48 (0.32-0.53)	1.50	0.0102*
(*SGIP1*)		A/G + G/G	100	0.32 (0.26-0.35)		
	D	A/A + A/G	69	0.34 (0.28-0.42)	1.00	0.4478
		G/G	51	0.34 (0.23-0.42)		
	OD	A/A + G/G	71	0.35 (0.29-0.43)	1.13	0.2359
		A/G	49	0.31 (0.24-0.35)		
rs873634	R	G/G	16	0.43 (0.34-0.53)	1.34	0.0207*
(*HCN1*)		GT + TT	103	0.32 (0.27-0.35)		
	D	G/G + GT	68	0.34 (0.27-0.43)	1.03	0.9829
		TT	51	0.33 (0.26-0.42)		
	OD	G/G + TT	67	0.35 (0.31-0.43)	1.21	0.1068
		GT	52	0.29 (0.24-0.41)		

3.10.1.2 Associations with ETDC

Only one SNP genotyped by PCR-RFLP – rs7501581 (*CACNA1G*) – was found to associate with ETDC. rs7501581 G/G homozygotes were found to have a 1.29-fold higher median ETDC than C/G heterozygotes (p = 0.0075), and C/G heterozygotes a 0.88-fold lower median ETDC than C/C homozygotes (p = 0.0383) (Appendix; Table 6.11). The strongest association was observed in the over-dominant model (p = 0.0071) and a weaker association was also observed the recessive model (p = 0206) (Table 3.13).

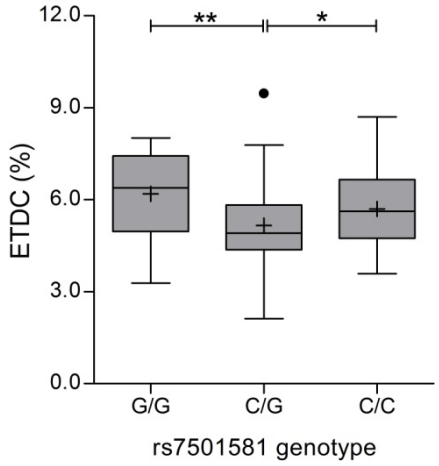

Figure 3.27: Associations of rs7501581 (*CACNA1G*) with ETDC.
Box and whisker plot shows median, minimum, maximum, and upper and lower quartiles for each genotype, the mean is marked with a cross and black circles indicate outliers. Significant differences in median are indicated with a single (p < 0.05) or double asterisk (p < 0.01) (Appendix; Table 6.11).

Table 3.13: Effects of rs7501581 (*CACNA1G*) on ETDC.
R = recessive model; D = dominant model; OD = over-dominant model. Significant p-values are indicated with a single (p < 0.05) or double (p < 0.01) asterisk.

SNP	Model	Genotype/s	n	Median (95% CI)	Fold Diff.	*p*-value
rs7501581	R	G/G	19	6.39 (4.96-7.36)	1.19	0.0206*
		C/G + C/C	103	5.38 (4.91-5.63)		
	D	G/G + C/G	71	5.34 (4.81-5.74)	0.95	0.3189
		C/C	51	5.62 (5.04-6.03)		
	OD	G/G + C/C	70	5.79 (5.35-6.18)	1.17	0.0071**
		C/G	52	4.95 (4.56-5.49)		

EDTC is in part controlled by the anaesthetist, therefore it was suggested rs7501581 might influence the relationship between BIS value and ETDC. A scatter plot of BIS value vs. ETDC categorised by rs7501581 in the over-dominant model, showed an effect of rs7501581 on the relationship between ETDC and BIS value (Figure 3.28), however, linear regression analysis found this to be non-significant (Appendix; Table 6.12). There was evidence of a negative relationship between BIS value and ETDC for C/G heterzygotes (r = 0.349, p = 0.0058) but not for the C/C + G/G homozygous group (r =-0.076, p = 0.6458). This linear regression analysis was also performed on rs7501581 in the recessive and dominant models. The difference in intercept or slope of the regression line between the groups was found not to be statistically significant in either of these models (Appendix; Table 6.12)

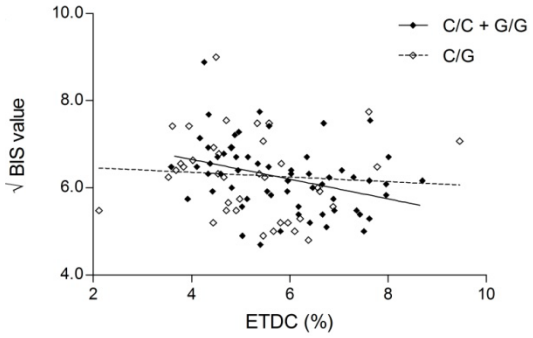

Figure 3.28: Scatter plot and regression lines showing relationship between BIS value and ETDC categorised by rs7501581 (*CACNA1G*) genotype in the over-dominant model. Solid black circles denote C/C + G/G homozygous patients, and black outlined circles C/G heterozygotes. Solid black line shows the relationship between BIS value and ETDC for C/C + G/G homozygotes, and dashed black line for C/G heterozygotes.

3.10.2 Association of SNPs in inflammatory genes

KW-ANOVA identified seven SNPs in or near five inflammatory genes associated with the EEG or ETDC ($p < 0.05$) (Table 3.14). A single SNP in *MYD88* (rs6853) had the strongest association with the EEG of all SNPs genotyped in this study and was associated with spindle amplitude ($p = 0.0040$), relative spindle amplitude ($p = 0.0006$) and ETDC ($p = 0.0095$). Two SNPs in *IL1B* (rs1143627 and rs16944) were also associated with spindle amplitude ($p = 0.0198$ and $p = 0.0222$, respectively), and a single SNP in *IL-10* (rs1800896) associated with delta frequency ($p = 0.0176$). In addition to rs6853, a further two SNPs in separate genes were associated with ETDC; rs2794521 in *CRP* ($p = 0.0381$), and rs1800469 in *TGFB1* ($p = 0.0367$).

Table 3.14: Association of SNPs genotyped by MassARRAY with ETDC and the EEG.

SNPs were tested for associations with ETDC and the EEG using KW-ANOVA. *p*-values for each test are shown and significant *p*-values are marked with a single ($p < 0.05$) or double ($p < 0.01$) asterisk. n_1 = number of samples tested for association with EEG traits excluding relative spindle amplitude (Relative spindle); n_2 = number of samples tested for association with ETDC and relative spindle amplitude.

Gene	SNP	ETDC	Delta amplitude	Delta frequency	Spindle amplitude	Spindle frequency	Relative spindle	n_1	n_2
IL6R	rs8192284	0.6726	0.7905	0.8512	0.6971	0.2381	0.6474	97	96
CRP	rs2794521	0.0381*	0.6964	0.7739	0.1236	0.6254	0.0530	97	96
IL10	rs1800871	0.4878	0.8088	0.5213	0.8982	0.4650	0.8995	99	98
	rs1800896	0.8142	0.2057	0.0176*	0.1671	0.9287	0.2590	99	98
IL1B	rs1143634	0.2900	0.2371	0.1925	0.2192	0.1262	0.1251	99	98
	rs1143627	0.0698	0.3828	0.8601	0.0198*	0.3021	0.0269*	97	96
	rs16944	0.1222	0.1818	0.9619	0.0222*	0.1595	0.0432*	99	98
MYD88	rs6853	0.0095**	0.0984	0.6288	0.0040**	0.6148	0.0006**	98	97
IL2	rs2069762	0.5595	0.3935	0.8795	0.6212	0.7916	0.4635	93	92
TLR2	rs3804100	0.6630	0.3026	0.9578	0.2643	0.4670	0.6599	99	98
TNF	rs1800629	0.1039	0.3886	0.7375	0.5477	0.2966	0.4918	99	98
OPRM1	rs1799971	0.9141	0.9206	0.8920	0.7330	0.4115	0.8699	99	98
IL6	rs10499563	0.1020	0.4094	0.9372	0.1091	0.3271	0.0522	88	87
TLR4	rs4986790	0.4767	0.6256	0.5489	0.6963	0.8344	0.8491	97	96
	rs4986791	0.4596	0.8527	0.7698	0.8175	0.1860	0.5772	98	97
BDNF	rs6265	0.9877	0.3893	0.7122	0.1214	0.9622	0.3737	99	98
CASP1	rs554344	0.8532	0.6344	0.0632	0.6753	0.0516	0.8497	98	87
	rs580253	0.5243	0.8996	0.4892	0.1489	0.1832	0.1652	98	97
TGFB1	rs1800469	0.0367*	0.3946	0.3352	0.2887	0.4170	0.2668	99	98

3.10.2.1 Association of *MYD88* with spindle amplitude and ETDC

rs6853G (minor allele) was only observed in heterozygotes and was found to be associated with increased spindle amplitude, increased relative spindle amplitude, and decreased ETDC (Table 3.14, Figure 3.29). rs6853 A/G heterozygotes had a 1.39-fold higher median spindle amplitude (p = 0.0040), 1.69-fold higher median relative spindle amplitude (p = 0.0006) and 0.88-fold lower median ETDC (p = 0.0095) than A/A homozygotes (Appendix; Table 6.9, Table 6.10, Table 6.11). Because no rs6853 G/G homozygotes were identified in this sample, tests for SNP effects in the various models were unable to be performed.

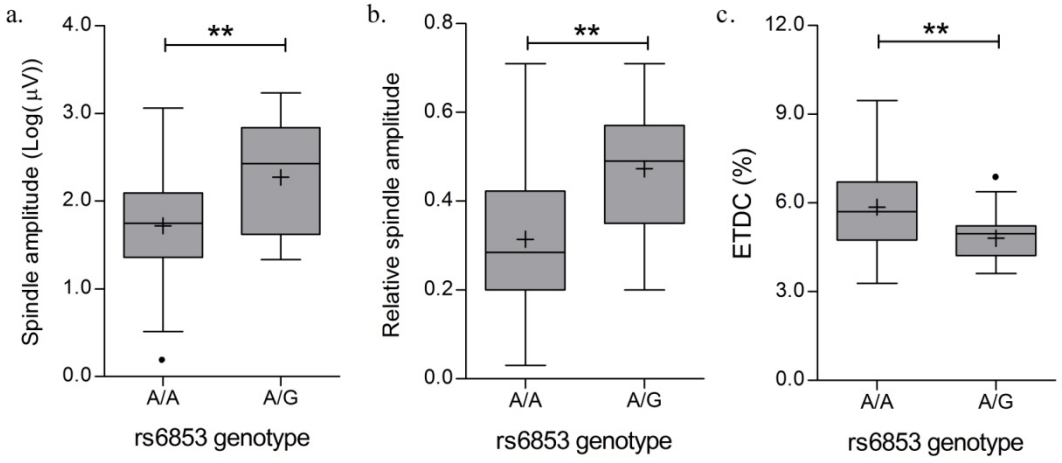

Figure 3.29: Association of rs6853 (*MYD88*) with spindle amplitude and ETDC.
Association of rs6853 with a. spindle amplitude; b. relative spindle amplitude; and c. ETDC. Box and whisker plots show median, minimum, maximum, and upper and lower quartiles for each genotype, the mean is marked with a cross and black circles denote outliers. Highly significant differences in median are indicated with a double asterisk (p < 0.01).

Based on histograms showing the distribution of spindle amplitude (Figure 3.1d), spindle amplitude was classified as either low (< 1.0 μV), moderate (1.0 μV to 2.5 μV) or high (> 2.5 μV), and distributions were compared between genotypes. Overall, approximately 80% of patients fell into the moderate group and the remaining were classified as either low or high. 40% of A/G heterozygotes fell into the high category compared with only 7.3% of A/A homozygotes, and no A/G heterozygotes fell into the low category compared with 8.4% of A/A homozygotes (p = 0.0013) (Table 3.15).

Table 3.15: Cross tabulation showing distribution of rs6853 (*MYD88*) genotypes with spindle amplitude categorised as either low, medium or high. (p = 0.0013).

rs6853 Genotype	Low (< 1.0 μV)	Medium (1.0 to 2.5 μV)	High (> 2.5 μV)
A/A	7 (8.4%)	70 (84.3%)	6 (7.3%)
A/G	0 (0.0%)	9 (60.0%)	6 (40.0%)

A scatter plot of spindle amplitude vs. ETDC, categorised by rs6853 genotype, showed that patients with the A/G genotype tended to cluster together at high spindle amplitude and low ETDC (Figure 3.30a). The relationship between spindle amplitude and ETDC was also influenced by rs6853 genotype. There was evidence of a negative relationship between ETDC and spindle amplitude for A/G heterozygotes (p = 0.0001), but not for A/G heterozygotes (Appendix; Table 6.13), and there was a significant difference in the intercept between A/G and G/G genotypes (p = 0.0087). No significant effects of rs6853 genotype on the relationship between BIS value and ETDC were observed (Figure 3.30b, Appendix; Table 6.13).

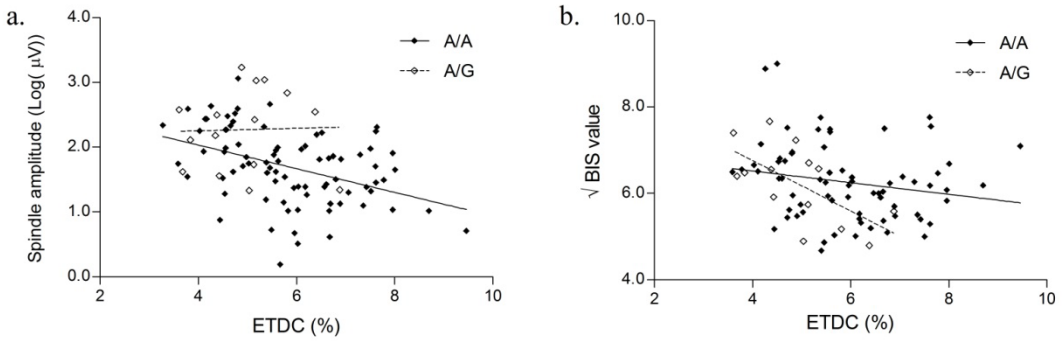

Figure 3.30: Scatter plots showing relationships between a. Spindle amplitude and ETDC, and b. BIS value and ETDC, categorised by rs6853 (*MYD88*) genotype.
Solid black circles denote A/A homozygous patients and black outlined circles A/G heterozygotes. Regression lines are also shown; solid black line shows the relationship between variables for A/A homozygotes, and dashed black line for A/G heterozygotes.

3.10.2.2 Associations with spindle amplitude

In addition to rs6853, KW-ANOVA identified two SNPs near *IL1B* – rs1143627 and rs16944 – associated with spindle amplitude and relative spindle amplitude (Table 3.14). For both SNPs, the strongest associations with spindle amplitude and relative spindle were observed in the over-dominant model. Weaker associations were also observed in the recessive model for spindle amplitude, and in the dominant model for relative spindle amplitude (Table 3.16, Table 3.17).

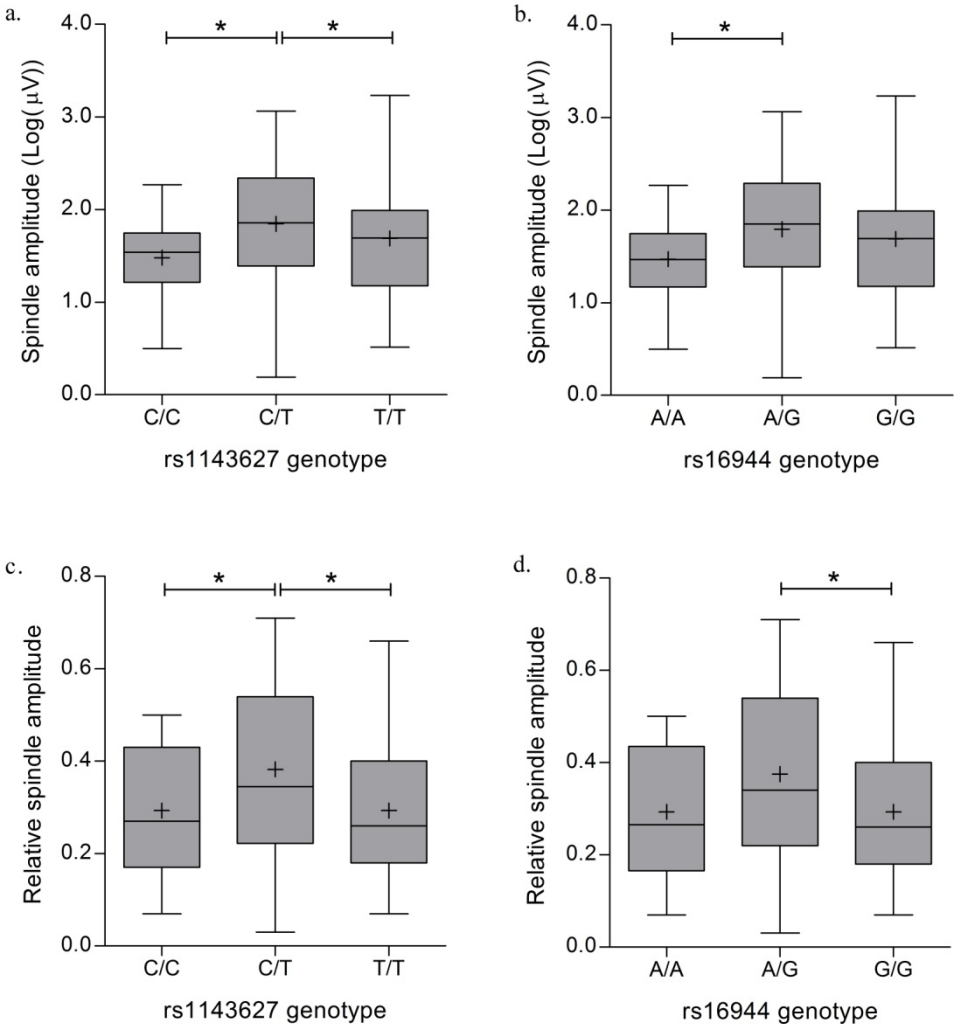

Figure 3.31: Association of *IL1B* SNPs with spindle amplitude.
a. Association of rs1143627 with spindle amplitude; b. rs16944 and spindle amplitude; c. rs1143627 and relative spindle amplitude; d. rs16944 and relative spindle amplitude. Box and whisker plots show median, minimum, maximum, and upper and lower quartiles of spindle amplitude for each genotype, the mean is marked with a cross and black circles indicate outliers. Significant differences in median are indicated with a single asterisk ($p < 0.05$) (Appendix; Table 6.9, Table 6.10).

Table 3.16: Individual *IL1B* SNP effects on spindle amplitude.
R = recessive model; D = dominant model; OD = over-dominant model. Significant *p*-values are indicated with a single ($p < 0.05$) or double ($p < 0.01$) asterisk.

SNP	Model	Genotype/s	n	Median (95% CI)	Fold Diff.	*p*-value
rs1143627	R	C/C	13	1.54 (1.13-1.75)	0.84	0.0495*
		C/T + T/T	84	1.84 (1.62-1.99)		
	D	C/C + C/T	61	1.83 (1.62-2.11)	1.08	0.1900
		T/T	36	1.69 (1.32-1.93)		
	OD	C/C + T/T	49	1.62 (1.39-1.79)	0.82	0.0092**
		C/T	48	1.97 (1.68-2.25)		
rs16944	R	A/A	12	1.47 (1.13-1.75)	0.80	0.0491*
		A/G + G/G	87	1.83 (1.62-1.97)		
	D	A/A + A/G	63	1.83 (1.62-2.04)	1.08	0.1917
		G/G	36	1.69 (1.32-1.93)		
	OD	A/A + G/G	48	1.58 (1.33-1.79)	0.84	0.0110*
		A/G	51	1.89 (1.71-2.25)		

Table 3.17: Individual *IL1B* SNP effects on relative spindle amplitude.
R = recessive model; D = dominant model; OD = over-dominant model. Significant *p*-values are indicated with a single ($p < 0.05$) or double ($p < 0.01$) asterisk.

SNP	Model	Genotype/s	n	Median (95% CI)	Fold Diff.	*p*-value
rs1143627	R	C+C	13	0.27 (0.16-0.44)	0.82	0.3015
		C/T + T/T	83	0.33 (0.28-0.35)		
	D	C/C + C/T	61	0.34 (0.28-0.44)	1.31	0.0395*
		T/T	35	0.26 (0.20-0.34)		
	OD	C/C + T/T	48	0.27 (0.21-0.34)	0.77	0.0072**
		C/T	48	0.35 (0.29-0.49)		
rs16944	R	A/A	12	0.27 (0.16-0.44)	0.84	0.3402
		A/A + A/G	86	0.32 (0.27-0.35)		
	D	A/A + A/G	63	0.34 (0.28-0.42)	1.31	0.0499*
		G/G	35	0.26 (0.20-0.34)		
	OD	A/A + G/G	47	0.26 (0.21-0.34)	0.76	0.0122*
		A/G	51	0.34 (0.29-0.47)		

3.10.2.3 Associations with delta frequency

A single SNP near *IL10* (rs1800896) associated with delta frequency ($p = 0.0176$). Mann-Whitney U tests identified a significant difference between the A/G and G/G genotypes ($p = 0.0055$), and no significant differences were observed between either the A/A and A/G or the A/A and G/G genotypes (Figure 3.32) (Appendix; Table 6.14) Associations were observed in both the over-dominant ($p = 0.0096$) and recessive models ($p = 0.0154$).

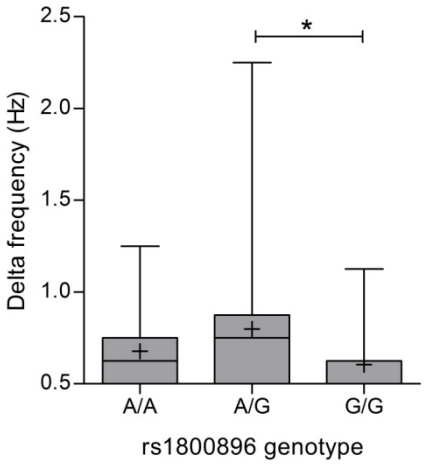

Figure 3.32: Association of rs1800896 (*IL10*) with delta frequency.
Box and whisker plot showing median, minimum, maximum, and upper and lower quartiles of delta frequency for each genotype, the mean is marked with a cross. Significant differences in median are indicated with a double asterisk ($p < 0.01$) (Appendix; Table 6.14).

Table 3.18: Effect of rs1800896 (*IL10*) on delta frequency.
R = recessive model; D = dominant model; OD = over-dominant model. Significant *p*-values are indicated with a single ($p < 0.05$) or double ($p < 0.01$) asterisk.

SNP	Model	Genotype/s	n	Median (95% CI)	Fold Diff.	*p*-value
rs1800896	R	A/A	19	0.50 (0.50-0.63)	0.72	0.0154*
(*IL10*)		A/G + G/G	80	0.69 (0.63-0.75)		
	D	A/A + A/G	66	0.63 (0.63-0.75)	1.00	0.4711
		G/G	33	0.63 (0.50-0.75)		
	OD	A/A + G/G	52	0.63 (0.50-0.63)	0.84	0.0096**
		A/G	47	0.75 (0.63-0.88)		

3.10.2.4 Associations with ETDC

In addition to rs6853, two other SNPs genotyped by MassARRAY were associated with ETDC – rs2794521 near *CRP* (p = 0.0381) and rs1800469 near *TGF1B* (p = 0.0367).

rs2794521C (minor allele) was associated with higher median ETDC and the strongest association was observed in the dominant model (p = 0.0119) (Table 3.19). A significant difference in median ETDC was observed between the rs2794521 C/T and T/T genotypes (p = 0.0306), with a 1.15-fold higher median ETDC observed in C/T heterozygotes relative to T/T homozygotes.

For rs1800469, a significant difference in mean ETDC was identified between the C/C and T/T genotypes (p = 0.0126) (Figure 3.33b). rs1800469T (minor allele) was associated with lower median ETDC with the strongest association observed in the recessive model (p = 02151) (Table 3.19).

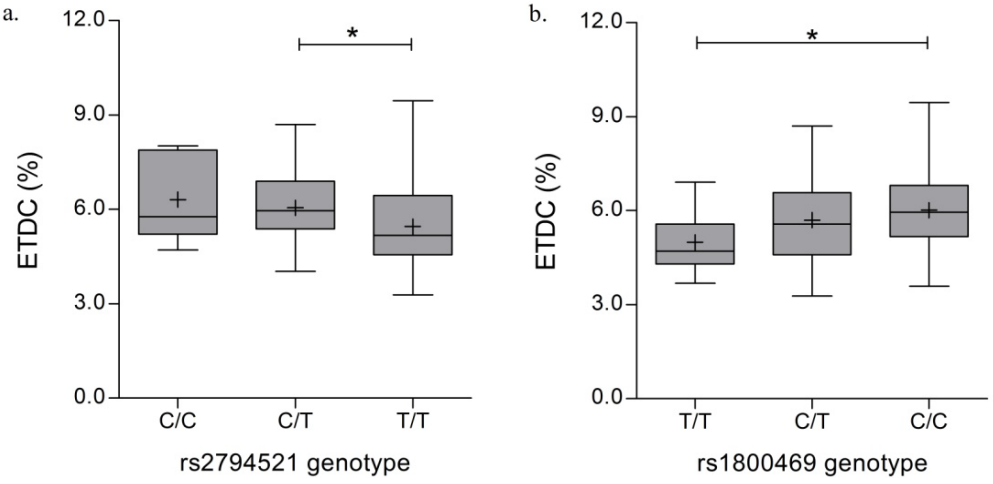

Figure 3.33: Association of a. 2794521 (*CRP*) and b. rs1800469 (*TGFB1*) with ETDC.
Box and whisker plots show median, minimum, maximum, and upper and lower quartiles for each genotype, the mean is marked with a cross. Significant differences in median are indicated with a single asterisk ($p < 0.05$) (Appendix; Table 6.11).

Table 3.19: Individual SNP effects on ETDC for associated SNPs genotyped by MassARRAY.

R = recessive model; D = dominant model; OD = over-dominant model. Significant *p*-values are indicated with a single ($p < 0.05$) or double ($p < 0.01$) asterisk.

SNP	Model	Genotype/s	n	Median (95% CI)	Fold Diff.	*p*-value
rs2794521	R	C/C	8	5.78 (4.71-7.96)	1.04	0.1785
(*CRP*)		C/T + T/T	88	5.58 (5.18-6.03)		
	D	C/C + C/T	39	5.83 (5.57-6.67)	1.13	0.0119*
		T/T	57	5.18 (4.80-5.62)		
	OD	C/C + T/T	65	5.39 (4.88-5.81)	0.90	0.0650
		C/T	31	5.96 (5.57-6.68)		
rs1800469	R	T/T	13	4.71 (4.26-5.67)	0.82	0.0215*
(*TGF1B*)		T/T + C/T	85	5.74 (5.39-6.10)		
	D	T/T + C/T	59	5.40 (4.80-5.83)	0.91	0.0685
		C/C	39	5.95 (5.39-6.66)		
	OD	T/T + C/C	52	5.60 (5.18-6.18)	1.00	0.8226
		C/T	46	5.58 (4.82-6.10)		

Chapter 4: Discussion

4.1 Genotyping results

Observed MAFs for all genotyped SNPs (excluding rs8066269) fell within ±0.16 of the corresponding MAF for the HapMap Caucasian population. SNPs rs7254543 and rs2069762 deviated the most from the HapMap MAF (+0.157 and +0.128, respectively). The differences in MAF between this sample and the HapMap are likely attributable to ancestral differences. The HapMap Caucasian population sample consists of Utah residents of northern and western European descent. The sample in the present study was of mixed descent; 77% of patients identified themselves as being of European ancestry and remainder as either Maori, Polynesian, or Asian.

For rs8066269, the MAF for the HapMap pilot Yoruban population was 0.157, and no frequency information was available for a Caucasian population. 25 samples were genotyped for rs8066269 and all were found to have the G/G genotype. Genotyping was not continued for this SNP as it was predicted that even if the A allele was identified in this sample, the low frequency would considerably limit statistical power in the association analysis.

Of the 34 SNPs included this study, two (rs13187565 and rs7254543) failed quality control tests for adherence to HWE and were therefore excluded from further analysis. The failure of SNPs to adhere to HWE can suggest problems in the dataset such as population stratification [179] or genotyping errors [180, 181]. Three SNPs (rs8066269, rs11466314 and rs11466004) were also found not to be polymorphic in this sample and were excluded from further analysis.

4.1.1 LD and haplotype phasing

Moderate to high levels of LD were observed for the majority of SNP loci in the same gene (*SGIP1*, *GABRA2*, *CACNA1G*, *IL10*, *IL1B*, *TLR4* and *CASP1*) (Table 3.7, Table 3.8). Plots of LD, as either D' or r^2, against distance between SNP loci, showed that LD tended to decrease only marginally with increasing distance (Figure 4.1) (Table 3.7, Table 3.8). All SNP pairs in complete LD were located within 5 kb of one another, however, high LD was observed for SNPs located as far as 48 kb apart, and moderate LD for SNP pairs as far as 89 kb apart. r^2 values showed the same general trend as D', with the exception that low r^2 values were observed for some SNP pairs even in very close proximity (<1 kb) (Figure 4.1b). D' provides a measure of recombinational history whereas r^2 measures both recombinational history *and* allele frequencies between two loci. High r^2 values indicate that SNPs have similar allele frequencies and are unlikely to have been separated by recombination. The average haplotype block size in European and Asian populations has previously been estimated to be around 20 kb, however, over half of the human genome is predicted to lie in a smaller number of large haplotypes blocks (>30 kb) [134]. Therefore it is not unexpected for SNPs nearly 50 kb apart to be in high LD.

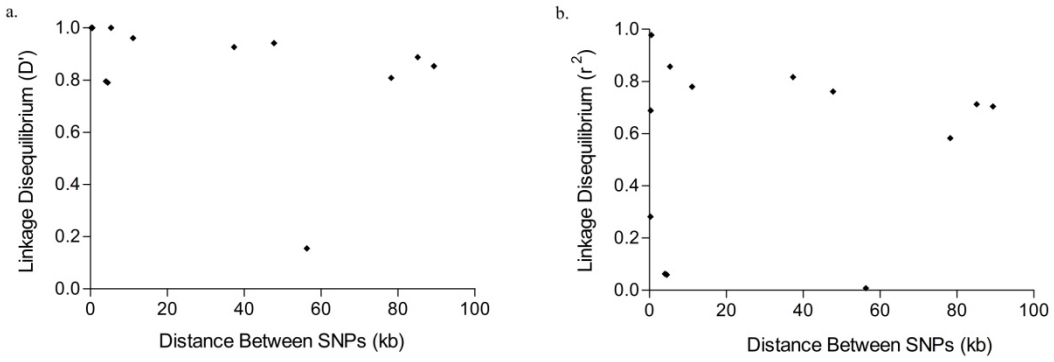

Figure 4.1: Relationship of LD with physical distance.
a. LD measured in D'; b. LD measured in r^2.

LD values determined in the present study were compared with the HapMap Caucasian population (Table 3.7, Table 3.8). Deviation from HapMap D' values ranged from -0.073 to +0.252 (mean = +0.017), and r^2 values from -0.119 to +0.027 (mean = -0.081). Differences in LD patterns between this sample

and the HapMap Caucasian population are suggested to in part be attributable to differences in ancestry. D' values can also be influenced by small sample size. However, small samples tend to lead to upwards fluctuations in D' [134, 135] and D' values were generally lower in this study than for the HapMap Caucasian population.

The EM algorithm in SNPAnalyzer 1.2A was investigated as a tool to resolve haplotype phase for three-SNP haplotypes in *SGIP1*, *GABRA2* and *IL1B*. The EM algorithm identified the same haplotypes as Haploview and one additional rare haplotype for *IL1B*, but the probability of over half of all haplotype calls for individual samples was below the desired threshold (90%). Because of the overall poor probability of calls, haplotype phase was not considered adequately resolved and haplotypes assignments were not used in the association analysis. It is suggested that the poor probability of the haplotype assignment is the result of a combination of small sample size, the low number of SNPs included in each haplotype, and only moderate LD between some SNP pairs.

Three-SNP haplotypes constructed in Haploview for *SGIP1*, *GABRA2* and *IL1B*, for this study were compared with haplotypes for the HapMap Caucasian population (Appendix; Table 6.8). For *SGIP1*, two additional rare haplotypes were identified in this study that are absent in HapMap Caucasians, and for *GABRA2* one additional rare haplotype was identified. As this study included participants of mixed ancestry, the additional rare haplotypes may have been contributed by participants of non-European descent, or alternatively, may be the result of genotyping errors. One of the requirements of performing a haplotype analysis is the need for a very low error rate as genotyping errors can create artificial rare haplotypes that are not truly present in the population [134]. Errors in PCR-RFLP genotyping can potentially arise as a result of incomplete digestion [182], or as result of polymorphisms in the primer binding region [183]. In order to reduce the likelihood of such errors, primer binding regions were checked for known polymorphisms using the UCSC Genome Browser; the ratio of band intensity was assessed for each sample; and any samples that gave unclear results were re-genotyped. It is also important to note that the haplotypes identified by Haploview are inferred using statistical algorithms, thus the haplotypes identified by the software are probable and may not represent the actual haplotypes present.

4.2 BIS value and ETDC

In accordance with previous studies, BIS value was found to decrease with increasing ETDC [184]. The correlation between EDTC and BIS value was weak (r = -0.2271, p = 0.0230). Other studies have also reported poor correlations between BIS value and ETAC of volatile anaesthetics [185, 186], furthermore, this relationship has been found to be significantly affected by age [187].

Two patients were found to have unexpectedly high median BIS values (81 and 79), which considered alone, would indicate inadequate anaesthesia. Both patients however were unconscious and ETDC values were within a suitable range for surgical anaesthesia. The high BIS values observed are likely to be artifactual, and highlight the fact that BIS value can be at times be misleading and cannot be relied on as a sole means to estimate anaesthetic depth. It is also important to note that these BIS values do not correspond to the median intra-operative BIS, but rather to a single a 60 sec EEG epoch recorded in the middle surgery.

4.3 Genetic associations with the EEG and EDTC

KW-ANOVA identified a total of nine SNPs located in eight different genes associated with the EEG or ETDC at $p < 0.05$, three of which were associated at $p < 0.01$. These are summarised in Table 4.1.

The associated SNPs were located in genes with four distinct types of function; ion channels, neurotransmitter signalling, endocytosis, and cytokine signalling. This is interpreted to suggest different pathways are involved in regulating the EEG during general anaesthesia. Sections 4.4 and 4.5 discuss the reported associations in more detail and the relevance of these associations to the EEG during general anaesthesia.

Table 4.1: Summary table of SNPs associated with the EEG or ETDC ($p < 0.05$).
Highly significant p-values ($p < 0.01$) are marked with an asterisk.

Gene	SNP	Phenotype	p-value
SGIP1	rs6681460	Spindle amplitude	0.0362
		Relative spindle amplitude	0.0357
GABRA2	rs279841	Spindle amplitude	0.0427
CACNA1G	rs7501581	ETDC	0.0097*
HCN2	rs873634	Relative spindle amplitude	0.0474
CRP	rs2794521	ETDC	0.0381
Il10	rs1800896	Delta Frequency	0.0176
IL1B	rs1143627	Spindle amplitude	0.0198
		Relative spindle amplitude	0.0269
	rs16944	Spindle amplitude	0.0222
		Relative spindle amplitude	0.0432
MYD88	rs6853	Spindle amplitude	0.0040*
		Relative spindle amplitude	0.0006*
		ETDC	0.0095*
TGF1B	rs1800469	ETDC	0.0367

4.3.1 The multiple testing problem

One difficulty with performing KW-ANOVA tests on all SNPs for all EEG traits and ETDC, is the multiple testing problem – the more simultaneous statistical tests performed the greater the likelihood of the null hypothesis being falsely rejected. The approach taken resulted in a total of 174 individual KW-ANOVA analyses being performed, which at an alpha level of 0.05 would be expected to result in 8-9 false positive results.

It is important that any adjustments for multiple comparisons finds a balance between decreasing the probability of false positives without over inflating the risk of false negatives, as this can result in important associations being over looked. One of the most commonly used methods to correct for multiple testing is the Bonferroni correction [188]. This method reduces the probability of false positives, however, it is often considered too conservative, particularly when variables are highly dependent [189].

The standard Bonferroni correction adjusts the significance threshold (α) based on the number of tests performed (n) (Equation 4.1).

$$\alpha/n = \text{adjusted } \alpha \qquad \text{(Equation 4.1)}$$

Using Equation 4.1, the Bonferroni correction gives an adjusted significance threshold value of $\alpha = 0.0003$ for this study. At this threshold no SNPs reach statistical significance.

Several SNPs in this study were found to be in high LD as measured by r^2 values, indicating that SNPs alleles are highly correlated. Moderate correlations were also observed between ETDC and spindle amplitude, and ETDC and delta amplitude. Therefore, within this data set, variables are not fully independent and the Bonferroni correction may indeed be too conservative. Rather than applying a correction for multiple testing, a lower significance level of $\alpha = 0.01$ is suggested as possibly more appropriate for this study. Using a significance threshold of $\alpha = 0.01$ only two SNPs (rs7501581 and rs6853) in this study achieve statistical significance and a further seven can be considered sub-threshold ($p = 0.01$ - 0.05). Additionally, while *p*-values measure the statistical significance of the result they do not provide a measure of effect sizes. A test may have a highly significant *p*-value yet this does not imply that the extent of effect is of biological or clinical importance, thus this also needs to be considered when evaluating the significance of association results.

4.4 Associations of candidate genes with the EEG and ETDC

4.4.1 *SGIP1*

SGIP1 encodes a protein involved in CME that plays an important role in the recycling of synaptic vesicles, channels, transporters and other membrane proteins in neuronal cells (Section 1.10.1). The present study identified a single SNP in *SGIP1* (rs6681406) associated with spindle amplitude at sub-threshold

significance ($p = 0.362$). The rs6681406 A/A genotype was found to be associated both with higher spindle amplitude ($p = 0.0103$) and relative spindle amplitude ($p = 0.0102$) in recessive models of effect. Effect sizes were only small, with 1.25- and 1.50-fold increases in median spindle amplitude and relative spindle amplitude, respectively, for A/A homozygous patients compared with carriers of the G allele.

rs6681406 is one of eight intronic SNPs previously associated with resting theta power in a GWAS of Plains American Indians by Hodgkinson et al. (2010) [95]. A recent study by Derringer and colleagues failed to replicate the association of any of these eight SNPs in a large European (n = 757) and an African sample (n = 309) [190], or for the combined data set. The failure to replicate was primarily attributed to differences in ancestry, in part resulting from differences in allele frequency or LD [190]. Of the eight significant SNPs identified by Hodgkinson et al. (2010), three were genotyped in this study, and only one was found putatively associated with the EEG. The failure to identify associations with the EEG for the other two SNPs (rs10889635 and rs2146904) may be the result of the difference in EEG phenotypes analysed in this study or ancestry differences. Participants in the present study data were of mixed, but predominantly European ancestry, and associations with delta and spindle oscillations were examined, but not with theta and alpha power.

The putative association of rs6681406 with spindle amplitude identified in the present study, in conjunction with the previously identified association with theta power [95], supports the earlier hypothesis that *SGIP1* may have broader effects on the EEG not solely limited to a single frequency band. Other loci that may regulate the EEG across the frequency spectrum have previously been identified, for example convergence of linkage peaks to alpha, beta and theta EEG power have been found on chromosome 5q13-14 [93].

All three *SGIP1* SNPs genotyped were intronic SNPs of unknown function and the underlying cause of the association of rs6681406 with spindle amplitude or ETDC is unknown. Association of intronic variants with disease of other phenotypes is often thought to be due to their being in LD with functional SNPs. Another possibility underlying associations of non-coding variants, such as rs6681406, is that they might alter the regulation of gene expression, for example,

by affecting transcription factor binding, RNA splicing, or via microRNA (miRNA) mediated gene regulation.

One mechanism by which *SGIP1* variation is suggested to influence the EEG, is through altered ion channel or receptor recycling by CME. Ion channel recycling plays an important role in the regulation of ion channels and their respective currents and CME has been directly shown to play a role in the regulation of various ion channels, including voltage gated potassium channels in neuronal cells [191]. Both over expression and knockdown of *SGIP1* have been shown to inhibit endocytosis [137], thus variability in the function or expression levels of *SGIP1* between individuals might also affect endocytosis and the efficiency of receptor and channel turnover or neurotransmitter uptake, thereby influencing neuronal activity. This in turn may potentially manifest not only as variability in the theta frequency band but extend to other EEG frequencies.

4.4.2 *GABRA2*

Three SNPs in *GABRA2* were genotyped by PCR-RFLP and tested for associations with the EEG and anaesthesia administration. Only one of these SNPs, rs279841, was associated with the EEG at sub-threshold significance (p = 0.0427) and no associations were identified for rs572227 and rs279845. rs279841A was associated with increased spindle amplitude and A/A homozygous patients had a 1.28-fold higher median spindle amplitude than carriers of the G allele (p = 0.0124).

rs279841 has previously been associated with alcohol dependency [92] and beta power in the resting EEG [92, 192]. Numerous other SNPs in *GABRA2* have also been associated with these phenotypes and associations with alcohol dependency replicated in various studies (reviewed in [145]). The association of *GABRA2* variants with both alcohol dependency and increased beta power has led to the hypothesis that *GABRA2* may influence risk for alcohol dependence by modulating neuronal activity [92]. While associations with beta power were not tested for in this study, the identification of a putative association with spindle amplitude suggests *GABRA2* variability might also influence other frequency bands.

Functional *GABRA2* SNP(s) have not yet been identified [171]. In all of the studies linking *GABRA2* with alcohol dependency or beta activity, only non-coding variants have been associated with either phenotype, suggesting that *GABRA2* variation may influence neuronal excitability by affecting gene regulation. Haughey and colleagues (2008), have previously reported differing *GABRA2* mRNA levels in the post-mortem prefrontal cortex between *GABRA2* genotypes, however, the difference in expression level between genotypes observed was less than two-fold [171]. Three SNPs in perfect LD; rs573400 in the 3' UTR, rs279871 in intron 7, and rs279858 – a synomynous coding SNP, were associated with mRNA *GABRA2* levels, leading the authors to speculate that *GABRA2* genotype may be involved in predetermining $GABA_A$ receptor subunit assembly and/or function [171].

The three SNPs genotyped in the current study are located in a 113 kb haplotype block beginning upstream of the gene 3′ end and spanning a large portion of *GABRA2* (Appendix; Figure 6.27). LD data was available for the HapMap Caucasian population for two of the three SNPs (rs573400 and rs279858) associated with *GABRA2* mRNA levels by Haughey et al. (2008). rs279841 is located in the same haplotype block and is in high LD with both of these SNPs (Table 4.2) (Appendix; Figure 6.27), prompting the suggestion that differential gene regulation may underlie the putative association identified in this study. It is unknown if rs279841 has a direct effect on gene expression itself, or whether its association is due to it being in high LD with an as yet unidentified functional SNP in this haplotype block.

Table 4.2: LD between rs279841 and SNPs previously associated with *GABRA2* mRNA levels in the pre-frontal cortex by Haughey et al. (2008) [171].

SNP 1	SNP 2	D'	r^2
rs573400	rs279858	1.0	0.934
rs573400	rs279841	0.93	0.835
rs279858	rs279841	1.0	0.902

The *GABRA1* gene encodes the $GABA_A$ receptor α1 subunit and presents another particularly viable candidate gene for association with the EEG during general anaesthesia. In the thalamus, α2 subunit expression is high during embryonic

development, and during postnatal development α2 is replaced by the α1 subunit [193]. Within the adult brain, the α2 subunit exhibits a localised distribution with preferential expression in the forebrain and cerebellum, and limited expression in the thalamus. Conversely, the α1 subunit is widely distributed and is highly expressed in thalamic neurons [194-196]. The incorporation of different α subunits into $GABA_A$ receptors effects neuronal excitability by influencing the kinetics of deactivation of GABA-induced current, with faster decay time observed in receptors containing the α1 subunit than those containing α2 [197]. Genetic variability affecting expression levels of the different α subunits, might affect the relative abundance of each which in turn might to lead to differences in neuronal excitability due to differences in $GABA_A$ receptor kinetics.

4.4.3 *CACNA1G*

T-type Ca^{2+} channels underlie the I_t current which plays an important role in the generation of both spindle and delta waves (Sections 01.4.3 and 1.4.4). A single T-type Ca^{2+} channel gene – *CACNA1G* – was investigated for associations with the EEG and ETDC in this study. Of the three *CACNA1G* SNPs genotyped, an association was only found for rs7501581 with ETDC (p = 0.0097). rs7501581 was selected based on MAF and its position upstream of the gene 5' end. SNPs in this region may affect gene regulation if they occur at transcription factor binding sites, or alternatively, might be in LD with SNPs with regulatory or other functional effects.

Associations of rs7501581 with ETDC were identified in both the recessive (p = 0.0206) and over-dominant models (p = 0.0071). It was suggested rs7501581 variability might affect the relationship between EDTC and the BIS value, however linear regression analysis found no significant effect of rs7501581 on this relationship in any of the effect models (Appendix; Table 6.12).

CACNA1G was selected as a candidate gene based on the role of I_t in the generation of synchronised EEG activity, and on previously reported findings showing altered slow wave EEG activity in *CACNA1G*$^{-/-}$ mice [155]. α1G is also strongly expressed within the thalamus in thalamic relay neurons [154]. In addition to its role in the generation of synchronised EEG activity, $Ca_v3.1$ is

implicated in pain signalling, sleep-wake cycles and absence epilepsy (reviewed in [41]). Interestingly, the results in this study suggest an association with ETDC, and no associations were identified between *CACNA1G* and the EEG. Associations of polymorphisms in any of the T-type Ca^{2+} genes with anaesthesia have not been reported to date.

Various general anaesthetics have previously been demonstrated to reversibly block I_t *in vitro* at clinically relevant concentrations in a dose dependent manner [198-201], and isoflurane has also been reported to inhibit LTS in TC neurons [202]. While the clinical effect of I_t blockade by certain anaesthetics is unclear [198], such results lend support for the putative association identified in the present study. Conversely, in a study by Petrenko et al. (2007) examining the effects of volatile anaesthetics on *CACNA1G*$^{-/-}$ mice, the hypnotic and immobilizing effects of volatile anaesthetics were not altered in *CACNA1G*$^{-/-}$ mice, however, KO mice took longer to develop hypnosis, suggesting T-type Ca^{2+} channels might be involved in the induction of anaesthesia by volatile anaesthetic agents [203].

4.4.4 *HCN1* and *HCN2*

Aside from a weakly significant association identified for rs873634 (*HCN1*) (p = 0.0474), *HCN1* and *HCN2* were not found to be associated with the EEG or ETDC.

There are over 900 SNPs in or near each of these genes listed in NCBI dbSNP. In the present study, just two SNPs located upstream of the gene 5' end were genotyped for each gene, and only one SNP in each gene passed quality control checks for inclusion in the association analysis. All four SNPs selected in these genes were chosen based on MAF and their location upstream of the gene 5' end. As the vast majority of *HCN1* and *HCN2* polymorphisms have not been tested for associations, the failure to identify associations for *HCN2*, and the identification of only one weak association for *HCN1*, does not imply that variability in these genes does not influence the EEG or ETDC.

4.5 Associations of inflammatory genes with the EEG and ETDC

For the inflammatory gene set, only one gene – *MYD88* – was found to be associated with the EEG at $p < 0.01$, and a further three genes were associated at sub-threshold significance. *MYD88* is involved in the IL-1R signalling pathway and was found to be associated with spindle amplitude and ETDC. Interestingly *IL1B*, which signals via IL-1R, was also associated with spindle amplitude at sub-threshold significance. Other than *MYD88*, no other genes involved in IL-1R mediated signalling were included in this study and no associations were identified for genes involved in toll-like receptor (TLR) signalling. Associations with the EEG or ETDC were also identified for SNPs in *Il10* (delta frequency, $p = 0.0176$), *CRP* (ETDC, $p = 0.0381$), and *TGFB1* (ETDC, $p = 0.0367$).

All associated SNPs were located in non-coding regions upstream of the gene 5' end and different gene regulation is predicted to underlie the identified associations (Sections 4.5.2-4.5.4). The cytokine genes *IL1B* and *IL10*, along with *MYD88*, were the most strongly associated with the EEG and these genes and their relevance to the EEG are discussed in more detail in the following sections.

4.5.1 Relevance of associations to the EEG

Systemic inflammation is mirrored by an inflammatory response in the brain involving an increase in the levels of pro-inflammatory cytokines [108]. Within the brain, cytokines are thought to act as neuronal modulators and have been demonstrated to influence ion channel and receptor function, thus regulating neuronal activity (reviewed in [119]).

Controlled changes in brain cytokine levels induced by systemic inflammation are thought to play an important role in mediating the behavioural changes required for recovery from infection or trauma (sickness behaviour) [106, 204]. Chronic changes in or disregulation of brain cytokine levels can lead to more adverse clinical symptoms [106], and have previously been associated with bipolar-disorder [205], and implicated in the pathophysiology of major depression, schizophrenia and Alzheimer’s disease (reviewed in [206]). The results from the

current study are interpreted to suggest that genetically determined variability in cytokine levels/signalling may influence the EEG during general anaesthesia. This effect is presumed to be mediated via cytokine modulation of ion channel or receptor activity, potentially involving upregulation of brain cytokine levels in response to surgical trauma.

In particular, the presently reported results suggest that *IL1B* and *MYD88* variability may underlie some of the variability in spindle wave activity observed during general anaesthesia. *IL1B* encodes IL-1β, a key pro-inflammatory cytokine that belongs to the IL-1R ligand family. IL-1β is primarily produced by macrophages, monocytes and endothelial cells, and is also constitutively expressed in the brain at low levels, along with its receptor IL-1R (reviewed in [207]). *MYD88* encodes the cytosolic adaptor protein – MyD88 – which acts a signal transducer in the IL-R and TLR mediated signalling pathways [208-210]. These homologous pro-inflammatory signalling pathways play important roles in mammalian host defences in both the innate and adaptive immune responses [211]. Upon activation, IL-1R interacts directly with MyD88 which activates signalling via IRAK (interleukin-1 receptor-associated) kinases and TRAF6 (TNF receptor associated factor 6) leading to NF-κB activation, and subsequently pro-inflammatory cytokine production and an inflammatory response [103, 212].

In addition regulating the inflammatory response in peripheral immune cells, IL-1β also has important effects on brain functioning and is thought to act as a primary mediator of immune system-to-brain communication [106]. *In vitro* studies investigating the electrophysiological effects of IL-1β on neuronal cells have demonstrated IL-1β can influence voltage dependent calcium currents and GABA-ergic signalling via $GABA_A$ receptors in certain cell types, as well TRPV1 (transient receptor potential vanilloid 1) and glutamate receptors (reviewed in [119, 213]). For example, IL-1β has been demonstrated to inhibit $GABA_A$ receptor mediated currents in hippocampal neurons *in vitro* [214], and also to reduce voltage-dependent Ca^{2+} currents mediated by N-type Ca^{2+} channels in cultured cortical neurons [215]. Furthermore, several studies have reported the effects of IL-1β on neuronal cells to be dose-dependent [214, 216-218]. IL-1β has also previously been suggested to affect I_h, however, regulation of I_h by IL-1β has not yet specifically been addressed [105]. At least some of the effects of IL-1β on

neuronal cells have been shown to require MyD88 [207], supporting the association of *MYD88* with the EEG. Tabarean et al. (2006) have demonstrated IL-1β induced hyperpolarisation and reduced firing rates in hypothalamic neurons and these effects were absent in mice lacking IL-1R and MyD88 – demonstrating that these effects require both IL-1R and MyD88 [207].

Brain mRNA levels of IL-1β, as well as IL-6 and TNFα, have been found to be elevated following peripheral lipopolysaccharide (LPS) administration in rodents [109-114], and peripheral LPS administration is also known to induce a behavioural response presumed to be mediated by elevated pro-inflammatory cytokine levels in the brain [204, 219]. As surgical trauma is associated with an inflammatory response involving the upregulation of these cytokines , it could reasonably be hypothesised that a similar elevation in brain cytokines occurs during surgery, however, to date no studies have directly examined the short-term effects of surgery on brain cytokines.

In all of the above mentioned studies investigating the effects of systemic inflammation on brain cytokine levels, the inflammatory response was stimulated by the administration of an exogenous endotoxin. The inflammatory response to surgery however, is induced under sterile conditions as a result of traumatic tissue injury. Therefore whether the same effects on brain cytokine levels induced by peripheral LPS occur in response to surgical trauma is not known. Elevated IL-6 and IL-8 levels in cerebrospinal fluid (CSF) following hip replacement surgery have been reported, conversely IL-1β, IL-10 and TNFα levels in the CSF have been found not to be elevated [220, 221]. A lack of correlation between plasma and CSF IL-6 levels was taken to suggest elevated CSF IL-6 levels resulted from central IL-6 secretion [221]. Moreover, elevated post-surgical CSF IL-6 levels have been found to correlate with sleep disturbances [220], suggesting effects of centrally expressed cytokines on neuronal function following surgery. Overall, these studies demonstrate elevated cytokine levels in the CNS following surgery, and suggest subsequent effects on neuronal functioning. However, cytokine levels were only measured pre- and post-operatively (hours to days) in the CSF, therefore the extent of any changes in brain cytokine levels within the intra-operative period remain unclear. Furthermore, IL-1β levels were found not be elevated in the CSF following surgery. Therefore, whether brain levels of this

cytokine are elevated during surgery, and to what extent if so, is unknown. As brain *IL1B* expression is found to be very low under basal conditions [110], it is uncertain if differences in basal levels between individuals would have a significant effect on neuronal activity that could result in differences in the EEG. It should also be noted that the duration and type of surgical procedure would likely affect the extent of any changes in cytokine gene expression, as the extent of the inflammatory response is related to the magnitude of surgical trauma [120].

IL-10 is a pro-inflammatory cytokine produced by a variety of immune cells, monocytes, macrophages and T-helper cells, and has also been demonstrated to be constitutively expressed by glial cells in the brain [222]. The primary function of IL-10 is to reduce the inflammatory response, this is achieved largely via modulation of cytokine release by monocytes and macrophages (reviewed in [223, 224]). Unlike IL-1β, the electrophysiological effects of IL-10 have not been well-studied and whether this cytokine has regulatory effects on ion channels and receptors is not known. IL-10 inhibits the expression of pro-inflammatory cytokines such as IL-1β [225], and has been shown to block the inhibitory effects of IL-1β on long-term potentiation in hippocampal cells [226] and to block LPS induced behavioural effects in rats [219]. It is therefore suggested variable *IL10* expression might influence the EEG via IL-10 mediated regulation of brain pro-inflammatory cytokines. Thus the balance between levels of pro- and anti-inflammatory cytokine levels in the brain may be an important contributing factor to the EEG during general anaesthesia.

While previous studies investigating the influence of cytokines on neuronal activity and behaviour support the association of cytokine genes (and mediators of cytokine signalling) with the EEG, an alternative explanation is that the identified SNPs are tagging functional effects of other nearby genes involved in regulation of the EEG. This alternative remains to be investigated.

4.5.2 *MYD88*

MYD88 is located on chromosome 3 at 3p22 on the forward strand, spans approximately 4.5kb, is alternatively spliced to produce 13 different transcripts, 8 of which are protein encoding (NCBI Gene ID: 4615) (Ensembl:

ENSG00000172936). The strongest association with the EEG and ETDC identified in this study was for a single SNP (rs6853), located in the 3' UTR of *MYD88*. In this study rs6853G was present at a frequency of only 7.7% and was only found in A/G heterozygotes (15.3% of patients). The observed MAF was lower than in the HapMap Caucasian population (MAF 11.5%). One of the limitations of this study that is particularly relevant to analysing associations of this SNP, is the small sample size (Section 4.6.2). The G allele was found to be associated 0.88-fold lower median ETDC (p = 0.0095), 1.39-fold higher median spindle amplitude (p = 0.0040) and 1.69-fold higher median spindle amplitude relative to ETDC (p = 0.0006). The EEG correlation analysis revealed a modest correlation between spindle amplitude and ETDC and rs6853 genotype was found to influence this relationship. The relationship between ETDC and BIS was not significantly affected by rs8365 genotype.

Previous studies have reported associations of *MYD88* variability with various conditions including Bueger disease (a rare vascular disorder) [227], Hogdkin's lymphoma [228] and response to the measles vaccine in adolescents [229]. The genomic region harbouring *MYD88* (3p22) has also been identified as a putative locus for autosomal dominant nocturnal frontal lobe epilepsy [230]. To date no associations been *MYD88* polymorphisms and the EEG or anaesthesia have been reported.

The SNP rs6853 is located in the 3' UTR of *MYD88* and effects on gene expression are predicted to underlie the identified association. Gene 3' UTRs contain polyadenylation sequences required for the addition of the poly(A) tail which is important for mRNA stability and translational efficiency. This region also contains binding sites for regulatory factors [231] and may contain target sites for regulation by miRNAs [232]. miRNAs are small single stranded RNA molecules that are involved in post-transcriptional regulation of gene expression. miRNAs recognise and bind to target mRNAs by base-pairing interactions, and act to down regulate gene expression either by repressing translation or bringing about the cleavage of target mRNAs [233]. They are often transcribed from intronic regions and predominantly target untranslated regions, in particular gene 3' UTRs [234, 235]. Polymorphisms in either miRNAs themselves, or in the target region to which they bind, might therefore influence gene expression by disrupting binding interactions between the miRNA and target region.

Accordingly, polymorphisms in the 3' UTR region have previously been associated with a variety of conditions and have been shown to affect expression of associated genes [236-240].

An alternative to the above suggestion is that rs6853 might not be functional itself, and instead be tagging the effects of a functional SNP in *MYD88*, or in another nearby gene. Using Haploview, downloaded data for the HapMap Caucasian population, and the haplotypes block definition of Gabriel et al. (2002), rs6853 was found to lie in a 29 kb LD block that encompasses all of *MYD88* along with the upstream gene *ACAA1* (Acetyl-CoA Acyltransferase 1) and part of *DLEC1* (Deleted in Lung and Esophageal Cancer 1) (Appendix; Figure 6.28a).

The rs6853G allele is only found on two rare haplotypes in HapMap Caucasians and tags several other SNPs not present on any other haplotypes (Appendix; Figure 6.28b). The free online tool F-SNP (http://compbio.cs.queensu.ca/F-SNP/) [241] was used to search for predicted functional SNPs in this block. Four non-synonymous SNPs with functional effects were predicted in or near *MYD88*, however, the MAF for each of these polymorphisms was <1%. F-SNP did not predict any functional effects for rs6853. Six SNPs with functional effects were predicted in or near *ACAA1*. Of these six SNPs, two had MAFs >5% in the HapMap Caucasian population, and a further two had MAFs of 1 to 5%. One of these SNPs – rs156265G>C (Glu172Asp), a non-synonymous coding SNP – is present at a frequency of 8.5% in the HapMap Caucasian population. F-SNP predicted functional effects of this SNP on mRNA splicing, transcriptional regulation and deleterious effects on protein coding. This SNP has previously been reported to be associated with the effects of endotoxin exposure on asthma risk in children, however, rs156265 was not found to be in LD with any SNPs in *MYD88* [242]. Another SNP in this block, rs5875 (MAF = 11.5%), is located in the *ACAA1* 3' UTR. F-SNP predicted a functional effect of rs5875 on transcription factor binding. This SNP is in perfect LD with rs6853 it is possible rs6853 is tagging the functional effects of rs5875, or another nearby functional SNP.

ACAA1 (NCBI Gene ID: 30) encodes an enzyme required for fatty acid β-oxidation in peroxisomes and is expressed throughout the body in a diverse array of tissues, including the brain (GeneNote Version 2.3 [243]). Based on the role of *MYD88* in cytokine signalling and the previously reported finding that some IL-1β cytokine effects on neuronal cells require functional *MYD88* [207], *MYD88* is

proposed as a more probable candidate for the association with the EEG, however an underlying association with *ACAA1* cannot be ruled out.

4.5.3 *IL1B*

Two SNPs in *Il1B* (rs1143627, rs16944) were associated with spindle amplitude and spindle amplitude relative to ETDC. *IL1B* spans approximately 7 kb, is comprised of six coding exons and is located in an interleukin gene cluster on the reverse strand of chromosome 2 at 2q14 (NCBI Gene ID: 3553).

SNPs rs1143627 (−31T>C) and rs16944 (−511C>T) have been extensively studied and have been associated with various and diverse diseases including psoriatic arthritis [244], schizophrenia [245, 246], febrile seizures [247], and breast, lung and gastric cancer [248-250]. Associations of either of these SNPs, or other *IL1B* polymorphisms, with the EEG have not been previously reported.

LD analysis in Haploview demonstrated that rs1143627 and rs16944 are in near perfect LD (D' = 1.0, r^2 = 0.98) (Section 3.8.2), indicating they have not been separated by recombination and each near perfectly tags the other. LD between rs1143627 and rs16944 was very similar in this sample and the HapMap Caucasian population (Table 3.8). Both SNPs are located upstream of the gene 5' end in a 3 kb haplotype block, no other genes are located in this block (Appendix; Figure 6.29).

The SNP rs1143627 is located in the *1L1B* TATA box [249] and has been identified as a transcription factor binding site for several transcription factors by ChIP-seq [251]. Furthermore, electrophoretic mobility shift assays have also revealed differential protein binding to the DNA region harbouring rs1143627 [250, 252]. Using promoter reporter assays, Lind et al. (2010) have reported higher expression levels from the T allele than the C allele [252], and 2.2 times higher expression from the from the T allele has also been reported using *in vitro* allele-specific transcript quantification [253]. Allelic differences in protein binding at rs16944 have failed to be identified [250, 254], suggesting that the association of rs16944 is due to its high LD with rs1143627.

Based on these previous studies, the effects of variant rs1143627 on the EEG are suggested to be due to by differential transcription factor binding and

consequently altered gene expression, and that rs16944 is likely tagging the functional effects of rs1143627. In this study, the “low expression” variant (rs1143627C), was observed at a frequency of 38.1%, similar to the HapMap Caucasian population (36.3%). Associations were observed in all three models for rs1143627C, and the strongest association was identified in the over-dominant model ($p = 0.0092$ and $p = 0.0072$) (Table 3.16, Table 3.18). Given the predicted function of this polymorphism on gene expression, the relevance of the association in the over-dominant model is unclear, although the effect of rs1143627 genotype may potentially be influenced by synergistic effects with other functional variants.

4.5.4 *IL10*

In the present study, a single SNP in *IL10* (rs1800896) was found to be associated with delta frequency ($p = 0.0176$). *IL10* is comprised of 5 exons, spans 5.1 kb and is located on the reverse strand of chromosome 1 at 1q31-q32 (NCBI Gene ID: 3586) [255].

SNP rs1800896 (−1082G>A) is one of three well studied SNPs located in the proximal promoter region of *IL10*, the other two being rs1800871 (−819C>T) and rs1800872 (−592C>A) [256]. *IL10* promoter SNPs and SNP haplotypes have been associated with various diseases including graft-versus-host disease [257, 258], advanced liver disease [259], and Alzheimer’s disease [260-262].

The association of rs1800896 identified in this study is suggested to be attributable to differences in *IL10* gene expression. Reuss et al. (2002) have studied the function of *IL10* promoter polymorphisms and found that rs1800896A confers optimal binding ability for the negative transcriptional regulator PU.1. Accordingly, the presence of the A allele has been found to lead to lower transcriptional activity and thereby lower IL-10 production than the G allele [256, 263]. The two *IL10* SNPs genotyped in this study (rs1800896 and rs1800871) and a third SNP (rs1800872), have previously been demonstrated to be complete LD and are found in only three possible haplotype combinations in Caucasians; GCC, ACC and ATA [256, 264, 265]. The ATA haplotype has been associated with lower transcriptional activity than the GCC haplotype, and the ATA/ATA

homozygous genotype with lower IL-10 production in whole blood cell cultures relative to all other genotypes [265]. In the present study, patients homozygous for the "high expression" variant (rs1800896G) were found to have a lower median delta frequency than A/G heterozygotes (0.67-fold, p = 0.0055), however, no significant difference was found between G/G and A/A homozygotes.

In addition to confirming the putative association identified in this study, a more comprehensive investigation of other *IL10* promoter polymorphisms is suggested. In addition to proximal-promoter SNPs, SNPs in the distal promoter region, and microsatellites in both the distal and proximal promoter regions (IL10.R $(CA)_n$ and IL10.G $(CA)_n$, respectively), have also been suggested to affect gene expression and susceptibility to a variety of diseases [266, 267] and might also influence the EEG.

4.6 Study limitations and confounding factors

4.6.1 Number of SNPs genotyped

A large scale study, such as GWAS, was beyond the scope of this project and only a limited number of SNPs were able to be included, limiting the amount of genotyping data able to be generated. Alternative feasible genotyping approaches include high resolution melting and RT-PCR based methods, however, these approaches would also have limited the number of SNPs genotyped and would also require tests to be performed in duplicate. The advantage of using PCR-RFLP over other such methods, was that it allowed DNA to be conserved as part of the larger study as tests were only performed once unless the genotyping result was unclear.

As only two to three SNPs per gene were genotyped in this study, only a small proportion of the genetic variability in each candidate gene was examined, potentially limiting the power of the approach to identify genes associated with the EEG. For example, only three SNPs in a single $GABA_A$ receptor gene were examined for associations in this study. The *GABRA2* SNPs genotyped are only three of 25 SNPs previously associated with beta oscillations by Edenberg et al.

(2004). The HapMap project contains information on over 150 *GABRA2* SNPs, and almost 3000 SNPs are listed in or near *GABRA2* in NCBI dbSNP. Furthermore, there are an additional 5 genes encoding α subunits and numerous genes encoding other $GABA_A$ receptor subunits. Therefore the potential contribution of the vast majority of $GABA_A$ receptor variability to the EEG is yet to be explored.

An alternative approach would have been to perform a more comprehensive analysis of a single gene using a SNP tagging approach. Such an approach may possibly have been more likely to detect potential associations in a single gene and provide a more refined picture. However, as no studies investigating genetic differences contributing to the EEG during general anaesthesia have yet been reported, the approach taken provided the advantage of giving a broader picture, and enabled identification of a number of genes putatively associated with the EEG that could be subject to more intense study in further work.

4.6.2 Multiple testing problem

The large number of statistical tests performed introduces the problem of multiple testing resulting in an increased likelihood of false positive results. This issue is addressed in section 4.3.1.

4.6.3 Sample size

This study included a total 125 participants. Samples from all patients were included in the PCR-RFLP genotyping, and only 100 were sent to AGRF for genotyping by MassARRAY. This small to moderate sample size often resulted in only a small number of patients homozygous (or even heterozygous) for the minor allele, hence limiting statistical power. For example, rs6853G was observed at a frequency of 7.7% and only 15 patients, all of whom were A/G heterozygous, were found to carry the G allele. In order to confirm the presently reported associations, these results need to be replicated in a larger sample. This may also help clarify the mode of effect of the examined SNPs, as associations were reported for several SNPs in more than one effect model.

4.6.4 Ancestry of participants

The participants included in this study were of mixed descent which may confound the association results. Because of the small sample size, performing statistical tests on each population group would markedly reduce statistical power and therefore all participants were pooled together. The study sample does however provide a reasonable subset of the New Zealand population which is approximately 68% European, 9% Asian, and 22% Maori and Polynesian [268].

4.6.5 Surgical procedures

Patients included in this study underwent one of three major categories of surgery; general (37%), gynaecological (51%) and orthopaedic (12%). The high proportion of gynaecological patients also introduced a sex bias into the study (82% of participants were female). The diversity of surgical procedures undertaken by participants potentially introduces an additional confounding factor. Different surgical procedures may cause different levels of trauma to the body, this may be particularly relevant to effects of cytokines on neuronal activity. As with ethnicity, the small sample size limited the ability to perform separate analysis, and due to limitations of the software, such confounding factors were not able to be incorporated into the non-parametric tests used.

4.6.6 Effect sizes and clinical relevance

The effect sizes for significant associations identified in this study were small – ranging from a fold-difference of 0.77 to 1.55. With such small effects, these SNPs are not likely to be clinically relevant or have useful clinical application. The association of numerous SNPs in various genes, each with small affect, suggests that the EEG during general anaesthesia is regulated by numerous genes in different pathways, each with a small effect.

4.7 Conclusions

This study identified a number of SNPs in a variety of genes putatively associated with the EEG during general anaesthesia with desflurane. Associations were identified for SNPs in genes with a variety of different functions and effect sizes were small, suggesting that the EEG during general anaesthesia is regulated by numerous genes in different pathways, possibly with an additive effect.

Putative associations with spindle amplitude (or relative spindle amplitude) were identified for five genes with four distinct types of function; ion channels (*HCN2*), neurotransmitter signalling (*GABRA2*), neuronal component recycling (*SGIP1*), and cytokine signalling (*MYD88* and *IL1B*). This prompts the suggestion that individual differences in the EEG during general anaesthesia may not only be attributable to variability in genes directly involved in the generation of synchronised EEG activity – such as ion channels and neurotransmitter signalling – but also to other pathways involved in regulating neuronal cell components involved in generating the synchronised EEG. Furthermore, two of the genes associated with spindle amplitude have previously been associated with resting theta and beta power (*SGIP1* and *GABRA2*, respectively), suggesting that the effects of some genetic loci on the EEG may not be restricted to single frequency bands.

Anaesthetic agents are thought to influence the inflammatory response following surgery by modulating cytokine release, resulting in a slight immune suppression following surgery (Section 1.7.3). The present study suggests that in addition to anaesthetics affecting cytokine release, cytokines themselves might play a role in regulating neuronal activity during general anaesthesia. This effect is predicted to be due to cytokine mediated modulation of neuronal activity, occurring via cytokine effects on ion channel function or neurotransmitter signalling. In particular, the present study suggests genetic differences in *MYD88* and *IL1B* might underlie some of the variability in spindle wave activity during general anaesthesia. It is speculated that cytokine mediated effects on the EEG involve upregulation of cytokines in the brain, mirroring the peripheral inflammatory response to surgery. However, at present, the effect of surgical trauma on brain cytokine levels remains uncertain. If the effect of cytokines on the EEG indeed

involves the upregulation of brain cytokine levels, the type and duration of surgical procedure undertaken will likely influence this effect as the inflammatory response is influenced by the extent of surgical trauma.

Further work needs to be undertaken to verify the reported associations in a larger more homogeneous patient sample, and a more comprehensive investigation of SNPs in strongly associated genes is suggested. In particular, further investigation of the influence of *MYD88* on the EEG during general anaesthesia is suggested. Functional *MYD88* variants are yet to be identified and it also remains to be determined if *MYD88* is indeed responsible for the reported association with the EEG. While the role of *MYD88* in cytokine signalling is presumed to underlie the reported associations, the mechanism by which this gene affects the EEG remains to be elucidated. The effect of surgery on brain cytokine levels also needs to be clarified. As differential gene expression is speculated to underlie the reported associations, it is hypothesised brain mRNA levels of the associated genes may correlate with EEG activity, however this is yet to be determined.

Despite the widespread use of qEEG monitors in anaesthesia monitoring, this study is the first that I am aware of investigating genetic contributors to individual variability in the EEG during general anaesthesia. While no SNPs with likely clinical applications were identified, the results presented here lend support for further, more comprehensive work investigating genetic polymorphisms associated with EEG variability during general anaesthesia. In the future, improved understanding of the genetic factors influencing the EEG during general anaesthesia will hopefully lead to improved use of the EEG and BIS monitors in anaesthesia monitoring and improved patient outcomes.

References

1. Iohom G, Fitzgerald D, Cunningham AJ: **Principles of pharmacogenetics--implications for the anaesthetist**. *British journal of anaesthesia* 2004, **93**(3):440-450.
2. Gurman GM, Popescu M, Weksler N, Steiner O, Avinoah E, Porath A: **Influence of the cortical electrical activity level during general anaesthesia on the severity of immediate postoperative pain in the morbidly obese**. *Acta Anaesthesiol Scand* 2003, **47**(7):804-808.
3. Myles PS, Leslie K, McNeil J, Forbes A, Chan MT: **Bispectral index monitoring to prevent awareness during anaesthesia: the B-Aware randomised controlled trial**. *Lancet* 2004, **363**(9423):1757-1763.
4. Ekman A, Lindholm ML, Lennmarken C, Sandin R: **Reduction in the incidence of awareness using BIS monitoring**. *Acta Anaesthesiol Scand* 2004, **48**(1):20-26.
5. Voss L, Sleigh J: **Monitoring consciousness: the current status of EEG-based depth of anaesthesia monitors**. *Best practice & research Clinical anaesthesiology* 2007, **21**(3):313-325.
6. Galley HF, Mahdy A, Lowes DA: **Pharmacogenetics and anesthesiologists**. *Pharmacogenomics* 2005, **6**(8):849-856.
7. Musizza B, Ribaric S: **Monitoring the depth of anaesthesia**. *Sensors (Basel)* 2010, **10**(12):10896-10935.
8. Schwender D, Kunze-Kronawitter H, Dietrich P, Klasing S, Forst H, Madler C: **Conscious awareness during general anaesthesia: patients' perceptions, emotions, cognition and reactions**. *British journal of anaesthesia* 1998, **80**(2):133-139.
9. Moerman N, Bonke B, Oosting J: **Awareness and recall during general anesthesia. Facts and feelings**. *Anesthesiology* 1993, **79**(3):454-464.

10. Osterman JE, Hopper J, Heran WJ, Keane TM, van der Kolk BA: **Awareness under anesthesia and the development of posttraumatic stress disorder**. *General hospital psychiatry* 2001, **23**(4):198-204.
11. Sebel PS, Bowdle TA, Ghoneim MM, Rampil IJ, Padilla RE, Gan TJ, Domino KB: **The incidence of awareness during anesthesia: a multicenter United States study**. *Anesth Analg* 2004, **99**(3):833-839.
12. Ghoneim MM: **Incidence of and risk factors for awareness during anaesthesia**. *Best practice & research Clinical anaesthesiology* 2007, **21**(3):327-343.
13. Sandin RH, Enlund G, Samuelsson P, Lennmarken C: **Awareness during anaesthesia: a prospective case study**. *Lancet* 2000, **355**(9205):707-711.
14. Phillips AA, McLean RF, Devitt JH, Harrington EM: **Recall of intraoperative events after general anaesthesia and cardiopulmonary bypass**. *Canadian journal of anaesthesia = Journal canadien d'anesthesie* 1993, **40**(10):922-926.
15. Lyons G, Macdonald R: **Awareness during caesarean section**. *Anaesthesia* 1991, **46**(1):62-64.
16. Ball C, Westhorpe RN: **The history of depth of anaesthesia monitoring**. *Anaesthesia and intensive care* 2010, **38**(5):797.
17. Topulos GP, Lansing RW, Banzett RB: **The experience of complete neuromuscular blockade in awake humans**. *Journal of clinical anesthesia* 1993, **5**(5):369-374.
18. Tunstall ME: **Detecting wakefulness during general anaesthesia for caesarean section**. *Br Med J* 1977, **1**(6072):1321.
19. Jameson LC, Sloan TB: **Using EEG to monitor anesthesia drug effects during surgery**. *Journal of clinical monitoring and computing* 2006, **20**(6):445-472.
20. Niedermeyer E: **Historical Aspects**. In: *Electroencephalography: Basic principles, clinical applications and related fields.* Edited by Niedermeyer E, Lopes da Silva FH, 5 edn. Baltimore: Lippincott Williams and Wilkins; 2005.
21. Olejniczak P: **Neurophysiologic basis of EEG**. *J Clin Neurophysiol* 2006, **23**(3):186-189.

22. Bennett C, Voss LJ, Barnard JP, Sleigh JW: **Practical use of the raw electroencephalogram waveform during general anesthesia: the art and science**. *Anesth Analg* 2009, **109**(2):539-550.
23. Sanei S, Chambers JA: **EEG signal processing**. Chichester, England John Wiley & Sons; 2007.
24. Bucci P, Galderisi S: **Physiologic Basis of the EEG Signal**. In: *Standard Electroencephalography in Clinical Psychiatry: A Practical Handbook.* Edited by Boutros N, Galderisi S, Pogarell O, Riggio S, 1 edn. Chichester, UK.: John Wiley & Sons, Ltd.; 2011.
25. Buzsaki G, Traub RD, Pedley TA: **The Cellular Basis of EEG Activity**. In: *Current Practice of Clinical Electroencephalography.* Edited by Pedley T, Ebersole J. Philadelphia: Lippincott Williams & Wilkins; 2003.
26. Steriade M, Gloor P, Llinas RR, Lopes de Silva FH, Mesulam MM: **Report of IFCN Committee on Basic Mechanisms. Basic mechanisms of cerebral rhythmic activities**. *Electroencephalography and clinical neurophysiology* 1990, **76**(6):481-508.
27. McCormick DA, Bal T: **Sleep and arousal: thalamocortical mechanisms**. *Annu Rev Neurosci* 1997, **20**:185-215.
28. Steriade M, McCormick DA, Sejnowski TJ: **Thalamocortical oscillations in the sleeping and aroused brain**. *Science* 1993, **262**(5134):679-685.
29. Sleigh JW, Scheib CM, Sanders RD: **General anaesthesia and electroencephalographic spindles**. *Trends in Anaesthesia and Critical Care* 2011, **1**(5):263-269.
30. Jahnsen H, Llinas R: **Ionic basis for the electro-responsiveness and oscillatory properties of guinea-pig thalamic neurones in vitro**. *J Physiol* 1984, **349**:227-247.
31. Steriade M: **Impact of network activities on neuronal properties in corticothalamic systems**. *J Neurophysiol* 2001, **86**(1):1-39.
32. Steriade M, Contreras D, Curro Dossi R, Nunez A: **The slow (< 1 Hz) oscillation in reticular thalamic and thalamocortical neurons: scenario of sleep rhythm generation in interacting thalamic and neocortical networks**. *J Neurosci* 1993, **13**(8):3284-3299.

33. von Krosigk M, Bal T, McCormick DA: **Cellular mechanisms of a synchronized oscillation in the thalamus**. *Science* 1993, **261**(5119):361-364.
34. Sherman SM: **Tonic and burst firing: dual modes of thalamocortical relay**. *Trends in neurosciences* 2001, **24**(2):122-126.
35. McCormick DA: **Cholinergic and noradrenergic modulation of thalamocortical processing**. *Trends in neurosciences* 1989, **12**(6):215-221.
36. Huguenard JR: **Low-threshold calcium currents in central nervous system neurons**. *Annu Rev Physiol* 1996, **58**:329-348.
37. Talavera K, Nilius B: **Biophysics and structure-function relationship of T-type Ca2+ channels**. *Cell calcium* 2006, **40**(2):97-114.
38. Jevtovic-Todorovic V, Todorovic SM: **The role of peripheral T-type calcium channels in pain transmission**. *Cell calcium* 2006, **40**(2):197-203.
39. Todorovic SM, Jevtovic-Todorovic V: **The role of T-type calcium channels in peripheral and central pain processing**. *CNS & neurological disorders drug targets* 2006, **5**(6):639-653.
40. Arnoult C, Cardullo RA, Lemos JR, Florman HM: **Activation of mouse sperm T-type Ca2+ channels by adhesion to the egg zona pellucida**. *Proc Natl Acad Sci U S A* 1996, **93**(23):13004-13009.
41. Shin HS, Cheong EJ, Choi S, Lee J, Na HS: **T-type Ca2+ channels as therapeutic targets in the nervous system**. *Current opinion in pharmacology* 2008, **8**(1):33-41.
42. Dogrul A, Gardell LR, Ossipov MH, Tulunay FC, Lai J, Porreca F: **Reversal of experimental neuropathic pain by T-type calcium channel blockers**. *Pain* 2003, **105**(1-2):159-168.
43. Self DA, Bian K, Mishra SK, Hermsmeyer K: **Stroke-prone SHR vascular muscle Ca2+ current amplitudes correlate with lethal increases in blood pressure**. *Journal of vascular research* 1994, **31**(6):359-366.
44. Nuss HB, Houser SR: **T-type Ca2+ current is expressed in hypertrophied adult feline left ventricular myocytes**. *Circ Res* 1993, **73**(4):777-782.
45. Lee JH, Daud AN, Cribbs LL, Lacerda AE, Pereverzev A, Klockner U, Schneider T, Perez-Reyes E: **Cloning and expression of a novel member of the low voltage-activated T-type calcium channel family**. *J Neurosci* 1999, **19**(6):1912-1921.

46. Coulter DA, Huguenard JR, Prince DA: **Calcium currents in rat thalamocortical relay neurones: kinetic properties of the transient, low-threshold current**. *J Physiol* 1989, **414**:587-604.
47. DiFrancesco D, Tortora P: **Direct activation of cardiac pacemaker channels by intracellular cyclic AMP**. *Nature* 1991, **351**(6322):145-147.
48. Biel M, Wahl-Schott C, Michalakis S, Zong X: **Hyperpolarization-activated cation channels: from genes to function**. *Physiol Rev* 2009, **89**(3):847-885.
49. Wahl-Schott C, Biel M: **HCN channels: structure, cellular regulation and physiological function**. *Cell Mol Life Sci* 2009, **66**(3):470-494.
50. Lewis AS, Chetkovich DM: **HCN channels in behavior and neurological disease: too hyper or not active enough?** *Mol Cell Neurosci* 2010, **46**(2):357-367.
51. Xue T, Marban E, Li RA: **Dominant-negative suppression of HCN1- and HCN2-encoded pacemaker currents by an engineered HCN1 construct: insights into structure-function relationships and multimerization**. *Circ Res* 2002, **90**(12):1267-1273.
52. Moosmang S, Stieber J, Zong X, Biel M, Hofmann F, Ludwig A: **Cellular expression and functional characterization of four hyperpolarization-activated pacemaker channels in cardiac and neuronal tissues**. *Eur J Biochem* 2001, **268**(6):1646-1652.
53. Ulens C, Tytgat J: **Functional heteromerization of HCN1 and HCN2 pacemaker channels**. *J Biol Chem* 2001, **276**(9):6069-6072.
54. Chen S, Wang J, Siegelbaum SA: **Properties of hyperpolarization-activated pacemaker current defined by coassembly of HCN1 and HCN2 subunits and basal modulation by cyclic nucleotide**. *J Gen Physiol* 2001, **117**(5):491-504.
55. Loomis AL: **Potential Rhythms of the Cerebral Cortex during Sleep**. *Science* 1935, **81**(2111):597-598.
56. Bal T, von Krosigk M, McCormick DA: **Role of the ferret perigeniculate nucleus in the generation of synchronized oscillations in vitro**. *J Physiol* 1995, **483 (Pt 3)**:665-685.

57. Bal T, von Krosigk M, McCormick DA: **Synaptic and membrane mechanisms underlying synchronized oscillations in the ferret lateral geniculate nucleus in vitro**. *J Physiol* 1995, **483 (Pt 3)**:641-663.
58. Kim U, Bal T, McCormick DA: **Spindle waves are propagating synchronized oscillations in the ferret LGNd in vitro**. *J Neurophysiol* 1995, **74**(3):1301-1323.
59. Fuentealba P, Steriade M: **The reticular nucleus revisited: intrinsic and network properties of a thalamic pacemaker**. *Progress in neurobiology* 2005, **75**(2):125-141.
60. Bonjean M, Baker T, Lemieux M, Timofeev I, Sejnowski T, Bazhenov M: **Corticothalamic feedback controls sleep spindle duration in vivo**. *J Neurosci* 2011, **31**(25):9124-9134.
61. Steriade M: **The corticothalamic system in sleep**. *Frontiers in bioscience : a journal and virtual library* 2003, **8**:878-899.
62. Luthi A, Bal T, McCormick DA: **Periodicity of thalamic spindle waves is abolished by ZD7288,a blocker of Ih**. *J Neurophysiol* 1998, **79**(6):3284-3289.
63. Luthi A, McCormick DA: **Periodicity of thalamic synchronized oscillations: the role of Ca2+-mediated upregulation of Ih**. *Neuron* 1998, **20**(3):553-563.
64. Bal T, McCormick DA: **What stops synchronized thalamocortical oscillations?** *Neuron* 1996, **17**(2):297-308.
65. McCormick DA, Pape HC: **Properties of a hyperpolarization-activated cation current and its role in rhythmic oscillation in thalamic relay neurones**. *J Physiol* 1990, **431**:291-318.
66. Steriade M, Dossi RC, Nunez A: **Network modulation of a slow intrinsic oscillation of cat thalamocortical neurons implicated in sleep delta waves: cortically induced synchronization and brainstem cholinergic suppression**. *J Neurosci* 1991, **11**(10):3200-3217.
67. **BIS™ Technology Enabling safety and quality improvements in the operating room** [http://www.covidien.com/imageServer.aspx/doc230269.pdf?contentID=28157&contenttype=application/pdf]

68. March PA, Muir WW: **Bispectral analysis of the electroencephalogram: a review of its development and use in anesthesia**. *Veterinary anaesthesia and analgesia* 2005, **32**(5):241-255.

69. Flaishon R, Windsor A, Sigl J, Sebel PS: **Recovery of consciousness after thiopental or propofol. Bispectral index and isolated forearm technique**. *Anesthesiology* 1997, **86**(3):613-619.

70. Glass PS, Bloom M, Kearse L, Rosow C, Sebel P, Manberg P: **Bispectral analysis measures sedation and memory effects of propofol, midazolam, isoflurane, and alfentanil in healthy volunteers**. *Anesthesiology* 1997, **86**(4):836-847.

71. Gan TJ, Glass PS, Windsor A, Payne F, Rosow C, Sebel P, Manberg P: **Bispectral index monitoring allows faster emergence and improved recovery from propofol, alfentanil, and nitrous oxide anesthesia. BIS Utility Study Group**. *Anesthesiology* 1997, **87**(4):808-815.

72. White PF, Ma H, Tang J, Wender RH, Sloninsky A, Kariger R: **Does the use of electroencephalographic bispectral index or auditory evoked potential index monitoring facilitate recovery after desflurane anesthesia in the ambulatory setting?** *Anesthesiology* 2004, **100**(4):811-817.

73. Wong J, Song D, Blanshard H, Grady D, Chung F: **Titration of isoflurane using BIS index improves early recovery of elderly patients undergoing orthopedic surgeries**. *Canadian journal of anaesthesia = Journal canadien d'anesthesie* 2002, **49**(1):13-18.

74. Kearse LA, Jr., Manberg P, Chamoun N, deBros F, Zaslavsky A: **Bispectral analysis of the electroencephalogram correlates with patient movement to skin incision during propofol/nitrous oxide anesthesia**. *Anesthesiology* 1994, **81**(6):1365-1370.

75. Vernon JM, Lang E, Sebel PS, Manberg P: **Prediction of movement using bispectral electroencephalographic analysis during propofol/alfentanil or isoflurane/alfentanil anesthesia**. *Anesth Analg* 1995, **80**(4):780-785.

76. Sebel PS, Lang E, Rampil IJ, White PF, Cork R, Jopling M, Smith NT, Glass PS, Manberg P: **A multicenter study of bispectral electroencephalogram analysis for monitoring anesthetic effect**. *Anesth Analg* 1997, **84**(4):891-899.

77. Mychaskiw G, 2nd, Horowitz M, Sachdev V, Heath BJ: **Explicit intraoperative recall at a Bispectral Index of 47**. *Anesth Analg* 2001, **92**(4):808-809.
78. Rampersad SE, Mulroy MF: **A case of awareness despite an "adequate depth of anesthesia" as indicated by a Bispectral Index monitor**. *Anesth Analg* 2005, **100**(5):1363-1364.
79. Dahaba AA: **Different conditions that could result in the bispectral index indicating an incorrect hypnotic state**. *Anesth Analg* 2005, **101**(3):765-773.
80. Ibrahim AE, Taraday JK, Kharasch ED: **Bispectral index monitoring during sedation with sevoflurane, midazolam, and propofol**. *Anesthesiology* 2001, **95**(5):1151-1159.
81. van Beijsterveldt CE, Boomsma DI: **Genetics of the human electroencephalogram (EEG) and event-related brain potentials (ERPs): a review**. *Hum Genet* 1994, **94**(4):319-330.
82. Gaillard JM, Blois R: **Spindle density in sleep of normal subjects**. *Sleep* 1981, **4**(4):385-391.
83. Gasser T, Bacher P, Steinberg H: **Test-retest reliability of spectral parameters of the EEG**. *Electroencephalography and clinical neurophysiology* 1985, **60**(4):312-319.
84. Napflin M, Wildi M, Sarnthein J: **Test-retest reliability of resting EEG spectra validates a statistical signature of persons**. *Clinical neurophysiology : official journal of the International Federation of Clinical Neurophysiology* 2007, **118**(11):2519-2524.
85. Salinsky MC, Oken BS, Morehead L: **Test-retest reliability in EEG frequency analysis**. *Electroencephalography and clinical neurophysiology* 1991, **79**(5):382-392.
86. Lennox WG, Gibbs EL, Gibbs FA: **The brain-wave pattern, an hereditary trait; evidence from 74 "normal" pairs of twins.** . *Journal of Heredity* 1945, **36**:233-243.
87. Lykken DT, Tellegen A, Iacono WG: **EEG spectra in twins: Evidence for a neglected mechanism of genetic determination.** . *Physiological Psychology* 1982, **10**(1):60-65.

88. Stassen HH, Lykken DT, Bomben G: **The within-pair EEG similarity of twins reared apart**. *European archives of psychiatry and neurological sciences* 1988, **237**(4):244-252.

89. van Beijsterveldt CE, Molenaar PC, de Geus EJ, Boomsma DI: **Heritability of human brain functioning as assessed by electroencephalography**. *Am J Hum Genet* 1996, **58**(3):562-573.

90. Dick DM, Jones K, Saccone N, Hinrichs A, Wang JC, Goate A, Bierut L, Almasy L, Schuckit M, Hesselbrock V *et al*: **Endophenotypes successfully lead to gene identification: results from the collaborative study on the genetics of alcoholism**. *Behavior genetics* 2006, **36**(1):112-126.

91. Ehlers CL, Gizer IR, Phillips E, Wilhelmsen KC: **EEG alpha phenotypes: linkage analyses and relation to alcohol dependence in an American Indian community study**. *BMC medical genetics* 2010, **11**:43.

92. Edenberg HJ, Dick DM, Xuei X, Tian H, Almasy L, Bauer LO, Crowe RR, Goate A, Hesselbrock V, Jones K *et al*: **Variations in GABRA2, encoding the alpha 2 subunit of the GABA(A) receptor, are associated with alcohol dependence and with brain oscillations**. *Am J Hum Genet* 2004, **74**(4):705-714.

93. Enoch MA, Shen PH, Ducci F, Yuan Q, Liu J, White KV, Albaugh B, Hodgkinson CA, Goldman D: **Common genetic origins for EEG, alcoholism and anxiety: the role of CRH-BP**. *PLoS One* 2008, **3**(10):e3620.

94. Ducci F, Enoch MA, Yuan Q, Shen PH, White KV, Hodgkinson C, Albaugh B, Virkkunen M, Goldman D: **HTR3B is associated with alcoholism with antisocial behavior and alpha EEG power--an intermediate phenotype for alcoholism and co-morbid behaviors**. *Alcohol* 2009, **43**(1):73-84.

95. Hodgkinson CA, Enoch MA, Srivastava V, Cummins-Oman JS, Ferrier C, Iarikova P, Sankararaman S, Yamini G, Yuan Q, Zhou Z *et al*: **Genome-wide association identifies candidate genes that influence the human electroencephalogram**. *Proc Natl Acad Sci U S A* 2010, **107**(19):8695-8700.

96. Gallinat J, Bajbouj M, Sander T, Schlattmann P, Xu K, Ferro EF, Goldman D, Winterer G: **Association of the G1947A COMT (Val(108/158)Met) gene polymorphism with prefrontal P300 during information processing**. *Biol Psychiatry* 2003, **54**(1):40-48.
97. Bombin I, Arango C, Mayoral M, Castro-Fornieles J, Gonzalez-Pinto A, Gonzalez-Gomez C, Moreno D, Parellada M, Baeza I, Graell M *et al*: **DRD3, but not COMT or DRD2, genotype affects executive functions in healthy and first-episode psychosis adolescents**. *Am J Med Genet B Neuropsychiatr Genet* 2008, **147B**(6):873-879.
98. Lydall GJ, Saini J, Ruparelia K, Montagnese S, McQuillin A, Guerrini I, Rao H, Reynolds G, Ball D, Smith I *et al*: **Genetic association study of GABRA2 single nucleotide polymorphisms and electroencephalography in alcohol dependence**. *Neurosci Lett* 2011, **500**(3):162-166.
99. Jones KA, Porjesz B, Almasy L, Bierut L, Goate A, Wang JC, Dick DM, Hinrichs A, Kwon J, Rice JP *et al*: **Linkage and linkage disequilibrium of evoked EEG oscillations with CHRM2 receptor gene polymorphisms: implications for human brain dynamics and cognition**. *International journal of psychophysiology : official journal of the International Organization of Psychophysiology* 2004, **53**(2):75-90.
100. Medzhitov R: **Inflammation 2010: new adventures of an old flame**. *Cell* 2010, **140**(6):771-776.
101. Libby P: **Inflammatory mechanisms: the molecular basis of inflammation and disease**. *Nutrition reviews* 2007, **65**(12 Pt 2):S140-146.
102. Lucas SM, Rothwell NJ, Gibson RM: **The role of inflammation in CNS injury and disease**. *Br J Pharmacol* 2006, **147**(S1):S232-240.
103. Vezzani A, Granata T: **Brain inflammation in epilepsy: experimental and clinical evidence**. *Epilepsia* 2005, **46**(11):1724-1743.
104. Lin E, Calvano SE, Lowry SF: **Inflammatory cytokines and cell response in surgery**. *Surgery* 2000, **127**(2):117-126.
105. Galic MA, Riazi K, Pittman QJ: **Cytokines and brain excitability**. *Frontiers in neuroendocrinology* 2012, **33**(1):116-125.
106. Capuron L, Miller AH: **Immune system to brain signaling: neuropsychopharmacological implications**. *Pharmacology & therapeutics* 2011, **130**(2):226-238.

107. Vezzani A, Maroso M, Balosso S, Sanchez MA, Bartfai T: **IL-1 receptor/Toll-like receptor signaling in infection, inflammation, stress and neurodegeneration couples hyperexcitability and seizures**. *Brain, behavior, and immunity* 2011, **25**(7):1281-1289.

108. Riazi K, Galic MA, Pittman QJ: **Contributions of peripheral inflammation to seizure susceptibility: cytokines and brain excitability**. *Epilepsy research* 2010, **89**(1):34-42.

109. Laye S, Parnet P, Goujon E, Dantzer R: **Peripheral administration of lipopolysaccharide induces the expression of cytokine transcripts in the brain and pituitary of mice**. *Brain Res Mol Brain Res* 1994, **27**(1):157-162.

110. Gabellec MM, Griffais R, Fillion G, Haour F: **Expression of interleukin 1 alpha, interleukin 1 beta and interleukin 1 receptor antagonist mRNA in mouse brain: regulation by bacterial lipopolysaccharide (LPS) treatment**. *Brain Res Mol Brain Res* 1995, **31**(1-2):122-130.

111. Gabellec MM, Griffais R, Fillion G, Haour F: **Interleukin-1 receptors type I and type II in the mouse brain: kinetics of mRNA expressions after peripheral administration of bacterial lipopolysaccharide**. *Journal of neuroimmunology* 1996, **66**(1-2):65-70.

112. Reinisch N, Wolkersdorfer M, Kahler CM, Ye K, Dinarello CA, Wiedermann CJ: **Interleukin-1 receptor type I mRNA in mouse brain as affected by peripheral administration of bacterial lipopolysaccharide**. *Neurosci Lett* 1994, **166**(2):165-167.

113. Gatti S, Bartfai T: **Induction of tumor necrosis factor-alpha mRNA in the brain after peripheral endotoxin treatment: comparison with interleukin-1 family and interleukin-6**. *Brain research* 1993, **624**(1-2):291-294.

114. Ban E, Haour F, Lenstra R: **Brain interleukin 1 gene expression induced by peripheral lipopolysaccharide administration**. *Cytokine* 1992, **4**(1):48-54.

115. Lancel M, Cronlein J, Muller-Preuss P, Holsboer F: **Lipopolysaccharide increases EEG delta activity within non-REM sleep and disrupts sleep continuity in rats**. *The American journal of physiology* 1995, **268**(5 Pt 2):R1310-1318.

116. Mullington J, Korth C, Hermann DM, Orth A, Galanos C, Holsboer F, Pollmacher T: **Dose-dependent effects of endotoxin on human sleep**. *American journal of physiology Regulatory, integrative and comparative physiology* 2000, **278**(4):R947-955.
117. Trachsel L, Schreiber W, Holsboer F, Pollmacher T: **Endotoxin enhances EEG alpha and beta power in human sleep**. *Sleep* 1994, **17**(2):132-139.
118. Pollmacher T, Schreiber W, Gudewill S, Vedder H, Fassbender K, Wiedemann K, Trachsel L, Galanos C, Holsboer F: **Influence of endotoxin on nocturnal sleep in humans**. *The American journal of physiology* 1993, **264**(6):R1077-1083.
119. Schafers M, Sorkin L: **Effect of cytokines on neuronal excitability**. *Neurosci Lett* 2008, **437**(3):188-193.
120. Toft P, Tønnesen E: **The systemic inflammatory response to anaesthesia and surgery**. *Current Anaesthesia & Critical Care* 2008, **19**(5):349-353.
121. Salo M: **Effects of anaesthesia and surgery on the immune response**. *Acta Anaesthesiol Scand* 1992, **36**(3):201-220.
122. Schneemilch CE, Schilling T, Bank U: **Effects of general anaesthesia on inflammation**. *Best practice & research Clinical anaesthesiology* 2004, **18**(3):493-507.
123. Kurosawa S, Kato M: **Anesthetics, immune cells, and immune responses**. *Journal of anesthesia* 2008, **22**(3):263-277.
124. Kelbel I, Weiss M: **Anaesthetics and immune function**. *Current opinion in anaesthesiology* 2001, **14**(6):685-691.
125. Evans WE, Relling MV: **Pharmacogenomics: translating functional genomics into rational therapeutics**. *Science* 1999, **286**(5439):487-491.
126. Roses AD: **Pharmacogenetics and the practice of medicine**. *Nature* 2000, **405**(6788):857-865.
127. Huang RS, Ratain MJ: **Pharmacogenetics and pharmacogenomics of anticancer agents**. *CA: a cancer journal for clinicians* 2009, **59**(1):42-55.
128. Sonner JM, Gong D, Eger EI, 2nd: **Naturally occurring variability in anesthetic potency among inbred mouse strains**. *Anesth Analg* 2000, **91**(3):720-726.
129. Kruglyak L, Nickerson DA: **Variation is the spice of life**. *Nature genetics* 2001, **27**(3):234-236.

130. Hinds DA, Stuve LL, Nilsen GB, Halperin E, Eskin E, Ballinger DG, Frazer KA, Cox DR: **Whole-genome patterns of common DNA variation in three human populations**. *Science* 2005, **307**(5712):1072-1079.
131. Wang DG, Fan JB, Siao CJ, Berno A, Young P, Sapolsky R, Ghandour G, Perkins N, Winchester E, Spencer J *et al*: **Large-scale identification, mapping, and genotyping of single-nucleotide polymorphisms in the human genome**. *Science* 1998, **280**(5366):1077-1082.
132. Cargill M, Altshuler D, Ireland J, Sklar P, Ardlie K, Patil N, Shaw N, Lane CR, Lim EP, Kalyanaraman N *et al*: **Characterization of single-nucleotide polymorphisms in coding regions of human genes**. *Nature genetics* 1999, **22**(3):231-238.
133. Manolio TA, Collins FS, Cox NJ, Goldstein DB, Hindorff LA, Hunter DJ, McCarthy MI, Ramos EM, Cardon LR, Chakravarti A *et al*: **Finding the missing heritability of complex diseases**. *Nature* 2009, **461**(7265):747-753.
134. Gabriel SB, Schaffner SF, Nguyen H, Moore JM, Roy J, Blumenstiel B, Higgins J, DeFelice M, Lochner A, Faggart M *et al*: **The structure of haplotype blocks in the human genome**. *Science* 2002, **296**(5576):2225-2229.
135. Barnes MR: **Navigating the HapMap**. *Briefings in bioinformatics* 2006, **7**(3):211-224.
136. Trevaskis J, Walder K, Foletta V, Kerr-Bayles L, McMillan J, Cooper A, Lee S, Bolton K, Prior M, Fahey R *et al*: **Src homology 3-domain growth factor receptor-bound 2-like (endophilin) interacting protein 1, a novel neuronal protein that regulates energy balance**. *Endocrinology* 2005, **146**(9):3757-3764.
137. Uezu A, Horiuchi A, Kanda K, Kikuchi N, Umeda K, Tsujita K, Suetsugu S, Araki N, Yamamoto H, Takenawa T *et al*: **SGIP1alpha is an endocytic protein that directly interacts with phospholipids and Eps15**. *J Biol Chem* 2007, **282**(36):26481-26489.
138. Conner SD, Schmid SL: **Regulated portals of entry into the cell**. *Nature* 2003, **422**(6927):37-44.
139. Brodin L, Low P, Shupliakov O: **Sequential steps in clathrin-mediated synaptic vesicle endocytosis**. *Current opinion in neurobiology* 2000, **10**(3):312-320.

140. Barnard EA, Skolnick P, Olsen RW, Mohler H, Sieghart W, Biggio G, Braestrup C, Bateson AN, Langer SZ: **International Union of Pharmacology. XV. Subtypes of gamma-aminobutyric acidA receptors: classification on the basis of subunit structure and receptor function**. *Pharmacol Rev* 1998, **50**(2):291-313.

141. Franks NP: **Molecular targets underlying general anaesthesia**. *Br J Pharmacol* 2006, **147** (S1):S72-81.

142. Buckle VJ, Fujita N, Ryder-Cook AS, Derry JM, Barnard PJ, Lebo RV, Schofield PR, Seeburg PH, Bateson AN, Darlison MG *et al*: **Chromosomal localization of GABAA receptor subunit genes: relationship to human genetic disease**. *Neuron* 1989, **3**(5):647-654.

143. Tian H, Chen HJ, Cross TH, Edenberg HJ: **Alternative splicing and promoter use in the human GABRA2 gene**. *Brain Res Mol Brain Res* 2005, **137**(1-2):174-183.

144. Porjesz B, Almasy L, Edenberg HJ, Wang K, Chorlian DB, Foroud T, Goate A, Rice JP, O'Connor SJ, Rohrbaugh J *et al*: **Linkage disequilibrium between the beta frequency of the human EEG and a GABAA receptor gene locus**. *Proc Natl Acad Sci U S A* 2002, **99**(6):3729-3733.

145. Cui WY, Seneviratne C, Gu J, Li MD: **Genetics of GABAergic signaling in nicotine and alcohol dependence**. *Hum Genet* 2012, **131**(6):843-855.

146. Mittman S, Guo J, Agnew WS: **Structure and alternative splicing of the gene encoding alpha1G, a human brain T calcium channel alpha1 subunit**. *Neurosci Lett* 1999, **274**(3):143-146.

147. Perez-Reyes E, Cribbs LL, Daud A, Lacerda AE, Barclay J, Williamson MP, Fox M, Rees M, Lee JH: **Molecular characterization of a neuronal low-voltage-activated T-type calcium channel**. *Nature* 1998, **391**(6670):896-900.

148. Emerick MC, Stein R, Kunze R, McNulty MM, Regan MR, Hanck DA, Agnew WS: **Profiling the array of Ca(v)3.1 variants from the human T-type calcium channel gene CACNA1G: alternative structures, developmental expression, and biophysical variations**. *Proteins* 2006, **64**(2):320-342.

149. Monteil A, Chemin J, Bourinet E, Mennessier G, Lory P, Nargeot J: **Molecular and functional properties of the human alpha(1G) subunit that forms T-type calcium channels**. *J Biol Chem* 2000, **275**(9):6090-6100.
150. Chemin J, Monteil A, Bourinet E, Nargeot J, Lory P: **Alternatively spliced alpha(1G) (Ca(V)3.1) intracellular loops promote specific T-type Ca(2+) channel gating properties**. *Biophysical journal* 2001, **80**(3):1238-1250.
151. Catterall WA, Goldin AL, Waxman SG: **International Union of Pharmacology. XLVII. Nomenclature and structure-function relationships of voltage-gated sodium channels**. *Pharmacol Rev* 2005, **57**(4):397-409.
152. Strong M, Chandy KG, Gutman GA: **Molecular evolution of voltage-sensitive ion channel genes: on the origins of electrical excitability**. *Molecular biology and evolution* 1993, **10**(1):221-242.
153. Cain SM, Snutch TP: **Contributions of T-type calcium channel isoforms to neuronal firing**. *Channels (Austin)* 2010, **4**(6):475-482.
154. Talley EM, Cribbs LL, Lee JH, Daud A, Perez-Reyes E, Bayliss DA: **Differential distribution of three members of a gene family encoding low voltage-activated (T-type) calcium channels**. *J Neurosci* 1999, **19**(6):1895-1911.
155. Kim D, Song I, Keum S, Lee T, Jeong MJ, Kim SS, McEnery MW, Shin HS: **Lack of the burst firing of thalamocortical relay neurons and resistance to absence seizures in mice lacking alpha(1G) T-type Ca(2+) channels**. *Neuron* 2001, **31**(1):35-45.
156. Lee J, Kim D, Shin HS: **Lack of delta waves and sleep disturbances during non-rapid eye movement sleep in mice lacking alpha1G-subunit of T-type calcium channels**. *Proc Natl Acad Sci U S A* 2004, **101**(52):18195-18199.
157. Ludwig A, Zong X, Jeglitsch M, Hofmann F, Biel M: **A family of hyperpolarization-activated mammalian cation channels**. *Nature* 1998, **393**(6685):587-591.
158. Santoro B, Grant SG, Bartsch D, Kandel ER: **Interactive cloning with the SH3 domain of N-src identifies a new brain specific ion channel protein, with homology to eag and cyclic nucleotide-gated channels**. *Proc Natl Acad Sci U S A* 1997, **94**(26):14815-14820.

159. Santoro B, Liu DT, Yao H, Bartsch D, Kandel ER, Siegelbaum SA, Tibbs GR: **Identification of a gene encoding a hyperpolarization-activated pacemaker channel of brain**. *Cell* 1998, **93**(5):717-729.
160. Santoro B, Chen S, Luthi A, Pavlidis P, Shumyatsky GP, Tibbs GR, Siegelbaum SA: **Molecular and functional heterogeneity of hyperpolarization-activated pacemaker channels in the mouse CNS**. *J Neurosci* 2000, **20**(14):5264-5275.
161. Notomi T, Shigemoto R: **Immunohistochemical localization of Ih channel subunits, HCN1-4, in the rat brain**. *J Comp Neurol* 2004, **471**(3):241-276.
162. Monteggia LM, Eisch AJ, Tang MD, Kaczmarek LK, Nestler EJ: **Cloning and localization of the hyperpolarization-activated cyclic nucleotide-gated channel family in rat brain**. *Brain Res Mol Brain Res* 2000, **81**(1-2):129-139.
163. Lorincz A, Notomi T, Tamas G, Shigemoto R, Nusser Z: **Polarized and compartment-dependent distribution of HCN1 in pyramidal cell dendrites**. *Nat Neurosci* 2002, **5**(11):1185-1193.
164. Ludwig A, Budde T, Stieber J, Moosmang S, Wahl C, Holthoff K, Langebartels A, Wotjak C, Munsch T, Zong X *et al*: **Absence epilepsy and sinus dysrhythmia in mice lacking the pacemaker channel HCN2**. *The EMBO journal* 2003, **22**(2):216-224.
165. Huang Z, Walker MC, Shah MM: **Loss of dendritic HCN1 subunits enhances cortical excitability and epileptogenesis**. *J Neurosci* 2009, **29**(35):10979-10988.
166. Sirois JE, Lynch C, 3rd, Bayliss DA: **Convergent and reciprocal modulation of a leak K+ current and I(h) by an inhalational anaesthetic and neurotransmitters in rat brainstem motoneurones**. *J Physiol* 2002, **541**(Pt 3):717-729.
167. Sirois JE, Pancrazio JJ, Iii CL, Bayliss DA: **Multiple ionic mechanisms mediate inhibition of rat motoneurones by inhalation anaesthetics**. *J Physiol* 1998, **512 (Pt 3)**:851-862.
168. Wan X, Mathers DA, Puil E: **Pentobarbital modulates intrinsic and GABA-receptor conductances in thalamocortical inhibition**. *Neuroscience* 2003, **121**(4):947-958.

169. Ying SW, Abbas SY, Harrison NL, Goldstein PA: **Propofol block of I(h) contributes to the suppression of neuronal excitability and rhythmic burst firing in thalamocortical neurons**. *Eur J Neurosci* 2006, **23**(2):465-480.

170. Chen X, Sirois JE, Lei Q, Talley EM, Lynch C, 3rd, Bayliss DA: **HCN subunit-specific and cAMP-modulated effects of anesthetics on neuronal pacemaker currents**. *J Neurosci* 2005, **25**(24):5803-5814.

171. Haughey HM, Ray LA, Finan P, Villanueva R, Niculescu M, Hutchison KE: **Human gamma-aminobutyric acid A receptor alpha2 gene moderates the acute effects of alcohol and brain mRNA expression**. *Genes, brain, and behavior* 2008, **7**(4):447-454.

172. Kent WJ, Sugnet CW, Furey TS, Roskin KM, Pringle TH, Zahler AM, Haussler D: **The human genome browser at UCSC**. *Genome research* 2002, **12**(6):996-1006.

173. Ovcharenko I, Nobrega MA, Loots GG, Stubbs L: **ECR Browser: a tool for visualizing and accessing data from comparisons of multiple vertebrate genomes**. *Nucleic Acids Res* 2004, **32**(Web Server issue):W280-286.

174. Consortium TIH: **The International HapMap Project**. *Nature* 2003, **426**(6968):789-796.

175. Zhang Z, Schwartz S, Wagner L, Miller W: **A greedy algorithm for aligning DNA sequences**. *Journal of computational biology : a journal of computational molecular cell biology* 2000, **7**(1-2):203-214.

176. Barrett JC, Fry B, Maller J, Daly MJ: **Haploview: analysis and visualization of LD and haplotype maps**. *Bioinformatics* 2005, **21**(2):263-265.

177. Don RH, Cox PT, Wainwright BJ, Baker K, Mattick JS: **'Touchdown' PCR to circumvent spurious priming during gene amplification**. *Nucleic Acids Res* 1991, **19**(14):4008.

178. Hecker KH, Roux KH: **High and low annealing temperatures increase both specificity and yield in touchdown and stepdown PCR**. *Biotechniques* 1996, **20**(3):478-485.

179. Cardon LR, Palmer LJ: **Population stratification and spurious allelic association**. *Lancet* 2003, **361**(9357):598-604.

180. Xu J, Turner A, Little J, Bleecker ER, Meyers DA: **Positive results in association studies are associated with departure from Hardy-Weinberg equilibrium: hint for genotyping error?** *Hum Genet* 2002, **111**(6):573-574.

181. Gomes I, Collins A, Lonjou C, Thomas NS, Wilkinson J, Watson M, Morton N: **Hardy-Weinberg quality control**. *Annals of human genetics* 1999, **63**(Pt 6):535-538.

182. Wu YY, Delgado R, Costello R, Sunderland T, Dukoff R, Csako G: **Quantitative assessment of apolipoprotein E genotypes by image analysis of PCR-RFLP fragments**. *Clinica chimica acta; international journal of clinical chemistry* 2000, **293**(1-2):213-221.

183. Fujimura FK, Northrup H, Beaudet AL, O'Brien WE: **Genotyping errors with the polymerase chain reaction**. *The New England journal of medicine* 1990, **322**(1):61.

184. Hans P, Lecoq JP, Brichant JF, Dewandre PY, Lamy M: **Effect of epidural bupivacaine on the relationship between the bispectral index and end-expiratory concentrations of desflurane**. *Anaesthesia* 1999, **54**(9):899-902.

185. Whitlock EL, Villafranca AJ, Lin N, Palanca BJ, Jacobsohn E, Finkel KJ, Zhang L, Burnside BA, Kaiser HA, Evers AS *et al*: **Relationship between bispectral index values and volatile anesthetic concentrations during the maintenance phase of anesthesia in the B-Unaware trial**. *Anesthesiology* 2011, **115**(6):1209-1218.

186. Pavlin DJ, Hong JY, Freund PR, Koerschgen ME, Bower JO, Bowdle TA: **The effect of bispectral index monitoring on end-tidal gas concentration and recovery duration after outpatient anesthesia**. *Anesth Analg* 2001, **93**(3):613-619.

187. Cortinez LI, Troconiz IF, Fuentes R, Gambus P, Hsu YW, Altermatt F, Munoz HR: **The influence of age on the dynamic relationship between end-tidal sevoflurane concentrations and bispectral index**. *Anesth Analg* 2008, **107**(5):1566-1572.

188. Cabin RJ, Mitchell RJ: **To Bonferroni or Not to Bonferroni: When and How Are the Questions**. *Bulletin of the Ecological Society of America* 2000, **81**(3):246-248

189. Silverstein AB: **Statistical Power Lost and Statistical Power Regained: The Bonferroni Procedure in in Exploratory Research**. *Educational and psychological measurement* 1986, **46**(2):303-307

190. Derringer J, Krueger RF, Manz N, Porjesz B, Almasy L, Bookman E, Edenberg HJ, Kramer JR, Tischfield JA, Bierut LJ: **Nonreplication of an association of SGIP1 SNPs with alcohol dependence and resting theta EEG power**. *Psychiatric genetics* 2011, **21**(5):265-266.

191. Nesti E, Everill B, Morielli AD: **Endocytosis as a mechanism for tyrosine kinase-dependent suppression of a voltage-gated potassium channel**. *Molecular biology of the cell* 2004, **15**(9):4073-4088.

192. Lydall GJ, Saini J, Ruparelia K, Montagnese S, McQuillin A, Guerrini I, Rao H, Reynolds G, Ball D, Smith I *et al*: **Genetic association study of GABRA2 single nucleotide polymorphisms and electroencephalography in alcohol dependence**. *Neurosci Lett* 2011, **500**(3):162-166.

193. Laurie DJ, Wisden W, Seeburg PH: **The distribution of thirteen GABAA receptor subunit mRNAs in the rat brain. III. Embryonic and postnatal development**. *J Neurosci* 1992, **12**(11):4151-4172.

194. Heldt SA, Ressler KJ: **Forebrain and midbrain distribution of major benzodiazepine-sensitive GABAA receptor subunits in the adult C57 mouse as assessed with in situ hybridization**. *Neuroscience* 2007, **150**(2):370-385.

195. Pirker S, Schwarzer C, Wieselthaler A, Sieghart W, Sperk G: **GABA(A) receptors: immunocytochemical distribution of 13 subunits in the adult rat brain**. *Neuroscience* 2000, **101**(4):815-850.

196. Wisden W, Laurie DJ, Monyer H, Seeburg PH: **The distribution of 13 GABAA receptor subunit mRNAs in the rat brain. I. Telencephalon, diencephalon, mesencephalon**. *J Neurosci* 1992, **12**(3):1040-1062.

197. Okada M, Onodera K, Van Renterghem C, Sieghart W, Takahashi T: **Functional correlation of GABA(A) receptor alpha subunits expression with the properties of IPSCs in the developing thalamus**. *J Neurosci* 2000, **20**(6):2202-2208.

198. Todorovic SM, Lingle CJ: **Pharmacological properties of T-type Ca2+ current in adult rat sensory neurons: effects of anticonvulsant and anesthetic agents**. *J Neurophysiol* 1998, **79**(1):240-252.

199. Takenoshita M, Steinbach JH: **Halothane blocks low-voltage-activated calcium current in rat sensory neurons**. *J Neurosci* 1991, **11**(5):1404-1412.

200. McDowell TS, Pancrazio JJ, Lynch C, 3rd: **Volatile anesthetics reduce low-voltage-activated calcium currents in a thyroid C-cell line**. *Anesthesiology* 1996, **85**(5):1167-1175.

201. Study RE: **Isoflurane inhibits multiple voltage-gated calcium currents in hippocampal pyramidal neurons**. *Anesthesiology* 1994, **81**(1):104-116.

202. Ries CR, Puil E: **Mechanism of anesthesia revealed by shunting actions of isoflurane on thalamocortical neurons**. *J Neurophysiol* 1999, **81**(4):1795-1801.

203. Petrenko AB, Tsujita M, Kohno T, Sakimura K, Baba H: **Mutation of alpha1G T-type calcium channels in mice does not change anesthetic requirements for loss of the righting reflex and minimum alveolar concentration but delays the onset of anesthetic induction**. *Anesthesiology* 2007, **106**(6):1177-1185.

204. Konsman JP, Parnet P, Dantzer R: **Cytokine-induced sickness behaviour: mechanisms and implications**. *Trends in neurosciences* 2002, **25**(3):154-159.

205. Kim YK, Jung HG, Myint AM, Kim H, Park SH: **Imbalance between pro-inflammatory and anti-inflammatory cytokines in bipolar disorder**. *Journal of affective disorders* 2007, **104**(1-3):91-95.

206. Kronfol Z, Remick DG: **Cytokines and the brain: implications for clinical psychiatry**. *The American journal of psychiatry* 2000, **157**(5):683-694.

207. Tabarean IV, Korn H, Bartfai T: **Interleukin-1beta induces hyperpolarization and modulates synaptic inhibition in preoptic and anterior hypothalamic neurons**. *Neuroscience* 2006, **141**(4):1685-1695.

208. Medzhitov R, Preston-Hurlburt P, Kopp E, Stadlen A, Chen C, Ghosh S, Janeway CA, Jr.: **MyD88 is an adaptor protein in the hToll/IL-1 receptor family signaling pathways**. *Molecular cell* 1998, **2**(2):253-258.

209. Muzio M, Ni J, Feng P, Dixit VM: **IRAK (Pelle) family member IRAK-2 and MyD88 as proximal mediators of IL-1 signaling**. *Science* 1997, **278**(5343):1612-1615.

210. Wesche H, Henzel WJ, Shillinglaw W, Li S, Cao Z: **MyD88: an adapter that recruits IRAK to the IL-1 receptor complex**. *Immunity* 1997, **7**(6):837-847.
211. Takeda K, Kaisho T, Akira S: **Toll-like receptors**. *Annual review of immunology* 2003, **21**:335-376.
212. Takeda K, Akira S: **Toll receptors and pathogen resistance**. *Cellular microbiology* 2003, **5**(3):143-153.
213. O'Connor JJ, Coogan AN: **Actions of the pro-inflammatory cytokine IL-1 beta on central synaptic transmission**. *Experimental physiology* 1999, **84**(4):601-614.
214. Wang S, Cheng Q, Malik S, Yang J: **Interleukin-1beta inhibits gamma-aminobutyric acid type A (GABA(A)) receptor current in cultured hippocampal neurons**. *The Journal of pharmacology and experimental therapeutics* 2000, **292**(2):497-504.
215. Zhou C, Ye HH, Wang SQ, Chai Z: **Interleukin-1beta regulation of N-type Ca2+ channels in cortical neurons**. *Neurosci Lett* 2006, **403**(1-2):181-185.
216. Yu B, Shinnick-Gallagher P: **Interleukin-1 beta inhibits synaptic transmission and induces membrane hyperpolarization in amygdala neurons**. *The Journal of pharmacology and experimental therapeutics* 1994, **271**(2):590-600.
217. Zhou C, Qi C, Zhao J, Wang F, Zhang W, Li C, Jing J, Kang X, Chai Z: **Interleukin-1beta inhibits voltage-gated sodium currents in a time- and dose-dependent manner in cortical neurons**. *Neurochemical research* 2011, **36**(6):1116-1123.
218. Zhu G, Okada M, Yoshida S, Mori F, Ueno S, Wakabayashi K, Kaneko S: **Effects of interleukin-1beta on hippocampal glutamate and GABA releases associated with Ca2+-induced Ca2+ releasing systems**. *Epilepsy research* 2006, **71**(2-3):107-116.
219. Bluthe RM, Castanon N, Pousset F, Bristow A, Ball C, Lestage J, Michaud B, Kelley KW, Dantzer R: **Central injection of IL-10 antagonizes the behavioural effects of lipopolysaccharide in rats**. *Psychoneuroendocrinology* 1999, **24**(3):301-311.220.

220. Buvanendran A, Kroin JS, Berger RA, Hallab NJ, Saha C, Negrescu C, Moric M, Caicedo MS, Tuman KJ: **Upregulation of prostaglandin E2 and interleukins in the central nervous system and peripheral tissue during and after surgery in humans**. *Anesthesiology* 2006, **104**(3):403-410.
221. Yeager MP, Lunt P, Arruda J, Whalen K, Rose R, DeLeo JA: **Cerebrospinal fluid cytokine levels after surgery with spinal or general anesthesia**. *Regional anesthesia and pain medicine* 1999, **24**(6):557-562.
222. Ledeboer A, Breve JJ, Wierinckx A, van der Jagt S, Bristow AF, Leysen JE, Tilders FJ, Van Dam AM: **Expression and regulation of interleukin-10 and interleukin-10 receptor in rat astroglial and microglial cells**. *Eur J Neurosci* 2002, **16**(7):1175-1185.
223. Sabat R, Grutz G, Warszawska K, Kirsch S, Witte E, Wolk K, Geginat J: **Biology of interleukin-10**. *Cytokine & growth factor reviews* 2010, **21**(5):331-344.
224. Moore KW, de Waal Malefyt R, Coffman RL, O'Garra A: **Interleukin-10 and the interleukin-10 receptor**. *Annual review of immunology* 2001, **19**:683-765.
225. de Waal Malefyt R, Abrams J, Bennett B, Figdor CG, de Vries JE: **Interleukin 10(IL-10) inhibits cytokine synthesis by human monocytes: an autoregulatory role of IL-10 produced by monocytes**. *The Journal of experimental medicine* 1991, **174**(5):1209-1220.
226. Kelly A, Lynch A, Vereker E, Nolan Y, Queenan P, Whittaker E, O'Neill LA, Lynch MA: **The anti-inflammatory cytokine, interleukin (IL)-10, blocks the inhibitory effect of IL-1 beta on long term potentiation. A role for JNK**. *J Biol Chem* 2001, **276**(49):45564-45572.
227. Chen Z, Nakajima T, Inoue Y, Kudo T, Jibiki M, Iwai T, Kimura A: **A single nucleotide polymorphism in the 3'-untranslated region of MyD88 gene is associated with Buerger disease but not with Takayasu arteritis in Japanese**. *J Hum Genet* 2011, **56**(7):545-547.
228. Mollaki V, Georgiadis T, Tassidou A, Ioannou M, Daniil Z, Koutsokera A, Papathanassiou AA, Zintzaras E, Vassilopoulos G: **Polymorphisms and haplotypes in TLR9 and MYD88 are associated with the development of Hodgkin's lymphoma: a candidate-gene association study**. *J Hum Genet* 2009, **54**(11):655-659.

229. Dhiman N, Ovsyannikova IG, Vierkant RA, Ryan JE, Pankratz VS, Jacobson RM, Poland GA: **Associations between SNPs in toll-like receptors and related intracellular signaling molecules and immune responses to measles vaccine: preliminary results**. *Vaccine* 2008, **26**(14):1731-1736.
230. Combi R, Ferini-Strambi L, Montruccoli A, Bianchi V, Malcovati M, Zucconi M, Dalpra L, Tenchini ML: **Two new putative susceptibility loci for ADNFLE**. *Brain research bulletin* 2005, **67**(4):257-263.
231. Wilkie GS, Dickson KS, Gray NK: **Regulation of mRNA translation by 5'- and 3'-UTR-binding factors**. *Trends in biochemical sciences* 2003, **28**(4):182-188.
232. Lai EC: **Micro RNAs are complementary to 3' UTR sequence motifs that mediate negative post-transcriptional regulation**. *Nature genetics* 2002, **30**(4):363-364.
233. Pillai RS: **MicroRNA function: multiple mechanisms for a tiny RNA?** *RNA* 2005, **11**(12):1753-1761.
234. John B, Enright AJ, Aravin A, Tuschl T, Sander C, Marks DS: **Human MicroRNA targets**. *PLoS biology* 2004, **2**(11):e363.
235. Huang Y, Shen XJ, Zou Q, Zhao QL: **Biological functions of microRNAs**. *Bioorganicheskaia khimiia* 2010, **36**(6):747-752.
236. Di Paola R, Frittitta L, Miscio G, Bozzali M, Baratta R, Centra M, Spampinato D, Santagati MG, Ercolino T, Cisternino C *et al*: **A variation in 3' UTR of hPTP1B increases specific gene expression and associates with insulin resistance**. *Am J Hum Genet* 2002, **70**(3):806-812.
237. Goto Y, Yue L, Yokoi A, Nishimura R, Uehara T, Koizumi S, Saikawa Y: **A novel single-nucleotide polymorphism in the 3'-untranslated region of the human dihydrofolate reductase gene with enhanced expression**. *Clinical cancer research : an official journal of the American Association for Cancer Research* 2001, **7**(7):1952-1956.
238. Miller GM, Madras BK: **Polymorphisms in the 3'-untranslated region of human and monkey dopamine transporter genes affect reporter gene expression**. *Molecular psychiatry* 2002, **7**(1):44-55.

239. Wang J, Pitarque M, Ingelman-Sundberg M: **3'-UTR polymorphism in the human CYP2A6 gene affects mRNA stability and enzyme expression**. *Biochemical and biophysical research communications* 2006, **340**(2):491-497.

240. Kamiyama M, Kobayashi M, Araki S, Iida A, Tsunoda T, Kawai K, Imanishi M, Nomura M, Babazono T, Iwamoto Y *et al*: **Polymorphisms in the 3' UTR in the neurocalcin delta gene affect mRNA stability, and confer susceptibility to diabetic nephropathy**. *Hum Genet* 2007, **122**(3-4):397-407.

241. Lee PH, Shatkay H: **F-SNP: computationally predicted functional SNPs for disease association studies**. *Nucleic Acids Res* 2008, **36**(Database issue):D820-824.

242. Sordillo JE, Sharma S, Poon A, Lasky-Su J, Belanger K, Milton DK, Bracken MB, Triche EW, Leaderer BP, Gold DR *et al*: **Effects of endotoxin exposure on childhood asthma risk are modified by a genetic polymorphism in ACAA1**. *BMC medical genetics* 2011, **12**:158.

243. Shmueli O, Horn-Saban S, Chalifa-Caspi V, Shmoish M, Ophir R, Benjamin-Rodrig H, Safran M, Domany E, Lancet D: **GeneNote: whole genome expression profiles in normal human tissues**. *Comptes rendus biologies* 2003, **326**(10-11):1067-1072.

244. Rahman P, Sun S, Peddle L, Snelgrove T, Melay W, Greenwood C, Gladman D: **Association between the interleukin-1 family gene cluster and psoriatic arthritis**. *Arthritis and rheumatism* 2006, **54**(7):2321-2325.

245. Xu M, He L: **Convergent evidence shows a positive association of interleukin-1 gene complex locus with susceptibility to schizophrenia in the Caucasian population**. *Schizophrenia research* 2010, **120**(1-3):131-142.

246. Shirts BH, Wood J, Yolken RH, Nimgaonkar VL: **Association study of IL10, IL1beta, and IL1RN and schizophrenia using tag SNPs from a comprehensive database: suggestive association with rs16944 at IL1beta**. *Schizophrenia research* 2006, **88**(1-3):235-244.

247. Kira R, Torisu H, Takemoto M, Nomura A, Sakai Y, Sanefuji M, Sakamoto K, Matsumoto S, Gondo K, Hara T: **Genetic susceptibility to simple febrile seizures: interleukin-1beta promoter polymorphisms are associated with sporadic cases**. *Neurosci Lett* 2005, **384**(3):239-244.

248. Liu X, Wang Z, Yu J, Lei G, Wang S: **Three polymorphisms in interleukin-1beta gene and risk for breast cancer: a meta-analysis**. *Breast cancer research and treatment* 2010, **124**(3):821-825.

249. Zienolddiny S, Ryberg D, Maggini V, Skaug V, Canzian F, Haugen A: **Polymorphisms of the interleukin-1 beta gene are associated with increased risk of non-small cell lung cancer**. *International journal of cancer Journal international du cancer* 2004, **109**(3):353-356.

250. El-Omar EM, Carrington M, Chow WH, McColl KE, Bream JH, Young HA, Herrera J, Lissowska J, Yuan CC, Rothman N *et al*: **Interleukin-1 polymorphisms associated with increased risk of gastric cancer**. *Nature* 2000, **404**(6776):398-402.

251. Consortium TEP: **A user's guide to the encyclopedia of DNA elements (ENCODE)**. *PLoS biology* 2011, **9**(4):e1001046.

252. Lind H, Haugen A, Zienolddiny S: **Differential binding of proteins to the IL1B -31 T/C polymorphism in lung epithelial cells**. *Cytokine* 2007, **38**(1):43-48.

253. Kimura R, Nishioka T, Soemantri A, Ishida T: **Cis-acting effect of the IL1B C-31T polymorphism on IL-1 beta mRNA expression**. *Genes and immunity* 2004, **5**(7):572-575.

254. Chen H, Wilkins LM, Aziz N, Cannings C, Wyllie DH, Bingle C, Rogus J, Beck JD, Offenbacher S, Cork MJ *et al*: **Single nucleotide polymorphisms in the human interleukin-1B gene affect transcription according to haplotype context**. *Human molecular genetics* 2006, **15**(4):519-529.

255. Kim JM, Brannan CI, Copeland NG, Jenkins NA, Khan TA, Moore KW: **Structure of the mouse IL-10 gene and chromosomal localization of the mouse and human genes**. *J Immunol* 1992, **148**(11):3618-3623.

256. Turner DM, Williams DM, Sankaran D, Lazarus M, Sinnott PJ, Hutchinson IV: **An investigation of polymorphism in the interleukin-10 gene promoter**. *European journal of immunogenetics : official journal of the British Society for Histocompatibility and Immunogenetics* 1997, **24**(1):1-8.

257. Lin MT, Storer B, Martin PJ, Tseng LH, Gooley T, Chen PJ, Hansen JA: **Relation of an interleukin-10 promoter polymorphism to graft-versus-host disease and survival after hematopoietic-cell transplantation**. *The New England journal of medicine* 2003, **349**(23):2201-2210.

258. Karabon L, Wysoczanska B, Bogunia-Kubik K, Suchnicki K, Lange A: **IL-6 and IL-10 promoter gene polymorphisms of patients and donors of allogeneic sibling hematopoietic stem cell transplants associate with the risk of acute graft-versus-host disease**. *Human immunology* 2005, **66**(6):700-710.

259. Grove J, Daly AK, Bassendine MF, Gilvarry E, Day CP: **Interleukin 10 promoter region polymorphisms and susceptibility to advanced alcoholic liver disease**. *Gut* 2000, **46**(4):540-545.

260. Bagnoli S, Cellini E, Tedde A, Nacmias B, Piacentini S, Bessi V, Bracco L, Sorbi S: **Association of IL10 promoter polymorphism in Italian Alzheimer's disease**. *Neurosci Lett* 2007, **418**(3):262-265.

261. Ma SL, Tang NL, Lam LC, Chiu HF: **The association between promoter polymorphism of the interleukin-10 gene and Alzheimer's disease**. *Neurobiology of aging* 2005, **26**(7):1005-1010.

262. Lio D, Licastro F, Scola L, Chiappelli M, Grimaldi LM, Crivello A, Colonna-Romano G, Candore G, Franceschi C, Caruso C: **Interleukin-10 promoter polymorphism in sporadic Alzheimer's disease**. *Genes and immunity* 2003, **4**(3):234-238.

263. Reuss E, Fimmers R, Kruger A, Becker C, Rittner C, Hohler T: **Differential regulation of interleukin-10 production by genetic and environmental factors--a twin study**. *Genes and immunity* 2002, **3**(7):407-413.

264. Hohler T, Grossmann S, Stradmann-Bellinghausen B, Kaluza W, Reuss E, de Vlam K, Veys E, Marker-Hermann E: **Differential association of polymorphisms in the TNFalpha region with psoriatic arthritis but not psoriasis**. *Annals of the rheumatic diseases* 2002, **61**(3):213-218.

265. Crawley E, Kay R, Sillibourne J, Patel P, Hutchinson I, Woo P: **Polymorphic haplotypes of the interleukin-10 5' flanking region determine variable interleukin-10 transcription and are associated with particular phenotypes of juvenile rheumatoid arthritis**. *Arthritis and rheumatism* 1999, **42**(6):1101-1108.

266. Gibson AW, Edberg JC, Wu J, Westendorp RG, Huizinga TW, Kimberly RP: **Novel single nucleotide polymorphisms in the distal IL-10 promoter affect IL-10 production and enhance the risk of systemic lupus erythematosus**. *J Immunol* 2001, **166**(6):3915-3922.

267. Bidwell J, Keen L, Gallagher G, Kimberly R, Huizinga T, McDermott MF, Oksenberg J, McNicholl J, Pociot F, Hardt C *et al*: **Cytokine gene polymorphism in human disease: on-line databases**. *Genes and immunity* 1999, **1**(1):3-19.

268. **2006 Census Data** [http://www.stats.govt.nz/Census/2006CensusHomePage]

Appendix

6.1 Buffers and other recipes

5 M GITC solution

295.4 g	GITC
2.5 g	N-Lauroylsarcosine sodium salt (sarkosyl)
3.9 g	Tri-sodium citrate
3.6 ml	2-mercaptoethanol
280 ml	DEPC treated MiliQ H_20

TE buffer

10 mM	Tris
1 mM	EDTA

CTAB/NaCl

10%	CTAB
0.7 M	NaCl

x10 Sodium borate gel running buffer

56 g	Boric Acid
10 g	Sodium Hydroxide
	Made up to 2 l with distilled water

x6 Loading buffer

30%	Glycerol
0.02%	Bromophenol Blue
0.02%	Xylene Cyanole

6.2 EEG data

Table 6.1: Processed EEG data supplied by the anaesthetist (part 1).

ID	ETDC (%)	BIS value	Spindle frequency (Hz)	Spindle amplitude (Log(μV))	Delta frequency (Hz)	Delta amplitude (Log(μV))	Relative spindle amplitude
1	7.51	25.00	8.500	1.979	0.750	6.878	0.263
2	7.62	28.00	7.125	2.245	2.250	5.746	0.295
3	7.78	41.80	7.750	1.495	0.625	4.895	0.192
4	4.03	44.30	8.375	2.252	0.500	4.411	0.559
5	4.91	30.00	7.250	1.708	0.625	6.547	0.348
6	6.35	44.60	15.500	0.580	0.500	5.550	0.091
7	6.18	30.60	10.250	1.390	0.500	7.134	0.225
8	6.69	56.25	8.875	1.129	0.500	7.322	0.169
9	3.59	42.20	9.625	1.745	0.875	6.234	0.486
10	4.82	35.50	10.125	2.043	0.500	5.458	0.424
11	5.63	–	11.250	1.785	0.625	8.317	0.317
12	3.53	38.80	9.875	2.477	0.625	5.917	0.702
13	4.11	42.40	10.250	1.934	0.625	5.371	0.471
14	6.18	29.30	8.125	2.019	1.125	5.541	0.327
15	5.81	25.20	8.250	2.164	0.500	7.119	0.373
16	4.66	45.60	10.750	2.330	0.625	5.307	0.500
17	4.34	40.10	9.125	2.364	0.750	6.306	0.545
18	5.35	43.20	11.875	3.043	0.500	4.405	0.569
19	7.96	37.00	15.875	1.036	0.500	6.980	0.130
20	7.06	40.80	8.000	1.302	0.875	6.317	0.184
21	7.36	30.30	9.000	1.099	0.875	6.311	0.149
22	6.61	34.90	8.000	1.428	0.750	5.562	0.216
23	7.62	38.20	7.500	1.453	0.750	5.608	0.191
24	5.83	42.70	16.375	1.020	0.750	5.517	0.175
25	4.53	45.40	10.250	1.928	0.500	5.832	0.426
26	6.21	28.30	7.625	1.263	1.125	6.346	0.203
27	5.49	39.10	13.875	0.726	0.750	4.358	0.132
28	2.12	29.70	8.750	1.790	0.500	5.462	0.844
29	4.60	40.30	9.875	2.477	0.625	5.917	0.538
30	5.58	56.10	11.875	1.951	0.750	5.229	0.350
31	4.45	48.00	9.750	2.700	1.000	5.936	0.607
33	5.40	21.90	8.625	1.606	1.250	6.932	0.297
34	6.88	31.20	7.500	1.342	0.625	5.564	0.195
35	4.75	31.60	7.875	2.521	0.500	7.323	0.531
36	3.61	54.80	11.125	2.579	0.500	4.405	0.714
37	4.56	46.40	9.875	1.987	0.875	5.222	0.436
38	6.03	40.60	10.000	1.031	0.500	5.825	0.171
39	7.30	39.30	9.750	1.886	0.875	5.929	0.258
40	4.35	58.80	12.875	2.181	0.500	5.629	0.501
41	4.95	41.30	11.500	2.174	0.500	7.430	0.439

Table 6.1 cont.: Processed EEG data (part 2).

ID	ETDC (%)	BIS value	Spindle frequency (Hz)	Spindle amplitude (Log(μV))	Delta frequency (Hz)	Delta amplitude (Log(μV))	Relative spindle amplitude
42	5.04	24.00	7.500	1.331	0.875	7.518	0.264
43	6.67	28.80	7.125	1.017	0.750	5.945	0.153
44	6.89	32.50	8.875	1.129	0.500	7.322	0.164
45	5.15	45.00	9.875	2.426	1.000	5.121	0.471
46	4.96	52.80	10.375	2.772	0.500	4.859	0.559
47	4.71	29.60	10.375	2.394	0.625	6.127	0.508
48	5.96	26.70	7.125	2.290	0.750	6.102	0.384
49	6.66	36.50	10.375	1.829	0.625	7.407	0.275
50	4.91	45.00	7.375	0.951	0.500	3.585	0.194
51	5.58	55.10	13.000	1.622	0.500	5.116	0.291
52	3.78	43.00	9.000	1.544	0.500	4.637	0.409
53	6.10	25.10	8.375	1.967	1.125	5.809	0.323
54	5.54	35.30	8.250	1.881	0.500	6.968	0.339
55	4.44	26.80	7.500	0.879	1.375	7.080	0.198
56	5.03	31.00	7.500	1.748	0.500	5.641	0.348
58	5.38	40.00	8.250	1.191	0.750	5.478	0.221
59	8.01	44.70	10.625	1.653	0.500	3.832	0.206
60	5.95	35.00	10.125	1.371	0.750	7.346	0.230
62	3.92	33.20	9.375	2.324	1.125	5.316	0.593
63	3.95	55.30	10.250	2.097	0.750	4.780	0.531
64	5.67	25.40	16.500	0.191	0.500	6.307	0.034
65	5.46	23.70	10.250	1.680	0.500	7.097	0.308
66	5.34	56.00	11.375	2.313	0.625	5.064	0.433
67	4.71	56.60	12.000	1.623	0.500	4.539	0.345
68	5.13	33.00	8.750	1.732	0.875	6.014	0.338
69	6.41	27.00	9.625	2.194	0.750	6.742	0.342
70	8.70	38.30	9.000	1.018	0.625	6.279	0.117
71	4.88	52.27	13.000	3.231	0.500	5.434	0.662
72	4.81	48.40	9.500	3.062	0.500	5.131	0.636
73	5.62	34.16	9.375	1.996	1.000	7.091	0.355
74	7.61	60.22	7.875	1.705	0.500	5.167	0.224
75	5.81	26.80	8.750	2.839	0.625	5.543	0.489
76	5.39	60.19	7.875	1.767	0.875	6.063	0.328
78	6.47	36.08	8.125	1.813	0.500	7.020	0.280
79	4.32	0.00	9.000	2.261	0.500	5.611	0.523
80	6.57	36.00	7.500	1.387	0.500	5.623	0.211
82	7.64	57.00	9.625	2.312	0.625	5.541	0.303
83	6.91	30.00	7.375	1.815	0.500	6.475	0.263
85	9.46	50.41	7.875	0.707	1.250	5.085	0.075
86	4.26	78.97	9.250	2.635	1.250	6.083	0.619
87	3.79	–	8.500	2.591	0.750	6.460	0.684
88	5.76	–	9.000	1.541	0.500	7.021	0.268
89	4.43	35.00	10.250	1.560	0.875	5.338	0.352
90	3.68	41.00	8.000	1.622	1.125	5.562	0.441
91	5.46	50.00	10.125	2.666	0.500	4.446	0.488

Table 6.1 cont.: Processed EEG data (part 3).

ID	ETDC (%)	BIS value	Spindle frequency (Hz)	Spindle amplitude (Log(μV))	Delta frequency (Hz)	Delta amplitude (Log(μV))	Relative spindle amplitude
90	3.68	41.00	8.000	1.622	1.125	5.562	0.441
91	5.46	50.00	10.125	2.666	0.500	4.446	0.488
92	6.39	40.00	8.125	1.177	0.500	6.565	0.184
93	6.75	26.00	7.625	1.860	0.500	6.358	0.276
94	4.98	33.00	9.625	1.848	1.125	6.603	0.371
95	5.57	42.00	10.125	1.473	1.000	5.443	0.265
96	4.56	–	12.250	2.269	0.875	5.221	0.498
97	4.14	–	9.250	2.435	0.750	5.917	0.588
99	4.38	43.00	8.500	2.499	0.500	5.529	0.571
100	4.50	81.04	9.250	1.523	0.625	5.764	0.338
101	7.96	34.00	8.375	1.907	0.625	5.203	0.240
102	4.57	–	12.125	2.268	0.750	5.900	0.496
103	4.66	39.00	9.500	1.994	0.500	5.854	0.428
104	4.80	48.00	11.375	2.596	0.750	4.697	0.541
105	4.74	–	7.125	2.056	0.500	6.213	0.434
106	7.43	–	8.250	1.189	0.750	7.233	0.160
108	5.18	–	9.250	3.027	0.750	4.948	0.584
109	6.03	–	8.625	1.440	0.625	5.242	0.239
110	4.01	–	10.625	2.432	1.125	6.897	0.606
111	6.68	–	8.750	0.613	0.500	5.319	0.092
112	6.04	–	10.125	1.393	0.625	5.328	0.231
114	3.28	–	11.875	2.340	0.875	4.014	0.713
115	7.44	–	15.875	1.144	0.500	7.138	0.154
116	–	–	11.125	2.059	0.500	5.825	–
117	7.52	–	9.500	1.323	0.500	7.159	0.176
118	6.52	–	8.375	2.224	0.500	4.886	0.341
119	4.34	48.00	11.500	2.379	0.875	5.572	0.548
120	3.84	42.00	11.375	2.111	1.250	5.232	0.550
121	4.17	51.00	10.750	2.436	0.750	4.455	0.584
122	6.38	23.00	9.250	2.545	0.625	7.131	0.399
123	7.51	25.00	8.250	0.499	0.500	10.222	0.066
124	–	–	9.375	2.713	0.625	5.048	–
125	–	–	10.250	2.930	0.500	4.810	–
128	5.28	–	9.250	2.675	0.750	6.161	0.507
130	4.37	–	12.250	2.306	0.500	3.358	0.528
131	5.01	–	8.750	2.080	0.500	5.907	0.415
158	7.43	29.20	8.000	1.387	0.500	6.282	0.187
159	6.03	39.50	15.250	0.512	1.125	6.294	0.085
163	5.74	–	10.375	1.149	0.750	5.941	0.200
165	5.96	38.30	8.000	0.674	0.750	6.594	0.113
167	4.54	40.30	11.375	1.283	0.625	6.006	0.283
170	6.80	38.90	8.625	1.505	0.625	6.009	0.221

Table 6.2: Correlations between EEG traits, ETDC and BIS value.
Significant *p*-values are marked with an asterisk ($p < 0.05$) or double asterisk ($p < 0.001$), respectively. N/A = Assumptions for linear regression model not able to be met.

Independent variable	Dependent variable	Intercept	Slope	r^2	*r*	*p*-value	n
ETDC	√(BIS value)	7.088	-0.149	0.052	-0.227	0.0230*	100
	Spindle frequency	N/A	N/A	N/A	N/A	N/A	N/A
	Spindle amplitude	3.054	-0.222	0.218	-0.467	<0.0001**	122
	Delta amplitude	4.768	0.202	0.070	0.265	0.0032**	122
	Log^{10} (delta frequency)	-0.139	-0.006	0.003	-0.058	0.5292	122
BIS value	Spindle frequency	N/A	N/A	N/A	N/A	N/A	N/A
	Spindle amplitude	1.298	0.012	0.050	0.223	0.0254*	100
	√ (delta amplitude)	0.941	-0.002	0.220	-0.469	<0.0001**	100
	Log^{10} (delta frequency)	-0.121	-0.001	0.009	-0.093	0.3564	100

6.3 Raw genotyping data

Table 6.3: Raw genotyping results for SNPs genotyped by PCR-RFLP (part 1a).

Patient ID	rs1088-9635	rs6681-460	rs2146-904	rs5722-27	rs2798-45	rs2798-41	rs1336-1609
1	A/G	A/G	A/G	A/G	A/T	A/G	T/T
2	A/A	G/G	G/G	A/G	A/T	A/G	C/T
3	A/A	G/G	G/G	G/G	T/T	G/G	C/T
4	G/G	A/G	A/G	A/G	A/T	A/G	C/T
5	A/G	A/G	A/G	G/G	T/T	G/G	T/T
6	G/G	A/A	A/A	A/G	A/T	A/G	T/T
7	A/A	G/G	G/G	G/G	T/T	–	T/T
8	A/G	A/G	A/G	A/A	A/T	A/G	T/T
9	A/G	A/G	A/G	G/G	T/T	G/G	T/T
10	A/A	G/G	G/G	A/A	A/A	A/A	T/T
11	G/G	A/A	A/A	A/G	A/T	A/G	C/T
12	G/G	A/A	A/A	G/G	T/T	G/G	T/T
13	G/G	A/A	A/A	G/G	T/T	G/G	T/T
14	A/G	A/G	A/G	A/G	A/T	A/G	C/T
15	A/G	A/G	A/G	G/G	T/T	G/G	C/T
16	A/G	A/G	A/G	A/G	A/A	A/A	C/T
17	A/A	G/G	G/G	A/A	A/A	A/A	T/T
18	A/A	G/G	G/G	A/G	A/A	A/G	T/T
19	A/A	G/G	G/G	A/G	A/T	A/G	T/T
20	A/A	G/G	G/G	G/G	T/T	G/G	T/T
21	A/G	G/G	G/G	A/A	A/T	A/G	C/T
22	A/G	A/G	A/G	G/G	A/T	A/G	T/T
23	A/G	G/G	G/G	A/A	A/T	A/G	T/T
24	G/G	A/G	A/G	G/G	T/T	G/G	T/T
25	A/A	G/G	G/G	A/G	A/T	A/G	T/T
26	A/G	A/G	A/G	G/G	T/T	G/G	C/T
27	A/A	G/G	G/G	G/G	A/T	G/G	T/T
28	A/G	A/G	A/G	A/G	A/T	A/G	T/T
29	A/G	A/G	G/G	G/G	A/T	A/A	T/T
30	A/G	A/G	A/G	A/A	A/A	A/A	C/T
31	A/A	–	G/G	G/G	T/T	G/G	T/T
33	A/G	A/G	A/G	A/G	A/T	A/G	C/T
34	–	–	–	A/G	A/T	A/G	C/C
35	G/G	A/A	A/A	A/G	A/T	A/G	T/T
36	A/G	A/G	A/G	A/G	A/T	A/G	T/T
37	A/G	G/G	G/G	A/G	A/A	A/G	C/T
38	A/G	A/G	A/G	G/G	T/T	G/G	C/C
39	A/A	G/G	A/G	A/G	A/T	A/G	C/C
40	G/G	A/A	A/A	A/G	A/T	A/G	T/T
41	A/G	A/G	A/G	A/G	A/T	A/G	T/T

Table 6.3 cont.: Raw genotyping results for SNPs genotyped by PCR-RFLP (part 1b).

Patient ID	rs1318-7565	rs7501-581	rs8066-527	rs8066-269	rs7254-543	rs8736-34
1	G/T	C/C	C/C	G/G	C/C	T/T
2	G/T	G/G	C/T	G/G	C/C	T/T
3	G/T	C/G	C/C	G/G	C/C	T/T
4	T/T	C/G	C/T	G/G	C/C	T/T
5	G/G	C/G	C/C	G/G	A/A	G/T
6	G/G	C/C	C/C	G/G	A/C	G/T
7	G/G	C/C	C/C	G/G	A/A	T/T
8	G/G	C/C	C/T	G/G	A/C	G/T
9	G/G	C/C	C/T	G/G	A/C	G/T
10	G/G	G/G	C/C	G/G	A/A	G/G
11	G/T	C/C	C/T	G/G	C/C	G/T
12	G/G	C/G	C/T	–	C/C	T/T
13	G/G	C/C	C/T	G/G	A/A	G/T
14	G/T	C/C	C/C	G/G	A/C	T/T
15	T/T	C/C	C/C	G/G	C/C	T/T
16	G/T	C/C	T/T	G/G	A/C	G/T
17	G/G	C/C	T/T	G/G	A/C	G/T
18	G/T	C/C	C/T	G/G	C/C	T/T
19	T/T	G/G	C/C	G/G	A/A	G/T
20	G/T	C/C	C/T	G/G	A/C	G/T
21	T/T	G/G	C/C	–	C/C	T/T
22	T/T	C/G	C/C	G/G	A/A	T/T
23	G/G	G/G	C/C	–	C/C	G/T
24	G/G	C/G	C/C	G/G	A/C	T/T
25	G/G	C/C	C/C	–	A/A	G/T
26	G/T	C/G	C/T	–	C/C	T/T
27	G/T	C/G	C/T	–	A/C	G/T
28	G/T	C/G	C/C	–	A/C	G/G
29	G/G	C/C	C/T	–	C/C	T/T
30	G/T	C/G	C/C	–	C/C	G/T
31	G/G	C/G	C/T	–	C/C	T/T
33	G/T	G/G	T/T	–	C/C	T/T
34	T/T	C/G	C/T	G/G	C/C	G/T
35	G/G	C/G	C/C	–	A/C	G/G
36	G/G	C/G	C/T	–	C/C	T/T
37	T/T	C/G	C/T	–	A/A	G/T
38	T/T	C/C	C/T	–	C/C	T/T
39	T/T	C/C	C/T	–	A/C	T/T
40	G/G	C/C	C/C	–	C/C	T/T
41	G/G	G/G	C/T	–	C/C	G/T

Table 6.3 cont.: Raw genotyping results for SNPs genotyped by PCR-RFLP (part 2a).

Patient ID	rs1088-9635	rs6681-460	rs2146-904	rs5722-27	rs2798-45	rs2798-41	rs1336-1609
42	G/G	A/A	A/A	G/G	A/T	G/G	T/T
43	A/A	G/G	G/G	A/G	T/T	G/G	T/T
44	A/A	G/G	G/G	A/G	A/T	A/G	T/T
45	A/G	A/G	A/G	A/G	A/T	A/G	C/T
46	A/A	G/G	G/G	A/G	A/T	A/G	T/T
47	A/A	G/G	A/G	G/G	T/T	G/G	T/T
48	G/G	A/A	A/A	G/G	T/T	G/G	T/T
49	A/G	A/G	A/G	A/G	A/T	A/G	C/C
50	A/A	G/G	G/G	A/G	T/T	G/G	T/T
51	A/A	G/G	G/G	A/G	A/T	A/G	C/T
52	A/G	A/G	A/G	A/G	A/T	A/G	T/T
53	A/A	G/G	G/G	A/G	A/T	A/G	T/T
54	A/A	G/G	A/G	G/G	T/T	G/G	C/T
55	A/G	A/G	A/G	A/G	A/T	A/G	C/T
56	A/G	A/G	A/G	A/G	A/T	A/G	T/T
58	A/G	A/G	A/G	A/G	A/T	A/G	T/T
59	A/G	A/G	A/G	G/G	T/T	G/G	C/T
60	A/G	A/G	A/G	A/G	A/T	A/G	C/T
62	A/G	A/G	A/G	A/G	A/T	A/G	T/T
63	G/G	A/A	A/A	A/G	A/T	A/G	T/T
64	A/G	A/G	A/G	G/G	T/T	G/G	–
65	A/G	A/G	A/G	A/A	A/T	A/G	T/T
66	A/G	A/G	A/G	A/G	A/T	A/G	T/T
67	A/A	G/G	G/G	G/G	A/T	G/G	C/T
68	A/A	G/G	G/G	A/G	A/T	A/G	T/T
69	A/G	A/G	A/G	A/G	A/T	G/G	T/T
70	A/G	A/G	A/G	G/G	A/T	A/G	T/T
71	A/G	A/G	A/G	G/G	A/T	A/G	C/T
72	A/A	G/G	G/G	A/G	A/T	A/G	T/T
73	A/A	G/G	G/G	G/G	T/T	G/G	T/T
74	A/G	G/G	G/G	A/G	T/T	G/G	–
75	A/G	G/G	G/G	A/G	A/T	A/G	C/T
76	A/G	A/G	A/A	A/G	A/T	A/G	T/T
78	G/G	A/A	A/A	A/G	A/T	A/G	T/T
79	A/A	G/G	G/G	G/G	A/A	G/G	T/T
80	A/A	G/G	G/G	A/G	A/T	A/G	C/T
82	G/G	A/A	A/A	A/A	A/A	A/A	T/T
83	A/A	G/G	G/G	G/G	T/T	G/G	C/T
85	A/G	A/G	A/G	A/G	A/T	A/G	C/T
86	G/G	A/A	A/A	G/G	T/T	G/G	T/T
87	A/A	G/G	G/G	A/G	A/T	A/G	C/T
88	A/G	A/G	A/G	G/G	T/T	G/G	T/T
89	A/A	G/G	G/G	A/A	A/A	A/A	C/T
90	A/A	G/G	G/G	G/G	T/T	G/G	T/T

Table 6.3 cont.: Raw genotyping results for SNPs genotyped by PCR-RFLP (part 2b).

Patient ID	rs1318-7565	rs7501-581	rs8066-527	rs8066-269	rs7254-543	rs8736-34
42	G/G	C/C	C/T	–	A/C	G/T
43	G/G	C/C	C/T	G/G	C/C	T/T
44	G/T	C/C	C/C	–	A/C	G/T
45	G/T	C/C	T/T	–	A/C	G/G
46	G/T	G/G	C/C	–	A/C	G/T
47	G/G	C/G	C/T	–	A/C	G/T
48	G/G	C/G	T/T	G/G	A/C	T/T
49	T/T	C/C	C/C	–	A/C	G/T
50	G/T	C/C	C/T	–	A/C	G/T
51	T/T	C/C	C/C	–	A/A	G/T
52	G/T	C/G	T/T	–	A/C	G/T
53	G/T	C/G	C/T	–	A/C	T/T
54	G/T	C/C	C/T	–	C/C	G/G
55	G/T	C/G	C/C	–	A/C	G/T
56	G/G	C/C	C/T	–	A/C	G/G
58	G/G	C/G	T/T	–	A/C	T/T
59	T/T	G/G	C/C	–	A/C	G/G
60	T/T	C/C	C/C	–	A/A	G/T
62	G/G	C/C	T/T	–	C/C	T/T
63	G/G	C/G	C/C	–	C/C	T/T
64	T/T	C/G	C/C	–	C/C	G/T
65	G/G	C/G	C/T	–	C/C	T/T
66	G/G	C/G	C/T	–	C/C	T/T
67	T/T	C/G	C/T	–	A/C	G/G
68	G/G	G/G	T/T	–	A/C	G/T
69	G/G	C/C	C/T	–	C/C	T/T
70	G/G	C/C	C/C	–	C/C	T/T
71	T/T	C/C	T/T	–	C/C	–
72	T/T	C/G	C/C	G/G	A/A	G/T
73	G/G	C/C	C/T	–	A/A	T/T
74	–	C/G	–	–	–	–
75	G/T	C/G	C/C	–	C/C	G/T
76	G/G	C/C	C/C	–	C/C	T/T
78	G/G	C/C	C/T	–	A/A	G/T
79	G/G	C/G	C/C	–	C/C	T/T
80	G/T	C/G	T/T	–	C/C	T/T
82	G/G	C/C	C/C	–	C/C	T/T
83	T/T	G/G	C/T	–	A/C	G/T
85	G/T	C/G	C/T	–	A/A	G/T
86	G/G	C/C	C/C	–	C/C	G/T
87	T/T	C/G	T/T	–	A/C	G/G
88	G/G	C/C	C/C	–	A/A	G/T
89	G/T	G/G	C/C	–	C/C	T/T
90	G/T	C/G	C/T	–	C/C	G/G

Table 6.3 cont.: Raw genotyping results for SNPs genotyped by PCR-RFLP (part 3a).

Patient ID	rs1088-9635	rs6681-460	rs2146-904	rs5722-27	rs2798-45	rs2798-41	rs1336-1609
91	A/G	A/G	A/G	G/G	T/T	G/G	T/T
92	A/G	A/G	A/G	G/G	T/T	G/G	T/T
93	A/G	A/G	A/G	A/G	A/T	A/G	T/T
94	A/A	G/G	G/G	G/G	T/T	G/G	T/T
95	A/A	G/G	G/G	G/G	T/T	G/G	T/T
96	A/A	G/G	G/G	G/G	A/T	G/G	C/T
97	A/A	G/G	G/G	A/A	A/A	A/A	C/T
99	G/G	A/A	A/A	G/G	T/T	G/G	C/C
100	A/A	G/G	G/G	A/G	A/A	A/A	T/T
101	G/G	A/A	A/A	G/G	T/T	G/G	T/T
102	G/G	A/A	A/A	G/G	A/T	G/G	C/T
103	A/A	G/G	G/G	A/A	A/A	A/A	C/T
104	G/G	A/A	A/A	A/G	A/T	A/G	T/T
105	G/G	A/A	A/A	G/G	T/T	G/G	C/T
106	A/G	A/G	A/G	A/G	A/A	A/G	T/T
108	A/G	A/G	A/G	A/G	A/T	A/G	T/T
109	A/G	A/G	A/G	G/G	T/T	G/G	T/T
110	G/G	A/A	A/A	A/A	A/A	A/A	C/T
111	A/G	G/G	G/G	A/G	A/T	A/G	T/T
112	A/A	G/G	G/G	A/A	A/A	A/A	T/T
114	A/A	G/G	G/G	A/G	A/T	A/G	C/T
115	A/A	G/G	G/G	A/A	T/T	G/G	T/T
116	G/G	A/A	A/A	G/G	T/T	G/G	C/T
117	A/A	G/G	G/G	A/A	A/A	A/A	C/C
118	A/G	A/G	A/G	G/G	T/T	G/G	C/C
119	A/G	G/G	G/G	G/G	T/T	G/G	C/T
120	A/A	G/G	G/G	A/A	A/A	A/A	T/T
121	A/G	A/G	A/G	A/A	A/A	A/A	T/T
122	A/G	A/G	A/G	A/G	A/T	A/A	T/T
123	A/G	A/G	A/G	A/G	A/T	A/G	C/T
124	A/G	G/G	A/G	G/G	T/T	G/G	C/T
125	A/G	A/G	G/G	A/A	A/A	A/A	T/T
128	A/G	G/G	A/G	A/A	A/A	A/A	C/T
130	A/A	A/A	A/G	A/G	A/T	A/G	C/T
131	A/G	A/A	A/G	G/G	T/T	G/G	C/T
158	A/A	G/G	G/G	G/G	T/T	G/G	T/T
159	A/G	A/G	A/A	A/G	A/T	A/G	C/T
163	A/G	G/G	G/G	A/G	T/T	–	C/T
165	A/A	G/G	G/G	G/G	T/T	G/G	C/C
167	A/G	A/G	A/G	A/G	A/T	A/G	–
170	A/G	A/G	A/G	A/G	A/A	A/G	T/T

Table 6.3 cont.: Raw genotyping results for SNPs genotyped by PCR-RFLP (part 3b).

Patient ID	rs1318-7565	rs7501-581	rs8066-527	rs8066-269	rs7254-543	rs8736-34
91	T/T	C/G	C/T	–	C/C	T/T
92	G/T	G/G	C/T	–	A/C	G/G
93	G/G	G/G	T/T	–	A/C	G/T
94	G/G	C/G	T/T	–	A/C	G/G
95	G/T	C/C	C/T	–	–	G/T
96	G/T	C/G	C/C	–	C/C	G/G
97	T/T	C/G	C/C	–	A/C	G/G
99	T/T	C/C	C/T	–	C/C	T/T
100	G/G	C/G	C/C	–	A/C	G/T
101	G/G	C/C	T/T	–	C/C	G/T
102	T/T	C/G	C/C	–	C/C	T/T
103	G/T	C/G	T/T	–	A/A	T/T
104	G/T	C/C	C/C	–	C/C	T/T
105	T/T	C/C	C/T	–	C/C	G/T
106	G/G	C/G	T/T	–	–	T/T
108	G/G	C/G	C/T	–	C/C	T/T
109	G/T	C/C	C/T	–	C/C	T/T
110	T/T	C/G	C/C	–	A/C	G/G
111	G/T	C/C	C/C	–	C/C	G/T
112	G/T	G/G	C/C	–	C/C	T/T
114	T/T	G/G	C/C	–	C/C	G/T
115	G/T	C/G	C/T	–	A/A	G/T
116	T/T	C/G	C/T	–	A/A	G/T
117	G/T	C/G	C/C	–	C/C	T/T
118	T/T	G/G	C/C	–	C/C	G/T
119	G/T	C/C	C/C	–	C/C	T/T
120	G/G	C/G	C/T	–	A/C	G/T
121	G/G	C/C	T/T	–	A/C	G/T
122	G/T	C/G	C/C	–	A/A	G/G
123	G/T	C/C	T/T	–	C/C	G/T
124	G/T	C/G	C/C	–	A/C	G/T
125	G/G	C/C	C/C	–	C/C	T/T
128	G/T	C/G	C/C	–	A/C	G/T
130	G/T	C/G	C/T	–	A/C	G/T
131	G/T	C/C	C/C	–	A/A	T/T
158	G/G	G/G	C/C	–	–	G/T
159	G/T	C/C	C/T	–	C/C	T/T
163	G/T	C/G	–	–	–	–
165	T/T	G/G	C/C	–	C/C	T/T
167	G/T	C/G	C/T	–	–	T/T
170	G/G	C/C	C/T	–	C/C	G/T

Table 6.4: Raw genotyping results for genotyped by MassARRAY. Data supplied by AGRF (part 1a).

Patient ID	rs8192-284	rs2794-521	rs1800-871	rs1800-896	rs1143-634	rs1143-627	rs16944
1	A/A	C/T	C/C	A/G	C/C	T/T	G/G
2	A/C	C/T	C/C	A/G	C/T	C/T	A/G
3	A/A	C/T	C/C	A/G	C/C	C/T	A/G
4	A/C	C/T	C/C	A/G	C/C	C/T	A/G
5	A/A	T/T	C/C	G/G	C/T	C/T	A/G
7	A/A	T/T	C/T	A/G	C/C	C/T	A/G
8	A/C	T/T	C/C	G/G	C/C	T/T	G/G
9	A/C	T/T	C/T	A/G	C/C	C/C	A/A
10	A/A	T/T	T/T	A/A	C/C	C/C	A/A
11	A/A	C/T	C/C	G/G	T/T	T/T	G/G
13	A/C	T/T	C/T	A/A	C/C	T/T	G/G
14	A/A	T/T	C/C	A/G	C/C	C/T	A/G
16	A/C	T/T	C/C	G/G	C/C	C/T	A/G
18	A/A	T/T	C/T	A/G	C/C	T/T	G/G
19	A/C	T/T	T/T	A/A	C/C	T/T	G/G
20	A/A	C/T	C/T	A/G	C/C	C/C	A/A
21	A/A	T/T	C/C	G/G	C/C	C/T	A/G
22	C/C	T/T	C/T	A/G	C/C	T/T	G/G
23	A/C	T/T	C/C	A/G	C/C	T/T	G/G
24	A/A	C/T	T/T	A/A	C/C	T/T	G/G
25	A/C	T/T	C/C	G/G	C/T	T/T	G/G
26	A/A	C/T	C/C	G/G	C/T	T/T	G/G
27	C/C	T/T	C/C	G/G	C/C	T/T	G/G
29	A/C	T/T	C/C	A/G	C/C	C/T	A/G
30	A/C	C/T	C/C	A/G	C/T	C/T	A/G
33	A/C	T/T	C/C	A/G	C/C	C/T	A/G
34	A/C	T/T	C/T	A/A	C/C	C/T	A/G
35	A/C	T/T	C/C	G/G	C/T	C/T	A/G
36	A/A	T/T	C/T	A/G	C/C	C/T	A/G
37	C/C	T/T	C/T	A/G	C/C	C/T	A/G
38	A/C	C/T	C/C	G/G	C/C	T/T	G/G
39	A/A	–	C/T	A/A	C/C	–	A/G
40	A/C	C/T	C/C	G/G	C/C	C/T	A/G
42	C/C	T/T	C/C	A/G	C/T	C/C	A/A
43	A/A	C/T	C/C	G/G	C/C	C/C	A/A
44	A/A	C/T	C/C	G/G	C/C	C/C	A/A
45	A/A	–	C/C	A/G	C/C	C/T	A/G
47	A/C	C/C	C/C	G/G	C/C	T/T	G/G
49	C/C	C/T	C/C	A/G	C/C	C/T	A/G
51	A/A	T/T	C/T	A/A	C/C	C/C	A/G
52	A/C	T/T	C/C	G/G	C/T	T/T	G/G
53	C/C	C/T	C/C	A/A	C/T	T/T	G/G
54	C/C	C/T	C/T	A/A	C/C	C/T	A/G
55	A/C	T/T	C/C	A/G	C/C	C/T	A/G

Table 6.4 cont.: Raw genotyping results for genotyped by MassARRAY (part 1b).

Patient ID	rs6853	rs2069-762	rs3804-100	rs1800-629	rs1799-971	rs1049-9563	rs1146-6004
1	A/A	T/T	T/T	A/A	A/A	T/T	C/C
2	A/A	G/T	T/T	G/G	A/G	T/T	C/C
3	A/A	G/T	T/T	A/A	A/A	C/T	C/C
4	A/A	T/T	T/T	G/G	A/A	T/T	C/C
5	A/A	G/T	T/T	G/G	A/G	C/T	C/C
7	A/A	G/G	T/T	G/G	G/G	T/T	C/C
8	A/A	G/T	T/T	A/G	A/G	T/T	C/C
9	A/A	G/T	T/T	G/G	A/A	T/T	C/C
10	A/A	G/G	T/T	G/G	A/G	T/T	C/C
11	A/A	G/T	T/T	G/G	A/G	C/T	C/C
13	A/A	T/T	C/T	A/G	A/A	T/T	C/C
14	A/A	G/T	T/T	G/G	A/A	T/T	C/C
16	A/A	G/T	T/T	G/G	A/A	T/T	C/C
18	A/G	–	T/T	G/G	A/A	–	–
19	A/A	G/T	C/T	G/G	A/G	T/T	C/C
20	A/A	G/G	T/T	G/G	A/A	T/T	C/C
21	A/A	T/T	T/T	G/G	A/A	C/T	C/C
22	A/A	T/T	C/T	G/G	A/G	T/T	C/C
23	A/A	G/T	C/T	G/G	A/G	T/T	C/C
24	A/A	G/G	T/T	G/G	A/G	–	C/C
25	A/A	T/T	T/T	G/G	A/A	T/T	C/C
26	A/A	T/T	T/T	G/G	A/A	T/T	C/C
27	A/A	T/T	T/T	G/G	A/A	T/T	C/C
29	A/A	T/T	T/T	A/G	A/G	T/T	C/C
30	A/A	T/T	C/T	G/G	A/A	T/T	C/C
33	A/A	T/T	T/T	G/G	A/A	C/T	C/C
34	A/G	T/T	T/T	G/G	A/A	T/T	C/C
35	A/A	G/T	T/T	A/G	A/A	T/T	C/C
36	A/G	T/T	T/T	G/G	A/A	T/T	C/C
37	A/A	T/T	T/T	G/G	A/G	T/T	C/C
38	A/A	G/T	T/T	G/G	A/G	T/T	C/C
39	A/A	–	T/T	A/G	A/A	–	–
40	A/G	T/T	T/T	G/G	A/A	C/T	C/C
42	A/G	G/T	T/T	G/G	A/A	T/T	C/C
43	A/A	G/G	T/T	G/G	A/A	T/T	C/C
44	A/A	G/T	T/T	G/G	A/A	T/T	C/C
45	A/G	T/T	T/T	A/G	A/A	T/T	C/C
47	A/A	G/T	T/T	G/G	A/A	C/T	C/C
49	A/A	G/T	T/T	A/G	A/A	T/T	C/C
51	A/A	G/T	T/T	G/G	A/A	T/T	C/C
52	A/A	G/T	T/T	G/G	A/A	C/T	C/C
53	A/A	T/T	T/T	G/G	A/A	T/T	C/C
54	A/A	G/G	T/T	G/G	A/A	T/T	C/C
55	A/A	G/T	T/T	A/G	A/A	T/T	C/C

Table 6.4 cont.: Raw genotyping results for genotyped by MassARRAY (part 1c).

Patient ID	rs4986-790	rs4986-791	rs6265	rs5543-44	rs5802-53	rs1146-6314	rs1800-469
1	A/A	C/C	G/G	C/G	C/T	G/G	C/C
2	A/A	C/C	A/G	G/G	C/C	G/G	C/C
3	A/A	C/C	G/G	G/G	C/C	G/G	C/T
4	A/A	C/C	G/G	G/G	C/C	G/G	T/T
5	A/G	C/T	G/G	G/G	C/C	G/G	C/C
7	A/A	C/C	G/G	G/G	C/C	G/G	C/C
8	A/A	C/C	G/G	C/G	C/T	G/G	C/C
9	A/G	C/T	A/G	C/G	C/T	G/G	C/C
10	A/A	C/C	A/G	G/G	C/C	G/G	C/T
11	A/A	C/T	G/G	C/G	C/T	G/G	C/T
13	A/A	C/C	G/G	G/G	C/C	G/G	C/C
14	A/A	C/C	G/G	G/G	C/C	G/G	C/T
16	A/A	C/C	G/G	C/G	C/T	G/G	C/T
18	A/A	C/T	A/A	G/G	C/C	G/G	C/C
19	A/A	C/C	A/G	G/G	C/C	G/G	C/C
20	A/A	C/C	G/G	G/G	C/C	G/G	C/T
21	A/A	C/C	G/G	C/G	–	G/G	C/C
22	A/A	C/C	A/G	G/G	C/C	G/G	C/T
23	A/A	C/C	G/G	G/G	C/C	G/G	C/T
24	A/A	C/C	A/G	G/G	C/C	G/G	C/T
25	A/A	C/C	G/G	C/C	T/T	G/G	C/T
26	A/A	C/C	A/G	G/G	C/C	G/G	C/T
27	A/A	C/C	G/G	G/G	C/C	G/G	T/T
29	A/A	C/C	G/G	C/G	C/T	G/G	C/T
30	A/A	C/C	G/G	C/G	C/T	G/G	C/C
33	A/A	C/C	A/G	G/G	C/C	G/G	C/T
34	A/A	C/C	G/G	G/G	C/C	G/G	C/C
35	A/A	C/C	G/G	G/G	C/C	G/G	C/T
36	A/G	C/T	G/G	G/G	C/C	G/G	C/T
37	A/A	C/C	A/G	G/G	C/C	G/G	T/T
38	A/A	C/C	G/G	G/G	C/C	G/G	C/C
39	A/A	–	G/G	G/G	C/C	G/G	C/T
40	A/A	C/C	G/G	C/G	C/T	G/G	T/T
42	A/A	C/C	G/G	C/G	C/T	G/G	C/C
43	A/A	C/C	G/G	G/G	C/C	G/G	C/C
44	A/A	C/C	A/G	C/G	C/T	G/G	T/T
45	–	C/T	G/G	C/G	C/T	G/G	C/T
47	A/A	C/C	G/G	G/G	C/C	G/G	C/C
49	A/G	C/T	G/G	G/G	C/C	G/G	C/C
51	A/A	C/C	G/G	G/G	C/C	G/G	C/T
52	A/A	C/C	G/G	G/G	C/C	G/G	C/C
53	A/A	C/C	A/G	G/G	C/C	G/G	C/T
54	A/A	C/C	G/G	G/G	C/C	G/G	C/T
55	A/A	C/C	A/G	G/G	C/C	G/G	C/T

Table 6.4 cont.: Raw genotyping results for genotyped by MassARRAY (part 2a).

Patient ID	rs8192-284	rs2794-521	rs1800-871	rs1800-896	rs1143-634	rs1143-627	rs16944
56	C/C	T/T	C/T	A/A	C/C	C/C	A/A
58	A/A	C/T	C/C	A/A	C/C	C/T	A/G
59	A/A	C/C	C/T	A/G	C/C	T/T	G/G
60	A/C	T/T	C/T	A/A	C/C	C/T	A/G
64	–	C/T	C/C	A/G	C/C	C/T	A/G
65	C/C	C/C	C/T	A/G	C/C	C/T	A/G
66	A/A	C/T	C/C	A/G	C/C	T/T	G/G
67	A/A	T/T	C/C	A/G	C/T	C/T	A/G
68	C/C	C/C	C/T	A/G	C/T	T/T	G/G
69	A/A	T/T	C/T	A/A	C/C	C/T	A/G
70	A/C	C/T	C/C	A/G	C/C	T/T	G/G
71	A/A	T/T	C/C	A/A	C/C	T/T	G/G
72	C/C	T/T	C/C	A/G	C/C	C/T	A/G
73	A/C	T/T	C/C	A/G	C/T	T/T	G/G
74	–	C/T	C/C	G/G	C/C	–	A/G
75	C/C	C/C	C/T	A/G	C/T	T/T	G/G
76	C/C	T/T	C/T	A/G	C/T	T/T	G/G
78	A/A	T/T	C/C	A/G	C/C	C/T	A/G
80	C/C	T/T	C/T	A/A	C/C	C/T	A/G
82	A/C	C/C	C/C	A/G	C/C	C/T	A/G
83	A/A	T/T	C/T	A/A	C/C	T/T	G/G
85	A/C	T/T	T/T	A/A	C/C	T/T	G/G
86	C/C	T/T	C/C	A/G	C/T	C/T	A/G
87	A/C	T/T	T/T	A/A	C/C	C/T	A/G
88	A/A	C/T	C/C	G/G	C/C	C/C	A/A
89	A/C	T/T	C/T	A/A	C/C	C/T	A/G
90	A/C	T/T	C/C	A/G	C/C	C/C	A/A
91	A/A	T/T	C/T	A/A	C/C	C/T	A/G
93	A/C	C/T	C/C	A/G	C/T	C/T	A/G
94	A/C	T/T	C/T	A/G	C/C	C/T	A/G
95	A/A	C/T	C/C	A/A	C/C	T/T	G/G
96	A/A	T/T	T/T	A/A	C/T	C/T	A/G
97	A/A	C/T	T/T	A/A	C/C	C/T	A/G
99	A/A	C/T	C/T	A/A	C/C	C/T	A/G
100	A/A	T/T	T/T	A/A	C/C	T/T	G/G
101	A/C	C/C	C/T	A/A	C/C	T/T	G/G
102	C/C	T/T	C/T	A/G	C/C	C/C	A/A
104	A/C	T/T	C/C	A/G	C/C	C/T	A/G
108	A/A	T/T	C/C	A/G	C/T	C/T	A/G
111	A/C	C/T	C/C	A/A	C/C	C/T	A/G
112	A/C	T/T	C/T	A/A	C/C	C/C	A/A
114	A/A	T/T	T/T	A/A	C/C	C/T	A/G
116	A/A	T/T	C/C	G/G	C/T	T/T	G/G
117	A/A	C/T	C/C	G/G	C/C	T/T	G/G

Table 6.4 cont.: Raw genotyping results for genotyped by MassARRAY (part 2b).

Patient ID	rs6853	rs2069-762	rs3804-100	rs1800-629	rs1799-971	rs1049-9563	rs1146-6004
56	A/A	T/T	T/T	G/G	A/A	T/T	C/C
58	A/A	–	T/T	G/G	A/A	–	–
59	A/A	G/T	C/T	G/G	A/G	T/T	C/C
60	A/A	G/T	T/T	G/G	A/G	T/T	C/C
64	A/A	G/G	T/T	A/G	A/A	T/T	–
65	A/A	G/T	T/T	G/G	A/A	–	C/C
66	A/A	G/T	T/T	G/G	A/A	C/C	C/C
67	A/A	G/T	T/T	G/G	A/A	T/T	C/C
68	A/G	G/T	T/T	A/G	A/G	C/T	C/C
69	A/A	T/T	T/T	A/G	A/A	T/T	C/C
70	A/A	G/G	C/T	G/G	A/A	T/T	C/C
71	A/G	–	T/T	G/G	A/A	–	–
72	A/A	G/T	T/T	G/G	A/G	T/T	C/C
73	A/A	T/T	T/T	G/G	A/A	T/T	C/C
74	A/A	–	T/T	G/G	A/A	–	–
75	A/G	G/T	T/T	A/G	A/G	C/T	C/C
76	A/A	T/T	T/T	G/G	A/A	–	C/C
78	A/A	T/T	T/T	G/G	A/A	T/T	C/C
80	A/A	T/T	T/T	G/G	A/A	T/T	C/C
82	A/A	G/G	T/T	G/G	A/G	T/T	C/C
83	A/A	G/G	C/T	G/G	A/A	C/T	C/C
85	A/A	T/T	T/T	G/G	A/A	T/T	C/C
86	A/A	G/T	C/T	A/G	A/A	T/T	C/C
87	A/A	G/T	T/T	G/G	A/A	T/T	C/C
88	A/A	T/T	C/T	G/G	A/A	C/T	C/C
89	A/G	G/T	C/T	G/G	A/A	T/T	C/C
90	A/G	G/G	T/T	G/G	A/G	C/T	C/C
91	A/A	T/T	T/T	G/G	A/G	C/T	C/C
93	A/A	T/T	T/T	G/G	A/A	T/T	C/C
94	A/A	G/T	C/T	G/G	A/G	C/T	C/C
95	A/A	G/T	T/T	G/G	A/A	T/T	C/C
96	A/A	G/G	C/T	G/G	A/A	C/T	C/C
97	A/A	T/T	T/T	G/G	A/G	T/T	C/C
99	A/G	T/T	T/T	G/G	A/A	C/T	C/C
100	A/A	G/T	T/T	G/G	A/A	T/T	C/C
101	A/A	T/T	T/T	A/G	A/A	T/T	C/C
102	A/A	G/G	T/T	G/G	A/A	T/T	C/C
104	A/A	G/T	C/T	A/G	G/G	C/T	C/C
108	A/G	T/T	T/T	G/G	A/A	T/T	C/C
111	A/A	G/T	C/T	G/G	A/A	T/T	C/C
112	A/A	G/T	C/T	G/G	A/A	T/T	C/C
114	A/A	T/T	T/T	G/G	A/G	T/T	C/C
116	A/A	G/T	T/T	A/G	A/A	C/T	C/C
117	A/A	T/T	T/T	G/G	A/A	T/T	C/C

Table 6.4 cont.: Raw genotyping results for genotyped by MassARRAY (part 2c).

Patient ID	rs4986-790	rs4986-791	rs6265	rs5543-44	rs5802-53	rs1146-6314	rs1800-469
56	A/A	C/C	G/G	G/G	C/C	G/G	C/T
58	A/A	C/C	G/G	G/G	C/C	G/G	C/C
59	A/A	C/C	A/G	G/G	C/C	G/G	C/C
60	A/A	C/C	G/G	G/G	C/C	G/G	C/C
64	A/A	C/C	G/G	C/G	C/C	G/G	T/T
65	A/A	C/C	A/G	C/C	T/T	G/G	C/C
66	A/A	C/C	G/G	C/G	C/T	G/G	C/T
67	A/A	C/C	A/G	G/G	C/C	G/G	T/T
68	A/A	C/C	G/G	G/G	C/C	G/G	C/T
69	A/A	C/C	G/G	G/G	C/C	G/G	C/T
70	A/A	C/C	G/G	C/G	C/T	G/G	C/T
71	A/A	C/C	G/G	G/G	C/C	G/G	C/C
72	A/A	C/C	G/G	G/G	C/C	G/G	T/T
73	A/A	C/C	A/A	C/G	C/T	G/G	C/C
74	–	C/C	G/G	G/G	C/C	G/G	C/C
75	A/A	C/C	G/G	G/G	C/C	G/G	C/T
76	A/A	C/C	G/G	C/G	C/C	G/G	C/C
78	A/A	C/C	G/G	G/G	C/C	G/G	C/C
80	A/A	C/C	G/G	G/G	C/C	G/G	C/T
82	A/A	C/C	G/G	G/G	C/C	G/G	C/T
83	A/A	C/C	A/A	G/G	C/C	G/G	T/T
85	A/A	C/C	G/G	–	T/T	G/G	C/C
86	A/A	C/C	G/G	G/G	C/C	G/G	T/T
87	A/A	C/C	A/G	G/G	C/C	G/G	C/C
88	A/A	C/C	A/G	G/G	C/C	G/G	C/C
89	A/A	C/C	G/G	C/G	C/T	G/G	C/T
90	A/A	C/C	G/G	G/G	C/C	G/G	T/T
91	A/A	C/C	G/G	C/G	C/T	G/G	C/C
93	A/A	C/C	G/G	C/G	C/T	G/G	C/T
94	A/A	C/C	G/G	G/G	C/C	G/G	T/T
95	A/A	C/C	G/G	C/G	C/T	G/G	C/T
96	A/G	C/T	G/G	G/G	C/C	G/G	C/T
97	A/A	C/C	A/G	G/G	C/C	G/G	C/T
99	A/A	C/C	G/G	G/G	C/C	G/G	C/C
100	A/A	C/C	A/A	G/G	C/C	G/G	C/T
101	A/A	C/C	G/G	G/G	C/C	G/G	C/T
102	A/A	C/C	G/G	C/G	C/T	G/G	C/T
104	A/A	C/C	G/G	G/G	C/C	G/G	C/T
108	A/A	C/C	A/G	C/G	C/T	G/G	C/C
111	A/G	C/T	A/G	C/C	T/T	G/G	C/C
112	A/A	C/C	G/G	G/G	C/C	G/G	C/T
114	A/A	C/C	G/G	G/G	C/C	G/G	C/T
116	A/A	C/C	G/G	G/G	C/C	G/G	C/T
117	A/A	C/C	A/G	C/G	C/T	G/G	C/T

Table 6.4 cont.: Raw genotyping results for genotyped by MassARRAY (part 3).

Patient ID	rs8192-284	rs2794-521	rs1800-871	rs1800-896	rs1143-634	rs1143-627	rs16944
118	C/C	T/T	C/C	A/G	C/C	T/T	G/G
120	A/A	T/T	C/T	A/G	C/C	C/T	A/G
121	A/C	C/T	C/C	A/G	C/T	C/T	A/G
122	A/C	T/T	C/T	A/A	C/C	T/T	G/G
123	A/C	T/T	C/T	A/A	C/C	C/C	A/A
158	A/A	T/T	C/T	A/A	C/C	C/T	A/G
159	A/A	T/T	C/T	A/G	T/T	T/T	G/G
163	A/A	C/C	C/C	A/G	C/T	T/T	G/G
165	A/A	C/T	T/T	A/A	C/C	C/T	A/G
167	A/A	C/T	C/C	A/G	C/T	T/T	G/G
170	A/A	T/T	C/C	A/G	C/T	C/T	A/G
Patient ID	**rs6853**	**rs2069-762**	**rs3804-100**	**rs1800-629**	**rs1799-971**	**rs1049-9563**	**rs1146-6004**
118	A/A	G/T	T/T	G/G	A/G	T/T	C/C
120	A/G	T/T	T/T	A/G	A/A	C/T	C/C
121	A/A	T/T	T/T	G/G	A/A	C/T	C/C
122	A/G	G/G	C/C	G/G	A/A	T/T	C/C
123	–	T/T	T/T	A/G	A/A	–	C/C
158	A/A	T/T	T/T	G/G	A/A	T/T	C/C
159	A/A	–	T/T	G/G	A/A	–	–
163	A/A	T/T	T/T	G/G	A/A	T/T	
165	A/A	G/T	T/T	G/G	A/G	T/T	C/C
167	A/A	T/T	C/T	A/G	A/A	–	–
170	A/A	T/T	T/T	G/G	A/A	T/T	C/C
Patient ID	**rs4986-790**	**rs4986-791**	**rs6265**	**rs5543-44**	**rs5802-53**	**rs1146-6314**	**rs1800-469**
118	A/A	C/C	G/G	G/G	C/C	–	C/C
120	A/A	C/C	G/G	C/G	C/T	G/G	C/T
121	A/A	C/C	G/G	C/G	C/T	G/G	C/T
122	A/A	C/C	A/A	G/G	C/C	G/G	C/T
123	A/G	C/T	G/G	G/G	C/C	G/G	C/C
158	A/A	C/C	G/G	G/G	C/C	G/G	C/T
159	A/A	C/C	G/G	C/G	C/C	G/G	C/C
163	A/A	C/T	A/G	C/G	C/C	G/G	C/C
165	A/A	C/C	G/G	G/G	C/C	G/G	C/T
167	A/A	C/C	A/G	G/G	C/C	G/G	T/T
170	A/A	C/C	G/G	G/G	C/C	G/G	C/C

6.4 Sequencing results

```
GGAGAAATACTGGGCCAACCTGACTAGGATGCTAGCAAACTTTTGAATTCAGCATATAATTTAT
CTTGTAAATGTGACTATTTTAGAAAAAACAAAATACATTTGTGGAGAGCACCACACAATTAACT
TCATTCAGATTTGGCATTTGGATCTTGGCTTTTCT[A]GAGATCCCATTTCTAATGATATCTTA
TTCTGGGCTTTTTTTTCATCATTATTAAAGTCACCCTTTACTTTCCTTCTGCCTTTGAAGTTAC
AATCTCGTCAGTTCAAAGTCTTTTTAGAGCACTTAACAGAAAATTTAATCAAAACGCTGAGCCA
AATTTCAGCTAAAAAGTTATTAGCGTCACTGGAAATTGTGAGTCA
```

Figure 6.1: Sequence of PCR product amplified for SNP rs10889635 (*SGIP1*).
Sequencing product size was 363 bp, 1 bp shorter than the expected 364 bp. The position of rs10889635 is indicated and shown in bold. Sample sequenced was determined to be A/A homozygous both by sequencing and PCR-RFLP.

```
>ref|NW_001838579.2| Homo sapiens chromosome 1 genomic contig,
alternate assembly HuRef SCAF_1103279188432, whole genome
shotgun sequence
Length=32841984

 Features in this part of subject sequence:
  SH3-containing GRB2-like protein 3-interacting protein 1

 Score = 660 bits (357), Expect = 0.0
 Identities = 362/364 (99%), Gaps = 2/364 (1%)
 Strand=Plus/Minus

Query 2         GGAGAAATA-CTGGGCCAACCTGACTAGGATGCTAGCAAACTTTTGAATTCAGCATATAA 60
                ||||||||| ||||||||||||||||||||||||||||||||||||||||||||||||||
Sbjct 16610096  GGAGAAATATCTGGGCCAACCTGACTAGGATGCTAGCAAACTTTTGAATTCAGCATATAA 16610037

Query 61        TTTATCTTGTAAATGTGACTATTTTAGAAAAAACAAAATACATTTGTGGAGAGCACCACA 120
                ||||||||||||||||||||||||||||||||||||||||||||||||||||||||||||
Sbjct 16610036  TTTATCTTGTAAATGTGACTATTTTAGAAAAAACAAAATACATTTGTGGAGAGCACCACA 16609977

Query 121       CAATTAACTTCATTCAGATTTGGCATTTGGATCTTGGCTTTTCTAGAGATCCCATTTCTA 180
                ||||||||||||||||||||||||||||||||||||||||||||||||||||||||||||
Sbjct 16609976  CAATTAACTTCATTCAGATTTGGCATTTGGATCTTGGCTTTTCTAGAGATCCCATTTCTA 16609917

Query 181       ATGATATCTTATTCTGGGCttttttttCATCATTATTAAAGTCACCCTTTACTTTCCTTC 240
                ||||||||||||||||||||||||||||||||||||||||||||||||||||||||||||
Sbjct 16609916  ATGATATCTTATTCTGGGCTTTTTTTTCATCATTATTAAAGTCACCCTTTACTTTCCTTC 16609857

Query 241       TGCCTTTGAAGTTACAATCTCGTCAGTTCAAAGTCTTTTTAGAGCACTTAACAGAAAATT 300
                ||||||||||||||||||||||||||||||||||||||||||||||||||||||||||||
Sbjct 16609856  TGCCTTTGAAGTTACAATCTCGTCAGTTCAAAGTCTTTTTAGAGCACTTAACAGAAAATT 16609797

Query 301       TAATCAAAACGCTGAGCCAAATTTCAGCTAAAAAGTTATTAGCGTCACTGGAAATTGTGA 360
                |||||||||||||||||||||||||||||||||||||||||||||||||||| ||||
Sbjct 16609796  TAATCAAAACGCTGAGCCAAATTTCAGCTAAAAAGTTATTAGCGTCACTGGAAAT-GTGA 16609738

Query 361       GTCA 364
                ||||
Sbjct 16609737  GTCA 16609734
```

Figure 6.2: BLAST nucleotide alignment of rs10889635 (*SGIP1*) sequencing product (Query) against the human genome.
The most highly significant alignment is shown.

```
GAGGAAGATTCAGGATACAGCCATCCTATTTTTAAGGTTCAATGATTGCAGACTCTTAAAAGGC
TTACAGATTCAACCTGACTTTTATGTCTTGATCCCACTCTATGATGCCTGATGCCAAAATTCCC
ATGGCAGCTCAATTCCTTGTTAAGCTAGGAAGCAAGCAG[G]GGTGTAATCAGAGCACGAAACC
TTC
```

Figure 6.3: Sequence of PCR product amplified for SNP rs6681460 (*SGIP1*).
Sequencing product size was 193 bp as expected. The position of rs6681460 is indicated and shown in bold. Sample sequenced was determined to be G/G homozygous by both sequencing and PCR-RFLP.

```
>ref|NW_001838579.2| Homo sapiens chromosome 1 genomic contig,
alternate assembly HuRef SCAF_1103279188432, whole genome
shotgun sequence
Length=32841984

 Features in this part of subject sequence:
  SH3-containing GRB2-like protein 3-interacting protein 1

 Score = 351 bits (190), Expect = 1e-94
 Identities = 192/193 (99%), Gaps = 0/193 (0%)
 Strand=Plus/Minus

Query 1         GAGGAAGATTCAGGATACAGCCATCCTATTTTTAAGGTTCAATGATTGCAGACTCTTAAA 60
                ||||||||||||||||||||||||||||||||||||||||||||||||||||||||||||
Sbjct 16562353  GAGGAAGATTCAGGATACAGCCATCCTATTTTTAAGGTTCAATGATTGCAGACTCTTAAA 16562294

Query 61        AGGCTTACAGATTCAACCTGACTTTTATGTCTTGATCCCACTCTATGATGCCTGATGCCA 120
                ||||||||||||||||||||||||||||||||||||||||||||||||||||||||||||
Sbjct 16562293  AGGCTTACAGATTCAACCTGACTTTTATGTCTTGATCCCACTCTATGATGCCTGATGCCA 16562234

Query 121       AAATTCCCATGGCAGCTCAATTCCTTGTTAAGCTAGGAAGCAAGCAGGGGTGTAATCAGA 180
                |||||||||||||||||||||||||||||||||||||||||||||| ||||||||||
Sbjct 16562233  AAATTCCCATGGCAGCTCAATTCCTTGTTAAGCTAGGAAGCAAGCAGGGATGTAATCAGA 16562174

Query 181       GCACGAAACCTTC 193
                |||||||||||||
Sbjct 16562173  GCACGAAACCTTC 16562161
```

Figure 6.4: BLAST nucleotide alignment of rs6681460 (*SGIP1*) sequencing product (Query) against the human genome.
The most highly significant alignment is shown.

```
TTTCAGATGCACCCTGTATATTTACTGTTGATC[A]TGGAACTCGTGCCACTGAAAATTTTTAA
GTGACTATATTCAAAAACAGCAGGTTGCATGACAGTTTCTCAGTGAAGAGGTTCAAAAAAGGTG
AGATGCTATTGCTTTGTGAATTTACAAAGGAAAGAATAATTTAACTGCTCAGAATTACATGTCC
GGTCACTGCTT
```

Figure 6.5: Sequence of PCR product amplified for SNP rs2146904 (*SGIP1*).
Sequencing product size was 201 bp as expected. The position of rs2146904 is indicated and shown in bold. Sample sequenced was determined to be A/A homozygous by both sequencing and PCR-RFLP.

```
>ref|NT_032977.9| Homo sapiens chromosome 1 genomic contig,
GRCh37.p5 Primary Assembly
Length=90908613

 Features in this part of subject sequence:
  SH3-containing GRB2-like protein 3-interacting protein 1

 Score = 363 bits (196), Expect = 5e-98
 Identities = 198/199 (99%), Gaps = 0/199 (0%)
 Strand=Plus/Plus

Query 3         TCAGATGCACCCTGTATATTTACTGTTGATCATGGAACTCGTGCCACTGAAAATTTTTAA 62
                |||||||||||||||||||||||||| ||||||||||||||||||||||||||||||||
Sbjct 37132223  TCAGATGCACCCTGTATATTTACTGTTCATCATGGAACTCGTGCCACTGAAAATTTTTAA 37132282

Query 63        GTGACTATATTCAAAAACAGCAGGTTGCATGACAGTTTCTCAGTGAAGAGGTTCAAAAAA 122
                ||||||||||||||||||||||||||||||||||||||||||||||||||||||||||||
Sbjct 37132283  GTGACTATATTCAAAAACAGCAGGTTGCATGACAGTTTCTCAGTGAAGAGGTTCAAAAAA 37132342

Query 123       GGTGAGATGCTATTGCTTTGTGAATTTACAAAGGAAAGAATAATTTAACTGCTCAGAATT 182
                ||||||||||||||||||||||||||||||||||||||||||||||||||||||||||||
Sbjct 37132343  GGTGAGATGCTATTGCTTTGTGAATTTACAAAGGAAAGAATAATTTAACTGCTCAGAATT 37132402

Query 183       ACATGTCCGGTCACTGCTT 201
                |||||||||||||||||||
Sbjct 37132403  ACATGTCCGGTCACTGCTT 37132421
```

Figure 6.6: LAST nucleotide alignment of rs2146904 (*SGIP1*) sequencing product (Query) against the human genome.
The most highly significant alignment is shown.

```
TTACGGGTGCTGGAGACTGGAAAAAGCATCCAGTTTGGTTGCTGTGGAGCAACATGCATATTGG
ATTAGAAAATTGTGCCAAAAACTCCCACTGATGAGAATTCATAGGTGCCCCACACT[G]TGACA
AACACTTATATGATTCTCCTCTTTCCTGTTTACTGCAAATTCTGCCTTAAGGCTTCTTTTCAAG
ACTCAGAAGCCACTAATTATAAAGGAAAGGGCAGTTAATTGGCA
```

Figure 6.7: Sequence of PCR product amplified for SNP rs572227 (*GABRA2*).
Sequencing product size was 234 bp as expected. The position of rs572227 is indicated and shown in bold. Sample sequenced was determined to be G/G homozygous by both sequencing and PCR-RFLP.

```
>ref|NW_001838903.1| Homo sapiens chromosome 4 genomic contig,
alternate assembly HuRef SCAF_1103279187004, whole genome
shotgun sequence
Length=8800796

 Features flanking this part of subject sequence:
  123291 bp at 5' side: gamma-aminobutyric acid receptor
  subunit gamma-1 precursor
 812 bp at 3' side: gamma-aminobutyric acid receptor subunit
  alpha-2 precursor

 Score = 433 bits (234), Expect = 7e-119
 Identities = 234/234 (100%), Gaps = 0/234 (0%)
 Strand=Plus/Minus

Query 1         TTACGGGTGCTGGAGACTGGAAAAAGCATCCAGTTTGGTTGCTGTGGAGCAACATGCATA 60
                ||||||||||||||||||||||||||||||||||||||||||||||||||||||||||||
Sbjct 5948072   TTACGGGTGCTGGAGACTGGAAAAAGCATCCAGTTTGGTTGCTGTGGAGCAACATGCATA 5948013

Query 61        TTGGATTAGAAAATTGTGCCAAAAACTCCCACTGATGAGAATTCATAGGTGCCCCACACT 120
                ||||||||||||||||||||||||||||||||||||||||||||||||||||||||||||
Sbjct 5948012   TTGGATTAGAAAATTGTGCCAAAAACTCCCACTGATGAGAATTCATAGGTGCCCCACACT 5947953

Query 121       GTGACAAACACTTATATGATTCTCCTCTTTCCTGTTTACTGCAAATTCTGCCTTAAGGCT 180
                ||||||||||||||||||||||||||||||||||||||||||||||||||||||||||||
Sbjct 5947952   GTGACAAACACTTATATGATTCTCCTCTTTCCTGTTTACTGCAAATTCTGCCTTAAGGCT 5947893

Query 181       TCTTTTCAAGACTCAGAAGCCACTAATTATAAAGGAAAGGGCAGTTAATTGGCA 234
                ||||||||||||||||||||||||||||||||||||||||||||||||||||||
Sbjct 5947892   TCTTTTCAAGACTCAGAAGCCACTAATTATAAAGGAAAGGGCAGTTAATTGGCA 5947839
```

Figure 6.8: BLAST nucleotide alignment of rs572227 (*GABRA2*) sequencing product (Query) against the human genome.
The most highly significant alignment is shown.

```
TGCCATGTTTGTCACAGGTTTTCTTAATGAACTACATTTACAAATGGCAACTTCTGATAAAGGA
TAACAGATTAAGTTCAGTGTCAATTTTGACCAGATATTAAAACTCACAACTCTCTAAACTTCCT
TGATATTAACTACTGAACTAATTAATATCCCAGTAGCTTCTGGAG[T]TTCTAAGAGATAATGC
ACTCTGTGTTTTTGCAGAGGAAG
```

Figure 6.9: Sequence of PCR product amplified for SNP rs279845 (*GABRA2*).
Sequencing product size was 213 bp as expected. The position of rs279845 is indicated and shown in bold. Sample sequenced was determined to be T/T homozygous by both sequencing and PCR-RFLP.

```
ref|NT_006238.11| Homo sapiens chromosome 4 genomic contig,
GRCh37.p5 Primary Assembly
Length=9041845

 Features in this part of subject sequence:
  gamma-aminobutyric acid receptor subunit alpha-2 precursor
  gamma-aminobutyric acid receptor subunit alpha-2 precursor

 Score = 394 bits (213), Expect = 2e-107
 Identities = 213/213 (100%), Gaps = 0/213 (0%)
 Strand=Plus/Plus

Query 1       TGCCATGTTTGTCACAGGTTTTCTTAATGAACTACATTTACAAATGGCAACTTCTGATAA 60
              ||||||||||||||||||||||||||||||||||||||||||||||||||||||||||||
Sbjct 6032454 TGCCATGTTTGTCACAGGTTTTCTTAATGAACTACATTTACAAATGGCAACTTCTGATAA 6032513

Query 61      AGGATAACAGATTAAGTTCAGTGTCAATTTTGACCAGATATTAAAACTCACAACTCTCTA 120
              ||||||||||||||||||||||||||||||||||||||||||||||||||||||||||||
Sbjct 6032514 AGGATAACAGATTAAGTTCAGTGTCAATTTTGACCAGATATTAAAACTCACAACTCTCTA 6032573

Query 121     AACTTCCTTGATATTAACTACTGAACTAATTAATATCCCAGTAGCTTCTGGAGTTTCTAA 180
              ||||||||||||||||||||||||||||||||||||||||||||||||||||||||||||
Sbjct 6032574 AACTTCCTTGATATTAACTACTGAACTAATTAATATCCCAGTAGCTTCTGGAGTTTCTAA 6032633

Query 181     GAGATAATGCACTCTGTGTTTTTGCAGAGGAAG 213
              |||||||||||||||||||||||||||||||||
Sbjct 6032634 GAGATAATGCACTCTGTGTTTTTGCAGAGGAAG 6032666
```

Figure 6.10: BLAST nucleotide alignment of rs279845 (*GABRA2*) sequencing product (Query) against the human genome.
The most highly significant alignment is shown.

```
CCTCTCTGTTCCTATCCATACAT[G]TTTTTTCTTGGATTAATTCTCAGGCTATTATTTTCTAT
GGCTAATGTCTCCTACCCATTTCTGACCTTCTAGTCTTACTATTTTCTTGGAGTTTGAGAGTAT
AAATAGACAGCTACTGAGAAGTAGAAAGGTTGGACCAGTTTTCTGACT
```

Figure 6.11: Sequence of PCR product amplified for SNP rs279841 (*GABRA2*).
Sequencing product size was 174 bp as expected. The position of rs279841 is indicated and shown in bold. Sample sequenced was determined to be G/G homozygous by both sequencing and PCR-RFLP.

```
>ref|NT_006238.11| Homo sapiens chromosome 4 genomic contig,
GRCh37.p5 Primary Assembly
Length=9041845

Features in this part of subject sequence:
  gamma-aminobutyric acid receptor subunit alpha-2 precursor
  gamma-aminobutyric acid receptor subunit alpha-2 precursor

Score = 316 bits (171), Expect = 4e-84
Identities = 173/174 (99%), Gaps = 0/174 (0%)
Strand=Plus/Plus

Query 1       CCTCTCTGTTCCTATCCATACATGTTTTTTCTTGGATTAATTCTCAGGCTATTATTTTCT 60
              |||||||||||||||||| ||||||||||||||||||||||||||||||||||||||||
Sbjct 6043644 CCTCTCTGTTCCTATCCATAGATGTTTTTTCTTGGATTAATTCTCAGGCTATTATTTTCT 6043703

Query 61      ATGGCTAATGTCTCCTACCCATTTCTGACCTTCTAGTCTTACTATTTTCTTGGAGTTTGA 120
              ||||||||||||||||||||||||||||||||||||||||||||||||||||||||||||
Sbjct 6043704 ATGGCTAATGTCTCCTACCCATTTCTGACCTTCTAGTCTTACTATTTTCTTGGAGTTTGA 6043763

Query 121     GAGTATAAATAGACAGCTACTGAGAAGTAGAAAGGTTGGACCAGTTTTCTGACT 174
              ||||||||||||||||||||||||||||||||||||||||||||||||||||||
Sbjct 6043764 GAGTATAAATAGACAGCTACTGAGAAGTAGAAAGGTTGGACCAGTTTTCTGACT 6043817
```

Figure 6.12: BLAST nucleotide alignment of rs279841 (*GABRA2*) sequencing product (Query) against the human genome.
The most highly significant alignment is shown.

```
ATTCCCTCTGCGTCTCTGAAACCCACTGGATTAGCTAAAGGAAGCAAAA[T]GTGCTGCCAAAC
CCACCAGTCACTCAGCAGGGGAGCCCCGGCGTCTGAAGAGCTTCAAGACTCCCGAATGTCCCAA
AACATCTGTTTCAGATACAAGCATTGCCTCCCTGCCCATAGCCTCTTCAAAGGAAATCTTGCCC
TG
```

Figure 6.13: Sequence of PCR product amplified for SNP rs13361609 (*HCN1*)
Sequencing product size was 192 bp as expected. The position of rs13361609 is indicated and shown in bold. Sample sequenced was determined to be T/T homozygous by both sequencing and PCR-RFLP.

```
ref|NT_006576.16| Homo sapiens chromosome 5 genomic contig,
GRCh37.p5 Primary Assembly
Length=46395641

Features flanking this part of subject sequence:
  1218 bp at 5' side: potassium/sodium hyperpolarization-
  activated cyclic nucle...

Score = 355 bits (192), Expect = 8e-96
Identities = 192/192 (100%), Gaps = 0/192 (0%)
Strand=Plus/Plus

Query 1         ATTCCCTCTGCGTCTCTGAAACCCACTGGATTAGCTAAAGGAAGCAAAATGTGCTGCCAA 60
                ||||||||||||||||||||||||||||||||||||||||||||||||||||||||||||
Sbjct 45687413  ATTCCCTCTGCGTCTCTGAAACCCACTGGATTAGCTAAAGGAAGCAAAATGTGCTGCCAA 45687472

Query 61        ACCCACCAGTCACTCAGCAGGGGAGCCCCGGCGTCTGAAGAGCTTCAAGACTCCCGAATG 120
                ||||||||||||||||||||||||||||||||||||||||||||||||||||||||||||
Sbjct 45687473  ACCCACCAGTCACTCAGCAGGGGAGCCCCGGCGTCTGAAGAGCTTCAAGACTCCCGAATG 45687532

Query 121       TCCCAAAACATCTGTTTCAGATACAAGCATTGCCTCCCTGCCCATAGCCTCTTCAAAGGA 180
                ||||||||||||||||||||||||||||||||||||||||||||||||||||||||||||
Sbjct 45687533  TCCCAAAACATCTGTTTCAGATACAAGCATTGCCTCCCTGCCCATAGCCTCTTCAAAGGA 45687592

Query 181       AATCTTGCCCTG 192
                ||||||||||||
Sbjct 45687593  AATCTTGCCCTG 45687604
```

Figure 6.14: BLAST nucleotide alignment of rs13361609 (*HCN1*) sequencing product (Query) against the human genome.
The most highly significant alignment is shown.

```
TCACCAACAAAGAGGCCATTATCAACTTGGAGTCTCAAAGCTGATTTTCTCCACCTCTTTAGCA
AGAAATTCAGTGAAATTCTGGAAATGAAATTACACACGATTATAAATGAGATTATTATTATTAT
TGTCTCTGAGTGAATTAAGATGCATAAATTGGGTTAAAGGGGTTTCCTCTTTATAATTATTTTT
ACC[G]TACCGATTTACAAAACTCCACAGTTC
```

Figure 6.15: Sequence of PCR product amplified for SNP rs13187565 (*HCN1*)
Sequencing product size was 222 bp as expected. The position of rs13187565 is indicated and shown in bold. Sample sequenced was determined to be G/G homozygous by both sequencing and PCR-RFLP.

```
>ref|NT_006576.16| Homo sapiens chromosome 5 genomic contig,
GRCh37.p5 Primary Assembly
Length=46395641

Features flanking this part of subject sequence:
  11148 bp at 5' side: potassium/sodium hyperpolarization-
  activated cyclic nucle...

Score = 405 bits (219), Expect = 1e-110
Identities = 221/222 (99%), Gaps = 0/222 (0%)
Strand=Plus/Plus

Query 1         TCACCaacaaagaggccattatcaacttggagtctcaaagctgattttctccacctcttt 60
                ||||||||||||||||||||||||||||||||||||||||||||||||||||||||||||
Sbjct 45697343  TCACCAACAAAGAGGCCATTATCAACTTGGAGTCTCAAAGCTGATTTTCTCCACCTCTTT 45697402

Query 61        agcaagaAATTCAGTGAAATTCTGGAAATGAAATTACACACGATTATAAATGAGATTATT 120
                ||||||||||||||||||||||||||||||||||||||||||||||||||||||||||||
Sbjct 45697403  AGCAAGAAATTCAGTGAAATTCTGGAAATGAAATTACACACGATTATAAATGAGATTATT 45697462

Query 121       ATTATTATTGTCTCTGAGTGAATTAAGATGCATAAATTGGGTTAAAGGGGTTTCCTCTTT 180
                ||||||||||||||||||||||||||||||||||||||||||||||||||||||||||||
Sbjct 45697463  ATTATTATTGTCTCTGAGTGAATTAAGATGCATAAATTGGGTTAAAGGGGTTTCCTCTTT 45697522

Query 181       ATAATTATTTTTACCGTACCGATTTACAAAACTCCACAGTTC 222
                |||||||||||||||| ||||||||||||||||||||||||
Sbjct 45697523  ATAATTATTTTTACCGTAGCGATTTACAAAACTCCACAGTTC 45697564
```

Figure 6.16: BLAST nucleotide alignment of rs13187565 (*HCN1*) sequencing product (Query) against the human genome.
The most highly significant alignment is shown.

```
GTGGTGCAGCCTTAGGTGAGTGAACAACGCCCAGGGTTGAAGGGCTCAGCAAGTGAGGGGTGGT
GATGGAGGTCATCCGACCCATCCCGCCGCCTCTCCGCAGTGGCGCAAGCGCCCCAAAATCTCCG
GAGAGGGAACTGA[C/G]TGACCCACTAGGTTCCGCCGTGTCTACCTCTCGCAGATGTTGGGGA
AGTGCTT
```

Figure 6.17: Sequence of PCR product amplified for SNP rs7501581 (*CACNA1G*).
Sequencing product size was 195 bp, 1 bp shorter than the expected 196 bp. The position of rs7501581 is indicated and shown in bold. Sample sequenced was determined to be C/G heterozygous by both sequencing and PCR-RFLP.

```
ref|NT_010783.15| Homo sapiens chromosome 17 genomic contig,
GRCh37.p5 Primary Assembly
Length=44983201

Features flanking this part of subject sequence:
  3496 bp at 5' side: spermatogenesis-associated protein 20
  2107 bp at 3' side: voltage-dependent T-type calcium channel
  subunit alpha-1G...

Score = 333 bits (180), Expect = 4e-89
Identities = 191/196 (97%), Gaps = 1/196 (1%)
Strand=Plus/Plus

Query 1         GTGGTGCAGCCTTAGGTGAGTGAACAACGCCCAGGGTTGAAGGGCTCAGC-AAGTGAGGG 59
                |||||||||||||||| |||||||||||||||||| ||| || |||||| |||||||||
Sbjct 13910671  GTGGTGCAGCCTTAGGAGAGTGAACAACGCCCAGGGGTGATGGCCTCAGCAAAGTGAGGG 13910730

Query 60        GTGGTGATGGAGGTCATCCGACCCATCCCGCCGCCTCTCCGCAGTGGCGCAAGCGCCCCA 119
                ||||||||||||||||||||||||||||||||||||||||||||||||||||||||||||
Sbjct 13910731  GTGGTGATGGAGGTCATCCGACCCATCCCGCCGCCTCTCCGCAGTGGCGCAAGCGCCCCA 13910790

Query 120       AAATCTCCGGAGAGGGAACTGACTGACCCACTAGGTTCCGCCGTGTCTACCTCTCGCAGA 179
                ||||||||||||||||||||||||||||||||||||||||||||||||||||||||||||
Sbjct 13910791  AAATCTCCGGAGAGGGAACTGACTGACCCACTAGGTTCCGCCGTGTCTACCTCTCGCAGA 13910850

Query 180       TGTTGGGGAAGTGCTT 195
                ||||||||||||||||
Sbjct 13910851  TGTTGGGGAAGTGCTT 13910866
```

Figure 6.18: BLAST nucleotide alignment of rs7501581 (*CACNA1G*) sequencing product (Query) against the human genome.
The most highly significant alignment is shown.

```
CCCAGGTAGGCG[C/T]GAGTGGACCAGCCATCTGGCCCCCCCACCTCCAGCTGAGGAACCTCT
GGGCAAGGTTAACACAGCCTGAGCCAGGGTACCTCTGTGCCAAGCAAGTGCTAGGCACACTACA
TGGGTTCCTCTTGTGCCCCTTGGAGGTGGGTATCATCTT
```

Figure 6.19: Sequence of PCR product amplified for SNP rs8066527 (*CACNA1G*).
Sequencing product size was 163 bp in length, 3 bp shorter than the expected 169 bp. The position of SNP rs8066527 is indicated and shown in bold. Sample sequenced was determined to be C/T heterozygous by both sequencing and PCR-RFLP.

```
ref|NT_010783.15| Homo sapiens chromosome 17 genomic contig,
GRCh37.p5 Primary Assembly
Length=44983201

Features in this part of subject sequence:
voltage-dependent T-type calcium channel subunit alpha-1G...

Score = 296 bits (160), Expect = 4e-78
Identities = 162/163 (99%), Gaps = 0/163 (0%)
Strand=Plus/Plus

Query 1         CCCAGGTAGGCGCGAGTGGACCAGCCATCTGGccccccccACCTCCAGCTGAGGAACCTCT 60
                |||||||||| ||||||||||||||||||||||||||||||||||||||||||||||||
Sbjct 13967021  CCCAGGTAGGAGCGAGTGGACCAGCCATCTGGCCCCCCCCACCTCCAGCTGAGGAACCTCT 13967080

Query 61        GGGCAAGGTTAACACAGCCTGAGCCAGGGTACCTCTGTGCCAAGCAAGTGCTAGGCACAC 120
                ||||||||||||||||||||||||||||||||||||||||||||||||||||||||||||
Sbjct 13967081  GGGCAAGGTTAACACAGCCTGAGCCAGGGTACCTCTGTGCCAAGCAAGTGCTAGGCACAC 13967140

Query 121       TACATGGGTTCCTCTTGTGCCCCTTGGAGGTGGGTATCATCTT 163
                  |||||||||||||||||||||||||||||||||||||||||
Sbjct 13967141  TACATGGGTTCCTCTTGTGCCCCTTGGAGGTGGGTATCATCTT 13967183
```

Figure 6.20: BLAST nucleotide alignment of rs8066527 (*CACNA1G*) sequencing product (Query) against the human genome.
The most highly significant alignment is shown.

```
CTCCGTCTTGTCCGTTCACTCCCAGCCAGCAGATACCAGCTACATCCTGCAGCTTCCCAAAGAT
GCACCTCATCTGCTCCAGCCCCACAGC[G]CCCCAACCTGGGGCACCATCCCCAAACTGCCCCC
ACCAGGACGCTCCCCTTTGGCTCAGAGGCCACTCAGGCGCCAGGTGAGCAGATGTGGAAAGGCA
GGCACAGGCCTGGGGGCTGGACCCTCTGCTGCTGGTGATGACCTGTGTT
```

Figure 6.21: Sequence of PCR product amplified for SNP rs8066269 (*CACNA1G*).
Sequencing product size was 239 bp as expected. The position of SNP rs8066269 is indicated and shown in bold. Sample sequenced was determined to be G/G homozygous by both sequencing and PCR-RFLP.

```
ref|NT_010783.15| Homo sapiens chromosome 17 genomic contig,
GRCh37.p5 Primary Assembly
Length=44983201

Features in this part of subject sequence:
 voltage-dependent T-type calcium channel subunit alpha-1G...

Score = 442 bits (239), Expect = 8e-122
Identities = 239/239 (100%), Gaps = 0/239 (0%)
Strand=Plus/Plus

Query 1         CTCCGTCTTGTCCGTTCACTCCCAGCCAGCAGATACCAGCTACATCCTGCAGCTTCCCAA 60
                ||||||||||||||||||||||||||||||||||||||||||||||||||||||||||||
Sbjct 13975874  CTCCGTCTTGTCCGTTCACTCCCAGCCAGCAGATACCAGCTACATCCTGCAGCTTCCCAA 13975933

Query 61        AGATGCACCTCATCTGCTCCAGCCCCACAGCGCCCCAACCTGGGGCACCATCCCCAAACT 120
                ||||||||||||||||||||||||||||||||||||||||||||||||||||||||||||
Sbjct 13975934  AGATGCACCTCATCTGCTCCAGCCCCACAGCGCCCCAACCTGGGGCACCATCCCCAAACT 13975993

Query 121       GCCCCCACCAGGACGCTCCCCTTTGGCTCAGAGGCCACTCAGGCGCCAGGTGAGCAGATG 180
                ||||||||||||||||||||||||||||||||||||||||||||||||||||||||||||
Sbjct 13975994  GCCCCCACCAGGACGCTCCCCTTTGGCTCAGAGGCCACTCAGGCGCCAGGTGAGCAGATG 13976053

Query 181       TGGAAAGGCAGGCACAGGCCTGGGGGCTGGACCCTCTGCTGCTGGTGATGACCTGTGTT 239
                |||||||||||||||||||||||||||||||||||||||||||||||||||||||||||
Sbjct 13976054  TGGAAAGGCAGGCACAGGCCTGGGGGCTGGACCCTCTGCTGCTGGTGATGACCTGTGTT 13976112
```

Figure 6.22: BLAST nucleotide alignment of rs8066269 (*CACNA1G*) sequencing product (Query) against the human genome.
The most highly significant alignment is shown.

GGCCTCTCCTCCCTCGTAC**[A/C]**CCCCACCCCAGTGGGAGCCCACAAGGACAGGGCCTGCCCC
ATCCCCTCCACTCTGGGCTGTGGCTCTAAGCAGCACGTCCCACTCTAGGGGCTCAGGGCAGGGA
CAGTGACTCATCCAAGGTCCCGCCGTGGAGGGCAGAGCTGAAGGAGTGAGAAGGAGCTGCTGAC
ATGGAA

Figure 6.23: Sequence of PCR product amplified for SNP rs7254543 (*HCN1*).
Sequencing product was 194 bp in length as expected. The position of rs725454 is shown in indicated and shown in bold. Sample sequenced was determined to be A/C heterozygous by both sequencing and PCR-RFLP.

```
>ref|NT_011255.14| Homo sapiens chromosome 19 genomic contig,
GRCh37.p5 Primary Assembly
Length=7286004

Features flanking this part of subject sequence:
  3209 bp at 5' side: basigin isoform 1 precursor
  3967 bp at 3' side: potassium/sodium hyperpolarization-
  activated cyclic nucle...

Score = 348 bits (188), Expect = 1e-93
Identities = 192/194 (99%), Gaps = 0/194 (0%)
Strand=Plus/Plus

Query 1       GGCCTCTCCTCCCTCGTACACCCCACCCCAGTGGGAGCCCACAAGGACAGGGCCTGCCCC 60
              ||||||||||||||| ||| ||||||||||||||||||||||||||||||||||||||||
Sbjct 525786  GGCCTCTCCTCCCTCTTACCCCCCACCCCAGTGGGAGCCCACAAGGACAGGGCCTGCCCC 525845

Query 61      ATCCCCTCCACTCTGGGCTGTGGCTCTAAGCAGCACGTCCCACTCTAGGGGCTCAGGGCA 120
              ||||||||||||||||||||||||||||||||||||||||||||||||||||||||||||
Sbjct 525846  ATCCCCTCCACTCTGGGCTGTGGCTCTAAGCAGCACGTCCCACTCTAGGGGCTCAGGGCA 525905

Query 121     GGGACAGTGACTCATCCAAGGTCCCGCCGTGGAGGGCAGAGCTGAAGGAGTGAGAAGGAG 180
              ||||||||||||||||||||||||||||||||||||||||||||||||||||||||||||
Sbjct 525906  GGGACAGTGACTCATCCAAGGTCCCGCCGTGGAGGGCAGAGCTGAAGGAGTGAGAAGGAG 525965

Query 181     CTGCTGACATGGAA 194
              ||||||||||||||
Sbjct 525966  CTGCTGACATGGAA 525979
```

Figure 6.24: BLAST nucleotide alignment of rs7254543 (*HCN1*) sequencing product (Query) against the human genome.
The most highly significant alignment is shown.

ACTGAAGGGGGTTCTTTTATGTTCACCCTGGGAAGATGTCAGGCCGGGCAGGTCGCCAGAGCCC
CAGGGCTCGCGGCTGGGAGCAGGGAGGAGGCGGGACCCGCACGGCACGAGAACCGCCCA**[T]**GC
CTGGCAGTGGGAGAAGCAGAAAGACGCCTCCTGCAGGCGCCGGCAGAACCCGCAAGTCACAAGG
GAGGCTGTG

Figure 6.25: Sequence of PCR product amplified for SNP rs873634 (*HCN2*).
Sequencing product size was 199 bp in length as expected. The position of rs873634 is indicated and shown in bold. Sample sequenced was determined to be T/T homozygous by both sequencing and PCR-RFLP.

```
>ref|NT_011255.14| Homo sapiens chromosome 19 genomic contig,
GRCh37.p5 Primary Assembly
Length=7286004

Features flanking this part of subject sequence:
  5653 bp at 5' side: basigin isoform 1 precursor
  1519 bp at 3' side: potassium/sodium hyperpolarization-
  activated cyclic nucle...

Score = 366 bits (198), Expect = 4e-99
Identities = 198/198 (100%), Gaps = 0/198 (0%)
Strand=Plus/Minus

Query 2      CTGAAGGGGGTTCTTTTATGTTCACCCTGGGAAGATGTCAGGCCGGGCAGGTCGCCAGAG 61
             ||||||||||||||||||||||||||||||||||||||||||||||||||||||||||||
Sbjct 528427 CTGAAGGGGGTTCTTTTATGTTCACCCTGGGAAGATGTCAGGCCGGGCAGGTCGCCAGAG 528368

Query 62     CCCCAGGGCTCGCGGCTGGGAGCAGGGAGGAGGCGGGACCCGCACGGCACGAGAACCGCC 121
             ||||||||||||||||||||||||||||||||||||||||||||||||||||||||||||
Sbjct 528367 CCCCAGGGCTCGCGGCTGGGAGCAGGGAGGAGGCGGGACCCGCACGGCACGAGAACCGCC 528308

Query 122    CATGCCTGGCAGTGGGAGAAGCAGAAAGACGCCTCCTGCAGGCGCCGGCAGAACCCGCAA 181
             ||||||||||||||||||||||||||||||||||||||||||||||||||||||||||||
Sbjct 528307 CATGCCTGGCAGTGGGAGAAGCAGAAAGACGCCTCCTGCAGGCGCCGGCAGAACCCGCAA 528248

Query 182    GTCACAAGGGAGGCTGTG 199
             ||||||||||||||||||
Sbjct 528247 GTCACAAGGGAGGCTGTG 528230
```

Figure 6.26: BLAST nucleotide alignment of rs873634 (*HCN2*) sequencing product (Query) against the human genome.
The most highly significant alignment is shown.

6.5 Haploview and haplotype phasing results

Table 6.5: Haploview quality control data for genotyped SNPs.
a. SNPs genotyped by PCR-RFLP; b. SNPs genotyped by MassARRAY. ObsHET = observed heterozygosity, PredHET = predicted heterozygosity, HWpval = HWE *p*-value, %Geno = % of samples successfully genotyped. Rating indicates SNPs that failed control checks on MAF (MAF < 0.05) or adherence to HWE ($p < 0.05$).

a.

SNP ID	Obs-HET	Pred-HET	HW-pval	%Geno	MAF	Alleles	Rating
rs10889635	0.476	0.483	0.9820	99.2	0.407	A:G	
rs6681460	0.407	0.468	0.1881	98.4	0.374	G:A	
rs2146904	0.427	0.473	0.3558	99.2	0.383	G:A	
rs572227	0.472	0.475	1	100	0.388	G:A	
rs279845	0.496	0.486	0.9985	100	0.416	T:A	
rs279841	0.472	0.472	1	98.4	0.382	G:A	
rs13187565	0.371	0.487	**0.0117**	99.2	0.419	G:T	BAD
rs13361609	0.328	0.362	0.3904	97.6	0.238	T:C	
rs7501581	0.432	0.465	0.5135	100	0.368	C:G	
rs8066527	0.398	0.457	0.2022	98.4	0.354	C:T	
rs8066269	0	0	1	20	**0**	G:G	BAD
rs873634	0.443	0.456	0.8509	97.6	0.352	T:G	
rs7254543	0.336	0.435	**0.0219**	95.2	0.319	C:A	BAD

b.

SNP ID	Obs-HET	Pred-HET	HW-pval	%Geno	MAF	Alleles	Rating
rs8192284	0.371	0.461	0.0793	98	0.361	A:C	
rs2794521	0.320	0.367	0.2911	98	0.242	T:C	
rs1800871	0.343	0.397	0.2563	100	0.273	C:T	
rs1800896	0.475	0.490	0.8754	100	0.429	A:G	
rs1143634	0.232	0.236	1	100	0.136	C:T	
rs1143627	0.495	0.472	0.8342	98	0.381	T:C	
rs16944	0.515	0.471	0.4985	100	0.379	G:A	
rs6853	0.153	0.141	1	99	0.077	A:G	
rs2069762	0.419	0.461	0.4827	93.9	0.360	T:G	
rs3804100	0.172	0.174	1	100	0.096	T:C	
rs1800629	0.192	0.205	0.7546	100	0.116	G:A	
rs1799971	0.253	0.25	1	100	0.146	A:G	
rs10499563	0.236	0.225	1	89.9	0.129	T:C	
rs11466004	0	0	1	90.9	**0**	T:T	BAD
rs4986790	0.072	0.070	1	98	0.036	A:G	
rs4986791	0.112	0.106	1	99	0.056	C:T	
rs6265	0.232	0.278	0.1922	100	0.167	G:A	
rs554344	0.286	0.287	1	99	0.173	G:C	
rs580253	0.235	0.266	0.3819	99	0.158	C:T	
rs11466314	0	0	1	99	**0**	G:G	BAD
rs1800469	0.475	0.466	1	100	0.369	C:T	

Table 6.6: Haplotype phasing results as determined by the EM algorithm in SNPAnalzyer 1.2A (part 1). Haplotype phase was determined for three-SNP haplotypes in *SGIP1*, *GABRA2* and *IL1B*, haplotypes assignments for each sample are shown (H1 and H2). Prob. = probability of the haplotype being correctly phased.

ID	*SGIP1*			*GABRA2*			*IL1B*		
	H1	**H2**	**Prob.**	**H1**	**H2**	**Prob.**	**H1**	**H2**	**Prob.**
1	AGG	GAA	49.88	GTG	AAA	49.70	CTG	CTG	100
2	AGG	AGG	100.00	GTG	AAA	49.70	TTG	CCA	45
3	AGG	AGG	100.00	GTG	GTG	100.00	CTG	CCA	50
4	GAA	GGG	49.85	GTG	AAA	49.70	CTG	CCA	50
5	AGG	GAA	49.88	GTG	GTG	100.00	TTG	CCA	45
6	GAA	GAA	100.00	GTG	AAA	49.70	–	–	–
7	AGG	AGG	100.00	–	–	–	CTG	CCA	50
8	AGG	GAA	49.88	ATG	AAA	50.00	CTG	CTG	100
9	AGG	GAA	49.88	GTG	GTG	100.00	CCA	CCA	100
10	AGG	AGG	100.00	AAA	AAA	100.00	CCA	CCA	100
11	GAA	GAA	100.00	GTG	AAA	49.70	TTG	TTG	100
12	GAA	GAA	100.00	GTG	GTG	100.00	–	–	–
13	GAA	GAA	100.00	GTG	GTG	100.00	CTG	CTG	100
14	AGG	GAA	49.88	GTG	AAA	49.70	CTG	CCA	50
15	AGG	GAA	49.88	GTG	GTG	100.00	–	–	–
16	AGG	GAA	49.88	GAA	AAA	100.00	CTG	CCA	50
17	AGG	AGG	100.00	AAA	AAA	100.00	–	–	–
18	AGG	AGG	100.00	GAG	AAA	49.93	CTG	CTG	100
19	AGG	AGG	100.00	GTG	AAA	49.70	CTG	CTG	100
20	AGG	AGG	100.00	GTG	GTG	100.00	CCA	CCA	100
21	AGG	GGG	100.00	ATG	AAA	50.00	CTG	CCA	50
22	AGG	GAA	49.88	GAA	GTG	47.59	CTG	CTG	100
23	AGG	GGG	100.00	ATG	AAA	50.00	CTG	CTG	100
24	GAA	GGG	49.85	GTG	GTG	100.00	CTG	CTG	100
25	AGG	AGG	100.00	GTG	AAA	49.70	CTG	TTG	100
26	AGG	GAA	49.88	GTG	GTG	100.00	CTG	TTG	100
27	AGG	AGG	100.00	GTG	GAG	100.00	CTG	CTG	100
28	AGG	GAA	49.88	GTG	AAA	49.70	–	–	–
29	AGG	GAG	43.84	GTA	GAA	100.00	CTG	CCA	50
30	AGG	GAA	49.88	AAA	AAA	100.00	TTG	CCA	45
31	–	–	–	GTG	GTG	100.00	–	–	–
33	AGG	GAA	49.88	GTG	AAA	49.70	CTG	CCA	50
34	–	–	–	GTG	AAA	49.70	CTG	CCA	50
35	GAA	GAA	100.00	GTG	AAA	49.70	TTG	CCA	45
36	AGG	GAA	49.88	GTG	AAA	49.70	CTG	CCA	50
37	AGG	GGG	100.00	GAG	AAA	49.93	CTG	CCA	50
38	AGG	GAA	49.88	GTG	GTG	100.00	CTG	CTG	100
39	AGG	AGA	100.00	GTG	AAA	49.70	–	–	–
40	GAA	GAA	100.00	GTG	AAA	49.70	CTG	CCA	50
41	AGG	GAA	49.88	GTG	AAA	49.70	–	–	–
42	GAA	GAA	100.00	GTG	GAG	100.00	CCA	CTA	100

Table 6.6 cont.: Haplotype phasing results (part 2).

ID	*SGIP1*			*GABRA2*			*IL1B*		
	H1	**H2**	**Prob.**	**H1**	**H2**	**Prob.**	**H1**	**H2**	**Prob.**
43	AGG	AGG	100.00	GTG	ATG	100.00	CCA	CCA	100
44	AGG	AGG	100.00	GTG	AAA	49.70	CCA	CCA	100
45	AGG	GAA	49.88	GTG	AAA	49.70	CTG	CCA	50
46	AGG	AGG	100.00	GTG	AAA	49.70	–	–	–
47	AGG	AGA	100.00	GTG	GTG	100.00	CTG	CTG	100
48	GAA	GAA	100.00	GTG	GTG	100.00	–	–	–
49	AGG	GAA	49.88	GTG	AAA	49.70	CTG	CCA	50
50	AGG	AGG	100.00	GTG	ATG	100.00	–	–	–
51	AGG	AGG	100.00	GTG	AAA	49.70	CCG	CCA	100
52	AGG	GAA	49.88	GTG	AAA	49.70	CTG	TTG	100
53	AGG	AGG	100.00	GTG	AAA	49.70	CTG	TTG	100
54	AGG	AGA	100.00	GTG	GTG	100.00	CTG	CCA	50
55	AGG	GAA	49.88	GTG	AAA	49.70	CTG	CCA	50
56	AGG	GAA	49.88	GTG	AAA	49.70	CCA	CCA	100
58	AGG	GAA	49.88	GTG	AAA	49.70	CTG	CCA	50
59	AGG	GAA	49.88	GTG	GTG	100.00	CTG	CTG	100
60	AGG	GAA	49.88	GTG	AAA	49.70	CTG	CCA	50
62	AGG	GAA	49.88	GTG	AAA	49.70	–	–	–
63	GAA	GAA	100.00	GTG	AAA	49.70	–	–	–
64	AGG	GAA	49.88	GTG	GTG	100.00	CTG	CCA	50
65	AGG	GAA	49.88	ATG	AAA	50.00	CTG	CCA	50
66	AGG	GAA	49.88	GTG	AAA	49.70	CTG	CTG	100
67	AGG	AGG	100.00	GTG	GAG	100.00	TTG	CCA	45
68	AGG	AGG	100.00	GTG	AAA	49.70	CTG	TTG	100
69	AGG	GAA	49.88	GAG	ATG	39.67	CTG	CCA	50
70	AGG	GAA	49.88	GAA	GTG	47.59	CTG	CTG	100
71	AGG	GAA	49.88	GAA	GTG	47.59	CTG	CTG	100
72	AGG	AGG	100.00	GTG	AAA	49.70	CTG	CCA	50
73	AGG	AGG	100.00	GTG	GTG	100.00	CTG	TTG	100
74	AGG	GGG	100.00	GTG	ATG	100.00	–	–	–
75	AGG	GGG	100.00	GTG	AAA	49.70	CTG	TTG	100
76	GAA	AGA	49.86	GTG	AAA	49.70	CTG	TTG	100
78	GAA	GAA	100.00	GTG	AAA	49.70	CTG	CCA	50
79	AGG	AGG	100.00	GAG	GAG	100.00	–	–	–
80	AGG	AGG	100.00	GTG	AAA	49.70	CTG	CCA	50
82	GAA	GAA	100.00	AAA	AAA	100.00	CTG	CCA	50
83	AGG	AGG	100.00	GTG	GTG	100.00	CTG	CTG	100
85	AGG	GAA	49.88	GTG	AAA	49.70	CTG	CTG	100
86	GAA	GAA	100.00	GTG	GTG	100.00	TTG	CCA	45
87	AGG	AGG	100.00	GTG	AAA	49.70	CTG	CCA	50
88	AGG	GAA	49.88	GTG	GTG	100.00	CCA	CCA	100
89	AGG	AGG	100.00	AAA	AAA	100.00	CTG	CCA	50
90	AGG	AGG	100.00	GTG	GTG	100.00	CCA	CCA	100
91	AGG	GAA	49.88	GTG	GTG	100.00	CTG	CCA	50
92	AGG	GAA	49.88	GTG	GTG	100.00	–	–	–

Table 6.6 cont.: Haplotype phasing results (part 3).

ID	*SGIP1*			*GABRA2*			*IL1B*		
	H1	**H2**	**Prob.**	**H1**	**H2**	**Prob.**	**H1**	**H2**	**Prob.**
93	AGG	GAA	49.88	GTG	AAA	49.70	TTG	CCA	45
94	AGG	AGG	100.00	GTG	GTG	100.00	CTG	CCA	50
95	AGG	AGG	100.00	GTG	GTG	100.00	CTG	CTG	100
96	AGG	AGG	100.00	GTG	GAG	100.00	TTG	CCA	45
97	AGG	AGG	100.00	AAA	AAA	100.00	CTG	CCA	50
99	GAA	GAA	100.00	GTG	GTG	100.00	CTG	CCA	50
100	AGG	AGG	100.00	GAA	AAA	100.00	CTG	CTG	100
101	GAA	GAA	100.00	GTG	GTG	100.00	CTG	CTG	100
102	GAA	GAA	100.00	GTG	GAG	100.00	CCA	CCA	100
103	AGG	AGG	100.00	AAA	AAA	100.00	–	–	–
104	GAA	GAA	100.00	GTG	AAA	49.70	CTG	CCA	50
105	GAA	GAA	100.00	GTG	GTG	100.00	–	–	–
106	AGG	GAA	49.88	GAG	AAA	49.93	–	–	–
108	AGG	GAA	49.88	GTG	AAA	49.70	TTG	CCA	45
109	AGG	GAA	49.88	GTG	GTG	100.00	–	–	–
110	GAA	GAA	100.00	AAA	AAA	100.00	–	–	–
111	AGG	GGG	100.00	GTG	AAA	49.70	CTG	CCA	50
112	AGG	AGG	100.00	AAA	AAA	100.00	CCA	CCA	100
114	AGG	AGG	100.00	GTG	AAA	49.70	CTG	CCA	50
115	AGG	AGG	100.00	ATG	ATG	100.00	–	–	–
116	GAA	GAA	100.00	GTG	GTG	100.00	CTG	TTG	100
117	AGG	AGG	100.00	AAA	AAA	100.00	CTG	CTG	100
118	AGG	GAA	49.88	GTG	GTG	100.00	CTG	CTG	100
119	AGG	GGG	100.00	GTG	GTG	100.00	–	–	–
120	AGG	AGG	100.00	AAA	AAA	100.00	CTG	CCA	50
121	AGG	GAA	49.88	AAA	AAA	100.00	TTG	CCA	45
122	AGG	GAA	49.88	AAA	GTA	49.74	CTG	CTG	100
123	AGG	GAA	49.88	GTG	AAA	49.70	CCA	CCA	100
124	AGG	GGA	37.49	GTG	GTG	100.00	–	–	–
125	AGG	GAG	43.84	AAA	AAA	100.00	–	–	–
128	AGG	GGA	37.49	AAA	AAA	100.00	–	–	–
130	AAG	AAA	100.00	GTG	AAA	49.70	–	–	–
131	GAA	AAG	49.67	GTG	GTG	100.00	–	–	–
158	AGG	AGG	100.00	GTG	GTG	100.00	CTG	CCA	50
159	GAA	AGA	49.86	GTG	AAA	49.70	TTG	TTG	100
163	AGG	GGG	100.00	–	–	–	CTG	TTG	100
165	AGG	AGG	100.00	GTG	GTG	100.00	CTG	CCA	50
167	AGG	GAA	49.88	GTG	AAA	49.70	CTG	TTG	100
170	AGG	GAA	49.88	GAG	AAA	49.93	TTG	CCA	45

Table 6.7: Summary of quality control data for haplotype phase reconstruction performed using the EM algorithm in SNPAnalyzer 1.2A.
Minimum, maximum and mean of haplotype call probabilities are shown together with percentage of samples that met the 90% probability threshold (Passed).

Gene	n	Min. probability	Max. probability	Mean probability	Passed
SGIP1	123	37%	100%	78%	56%
GABRA2	123	40%	100%	75%	51%
IL1B	97	45%	100%	75%	51%

6.6 HapMap haplotypes and haplotype blocks

The following LD plots and haplotypes were constructed in Haploview using downloaded HapMap data (V3/R27/CEU) and the haplotype block definitions of Gabriel et al. (2002) [134]. For LD plots, the value in each square corresponds level of LD between SNP loci in D' – for example, a value of 94 corresponds to D' = 0.94, and empty squares correspond to D' = 1. Dark black squares indicate high levels of LD between SNP loci, and white and pale grey squares weaker LD.

Table 6.8: Comparison of haplotypes and their frequencies constructed for SNPs genotyped in this study with the HapMap Caucasian population.
a. *SGIP1* haplotypes, 1 = rs10889635, 2 = rs6681460, 3 = rs2146904; b. *GABRA2* haplotypes, 1 = rs572227, 2 = 279845, 3 = rs279841; c. *IL1B* haplotypes, 1 = rs1143634, 2 = rs1143627 and 3 = rs16944. N/P = haplotype not present in HapMap Caucasians.

a.

SGIP1			**Genotyped**	**HapMap**
1	**2**	**3**	**HF**	**HF**
A	G	G	0.558	0.509
G	A	A	0.350	0.453
G	G	G	0.043	0.004
A	G	A	0.022	0.017
A	A	G	0.009	N/P
G	A	G	0.008	0.009
G	G	A	0.007	N/P
A	A	A	0.004	0.009

b.

GABRA2			**Genotyped**	**HapMap**
1	**2**	**3**	**HF**	**HF**
G	T	G	0.530	0.491
A	A	A	0.343	0.432
G	A	G	0.048	0.030
G	T	A	0.009	N/P
G	A	A	0.025	0.017
A	T	G	0.045	0.021

c.

IL1B			**Genotyped**	**HapMap**
1	**2**	**3**	**HF**	**HF**
C	T	G	0.490	0.470
C	C	A	0.368	0.321
T	T	G	0.126	0.171
T	C	A	0.011	0.034

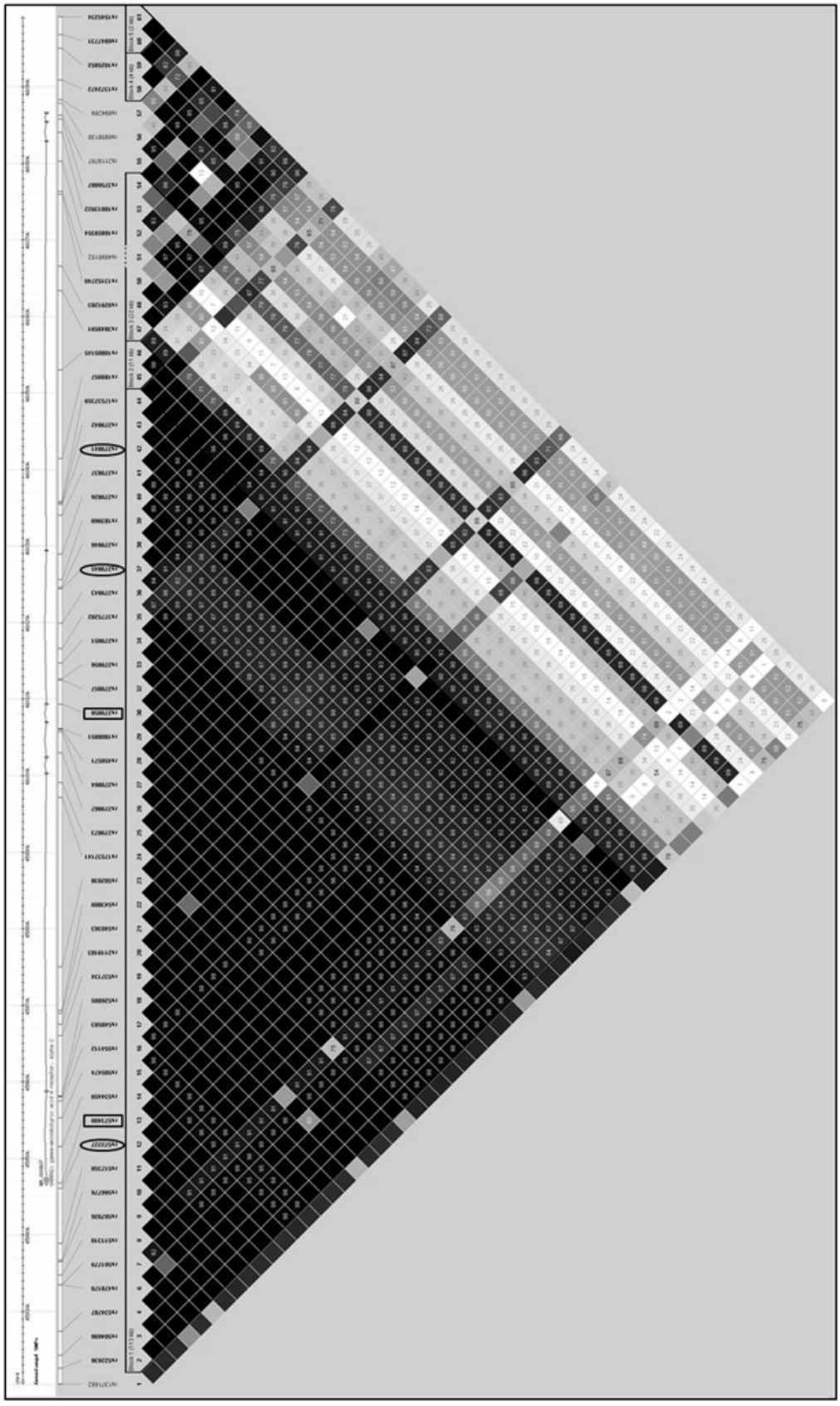

Figure 6.27: LD plot showing the haplotype block structure of *GABRA2*.
SNPs genotyped by PCR-RFLP in this study are circled. SNPs previously associated with *GABRA2* mRNA levels [171] are marked with square boxes (rs279871 was not in the HapMap Caucasian database).

a.

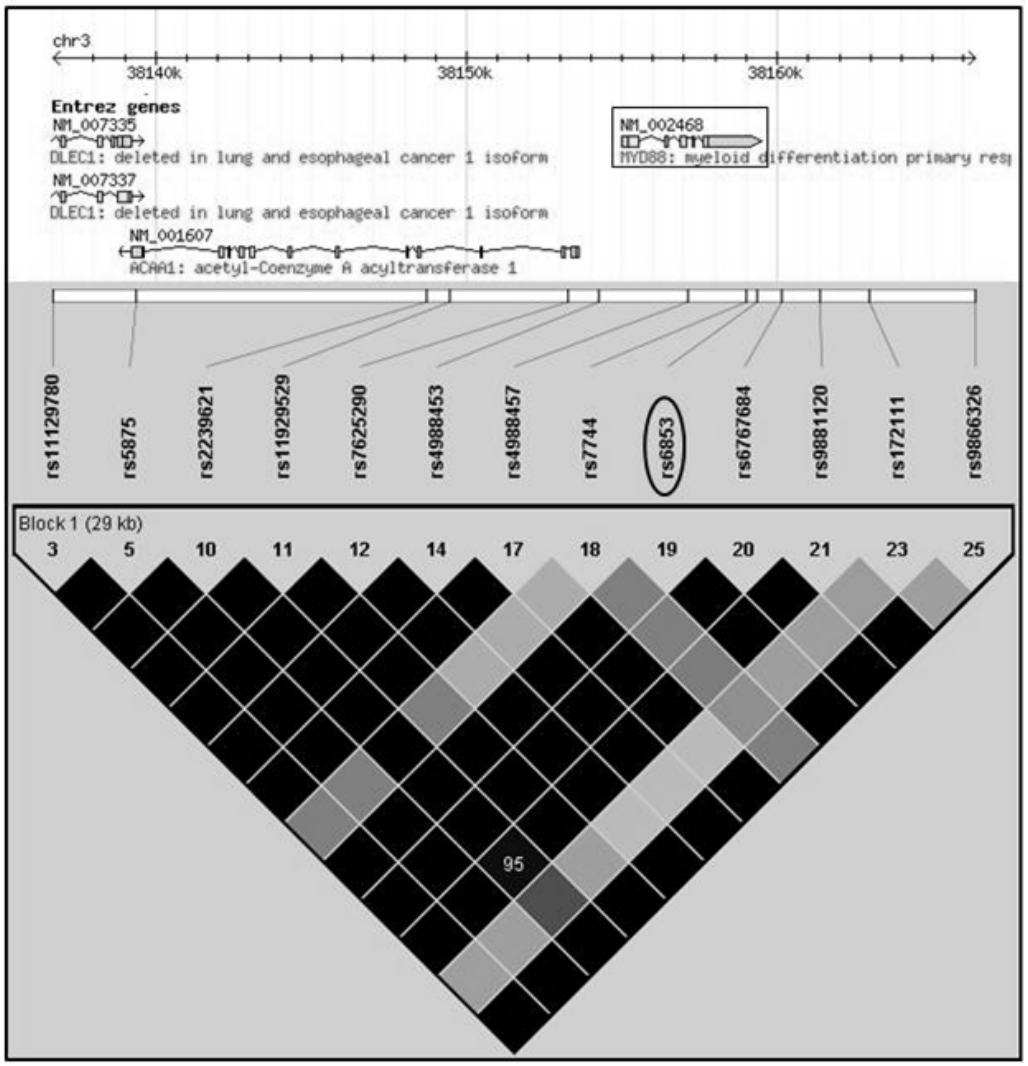

b.

Figure 6.28: Haplotype block structure and haplotypes for *MYD88* and surrounding genomic region.

a. LD plot for *MYD88* and surrounding genomic region. rs6853 (circled) is located in a 29 kb haplotype block encompassing all of *MYD88* (indicated by a black square) along with *ACAA1* and part of *DLEC1*. b. rs6853G (circled) is present on two rare haplotypes located in a 29 kb haplotype in Caucasians.

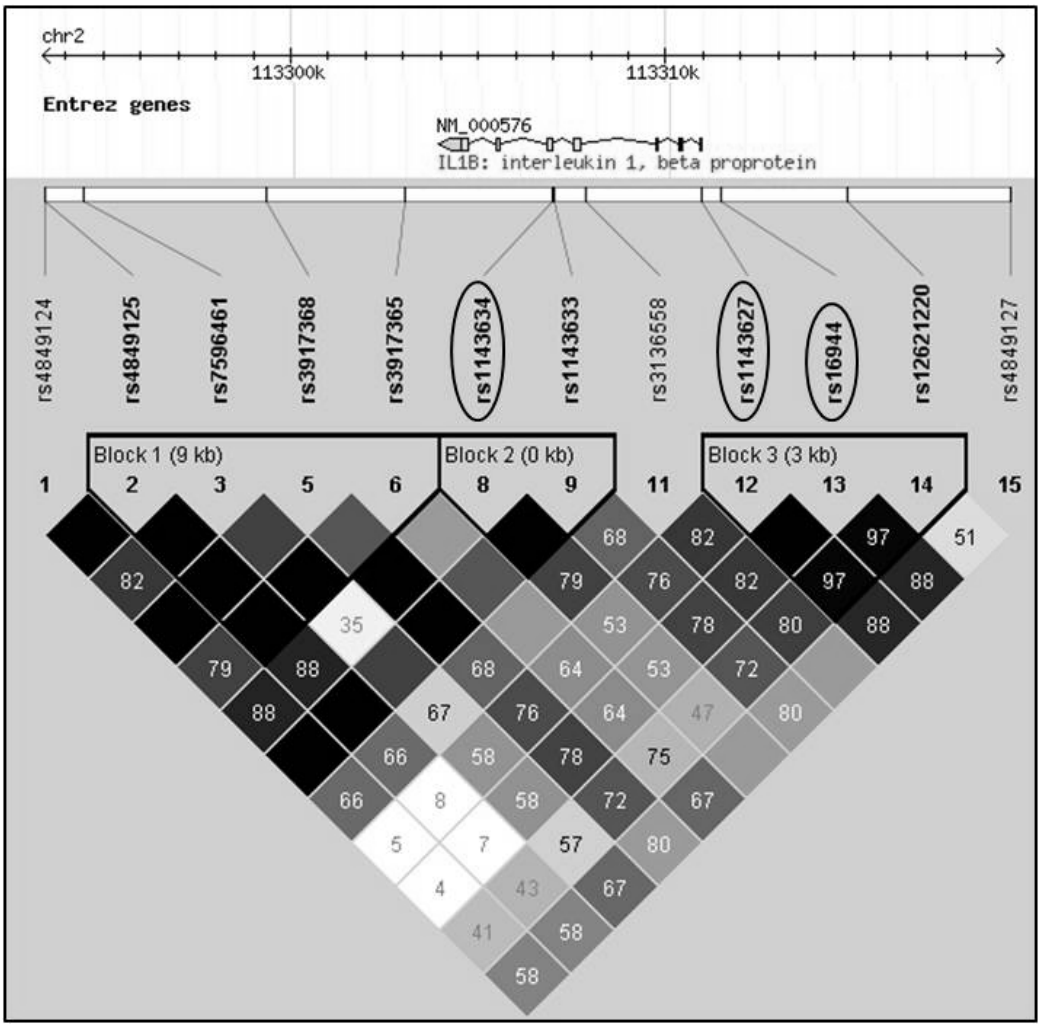

Figure 6.29: LD plot showing gene and haplotype block structure of *IL1B* and surrounding genomic region.
Genotyped SNPs are circled.

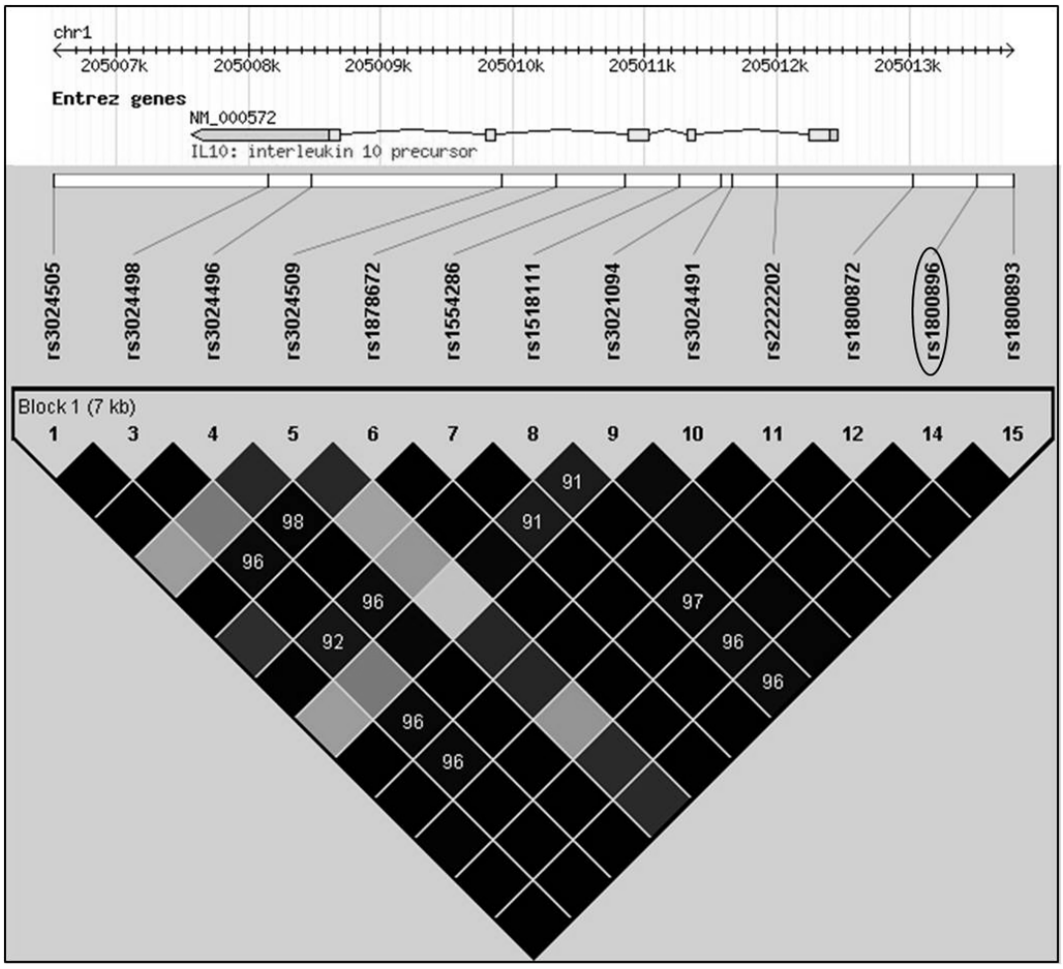

Figure 6.30: LD plot showing gene and haplotype block structure of *IL10*.
rs1800896 (circled) is located in a 7 kb haplotype block encompassing all of *IL10*.

6.7 Association analysis results

Table 6.9: Effect of SNP genotypes on spindle amplitude.
Significant ($p < 0.05$), and highly significant ($p < 0.01$), *p*-values are marked by an asterisk and double asterisk, respectively.

SNP	Test	Genotype	n	Median (95% CI)	Fold Diff.	*p*-value
rs6681406	AA vs. AG	AA	21	2.18 (1.93-2.43)	1.25	0.0158*
(*SGIP1*)		AG	50	1.74 (1.51-1.98)		
	AA vs. GG	AA	21	2.18 (1.93-2.43)	1.23	0.0206*
		GG	52	1.77 (1.50-1.99)		
	AG vs. GG	AG	50	1.74 (1.51-1.98)	0.98	0.7863
		GG	52	1.77 (1.50-1.99)		
rs279841	AA vs. AG	AA	18	2.32 (1.95-2.44)	1.29	0.0262*
(*GABRA2*)		AG	58	1.80 (1.61-1.99)		
	AA vs. GG	AA	18	2.32 (1.95-2.44)	1.28	0.0141*
		GG	47	1.81 (1.54-2.06)		
	AG vs. GG	AG	58	1.80 (1.61-1.99)	0.99	0.8467
		GG	47	1.81 (1.54-2.06)		
rs1143627	CC vs. CT	CC	13	1.54 (1.13-1.75)	0.78	0.0118*
(*IL1B*)		CT	48	1.97 (1.68-2.25)		
	CC vs. TT	CC	13	1.54 (1.13-1.75)	0.91	0.3358
		TT	36	1.69 (1.32-1.93)		
	CT vs. TT	CT	48	1.97 (1.68-2.25)	1.17	0.0488*
		TT	36	1.69 (1.32-1.93)		
rs16944	AA vs. AG	AA	12	1.47 (1.13-1.75)	0.78	0.0129*
(*IL1B*)		AG	51	1.89 (1.71-2.25)		
	AA vs. GG	AA	12	1.47 (1.13-1.75)	0.87	0.3230
		GG	36	1.69 (1.32-1.93)		
	AG vs. GG	AG	51	1.89 (1.71-2.25)	1.12	0.0568
		GG	36	1.69 (1.32-1.93)		
rs6853	AG vs. AA	AG	15	2.43 (1.62-2.84)	1.39	0.0040**
(*MYD88*)		AA	83	1.75 (1.54-1.88)		

Table 6.10: Effect of SNP genotypes on relative spindle amplitude.
Significant ($p < 0.05$), and highly significant ($p < 0.01$), *p*-values are marked by an asterisk and double asterisk, respectively.

SNP	Test	Genotype	n	Median (95% CI)	Fold Diff.	*p*-value
rs6681406	AA vs. AG	AA	20	0.48 (0.32-0.53)	1.55	0.0115*
(*SGIP1*)		AG	49	0.31 (0.24-0.35)		
	AA vs. GG	AA	20	0.48 (0.32-0.53)	1.41	0.0261*
		GG	51	0.34 (0.23-0.42)		
	AG vs. GG	AG	49	0.31 (0.24-0.35)	0.91	0.8307
		GG	51	0.34 (0.23-0.42)		
rs873634	GG vs. GT	GG	16	0.43 (0.34-0.53)	1.48	0.0164*
(*HCN1*)		GT	52	0.29 (0.24-0.41)		
	GG vs. TT	GG	16	0.43 (0.34-0.53)	1.30	0.0540
		TT	51	0.33 (0.26-0.42)		
	GT vs. TT	GT	52	0.29 (0.24-0.41)	0.88	0.3732
		TT	51	0.33 (0.26-0.42)		
rs1143627	CC vs. CT	CC	13	0.27 (0.16-0.44)	0.77	0.0724
(*IL1B*)		CT	48	0.35 (0.29-0.49)		
	CC vs. TT	CC	13	0.27 (0.16-0.44)	1.04	0.8985
		TT	35	0.26 (0.20-0.34)		
	CT vs. TT	CT	48	0.35 (0.29-0.49)	1.35	0.0145*
		TT	35	0.26 (0.20-0.34)		
rs16944	AA vs. AG	AA	12	0.27 (0.16-0.44)	0.79	0.1073
(*IL1B*)		AG	51	0.34 (0.29-0.47)		
	AA vs. GG	AA	12	0.27 (0.16-0.44)	1.04	0.9223
		GG	35	0.26 (0.20-0.34)		
	AG vs. GG	AG	51	0.34 (0.29-0.47)	1.31	0.0220*
		GG	35	0.26 (0.20-0.34)		
rs6853	AG vs. AA	AG	15	0.49 (0.35-0.57)	1.69	0.0006**
(*MYD88*)		AA	82	0.29 (0.24-0.33)		

Table 6.11: Effect of SNP genotypes on ETDC.
Significant ($p < 0.05$), and highly significant ($p < 0.01$), *p*-values are marked by an asterisk and double asterisk, respectively.

SNP	Test	Genotype	n	Median (95% CI)	Fold Diff.	*p*-value
rs7501581 (*CACNA1G*)	GG vs. CG	GG	19	6.39 (4.96-7.36)	1.29	0.0075**
		CG	52	4.95 (4.56-5.49)		
	GG vs. CC	GG	19	6.39 (4.96-7.36)	1.14	0.1071
		CC	51	5.62 (5.04-6.03)		
	CG vs. CC	CG	52	4.95 (4.56-5.49)	0.88	0.0383*
		CC	51	5.62 (5.04-6.03)		
rs2794521 (*CRP*)	CC vs. CT	CC	8	5.78 (4.71-7.96)	0.97	0.6764
		CT	31	5.96 (5.57-6.68)		
	CC vs. TT	CC	8	5.78 (4.71-7.96)	1.12	0.0739
		TT	57	5.18 (4.80-5.62)		
	CT vs. TT	CT	31	5.96 (5.57-6.68)	1.15	0.0306*
		TT	57	5.18 (4.80-5.62)		
rs6853 (*MYD88*)	AG vs. AA	AG	15	5.04 (4.35-5.35)	0.88	0.0095**
		AA	82	5.71 (5.46-6.1)		
rs1800469 (*TGF1B*)	TT vs. CT	TT	13	4.71 (4.26-5.67)	0.84	0.0634
		CT	46	5.58 (4.82-6.10)		
	TT vs. CC	TT	13	4.71 (4.26-5.67)	0.79	0.0126*
		CC	39	5.95 (5.39-6.66)		
	CT vs. CC	CT	46	5.58 (4.82-6.10)	0.84	0.2408
		CC	39	5.95 (5.39-6.66)		

Table 6.12: Effect of rs7501581 (*CACNA1G*) on relationship between BIS and ETDC.
a. Linear regression analysis results for √BIS value vs. ETDC categorised by rs7501581 genotype. b. *p*-values for differences in slope and intercept between lines. Significant ($p < 0.05$), and highly significant ($p < 0.01$), *p*-values are marked by an asterisk and double asterisk, respectively.

a.

Model	Genotype/s	n	Intercept	Slope	r^2	*r*	*p*-value
R	G/G	16	6.396	-0.080	0.024	-0.155	0.5663
	C/G + C/C	84	7.067	-0.136	0.040	-0.200	0.0693
D	G/G + C/G	55	6.725	-0.099	0.025	-0.158	0.2492
	C/C	45	7.734	-0.243	0.126	-0.112	0.0169*
OD	C/C + G/G	61	7.558	-0.226	0.122	-0.349	0.0058**
	C/G	39	6.568	-0.053	0.006	-0.076	0.6458

b.

Model	Genotype/s	*p*-value for difference in intercept	*p*-value for difference in slope
R	G/G vs. C/G + C/C	0.1786	0.7765
D	G/G + C/G vs. C/C	0.2476	0.2804
OM	C/C + G/G vs. C/G	0.8393	0.1990

Table 6.13: Effect of rs6853 (*MYD88*) genotype on relationship of ETDC with spindle amplitude and BIS value.

a. Linear regression analysis results for spindle amplitude (Spindle A.) vs. ETDC, and √BIS value vs. ETDC, categorised by res6853 genotype. b. *p*-values for differences in slope and intercept between lines. Significant ($p < 0.05$), and highly significant ($p < 0.01$), *p*-values are marked by an asterisk and double asterisk, respectively.

a.

ETDC vs.	Genotype	n	Intercept	Slope	r^2	*r*	*p*-value
Spindle A.	A/A	82	0.019	-0.183	0.172	-0.415	0.0001**
	A/G	15	2.177	2.764	0.001	0.028	0.9208
√BIS	A/A	82	-0.5836	-0.1348	0.038	-0.194	0.1075
	A/G	15	9.097	7.059	0.394	0.627	0.0163

b.

ETDC vs.	Test	*p*-value for difference in intercept	*p*-value for difference in slope
Spindle A.	A/A vs. A/G	0.0087**	0.2139
√BIS	A/A vs. A/G	0.4216	0.8594

Table 6.14: Effect of rs1800896 (*IL10*) genotype on delta frequency.

Significant ($p < 0.05$), and highly significant ($p < 0.01$), *p*-values are marked by an asterisk and double asterisk, respectively.

SNP	Test	Genotype	n	Median (95% CI)	Fold Diff.	*p*-value
rs1800896	GG vs. AG	GG	19	0.50 (0.05-0.63)	0.67	0.0055**
(*IL10*)		AG	47	0.75 (0.63-0.88)		
	GG vs. AA	GG	19	0.50 (0.05-0.63)	0.79	0.1385
		AA	33	0.63 (0.50-0.75)		
	AG vs. AA	AG	47	0.75 (0.63-0.88)	1.19	0.0935
		AA	33	0.63 (0.50-0.75)		